



Terms and Conditions of Use of Digitised Theses from Trinity College Library Dublin

Copyright statement

All material supplied by Trinity College Library is protected by copyright (under the Copyright and Related Rights Act, 2000 as amended) and other relevant Intellectual Property Rights. By accessing and using a Digitised Thesis from Trinity College Library you acknowledge that all Intellectual Property Rights in any Works supplied are the sole and exclusive property of the copyright and/or other IPR holder. Specific copyright holders may not be explicitly identified. Use of materials from other sources within a thesis should not be construed as a claim over them.

A non-exclusive, non-transferable licence is hereby granted to those using or reproducing, in whole or in part, the material for valid purposes, providing the copyright owners are acknowledged using the normal conventions. Where specific permission to use material is required, this is identified and such permission must be sought from the copyright holder or agency cited.

Liability statement

By using a Digitised Thesis, I accept that Trinity College Dublin bears no legal responsibility for the accuracy, legality or comprehensiveness of materials contained within the thesis, and that Trinity College Dublin accepts no liability for indirect, consequential, or incidental, damages or losses arising from use of the thesis for whatever reason. Information located in a thesis may be subject to specific use constraints, details of which may not be explicitly described. It is the responsibility of potential and actual users to be aware of such constraints and to abide by them. By making use of material from a digitised thesis, you accept these copyright and disclaimer provisions. Where it is brought to the attention of Trinity College Library that there may be a breach of copyright or other restraint, it is the policy to withdraw or take down access to a thesis while the issue is being resolved.

Access Agreement

By using a Digitised Thesis from Trinity College Library you are bound by the following Terms & Conditions. Please read them carefully.

I have read and I understand the following statement: All material supplied via a Digitised Thesis from Trinity College Library is protected by copyright and other intellectual property rights, and duplication or sale of all or part of any of a thesis is not permitted, except that material may be duplicated by you for your research use or for educational purposes in electronic or print form providing the copyright owners are acknowledged using the normal conventions. You must obtain permission for any other use. Electronic or print copies may not be offered, whether for sale or otherwise to anyone. This copy has been supplied on the understanding that it is copyright material and that no quotation from the thesis may be published without proper acknowledgement.

Investigation of
Microtubule Inhibitors as
Potential Antimalarial Agents

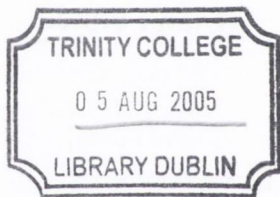
A thesis submitted for the degree of Doctor of Philosophy

by

Brian Fennell

Department of Microbiology
Moyne Institute of Preventive Medicine
Trinity College
University of Dublin

December 2004



THESIS

7A03

DECLARATION

This is to certify that the experimentation recorded herein represents my own work, unless otherwise stated, and has not been submitted for higher degree at this or any other university. The thesis may be lent or copied at the discretion of the librarian, Trinity College.

Brian Fennell.

Brian Fennell,
December, 2004.

SUMMARY

Malaria is a parasitic infection of immense global importance. The most common and severe form of the disease is caused by the blood-borne apicomplexan parasite *Plasmodium falciparum*. The lack of an effective vaccine coupled with the emergence and spread of resistance to currently-used antimalarial agents highlights the need for the discovery and development of novel antimalarial drugs.

Microtubules are cytoskeletal polymers containing repeating α/β -tubulin heterodimers and are found in all eukaryotes including *P. falciparum*. Diverse cellular functions such as chromosomal segregation, organelle transport and the determination of cell shape and motility are all dependent on microtubules. This essential role played by tubulin in cells has resulted in the effective use of anti-microtubule agents for application as fungicides, herbicides, antiparasitics and anticancer agents. Given the fact that *P. falciparum* is also highly susceptible to some of these agents suggests that tubulin from the malarial parasite may present an excellent drug target.

The objective of this project was to characterise the effects of established and novel classes of antimicrotubule agent on *P. falciparum*, and in particular to investigate their possible anti-tubulin mechanism of action at the cellular and molecular level. A series of naturally-occurring and synthetic inhibitors from both anti-cancer and herbicide stables was investigated. The likelihood that such agents could be candidates for development into new antimalarial drugs was also considered.

Dolastatin 10 was a potent inhibitor of *P. falciparum*, while the related auristatins had variable potencies. All agents displayed unusual dose-response relationships, which were deemed to reflect the varying susceptibilities of the different cellular forms of asexual erythrocytic parasites. Concentrations of dolastatin 10 and auristatin PE in the low nanomolar range hindered parasite schizogony and nuclear division, caused various cellular abnormalities and resulted in loss of normal mitotic microtubular structures and their replacement by diffuse or fragmented tubulin labelling. These findings are consistent with an anti-tubulin mechanism of action of the dolastatin/auristatin series similar to that of the “*Vinca*” alkaloid vinblastine. However, no markedly selective compound from the dolastatin/auristatin series was identified that might be progressed as an antimalarial drug.

Ligands from structurally diverse herbicide classes, namely the dinitroanilines and phosphorothioamidates, which have previously been shown to have no effect on

microtubules in mammalian cells, displayed moderate antimalarial activity. They also caused a block on nuclear division and perturbed normal parasite microtubular architecture in a manner different from the “*Vinca*” domain-binding agents vinblastine and dolastatin 10. Furthermore, the radiolabelled dinitroaniline [¹⁴C]trifluralin was found to bind to recombinant *P. falciparum* tubulins with a higher affinity than mammalian tubulins, consistent with the premise that the inhibition of cultured *P. falciparum* was caused by binding of these ligands to parasite tubulin. Molecular modeling studies of the *P. falciparum* α I/ β -tubulin dimer based on the crystal structure of the bovine tubulin heterodimer identified a putative dinitroaniline-binding site on modelled *P. falciparum* α I-tubulin but not on the bovine α -tubulin subunit.

Studies on α I- and β -tubulin in the parasite’s intra-erythrocytic cycle indicated that the production of these proteins was stage-dependent, in agreement with their expression at the mRNA level. Ring-stage parasites contained the lowest amounts of tubulin and schizonts the highest. Low levels of α II-tubulin production, previously thought to be exclusive to gametocytes, were also detected in schizont-stage parasites. In addition, both native and recombinant *P. falciparum* α I- and β -tubulins displayed a reversed order of electrophoretic mobility compared to the migratory behaviour of vertebrate (bovine brain) tubulins, a property common to a number of lower eukaryotic organisms. Functional studies described here indicated that refolded recombinant *P. falciparum* tubulins, produced in *Escherichia coli*, were non-functional as they failed to polymerise into microtubules. However, α I-tubulin expressed as a soluble fusion protein displayed assembly competency as it could be incorporated into microtubules assembled from bovine brain tubulin.

In summary, these findings have provided experimental evidence both directly in the parasite and *in vitro* that *P. falciparum* tubulins are the target for a diverse range of microtubule inhibitors. The selective actions of the antimitotic herbicides suggest that derivatives of them may have great potential as future anti-malarial drugs.

For Mam and Dad

ACKNOWLEDGEMENTS

Firstly, I would like to thank Gus for his brilliant supervision, his constant support, guidance and friendship. You have all the great qualities one needs in a supervisor and I count myself very lucky to have had the opportunity to work in your fine research group.

A big thanks must also go to all the members of the Bell lab - Clare, Paul, Gerry, Julie, Eithne, Zenab, and Kate. Clare or "CSG" what can I say!! I've had so much fun working with you, thanks for all the help! Hope everything goes well for you in Sligo, you'll love it down (or even across) the country! Paul - The Karaoke King, thanks a mill for all (actually lots) the help you've given me, it's very much appreciated. I hope everything works out really well for you in Boston and if you get a chance to go to New York remember not to get the bus because it takes nearly 8 hours!! Gerry Dowd, it's been great working with you! Mayo abú!! Ye were unlucky last year Ger, but I reckon it's the Lillies for Sam this year! Julie my bay partner, I hope I haven't driven you mad; my music collection is a little repetitive, well so I'm told! Eithne can't believe you're off to Oz, I reckon there should be a lab outing there next year to visit you to make sure things are going well!

Thanks to all the members, past and present, of the West Bunker Lab! A special thanks must go to the mercaptoethanol bandit Mary Meehan. Without your help I'm sure I'd still be lost! Your help and guidance is very much appreciated. Sharkey (Dee), my fellow culchie, thanks for all the bits and bobs I borrowed, right then nicked!! I reckon I might owe yourself and Mary a couple of boxes of chocs as well!

Thanks to all those who have gone along the PhD trail with me - Alan, Blanca, Matt and Judy. Judy thanks ever so much for all your help with the broad curriculum-teaching course. It was a tough year but you definitely lightened the load - cheers! Thanks must also go to Fred, Jamie, Christopher, Ronan, Jenny, Sorcha and David for all those crazy nights out, place just won't be the same with ye guys gone!

A big thanks must also go to the members of the prep-room - Paddy, Joe, Ronan, Dave, Margaret, Fionnuala and Henry. Paddy thanks for always having a puncture repair kit on hand for the much trouble I've had with my bike over the last five years. If you have a spare set of brakes now that would be great!! I would also like to express my gratitude to the various members of my committee and to Prof. Tim

Foster, for giving me the opportunity to teach the broad curriculum course last year. Thanks also to the British society for Antimicrobial Chemotherapy for the financial support. I am also very grateful to Dr Neil McFerran in Queens University, Belfast for all the help and advise you have given me with regards to molecular modelling.

A special thanks goes to all my family and friends. Mossy you've been a top mate, thanks for all the lifts you've given me over the years to the train station, to the footie matches and so on. Been some tough times in the last few years so thanks for been there. Thanks to Mossys better half, Eithne, for use of the swimming pool and more so the Jacuzzi, was great for those stressful days. Thanks to all the lads, Mick, Maca, Rooster, Mooney, George, Leo and Trev, all great school friends who still give me so much grief over still been a student! Mam, I owe you so much, thanks for supporting me in college for all these years. I know times have been tough but I could have never got this far without you, thanks for all the encouragement. This thesis is for you and Dad.

Yvonne, you have been brilliant to me in more ways that you'll ever know. I am so grateful to you for your constant love, support and encouragement. Thank you for everything, I love you very much.

PUBLICATIONS ORIGINATING FROM THIS STUDY

Fennell, B. J., Carolan, S., Pettit, G. R., and Bell, A. 2003. Effects of the antimitotic natural product dolastatin 10, and related peptides, on the human malarial parasite *Plasmodium falciparum*. *J Antimicrob Chemother* **51**: 833-841.

Fennell, B. J., Naughton, J. A., Dempsey, E., and Bell, A. Cellular and molecular actions of dinitroaniline and phosphorothioamidate herbicides on *Plasmodium falciparum*: tubulin as a specific antimalarial target. *Manuscript in preparation*.

Dascombe, M. J., Bell, A., Drew, M. G. B., Bhatt, R., Fennell, B. J., and Ismail, F. M. D. Establishing structure-bioactivity relationships amongst potential dinitroaniline antimalarials active *in vitro* and *in vivo*. *Manuscript in preparation*.

TABLE OF CONTENTS

Declaration	ii
Summary	iii
Acknowledgements	vi
Publications originating from this study	viii
List of tables	xv
List of figures	xvi
Abbreviations	xix
Chapter 1: General Introduction	1
1.1. Malaria.....	1
1.1.1. Malaria: an introduction.....	1
1.1.2. Developmental cycle of <i>P. falciparum</i>	2
1.1.3. Intra-erythrocytic stages of <i>P. falciparum</i> development.....	3
1.1.4. Clinical symptoms of malaria infection.....	6
1.1.5. Malaria: control, treatment and prevention.....	7
1.1.6. Brief overview of promising antimalarial drugs and drug targets....	9
1.2. Tubulin and microtubules.....	10
1.2.1. Tubulin and microtubules: an introduction.....	10
1.2.2. Tubulin and microtubule structure.....	11
1.2.2.1. Structure of the tubulin heterodimer.....	11
1.2.2.2. Microtubule structure and dynamics.....	13
1.2.2.3. Microtubule nucleation.....	16
1.2.2.4. Cellular organisation of microtubules: general overview.....	16
1.2.3. Tubulin diversity.....	18
1.2.3.1. Tubulin isotypes.....	18
1.2.3.2. Post-translational modifications of tubulin.....	19
1.2.4. Tubulin/microtubule-drug interactions.....	21
1.2.4.1. Colchicine-site agents.....	21
1.2.4.2. “ <i>Vinca</i> ” domain agents.....	23
1.2.4.3. Taxol-site agents.....	24
1.2.4.4. Other agents.....	25

1.3.	Microtubules in <i>Plasmodium</i>	
1.3.1.	Tubulin: genes and proteins.....	26
1.3.2.	Functional classes of microtubules in <i>Plasmodium</i>	27
1.3.3.	Effects of microtubule inhibitors on <i>Plasmodium</i>	29
1.3.3.1.	Colchicine-site agents.....	30
1.3.3.2.	“ <i>Vinca</i> ” domain agents.....	30
1.3.3.3.	Taxol-site agents.....	31
1.3.3.4.	Other agents.....	32
1.4.	Project objectives.....	32
Chapter 2: Materials and Methods.....		34
2.1.	Chemicals, reagents and inhibitors.....	34
2.2.	Culture of <i>P. falciparum</i>	34
2.2.1.	Routine culture.....	34
2.2.2.	Gametocyte culture.....	35
2.2.3.	Synchronisation of cultures.....	35
2.2.4.	Harvesting of parasites.....	36
2.3.	Preparation of fractions of harvested parasites.....	37
2.3.1.	Preparation of whole cell extracts.....	37
2.3.2.	Isolation of RNA.....	37
2.4.	Assessment of antimalarial activity of microtubule inhibitors.....	38
2.4.1.	Inhibition of parasite proliferation assessed using the lactate dehydrogenase (pLDH) method.....	38
2.4.2.	Effects of inhibitors on synchronised cultures of different initial ages.....	39
2.4.3.	Effects of inhibitors on parasite morphology.....	39
2.4.4.	Activity of inhibitors on different developmental stages.....	40
2.4.5.	Effects of inhibitors on mitotic microtubular structures.....	40
2.5.	Cloning of <i>P. falciparum</i> α I- and β -tubulin genes.....	41
2.5.1.	Amplification of <i>P. falciparum</i> α I- and β -tubulin genes by reverse-transcriptase polymerase chain reaction (RT-PCR).....	41
2.5.2.	Visualisation of DNA by agarose gel electrophoresis.....	42
2.5.3.	Purification of PCR products.....	42
2.5.4.	Generation of pTrp2- β Tub.....	42

2.5.5.	Generation of pET11a- α Tub and pET11a- β Tub.....	43
2.5.6.	Generation of pMAL-c2X- α Tub and pMAL-c2X- β Tub.....	44
2.5.7.	Recovery of DNA by ethanol precipitation.....	44
2.5.8.	Preparation of competent <i>E. coli</i> cells.....	45
2.5.9.	Transformation of competent <i>E. coli</i> strains.....	45
2.5.10.	Screening of transformants.....	46
2.5.10.1.	Screening by small-scale plasmid isolation.....	46
2.5.10.2.	Rapid colony screening.....	47
2.5.10.3.	Screening by restriction endonuclease digestion.....	47
2.5.10.4.	Screening by PCR.....	48
2.6.	Protein quantification and analysis.....	48
2.6.1.	Quantification of protein concentration by Bradford assay.....	48
2.6.2.	SDS-polyacrylamide gel electrophoresis (SDS-PAGE).....	48
2.6.3.	Visualisation of protein samples on polyacrylamide gels.....	49
2.6.4.	Precipitation of protein with trichloroacetic acid (TCA).....	50
2.6.5.	Western Immunoblotting.....	50
2.6.6.	Stripping and re-probing PVDF membranes.....	51
2.7.	Recombinant tubulin production, purification and refolding.....	51
2.7.1.	Expression studies with pTrp2- β tub construct.....	51
2.7.2.	Expression studies with pET11a-tubulin constructs.....	52
2.7.3.	Determination of recombinant protein solubility.....	52
2.7.4.	<i>E. coli</i> cell lysis and purification of inclusion bodies containing recombinant protein.....	53
2.7.5.	Solubilisation of inclusion bodies and renaturation of tubulin.....	53
2.7.6.	Expression studies with pMAL-c2X-tubulin constructs.....	54
2.7.7.	Amylose affinity chromatography.....	55
2.7.8.	Ion-exchange chromatography.....	55
2.7.9.	Purification of antibodies specific to <i>P. falciparum</i> tubulins.....	55
2.8.	Functional analysis of recombinant <i>P. falciparum</i> tubulins.....	56
2.8.1.	Tubulin co-sedimentation assay.....	56
2.8.1.1.	Sedimentation of bovine brain tubulin alone.....	56
2.8.1.2.	Sedimentation of bovine brain tubulin in the presence of other proteins.....	58

2.8.1.3.	Sedimentation of recombinant MBP- α I- and MBP- β - tubulin fusions combined.....	58
2.8.2.	Turbidimetric assay of microtubule polymerisation.....	58
2.9.	Stage-dependent production and electrophoretic behaviour of tubulins in <i>P. falciparum</i>	59
2.9.1.	Investigation of the “ α / β inversion” of <i>P. falciparum</i> tubulins.....	59
2.9.2.	Stage-specific expression and quantitation of <i>P. falciparum</i> α I- and β -tubulin during the intra-erythrocytic cycle.....	60
2.9.3.	Investigation of α II-tubulin expression in asexual stages of <i>P. falciparum</i> erythrocytic development.....	60
2.10.	Investigation of the dinitroaniline binding site on <i>P. falciparum</i> tubulins....	61
2.10.1.	Investigation of interaction of [¹⁴ C] trifluralin with recombinant <i>P.</i> <i>falciparum</i> tubulin fusion proteins.....	61
2.10.2.	Sequence alignments.....	62
2.10.3.	Molecular modeling of <i>P. falciparum</i> tubulins.....	62
2.10.4.	Identification of a putative trifluralin-binding site.....	63

Chapter 3: Antimalarial Activity and Mechanisms of Action of the

	Dolastatin / Auristatin Family of Compounds.....	65
3.1.	Introduction.....	65
3.2.	Results.....	66
3.2.1.	Growth inhibition of cultured <i>P. falciparum</i> by microtubule inhibitors.....	66
3.2.1.1.	Dolastatin 10.....	66
3.2.1.2.	Auristatins.....	67
3.2.2.	Stage-specific sensitivities of <i>P. falciparum</i> to microtubule inhibitors.....	68
3.2.3.	Effects of inhibitors on parasite maturation and morphology.....	69
3.2.4.	Stage-dependent susceptibility and inhibitor reversibility studies....	70
3.2.5.	Effects of inhibitors on mitotic microtubular structures.....	70
3.3.	Discussion.....	72

Chapter 4: Recombinant Expression, Purification and Functional Analysis

	of <i>P. falciparum</i> Tubulins.....	78
4.1.	Introduction.....	78
4.2.	Results.....	79
4.2.1.	Amplification of <i>P. falciparum</i> α I- and β -tubulin genes.....	79
4.2.2.	Recombinant production of <i>P. falciparum</i> α I- and β -tubulin.....	80
4.2.2.1.	Generation of β -tubulin using pTrp2.....	80
4.2.2.2.	Generation of α I-tubulin and β -tubulin using pET11a.....	82
4.2.2.3.	Generation of MBP- α I-tubulin and MBP- β -tubulin.....	84
4.2.3.	Functional analysis of <i>P. falciparum</i> recombinant tubulins.....	86
4.2.3.1.	Turbidimetric assay of the polymerisation of recombinant tubulin monomers.....	86
4.2.3.2.	Co-polymerisation studies of recombinant tubulins with bovine brain tubulin as assessed by sedimentation assay....	87
4.3.	Discussion.....	90

Chapter 5: Stage-Dependent Production and Electrophoretic Behaviour

	of Tubulins in <i>P. falciparum</i>.....	96
5.1.	Introduction.....	96
5.2.	Results.....	97
5.2.1.	Quantification of α I- and β -tubulin expression in asexual erythrocytic stages of <i>P. falciparum</i> development.....	97
5.2.2.	Analysis of α II-tubulin expression in <i>P. falciparum</i> asexual stages.....	98
5.2.3.	Investigation of the α/β -inversion of <i>P. falciparum</i> recombinant and native tubulins.....	99
5.3.	Discussion.....	100

Chapter 6: Antimalarial Activity and Mechanisms of Action of

	Dinitroaniline and Phosphorothioamidate Herbicides.....	105
6.1.	Introduction.....	105
6.2.	Results.....	106

6.2.1.	Growth inhibition of cultured <i>P. falciparum</i> by antimitotic herbicides.....	106
6.2.1.1.	Dinitroanilines.....	106
6.2.1.2.	Phosphorothioamidate and <i>N</i> -phenyl carbamate herbicides.....	106
6.2.2.	Effects of herbicides on mitotic microtubular structures.....	107
6.2.3.	Investigation of the interaction of [¹⁴ C] trifluralin with recombinant <i>P. falciparum</i> tubulin fusion proteins.....	108
6.2.4.	Investigation of the dinitroaniline binding site(s) on <i>P. falciparum</i> tubulins.....	109
6.2.4.1.	Sequence alignments.....	109
6.2.4.2.	Homology modeling of <i>P. falciparum</i> tubulins.....	110
6.2.4.3.	Identification of a possible trifluralin-binding cavity.....	111
6.3.	Discussion.....	112
Chapter 7: General Discussion.....		119
7.1.	Effects of Microtubule Inhibitors on <i>P. falciparum</i>	119
7.2.	Tubulins of <i>P. falciparum</i>	121
7.3.	<i>Plasmodium falciparum</i> tubulin as a chemotherapeutic target: future directions.....	122
References.....		128

List of Tables

	Following Page
1.1. Targets for new and existing antimalarial compounds.....	8
2.1. Standard Broad Range molecular weight protein markers.....	49
2.2. Prestained Broad Range molecular weight protein markers.....	49
2.3. Tubulin sequences used in alignment studies.....	62
3.1. Inhibitory effects on growth of <i>P. falciparum</i> and mammalian cells (various lines) by dolastatin 10 and derivatives.....	66
3.2. Susceptibilities of synchronous cultures of different initial ages upon 48 h exposure to inhibitors.....	68
3.3. Quantitative analysis of effects of inhibitors on mitotic microtubular structures.....	71
4.1. Overview of approaches previously used to produce recombinant tubulins in <i>E. coli</i>	79
4.2. Plasmid constructs used in this study.....	80
4.3. Comparative codon usage for particular codons by <i>E. coli</i> and <i>P. falciparum</i>	81
6.1. Inhibitory effects on growth of <i>P. falciparum</i> by dinitroaniline herbicides and derivatives.....	106
6.2. Quantitative analysis of effects of inhibitors on mitotic microtubular structures.....	108

List of Figures

	Following Page
1.1. Worldwide incidence of malaria in 2003.....	1
1.2. Developmental cycle of <i>Plasmodium falciparum</i>	2
1.3. Ribbon diagram of the crystal structure of the α/β -tubulin dimer.....	12
1.4. Schematic diagram of microtubule formation and structure.....	13
1.5. Microtubule nucleation, assembly and depolymerisation.....	15
1.6. Current model of microtubule structure at atomic resolution.....	15
1.7. Highly schematic diagram of the organisation of microtubule containing structures in a simple eukaryotic cell.....	17
1.8. Ribbon diagram of two tubulin heterodimers complexed with colchicine and RB3-SLD.....	22
3.1. Susceptibilities of asynchronous cultures to GRP18290 and auristatin PE as measured by the pLDH method.....	67
3.2. Chemical structures of vinblastine and Taxol.....	67
3.3. Development of parasites in the presence of inhibitors.....	69
3.4. Effects of microtubule inhibitors on different developmental stages.....	70
3.5. Mitotic microtubular structures of cultured parasites viewed by immuno- fluorescence using antibodies to <i>P. falciparum</i> β -tubulin and DAPI nuclear stain.....	71
3.6. Proposed model for typical biphasic dose-response curves observed after 48 h treatment of asynchronous cultures of <i>P. falciparum</i> with dolastatin 10 and auristatin PE.....	73
3.7. Proposed + end binding site for dolastatin 10 on mammalian β -tubulin.....	76
4.1. Nucleotide sequence of the α I-tubulin gene of <i>P. falciparum</i> K1/Thailand and its derived amino acid sequence.....	79
4.2. Nucleotide sequence of the β -tubulin gene of <i>P. falciparum</i> K1/Thailand and its derived amino acid sequence.....	79
4.3. Amplification of <i>P. falciparum</i> α I- and β -tubulin cDNA.....	79
4.4. Analysis of the clone pTrp2- β Tub.....	80
4.5. Analysis of production of β -tubulin from <i>E. coli</i> containing the pTrp2- β Tub plasmid.....	80
4.6. Effect of the RIG plasmid on overproduction of β -tubulin.....	82

4.7.	Cloning of <i>P. falciparum</i> tubulin genes into the expression vector pET11a.....	82
4.8.	Analysis of the clone pET11a- α ITub.....	83
4.9.	Expression of <i>P. falciparum</i> α I- and β - tubulin in <i>E. coli</i>	83
4.10.	Purification of <i>P. falciparum</i> α I- and β - tubulin overexpressed in <i>E. coli</i>	83
4.11.	Recombinant production and purification of <i>P. falciparum</i> α I- and β - tubulins as MBP-fusion proteins under optimised conditions.....	85
4.12.	Turbidimetric analysis of bovine brain tubulin and recombinant <i>P. falciparum</i> tubulin polymerisation.....	86
4.13.	Analysis of bovine brain tubulin polymerisation by the sedimentation assay.....	88
4.14.	Analysis of the dose-dependent co-polymerisation of MBP- α I-tubulin with bovine brain tubulin.....	88
4.15.	Analysis of the dose-dependent co-polymerisation of BSA with bovine brain tubulin.....	89
4.16.	Analysis of the dose-dependent co-polymerisation of MBP with bovine brain tubulin.....	89
4.17.	Analysis of the dose-dependent co-polymerisation of MBP- β -tubulin with bovine brain tubulin.....	89
5.1.	Stage-specific quantitation of <i>P. falciparum</i> α I- and β -tubulin expression during the asexual erythrocytic cycle.....	97
5.2.	The transcription profile of α I- and β -tubulin genes in the development cycle of <i>P. falciparum</i> as determined by the Scripps/GNF malaria array.....	97
5.3.	Analysis of α II-tubulin expression at the mRNA level and protein level in asexual stages of <i>P. falciparum</i>	98
5.4.	pH effects on tubulin separation in high-grade SDS-PAGE.....	100
5.5.	pH effects on tubulin separation in low-grade SDS-PAGE.....	100
5.6.	Tubulin diversity in <i>P. falciparum</i> , plants and various protist organisms....	102
6.1.	Chemical structures of oryzalin, trifluralin, RBO48, amiprofos-methyl and chloroprotham.....	105
6.2.	Inhibition of the growth of <i>P. falciparum</i> in culture by the phosphorothioamidate herbicide amiprofos-methyl.....	107

6.3.	Mitotic microtubular structures of cultured parasites viewed by immunofluorescence using antibodies to <i>P. falciparum</i> β -tubulin and DAPI nuclear stain.....	107
6.4.	Assay of [^{14}C]trifluralin binding to recombinant <i>P. falciparum</i> tubulin fusion proteins.....	108
6.5.	Assay of [^{14}C]trifluralin binding to maltose binding protein (MBP) and bovine brain tubulin.....	109
6.6.	Comparison of the amino acid sequences of the α -tubulins of dinitroaniline-sensitive plants.....	109
6.7.	Comparison of the amino acid sequences of the β -tubulins of dinitroaniline-sensitive plants.....	109
6.8.	Comparison of the amino acid sequences of the α -tubulins of dinitroaniline-insensitive mammals.....	109
6.9.	Comparison of the amino acid sequences of the β -tubulins of dinitroaniline-insensitive mammals.....	109
6.10.	Alignment of representative plant [<i>E. indica</i> (<i>Ei</i> 1)] and animal [<i>S. scrofa</i> (<i>Ss</i> 1)] α -tubulin amino acid sequences with those of <i>P. falciparum</i> (<i>Pf</i> 1).....	110
6.11.	Alignment of representative plant [<i>A. thaliana</i> (<i>At</i> 2)] and animal [<i>S. scrofa</i> (<i>Ss</i> 1)] β -tubulin amino acid sequences with those of <i>P. falciparum</i> (<i>Pf</i>).....	110
6.12.	Ribbon diagram of the proposed structure of α I/ β -tubulin heterodimer of <i>P. falciparum</i> obtained by homology modelling.....	110
6.13.	Spatial distribution and location of amino acid positions where <i>P. falciparum</i> and various plants differ from mammalian tubulins.....	111
6.14.	Potential binding site for the dinitroaniline trifluralin in modelled <i>P. falciparum</i> α I-tubulin.....	111

Abbreviations

A.....	absorbance
APAD.....	3-acetyl pyridine adenine dinucleotide
APS.....	ammonium persulfate
bp.....	base pair(s)
BSA.....	bovine serum albumin
cDNA.....	complementary deoxyribonucleic acid
ddH ₂ O.....	deionised water
dpm.....	disintegrations per minute
DMSO.....	dimethylsulphoxide
DTNB.....	5, 5'-dithio-bis(2-nitrobenzoic acid)
DTT.....	dithiothreitol
DV.....	digestive vacuole
EDTA.....	ethylenediaminetetraacetic acid
EGTA.....	etheleneglycolbis(aminoethyl)- tetra-acetic acid
IC ₅₀	median inhibitory concentration
kbp.....	kilobase pair
LDH.....	lactate dehydrogenase
MBP.....	maltose binding protein
MCS.....	multiple cloning site
min.....	minute(s)
NBT.....	nitroblue tetrazolium
PAGE.....	polyacrylamide gel electrophoresis
PBS.....	phosphate buffered saline
PCR.....	polymerase chain reaction
PES.....	phenazine ethosulphate
pLDH.....	parasite lactate dehydrogenase
PMSF.....	phenylmethylsulphonyl fluoride
PVDF.....	polyvinylidene fluoride
rpm.....	revolutions per minute

RT-PCR.....	reverse transcriptase polymerase chain reaction
SDS.....	sodium dodecyl sulphate
SDS-PAGE.....	sodium dodecyl sulphate- polyacrylamide gel electrophoresis
SEM.....	standard error of the mean
SSC.....	saline sodium citrate
TAE.....	tris-acetate-EDTA
TCA.....	trichloroacetic acid
TE.....	tris-EDTA
TEMED.....	N, N, N', N'-tetramethyl- ethylenediamine
Tris.....	tris(hydroxymethyl)aminomethane
TVM.....	tubovesicular membrane
UV.....	ultraviolet

Chapter 1

General Introduction

1.1. MALARIA

1.1.1. Malaria: an introduction

Malaria is one of the most prevalent human infections worldwide and probably kills more people than any other communicable disease apart from tuberculosis and HIV infection (Sachs *et al*, 2002). Once endemic in North America, Europe and Russia, it is now confined to regions that experience more tropical and subtropical climates such as parts of Asia and Central and South America. However, the greatest burden of malaria is borne by sub-Saharan Africa where an estimated 90% of global malaria occurs (Breman *et al*, 2004) (Fig 1.1). In such endemic regions, malaria is a significant cause of morbidity and mortality and imposes enormous social and economic burdens. An estimated 300 - 500 million clinical cases of malaria occur every year with 1.5 - 2.7 million deaths, mostly of children under the age of five, attributable to this disease (Suh *et al*, 2004). In recent years, the burden of this disease and death has increased significantly in malaria-endemic countries, and transmission has spread to new areas, in particular to central Asia (Moorthy *et al*, 2004). The major causes of this resurgence are global climate and environmental change, the development of resistance to affordable antimalarial drugs and insecticides, war and civil disturbance, increasing human migration, and deterioration of health services and national control programmes. With 41% of the world's population now at risk of malaria and with worldwide cases expected to exceed 2 billion by 2010 (Breman, 2001), efforts towards controlling this debilitating disease are urgently required.

Malaria is caused by protozoan parasites of the genus *Plasmodium*. There are nearly 120 species of *Plasmodium* of which four are known to cause malaria in humans, namely *P. falciparum*, *P. vivax*, *P. malariae* and *P. ovale* (López-Antuñano *et al*, 1992). These four species are obligate intracellular parasites whose developmental cycle occurs in two host organisms: humans and mosquitoes. There are approximately 60 different species of mosquito belonging to the genus *Anopheles* that can transmit the parasites to humans (News, 2002). The most notorious of these mosquitoes is *Anopheles gambiae*, which is native to Africa and is one of the most efficient malaria vectors in the world. Although mosquitoes are found in most countries, *Anopheles* predominates mostly in the tropics at low elevations, thereby largely restricting transmission of malaria to these regions.

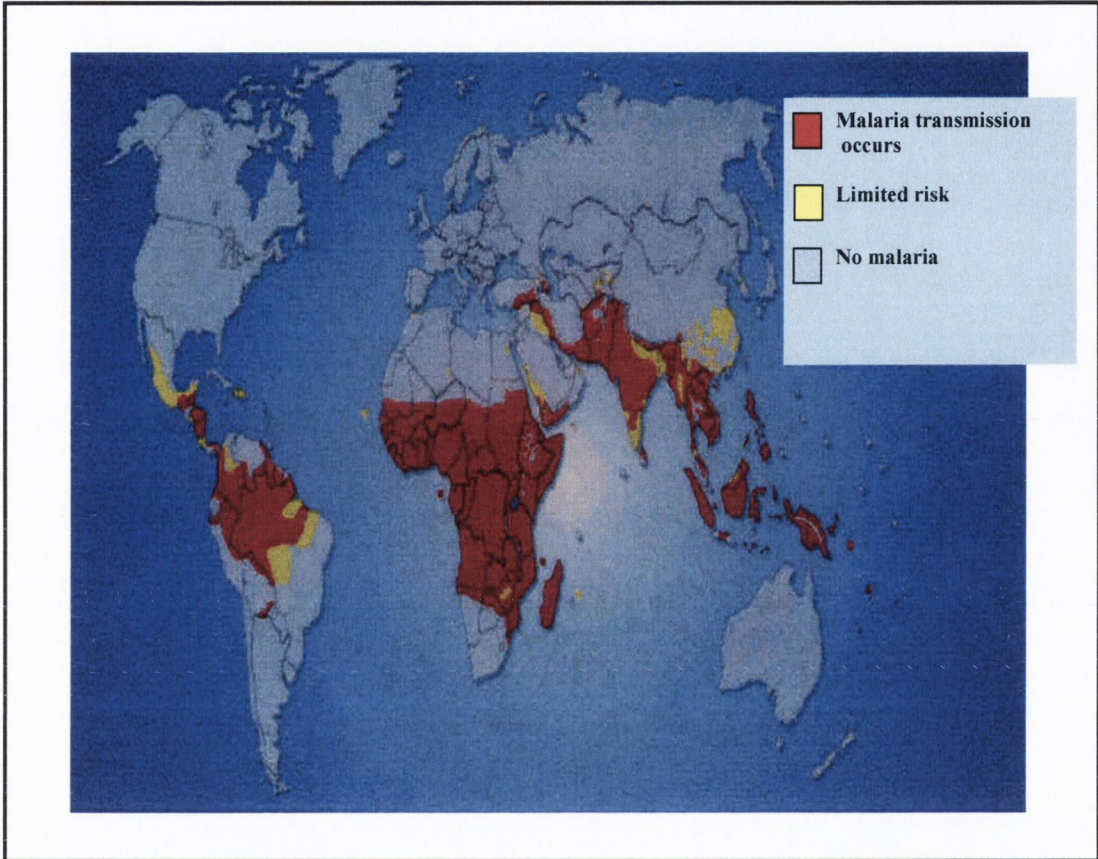


Figure 1.1. Worldwide incidence of malaria in 2003 (adapted from Greenwood, 2004).

1.1.2. Developmental cycle of *P. falciparum*

The developmental cycle of all species of human malaria is effectively the same (Fig. 1.2). However, from hereon, only *P. falciparum* will be described, as it is the most significant of the four *Plasmodium* species that infect man, causing most malaria-related deaths, and is the subject of this thesis. The developmental cycle of *P. falciparum* involves numerous cellular differentiations and nuclear divisions and is one of the most intricate of any human infection. The cycle can be divided into two stages: a sexual phase mainly within an invertebrate host, the *Anopheles* mosquito and an asexual phase within the vertebrate host, humans. In addition, the latter stage can be subdivided into the liver phase and the intra-erythrocytic phase of parasite development.

The cycle commences when an infected female anopheline mosquito requiring a blood meal for egg production bites a human host and inadvertently injects 5 - 20 sporozites (Rosenberg *et al*, 1990) into the tissue or bloodstream of the individual. The sporozites migrate quickly from the site of the bite via the bloodstream to the liver, where they invade hepatocytes and develop to become schizonts, a process known as exoerythrocytic schizogony. Rupture of the hepatocytes releases 20,000 - 30,000 merozoites per original sporozoite into the bloodstream, from which they disseminate systemically. Each merozoite that is not engulfed by phagocytic cells may invade an erythrocyte and develop by one of two distinct developmental pathways. The asexual pathway entails parasite growth and asexual multiplication, with the production of up to 24 merozoites, a process known as erythrocytic schizogony. Lysis of the erythrocyte by a protease-dependent process releases merozoites for a brief extracellular phase until they re-invade new erythrocytes and re-initiate the asexual, intra-erythrocytic stage. Alternatively, some merozoites initiate the sexual pathway by differentiating into micro- (male) or macro- (female) gametocytes within the erythrocyte. Ingestion of erythrocytes containing gametocytes by another anopheline mosquito results in the re-initiation of the insect stage of parasite development. On entering the midgut of the insect, the macrogametocyte escapes from the erythrocyte to form a macrogamete. At the same time, the microgametocyte divides rapidly by mitosis three times to produce flagellated microgametes, which are released from the parent cell and move quickly away to fertilise a macrogamete. This results in the formation of a zygote, which in turn develops into a motile ookinete that penetrates the mosquito gut wall and settles

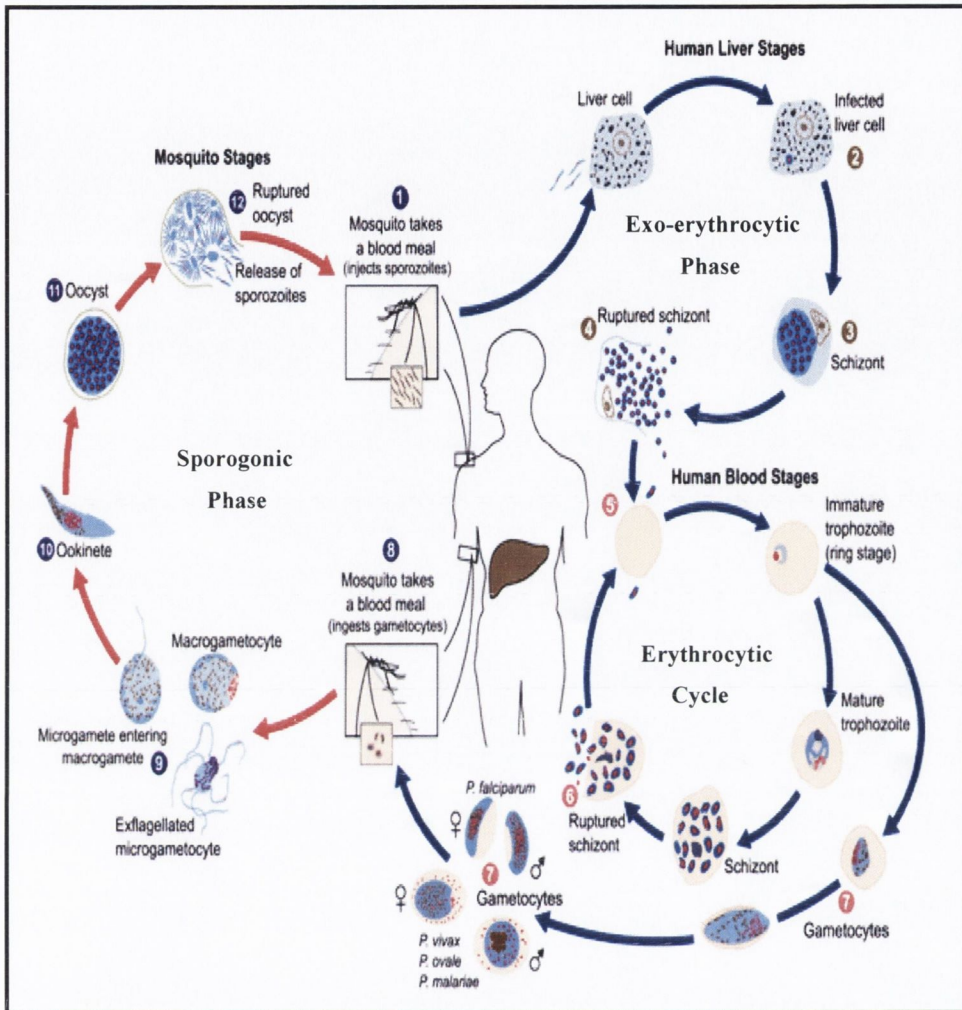


Figure 1.2. Development cycle of *Plasmodium falciparum*. Obtained from http://www.dpd.cdc.gov/dpdx/HTML/ImageLibrary/Malaria_il.htm

beneath the elastic outer membrane covering the gut. Here it grows into an oocyst with a thin cell wall. The oocyst matures and undergoes nuclear division to produce thousands of sporozoites. Rupture of the oocyst releases the sporozoites into the mosquito gut, from where they migrate to the salivary glands of the mosquito. Hence, when the mosquito feeds on its next bloodmeal, the sporozoites are transmitted into the human host and so begins a new cycle of infection.

Approaches to malaria control have focused on numerous points of the parasite's developmental cycle. However, the majority of drugs in use today, except for primaquine, are effective on blood-stage parasites (Bell, 2000). This is probably due to the fact that the parasite's intra-erythrocytic stage is the easiest to maintain in culture and most clinical symptoms of malaria are related to this stage. Given the likelihood that antimalarial agents will continue to be developed against blood-stage parasites (Fidock *et al*, 2004), a clear understanding of the underlying biology and development of the parasite within the erythrocyte is essential for the success of such drug-development projects.

1.1.3. Intra-erythrocytic stages of *P. falciparum* development

The invasion of human erythrocytes by the extracellular merozoite form of *P. falciparum* is a process fundamental to the pathogenesis of this devastating parasite. It is an intricate process that is highly dependent on the ability of the merozoite to select and adhere to a fresh erythrocyte and to subsequently enter and seal itself inside. The involvement of, and interactions between, both parasite and host proteins are essential to this process. Although the merozoite is very small (~ 1.6 μM long and ~1.0 μM wide) (Bannister *et al*, 2000) it contains all the necessary tools to escape from the remnants of its host erythrocyte and to establish itself in a new erythrocyte.

The process of invasion initially involves adherence of the merozoite to an erythrocyte by means of its bristly coat. The merozoite then manages to align its apical end with the erythrocyte to form a tight junction between the two cells (Bannister *et al*, 2003). A number of proteins such as merozoite surface proteins (MSPs) (Cowman *et al*, 2002) are believed to play a role in the initial capture of the erythrocyte and have now become leading candidates for the development of a blood-stage vaccine (Moorthy *et al*, 2004). The formation of the apical junction triggers the development of a deep membrane-lined cavity within the erythrocytic

surface known as the parasitophorous vacuole (PV). Key to its formation are the discharges from three sets of secretory vesicles, namely the rhoptries, micronemes and dense granules, located at the apex of the merozoite (Bannister *et al*, 2000). As the invasion cavity begins to form, the merozoite begins to glide into it, propelled by an actin-myosin motor (Pinder *et al*, 2000). Movement of the merozoite into the PV results in the removal of the bristly coat and most of the merozoite surface protein-1 (MSP-1). Once enclosed in the erythrocyte, the merozoite discharges the contents of the dense granules into the PV at various points around its boundary (Culvenor *et al*, 1991). Examples of molecules secreted include ring membrane antigen (RIMA) (Trager *et al*, 1992) and ring-infected erythrocyte surface antigen (RESA) (Culvenor *et al*, 1991) which result in the enlargement of the PV presumably to create space for the growth of the parasite. As the merozoite matures, the invasion related-structures are destroyed, the parasite spreads itself into a disc-like structure called the ring stage and active feeding commences.

The ring stage encompasses approximately the first 16 hours of intra-erythrocytic parasite growth. During this time, the parasite feeds on portions of the surrounding erythrocyte cytoplasm, through a dense ring at the surface of the parasite, known as the cytostome. Haemoglobin, the major protein of the erythrocyte cytosol (Banerjee *et al*, 2001) is degraded in a specialised lysosome-like organelle known as the digestive vacuole (DV) into its constituent amino acids and cytotoxic haem. As the parasite lacks the enzymes to degrade haem it sequesters it by a parasite-specific aggregation process resulting in an inert, insoluble crystal form, called haemozoin or malaria pigment (Senge *et al*, 2000). The process of haem detoxification is essential for intra-erythrocytic parasite development and several antimalarial drugs such as chloroquine are believed to act by interfering with the process of haemozoin formation.

As the ring grows, a corresponding increase in the area of the surrounding PV occurs and extends narrow finger-like projections, the tubovesicular membranes (TVM), into the periphery of the erythrocyte (Halder *et al*, 2001). While the functions of this organelle remain to be resolved, it is believed to aid parasite uptake of nutrients from the host cell. In addition, a number of ring-specific molecules are synthesised and exported into the erythrocyte to facilitate modification of the erythrocyte membrane (Das *et al*, 1994). Such alterations allow infected host cells to adhere to non-infected erythrocytes, a process known as rosetting, or to parasitised

erythrocytes, a process known as auto-agglutination. The ring eventually grows into the more metabolically-active trophozoite stage, which covers approximately the next 20 hours of intra-erythrocytic development of the parasite.

Unlike ring-stage parasites, which can be found circulating in the bloodstream, trophozoites adhere to the endothelial cells of blood vessels (Miller *et al*, 2002). To facilitate this linkage the trophozoite secretes a number of molecules such as erythrocyte membrane protein 1 (PfEMP1) that penetrate the host cell surface and mediate binding to the endothelial cell (Bannister *et al*, 2003). Other exported molecules induce membrane and cytoskeletal components of the erythrocyte to rearrange into small knobs that increase the selective adhesiveness of the parasitised host cell membrane. Adherence of the trophozoite-infected erythrocyte is central to its protection from destruction, as non-adherent parasitised erythrocytes are cleared by the spleen, whose function is to remove old and damaged erythrocytes from the circulatory system. In addition to the intra-erythrocytic location of the parasite, antigenic variation of PfEMP1 together with the variety of proteins used for erythrocyte adherence allows the parasite to outwit the vast array of protective components of the host immune system.

As the trophozoite continues to feed on haemoglobin it increases in size and the malaria pigment becomes more prominent. Other exported molecules increase erythrocytic permeability to nutrients and generate flat membrane-bound structures termed Maurer's clefts within the cytosol of the erythrocyte, which are proposed to play a role in protein-trafficking (Das *et al*, 1994). In the late trophozoite stage, the parasite initiates DNA synthesis and begins erythrocytic schizogony, while still adhering to the blood vessel wall. This involves a series of nuclear divisions to produce about 16 nuclei, although sometimes more are found in a singly-infected erythrocyte, indicating the rather relaxed nature of nuclear division in the schizont (Bannister, 2000). Nuclear division is accompanied by numerous cytosolic changes in preparation for merozoite formation. Partitioning of the nuclei, cytoplasm and organelles results in the formation of up to 24 merozoites and the parasite is now termed a segmenter. Finally, the erythrocytic membrane and the PV membrane lyse and the released merozoites proceed to find and invade new erythrocytes.

The asexual intra-erythrocytic cycle of *P. falciparum* occurs over a 48-hour time period and is the phase of the parasite's development cycle responsible for the clinical manifestations of malaria in humans. While much information has been

gleamed on the molecular and cellular events during this cycle, many unanswered questions remain with particular regard to signalling pathways that trigger erythrocyte invasion and the diversion from the asexual to the sexual stages. The release of the *P. falciparum* genome sequence (Gardner *et al*, 2002) should prove to be a major aid in increasing our knowledge of the intricate biology and pathogenesis of this unique unicellular organism.

1.1.4. Clinical symptoms of malaria infection

The diverse symptoms of malaria are exclusively associated with the parasite's asexual intra-erythrocytic stage of development and can range from a mild headache to anaemia or even death. One of the most common features of this disease is fever, which usually occurs every 48 hours in accordance with the release of merozoites from infected erythrocytes. Malarial fever is characterised by a feeling of intense chills and a period of drenching sweats. The cessation of fever usually indicates that merogony (i.e. release of merozoites) is complete. Additional symptoms may also include headaches and vomiting. While fever causes untold suffering to millions of victims, malaria-induced anaemia causes more deaths than any other manifestation of this disease (Breman *et al*, 2004). Anaemia results from both parasite-induced lysis of host erythrocytes and the removal of infected and damaged erythrocytes by the spleen. As a result, the spleen becomes enlarged and swollen and this process is known as splenomegaly.

The clinical outcome of malarial infection depends on many parasitic, host, and social factors, most notably the age and immune status of the individual, the multiplication rate of the parasite, the proportion of infected erythrocytes (i.e. parasitemia) and the drug resistance status of the parasite. At highest risk of infection are children, pregnant women and non-immune people who live in endemic regions. Given the right conditions, the clinical outcome can progress to “severe” malaria, a disorder that affects several tissues and organs. The cytoadherence mechanisms of *P. falciparum* infected erythrocytes as outlined in section 1.1.3 play a pivotal role in this progression. Accumulation of parasitised and non-parasitised erythrocytes by autoagglutination and rosetting can obstruct blood flow and allow the parasites to sequester themselves in the circulatory systems of various organs including lung, brain, liver, kidney and placenta. This facilitates one of the most serious complications of the disease, cerebral malaria, manifested by altered levels of

consciousness, seizures, hearing and neurological damage (Clark *et al*, 2000). Other major malaria-induced complications include respiratory distress, hypoglycaemia, bacterial infection, low birth-weight and impaired growth and development. “Severe” malaria typically occurs with a parasitemia of 5% or more, and even with optimal clinical management, the mortality rate still surpasses 20% (Suh *et al*, 2004).

1.1.5. Malaria: control, treatment and prevention

During the mid-twentieth century, the World Health Organisation (WHO) made significant progress in its efforts to eradicate malaria from numerous countries, but this momentum slowed with the appearance of mosquitoes resistant to DDT and with public health concerns pertaining to insecticide use. Since then prospects for antimalarial chemotherapy have also become increasingly bleak owing to growing parasite resistance to the most widely used antimalarial drugs, namely chloroquine and the combination of sulphadoxine and pyrimethamine. To make matters worse efforts to develop new antimalarials have had a significant setback by the decision of some major pharmaceutical companies to pull out of the antimalarial research and development field (Butler *et al*, 1997).

However, in these challenging times the outlook for malaria treatment and prevention is better than it has been for decades. Poor countries now have access to increasingly large sums of money for malaria prevention obtained from international organisations such as the Global Fund and from donors such as the Bill and Melinda Gates Foundation (Greenwood, 2004). The development of new antimalarials is now more promising primarily due to public-private partnerships involving organisations such as Medicines for Malaria Venture (MMV) and Multilateral Initiative on Malaria. For example, LapdapTM (a combination of existing compounds, chlorproguanil and dapsone) is effective against malaria in areas where other therapies have encountered resistance and resulted from collaboration between Glaxo SmithKline and the WHO Special Programme for Research and Training in Tropical Diseases (TDR) (Ridley *et al*, 2004). In addition, advances in malarial genetics coupled with the recent sequencing of the *P. falciparum* genome (Gardner *et al*, 2002) should facilitate the identification and validation of potential new parasite drug targets, offering hope for the development of novel and affordable drugs.

The likelihood of developing antimalarials of therapeutic value stems from the success of chloroquine, one of the oldest and most recognised antimalarial agents.

In the 1940's, the use of chloroquine, a synthetic derivative of quinine (an alkaloid derived from the bark of the cinchona tree: Meshnick *et al*, 2001) led to marked reductions in morbidity and mortality across the Americas, Africa, Asia and Oceania. However, such immense worldwide use was followed some years later by the first reports of chloroquine-resistant strains of *P. falciparum*. Today, chloroquine resistance has spread to the vast majority of malaria-endemic areas including much of sub-Saharan Africa and South-East Asia, rendering this drug increasingly ineffective. Mefloquine and halofantrine are structurally-related drugs that are active against most chloroquine-resistant strains, but resistance has also developed to both of these drugs (Wellems *et al*, 2001) meaning that, for the first time in nearly 300 years, we are at risk of having no effective quinolines for use in the fight against malaria.

The replacement of chloroquine for clinical therapy of malaria has already begun in many regions, in particular in Southeast Asia and parts of South America. However, chloroquine remains the first-line therapy for falciparum malaria in much of Africa despite a high prevalence of resistant parasites. Some of the reasons for this can be gleaned from Table 1.1 (modified from Fidock *et al*, 2004) where it can be seen that few therapies currently exist for the successful clinical treatment of malaria. Of these, resistance has already developed to sulfadoxine, pyrimethamine, proguanil and the previously mentioned quinolines. Resistance to such compounds arises for numerous reasons including their over-use, their lack of chemical diversity, the limited range of targets on which they exert their actions and of course the evolution of spontaneous mutations in parasite genomes that confer the resistance. Therefore, to combat malaria, new drugs and drug combinations are urgently needed.

Multiple approaches to the identification of new antimalarials are being pursued. These include (i) the optimisation of existing drugs by chemical modification, (ii) use of new combination therapies (e.g. lumefantrine and artemether), (iii) development of natural-product-derived compounds such as the artemisinins, (iv) use of agents earmarked for other diseases (e.g. folate inhibitors developed as antibacterials were later found to be antimalarial (Ridley, 2002)) and (v) detection of new targets and the subsequent discovery of agents that act on these targets. In terms of the last approach, much progress is being made (Table 1.1: see column on new compounds) suggesting that safe and affordable new drugs to counter the spread of malaria parasites that are resistant to existing agents may soon be

Table 1.1. Targets for new and existing antimalarial compounds.

Target location	Pathway/mechanism	Target molecule	Established compounds	Advantages	Disadvantages	New compounds
Cytosol	Folate metabolism	Dihydrofolate reductase	Pyrimethamine	Low cost	Resistance	Chlorproguanil
		Dihydropteroate synthase	Proguanil	Low cost	Low efficacy	
	Glycolysis	Thymidylate synthase	Sulphadoxine	Low cost	Resistance	5-fluoroorotate
		Lactate dehydrogenase	Dapsone	Low cost	Low efficacy	Gossypol derivatives
Glutathione Metabolism	Signal transduction	Glutathione reductase				Enzyme inhibitors
		Protein kinases				Oxindole derivatives
	Unknown	Ca ²⁺ -ATPase	Artemisinins	Rapid action	Recrudescence	
Parasite membrane	Phospholipid synthesis	Choline transporter				G25
	Membrane transport	Unique channels				Dinucleoside dimers
Food vacuole	Haem polymerisation	Haemozoin	Chloroquine	Low cost; prophylactic use	Resistance	New quinolines
	Haemoglobin hydrolysis	Plasmepsins Falcipains				Protease inhibitors Protease inhibitors
Mitochondrion	Electron transport	Cytochrome <i>c</i> oxidoreductase	Atovaquone	Low toxicity	High cost; Recrudescence	
Apicoplast	Protein synthesis	Apicoplast ribosome	Tetracyclines	Low cost	Slow to act	
	Transcription	RNA polymerase	Rifampicin	Suitable for young children and pregnant women	High cost	
	Isoprenoid synthesis	DOXP reductoisomerase				Fosmidomycin
	Protein farnesylation	Farnesyl transferase				Peptidomimetics
Extracellular	Erythrocyte invasion	Subtilisin serine proteases				Protease inhibitors

DOXP: 1-deoxy-D-zylulose 5-phosphate

Modified from Fidock *et al* (2004).

realised. The importance of developing new antimalarials is further emphasised by the current absence of an effective vaccine against malaria and the extensive spread of insecticide resistance among the *Anopheles* mosquitoes.

1.1.6. Brief overview of promising antimalarial drugs and drug targets

Although it is not possible to discuss all the targets that are presenting themselves for malaria drug discovery, several would appear to be quite promising, particularly those located within the apicoplast and food vacuole.

The apicoplast or plastid is an organelle believed to have been acquired during the course of evolution through the endosymbiosis of a unicellular alga (Clough *et al*, 2001). It contains a 35-kilobase genome that encodes elements of a prokaryotic transcription and translation system believed to be the target of antibiotics such as the tetracyclines. Although such antibiotics inhibit *P. falciparum*, their actions are slow. However, recent advances such as the completion of the *P. falciparum* genome sequence (Gardner *et al*, 2002) have facilitated the discovery of several key metabolic pathways in the plastid, the disruption of which results in a more rapid cell death. For example, thiolactomycin inhibits *P. falciparum* growth by interfering with the Type II fatty acid biosynthesis pathway, which is also found in plants and bacteria (Ridley, 2002). This inhibition is selective in that humans generate fatty acids by a different pathway, namely the Type I biosynthetic pathway. Another enzyme pathway associated with the plastid is the non-mevalonate pathway that leads to synthesis of isoprenoids (chemical precursors used for the formation of numerous cellular molecules) which is selectively inhibited by the actions of fosmidomycin (Jomaa *et al*, 1999). In view of the selective antimalarial activity of such agents, it would appear that the prokaryotic-like biosynthetic pathways present in the apicoplast present exciting targets for the development of novel antimalarials.

The parasite digestive vacuole (DV) (as mentioned in section 1.1.3) also presents an excellent location for the activity of a number of diverse drug groups (Table 1.1). The artemisinins, for example, which appear to be one of our most useful groups of antimalarials (Haynes *et al*, 2004) are believed to interact with haem in the parasite DV. As of yet there have been no clinical reports of artemisinin resistance among the malarial parasites, however their use is limited by their short half-life, short shelf-life and cost (Bell, 2000; Ridley, 2002). New synthetic derivatives are presently being designed which may help overcome such limitations.

Aside from the artemisinins, protease inhibitors offer much hope as chemotherapeutic agents. In erythrocytic parasites, proteases play an important role in the sequential degradation of haemoglobin into its constituent amino acids and studies have shown the anti-malarial potential of inhibitors of such proteases (Rosenthal, 2001). In addition, the critical role of proteases in the invasion of erythrocytes by free merozoites and in erythrocytic lysis during merogony further underlines their potential as targets for drug development. The apicoplast and parasite DV represent just two of many potential drug target locations within the malarial parasite. The deciphering of the complete genome sequence of *P. falciparum* coupled with transcriptomic, proteomic and comparative genomic technologies should facilitate the identification of many more. For example, gene chip technologies have already been used to determine how each of the more than 5,400 parasite genes are switched on and off in the intra-erythrocytic stage of the parasite development cycle and to assign functions to the proteins involved (Le Roch *et al*, 2003). With such tools in hand to enhance our understanding of the cellular and molecular biology of the malarial parasites, the future identification, characterisation and validation of novel antimalarial drug targets would appear to look a lot brighter.

1.2. TUBULIN AND MICROTUBULES

1.2.1. Tubulin and microtubules: an introduction

Microtubules are cylindrical cytoskeletal polymers composed primarily of equal amounts of two repeating structural proteins, α - and β -tubulin. They have been identified in almost all eukaryotic cells and play crucial roles in diverse cellular processes such as chromosome segregation, intracellular transport, organisation and positioning of membranous organelles and the determination of cell shape and motility. Many of these activities are associated with the ability of microtubules to grow or shorten at various speeds, a unique phenomenon amongst cell organelles. This dynamic process of assembly and disassembly is regulated by numerous cellular factors including microtubule-associated proteins (MAPs), post-translational modifications of the tubulin subunits, local environmental conditions and the intrinsic ability of the tubulin heterodimers to form non-equilibrium, dynamic

polymers. Exogenous ligands can also have striking effects on microtubule stability, dynamics and function and thus on the health and viability of the cell.

Although microtubules have been identified in most stages of the development cycle of *P. falciparum*, little information currently exists pertaining to their structure and biochemistry. Thus, to aid our subsequent overview on the microtubules of the malarial parasite and their potential as an antimalarial drug target, the following sections will initially concentrate on general aspects of microtubule structure, dynamics, function and pharmacology as determined in a range of other eukaryotic organisms. As tubulin is a highly conserved protein across the eukaryotic kingdom, much of this information should be relevant to the microtubules of *P. falciparum*.

1.2.2. Tubulin and microtubule structure

1.2.2.1. Structure of the tubulin heterodimer

The α - and β -tubulin monomers, which form the heterodimer subunit of a microtubule, are closely-related proteins of approximately equal molecular mass of about 50,000 and sequence lengths of around 450 amino acids. Both monomers are highly acidic (pI 4 - 6) and share approximately 36 - 42% identity at the amino acid level (Ludueña *et al*, 1992). Sequence studies have shown that the amino acid identity among either α - or β -tubulins from different species generally exceeds 60% (Oakley, 2000). For example, tubulins from plants and animals typically share between 79 - 87% identity (Morejohn *et al*, 1991), while tubulins from protozoa and plants/algae are even more alike with identities of 88 - 93% (Burns *et al*, 1994). Although α - and β -tubulin have been highly conserved over the course of eukaryotic evolution, immunological, pharmacological and electrophoretic differences have been reported between the tubulins of higher and lower eukaryotes (Bell, 1998; Morejohn *et al*, 1991; Ochola *et al*, 2002; Werbovetz, 2002) making it possible selectively to target parasite tubulin with inhibitors (Lacey, 1988). However, given these subtle differences, it is evident that the remarkable conservation of the primary sequences of both tubulin monomers stems from the constraints imposed by the formation of the tertiary structure of the tubulin heterodimer.

The structure of the tubulin heterodimer had eluded crystallographers for many years due to tubulins' propensity to polymerise into various aggregated structures, which are unsuitable for diffraction studies. However, Nogales and co-

workers recently solved the structure of the tubulin dimer at 3.7 Å resolution by electron crystallography of zinc-induced bovine tubulin sheets stabilised with Taxol (Nogales *et al*, 1998). The structure of the tubulin dimer was mapped onto the amino acid sequence of pig tubulin in the absence of the amino acid sequence of bovine tubulin. The model was later refined to 3.5 Å resolution (Löwe *et al*, 2001) and consists of residues 2 - 34 and 61 - 439 of α -tubulin (total 451 residues), 2 - 437 of β -tubulin (total 445 residues), one molecule of guanosine triphosphate (GTP), one of guanosine diphosphate (GDP), and one of Taxol (microtubule-stabilising drug), as well as ions of magnesium and zinc. The determined structure clearly shows that the α - and β -tubulin monomers are very similar in overall fold, in agreement with their approximate 40% similarity at the amino acid level (Fig. 1.3).

The structure of each monomer consists of a core of two beta sheets surrounded by a number of helices and can be divided into three domains. (1) The N-terminal domain (residues 1 - 206) consists of six parallel β -strands alternating with six α -helices, forms a structure known as a Rossmann fold and creates the GTP-binding domain. This nucleotide-binding domain is different in structure to that of typical GTPases such as EF-Tu and transducin and has been reported to resemble more closely the topology of dinucleotide-binding proteins (Downing *et al*, 1999). In the dimer, α -tubulin is always found with GTP bound non-exchangeably at the so-called N-site, which is located at the intradimer interface, readily explaining the non-exchangeability. In contrast, the nucleotide bound to β -tubulin at the E-site can exchange freely as this site is partially exposed on the surface of the dimer. Furthermore, when the unpolymerised tubulin dimer has GTP bound to the E-site it maintains a straight conformation but with bound GDP the dimer conformation becomes more curved (Amos, 2004). (2) The second or intermediate domain (residues 207 - 384) consists of four mixed β -sheets and three helices and shows little structural homology to other proteins except for proteins of the YgjF family, whose function(s) are yet to be elucidated (Downing, 2000). This domain is involved in nucleotide hydrolysis, facilitates intra-monomer contact in the microtubule structure and forms the binding site for the microtubule-stabilising drug Taxol (Nogales *et al*, 1998). (3) The third domain comprises two antiparallel helices that cross over the previous two domains, the loop that connects them and the C-terminal residues. The extreme C-terminal regions of both monomers were not resolved in the atomic model, but are believed to be exposed on the outside surface of the microtubule and may

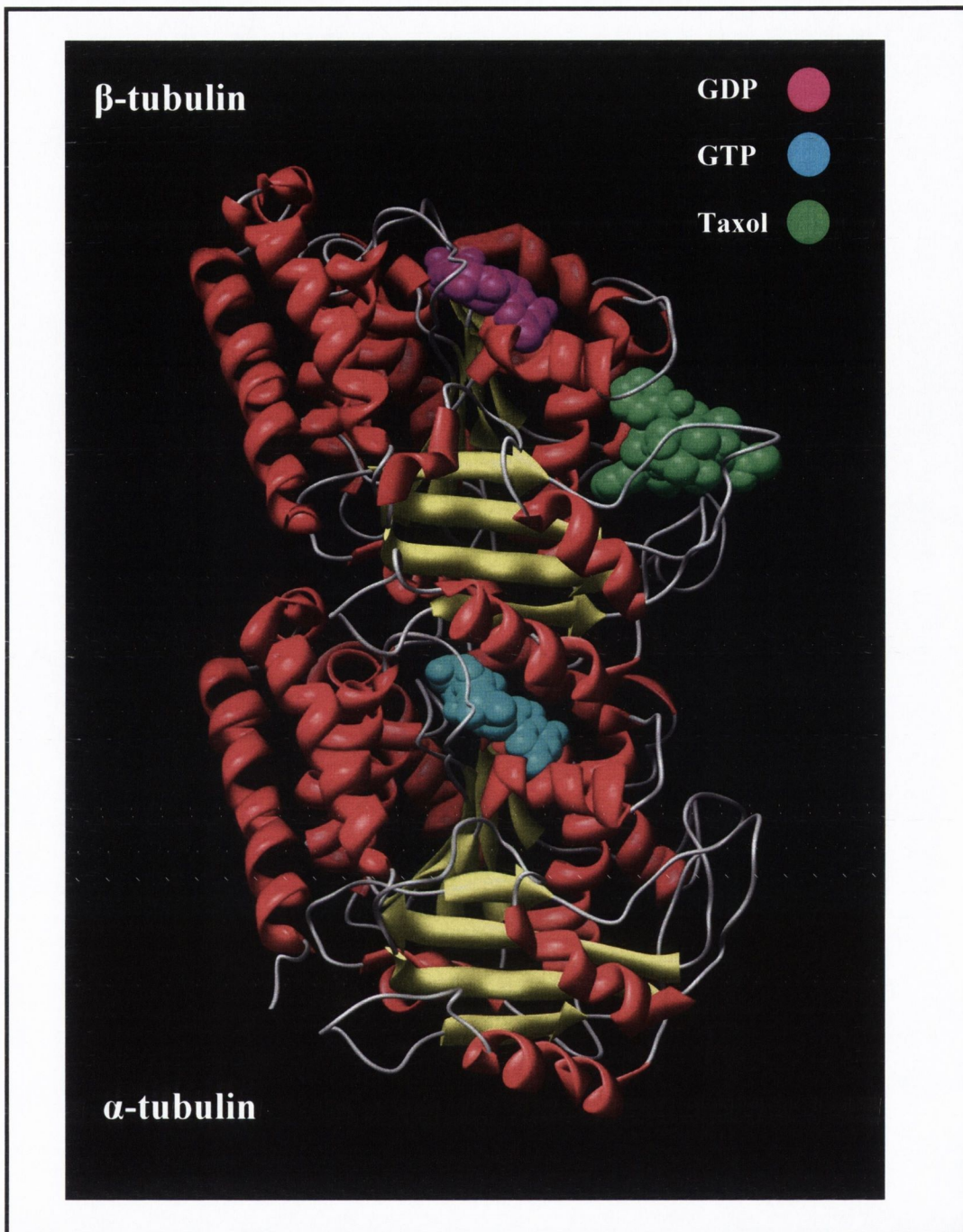


Figure 1.3. Ribbon diagram of the crystal structure of the α/β -tubulin dimer complexed with Taxol. α helices are shown as red helical ribbons and β strands are shown as yellow arrows. Loop regions are shown in gray. The nucleotides (GTP, GDP) and the microtubule-stabilising drug Taxol are shown as space-filling molecules as indicated. The β -monomer is at the top, which would correspond to the plus end of a microtubule. Accession no. 1JFF.

play a significant role in binding MAPs and the motor proteins kinesin and dynein. Overall, both tubulin monomers show very little structural homology to any other protein, with the exception of the bacterial cell-division protein FtsZ (Löwe *et al*, 1998). Remarkably, FtsZ shares only ~ 10% sequence identity with tubulin, yet the two proteins are structurally alike, with the same topology throughout the N-terminal and intermediate domains. In addition, limited sequence identity has also been found between tubulin and the protein Misato, which is involved in cell division in *Drosophila* (Nogales *et al*, 1998).

Prior to microtubule formation, both tubulin subunits must be correctly folded by the cytosolic chaperonin complex CCT, also known as TriC or TCP-1 (Gao *et al*, 1993). This 800-kDa structure is formed by eight different subunits arranged into a hexadecamer of two double rings. It binds to and releases each of the tubulin subunits in a number of ATP-dependent cycles, and the subunits are then captured, stabilised and complexed together by a number of additional cofactors (Linder *et al*, 1998). With the hydrolysis of GTP by β -tubulin comes the release of the properly folded α/β -tubulin dimer from the chaperonin complex (Nogales, 2000), which must now bind to another molecule of GTP to facilitate its successful assembly into the microtubule lattice.

1.2.2.2. Microtubule structure and dynamics

Microtubules are formed when tubulin dimers, each with two bound molecules of GTP, co-assemble in a head-to-tail fashion to form a protofilament, and protofilaments assemble side by side to form the cylindrical structure of the microtubule (Fig. 1.4). Microtubules typically contain 13 protofilaments laterally associated but slightly offset relative to each other by a 10° helical pitch, producing what is known as a “B” lattice structure (Oakley, 2000). However, protofilament numbers can vary from 9 to 18 in microtubules formed intracellularly and *in vitro* (Li *et al*, 2002) suggesting that there is a high degree of flexibility in the lateral associations of the adjacent protofilaments. Microtubules containing 13 protofilaments tend to run straight, whereas microtubules containing more or less than 13 protofilaments invoke a greater pitch around the microtubule axis to maintain a straight structure (Amos, 2004). Microtubule dimensions are typically 25 nm in diameter with variable length up to more than several μm . In the microtubule, the principal lateral contacts are made between homologous subunits (i.e. α - α and β - β),

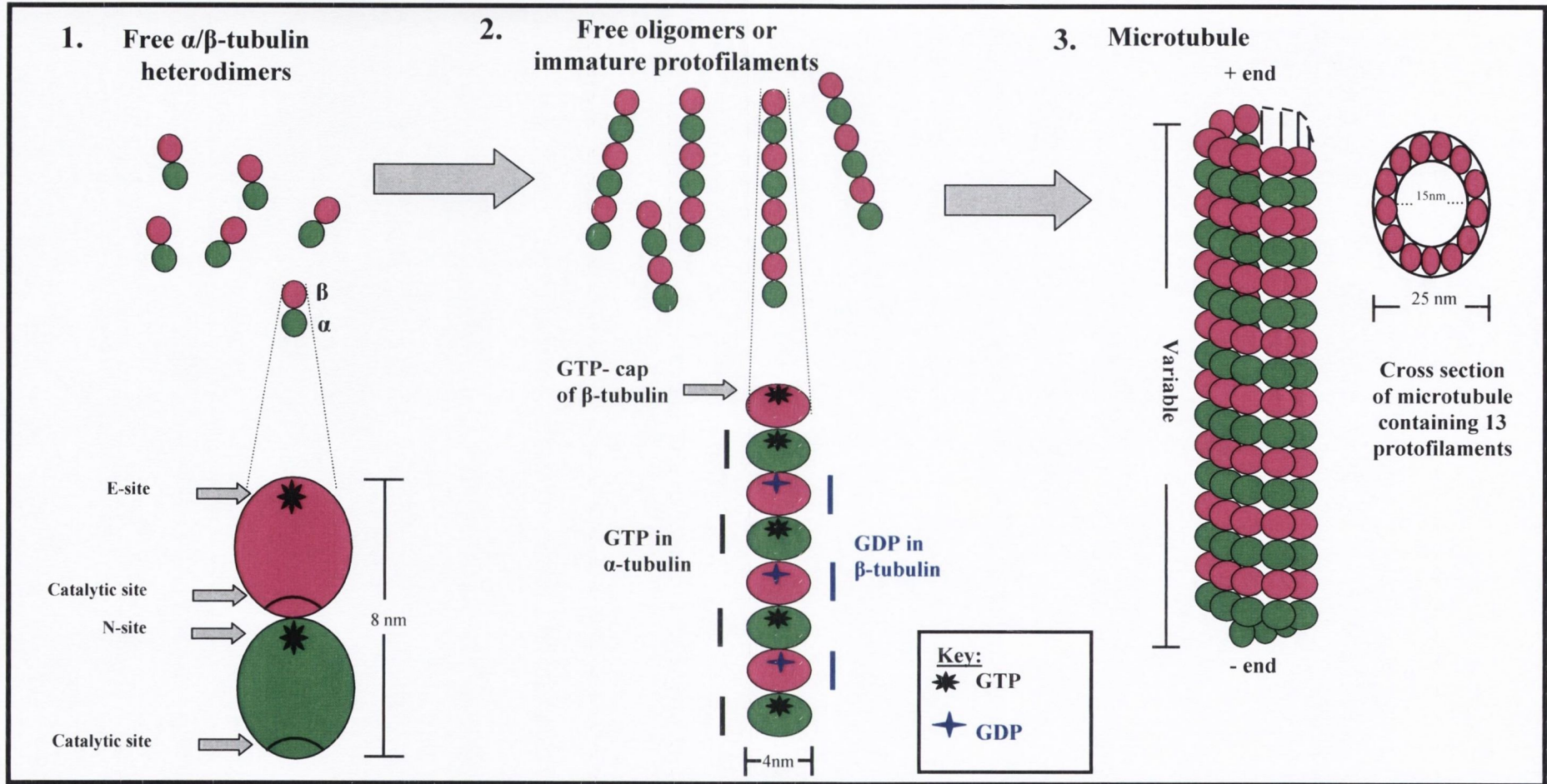


Figure 1.4. Schematic diagram of microtubule formation and structure. (1) Heterodimers comprising α - and β -tubulin (each containing one molecule of GTP in the N- and E- sites, respectively) (2) associate linearly to form oligomers or short protofilaments, which accompanies the hydrolysis of GTP to GDP in the β - but not the α -subunit or the β -tubulin cap. (3) The lateral association of the protofilaments forms a cylindrical polar microtubule with an outer diameter of 25 nm and variable length up to more than several μm . Lateral contacts in the microtubule are between the subunits α - α and β - β , however there may be a line of discontinuity where α and β subunits meet, producing a seam that runs the length of the microtubule (not observed in above schematic).

but there may also be a seam or line of connection in which contact is made among the heterologous subunits (i.e. α - β and β - α). The function of the seam remains to be elucidated but is believed to be involved in interactions with MAPs and/or microtubule stability (Nogales, 2000).

Central to microtubule functioning is the distinct polarity of the microtubule, consisting of a plus end which is kinetically more dynamic than the other (minus end) (Fig. 1.4). This polarity arises from the specific orientation of the protofilament within the microtubule so that the plus end is crowned by a β -tubulin subunit exposing its GTP nucleotide end into solution, whereas the minus end terminates with the α -subunit exposing its catalytic domain (Inclán *et al*, 2001) (Fig. 1.4). When a tubulin dimer is added to the plus end, its catalytic domain within the α -subunit contacts the E-site GTP nucleotide of the previous subunit and this nucleotide becomes hydrolysed to GDP. The newly added GTP-tubulin dimer, however, will not be hydrolysed until a new tubulin dimer is added. This cap of β -tubulin containing GTP on the microtubule plus end may be as little as one subunit deep, but is sufficient to stabilise the microtubule structure. At the minus end, the addition of tubulin dimers is much slower and results in contact between the catalytic region of the last α -tubulin subunit and the E-site nucleotide of the new subunit, thus preventing the formation of a GTP cap at the minus end.

The polar nature of the microtubule makes it a highly dynamic polymer, which can switch stochastically between growing and shrinking phases both intracellularly and *in vitro* (Heald *et al*, 2002). Microtubules have been found to exhibit two types of dynamic behaviour, namely treadmilling and dynamic instability (Mandelkow *et al*, 1995). Both of these provide the cell with continuous opportunities for cytoskeletal rearrangement, which is presumably required during the cell cycle and cell differentiation stages of growth as microtubules associated with cell shape and motility (e.g. flagella and cilia) are intrinsically more stable. Treadmilling occurs when dimers are added to the plus end of the microtubule and are lost from the minus end, resulting in a GTP hydrolysis-driven net flux of dimers through the polymer without a significant change in microtubule length. This phenomenon is widely believed to be critical in the polar movement of chromosomes during anaphase (Dumontet, 2000). Dynamic instability, on the other hand, involves a population of microtubules with dramatically different behaviour; some of the microtubules are shrinking or disassembling rapidly while others are growing slowly.

This sudden change from growth to shrinkage is known as a “catastrophe”, while the cessation of shrinkage and the re-growth of the microtubule is termed a “rescue” (Amos, 2004). Even after a “catastrophe” some of the protofilaments can remain intact, forming rings and spirals that eventually break off and dissociate into dimers (Fig. 1.5). However, the high curvature of the protofilaments is usually only seen with GDP bound to the E-site of the tubulin dimer.

A wide range of factors are known to control microtubule dynamics in the cell. For example, intracellular levels of free tubulin dimers can have dramatic effects on microtubule behaviour. However, even when tubulin concentrations are above the critical concentration (the minimum concentration of tubulin required for microtubule formation) microtubules can still demonstrate dynamic instability. Local environmental conditions such as low temperature (generally less than 10°C), fluctuating pH, low GTP levels and high calcium levels can also increase the rate of microtubule disassembly and under certain conditions can cause catastrophic depolymerisation of the entire microtubule in a non-polar fashion (Lacey, 1988). Similarly, a number of MAPs can act to destabilise the microtubule lattice by a variety of mechanisms. For example, katanin acts as a severing factor to generate microtubule ends lacking a GTP cap, while depolymerising kinesins of the KinI family bind to microtubule ends and cause protofilament peeling (Heald *et al*, 2002) (Fig. 1.5). However, several other classes of MAPs (e.g. MAP2 and Tau) can also act to stabilise microtubules by binding to their surfaces, bridging several tubulin subunits and preventing their disassembly (Amos, 2004).

A model of the atomic structure of a microtubule has now been obtained by a number of groups by docking the high-resolution structure of the tubulin dimer into the lower-resolution map of an intact microtubule (Nogales, 2000; Amos, 2000; Li *et al*, 2002). These models detail the elaborate architecture of the microtubule and offer novel insight into the molecular interactions between the tubulin subunits. Such studies have revealed that most of the lateral interactions between tubulin protofilaments occur through the M-loops of one protofilament making contact with the H3 helix of the N-terminal domain of the next protofilament (Fig. 1.6). Such lateral contacts are responsible for microtubule stability. They counteract the constraining influence of GDP that exists throughout most of the polymer lattice, maintaining a straight protofilament structure, which is central to the dynamic instability of microtubules (Amos, 2004). Such lateral contacts may be further

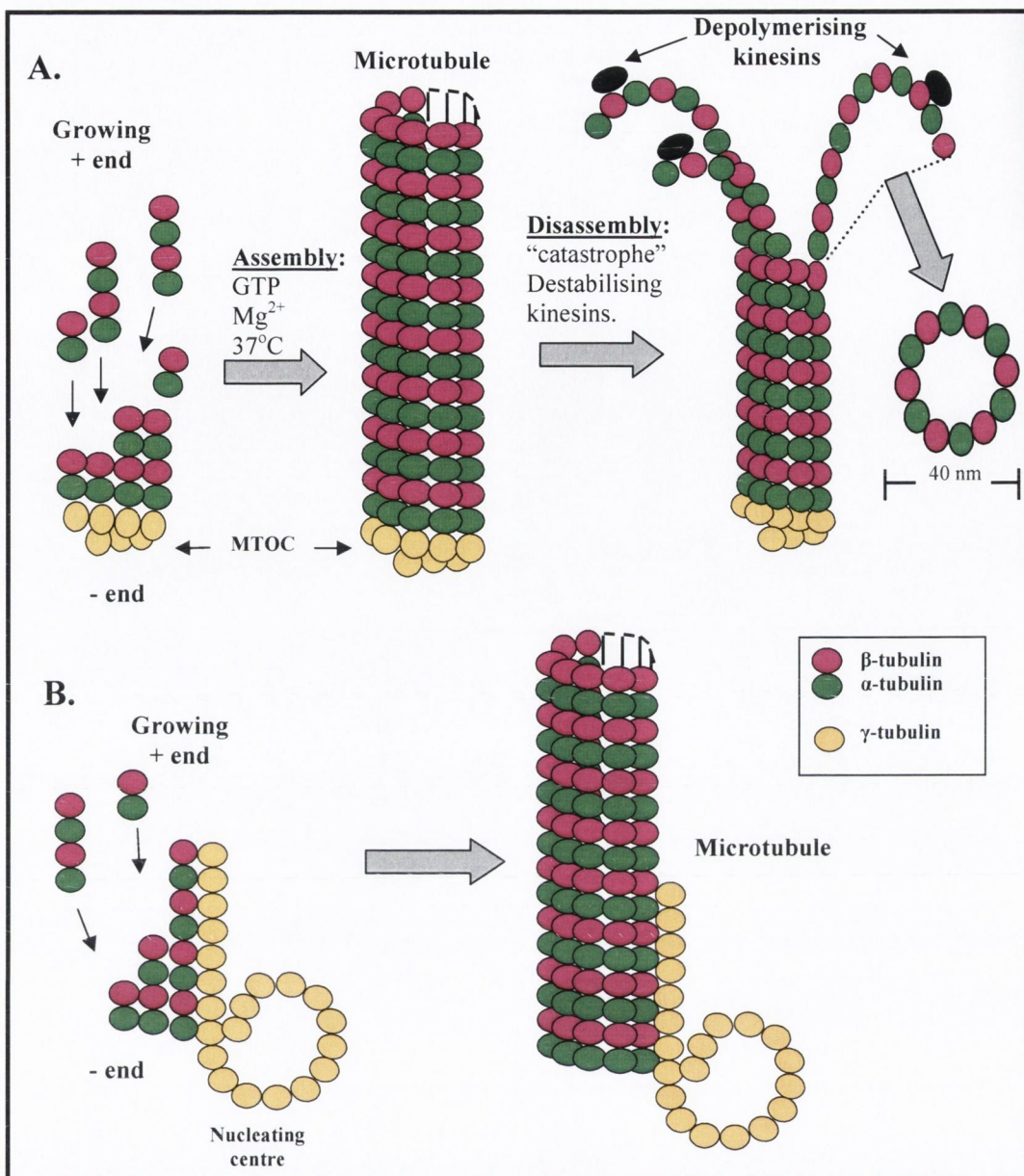


Figure 1.5. Microtubule nucleation, assembly and depolymerisation. **A.** Proposed model for microtubule nucleation (modified from Nogales, 2000) in which γ -tubulin comprises the first helical turn of the microtubule, providing a platform for microtubule growth and making longitudinal contacts with the α -subunit of the tubulin dimer. Following microtubule formation an example of microtubule disassembly is shown induced by the actions of depolymerising kinesins. Note the peeling or spiralling of protofilaments from the microtubule lattice as well as their ability to form ring-like structures up to 30 - 40 nm in diameter. **B.** Alternative model for microtubule nucleation in which a spiral-like protofilament of γ -tubulin acts to stabilise the $\alpha\beta$ -tubulin microtubule lattice by lateral interactions, thus facilitating microtubule assembly. Note: In addition to γ -tubulin, the microtubule-organising centre (MTOC) is comprised of various other proteins, which for reasons of simplicity are not shown.

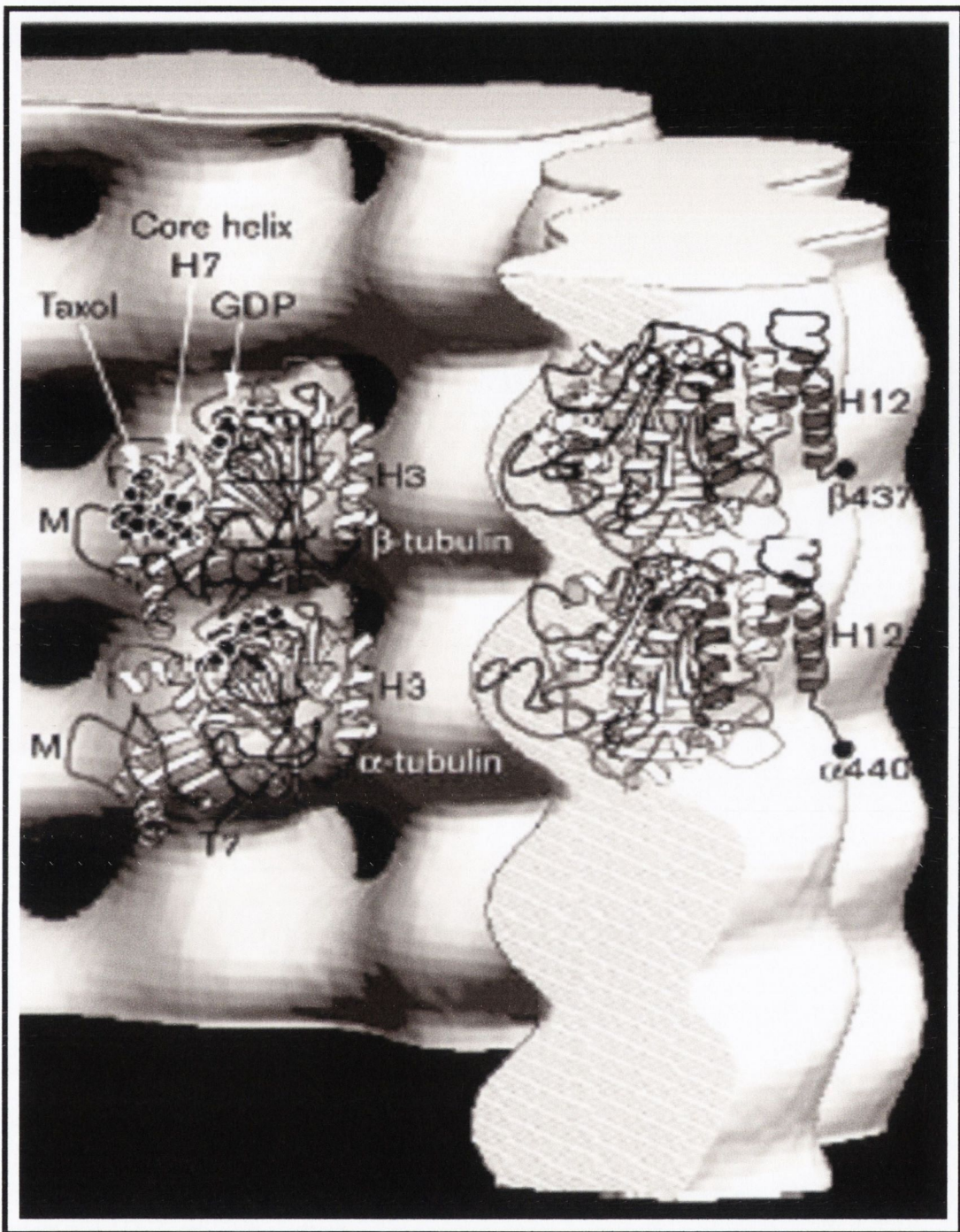


Figure 1.6. Current model of microtubule structure at atomic resolution. The crystal structure of tubulin shown as a ribbon model is docked into a low-resolution 3-D image of tubulin protofilaments. This diagram shows a section through a microtubule; on the left is the view inside a microtubule and on the right is from one side of a protofilament. A nucleotide occupies the top of each monomer (GTP bound to α -tubulin, GDP bound to β -tubulin) and each nucleotide is in contact with the T7 loop of the next subunit in the protofilament. The microtubule stabilising drug Taxol is shown as a space-filling molecule in a cavity on the inside surface of β -tubulin. Lateral interactions between the protofilaments involve contact between the M-loop and H3 helix of tubulin subunits in adjacent protofilaments. Note the positions of the last visible residues (α 440 and β 437) near the outside surface of the microtubule denoted by black circles. Reproduced from Amos (2000).

strengthened by the actions of the microtubule stabilising drug Taxol that binds to β -tubulin near the M - loop region (Amos, 2000).

1.2.2.3. Microtubule nucleation

Microtubule assembly *in vitro* generally involves the formation of a cylindrical polymer comprising two free ends (Fig. 1.4). Microtubules in cells, however, usually grow out from a microtubule organising centre (MTOC), which is crucial to their functioning and dynamic behaviour. The MTOC is commonly termed a centrosome in animal cells or a spindle pole body in the case of fungi. The minus end of the microtubule is typically embedded or nucleated into the MTOC and may not be subject to change, while the more dynamic plus end can switch between phases of growth and shrinkage (Oakley, 2000).

Central to microtubule nucleation is a relatively new member of the tubulin family, γ -tubulin, a protein with high homology to α - and β -tubulin that forms a key component of MTOC's (Oakley *et al*, 1989) and has also been located in the mitotic spindle (Lajoie-Mazenc *et al*, 1994). Studies have revealed that γ -tubulin is found in the MTOC in two types of complex: the γ -tubulin ring complex (γ -TuRC) which is approximately the same diameter as the microtubule (25 nm) and comprises up to eight proteins in addition to γ -tubulin or the γ -tubulin small complex (γ -TuSC) which contains two molecules of γ -tubulin and one molecule each of two related, conserved proteins termed Dgrip84 and Dgrip91 in *Drosophila melanogaster* (Oakley, 2000). Such complexes are believed to serve as the effective basal template for the nucleation of the microtubule lattice (Amos, 2004). Two models have been proposed for this process suggesting that either the ring complexes form the first helical turn of the growing microtubule or that γ -tubulin forms a rolled-up, protofilament-like structure, which can serve as a template for lateral contacts with α/β -tubulin protofilaments (Nogales, 2000) (Fig. 1.5). It is also interesting to note that further members of the tubulin family have recently been discovered, namely delta (δ)-, epsilon (ϵ)-, zeta (ζ)- and eta (η)-tubulin, that appear to be located in the MTOC and may play an important role in microtubule nucleation (reviewed in McKean *et al*, 2001).

1.2.2.4. Cellular organisation of microtubules: general overview

In different eukaryotic cells, or at different times or places in the same cell,

many diverse kinds of microtubule-based structures are assembled, each unique in architecture and mode of function (Fig. 1.7). One such kind are the mitotic microtubular spindles, which play a key role in cell division (mitosis and cytokinesis) in nearly all eukaryotic cells. Mitotic spindle formation firstly involves a prophase stage where intense networks of microtubules are formed between the poles (MTOC) of the cells that are soon to be created. During metaphase, the microtubules form the spindle, which binds to and orients the duplicated chromosomes in the central plain of the mitotic cell. At the same time, other microtubules bypass the kinetochores (points of attachment of microtubule to chromosome) and terminate elsewhere in the body of the spindle, often reaching the opposite pole (Fig. 1.7 C). Such polymers are known as astral microtubules and their function in mitosis is not certain but they are believed to help to define the plane of cytokinesis in cells that form a cleavage furrow (McIntosh, 1994). In anaphase, microtubules facilitate chromosome separation and move them to opposite ends of the cell. Finally, in teleophase, microtubules play an important role in cytokinesis and in the formation of the cell plane, which separates the two new cells.

Another important functional class of microtubules, together with a number of accessory proteins, are found to constitute the axoneme of cilia and flagella, which contribute to cell motility. Microtubules of the axoneme are organised into the characteristic “9 + 2” arrangement (Fig. 1.7 A) which consists of nine peripheral doublet microtubules (termed A- and B-tubules) and a central pair of singlet microtubules. Movement of cilia and flagella is believed to result from the sliding movements between the doublet microtubules. The force for such movement is supplied by the dynein motor proteins, which are attached to the A-tubules of each doublet. The central, radial spokes are believed to convert this dynein-driven microtubule sliding action into the characteristic bending motions often observed with flagella (Smith *et al*, 1994). Flagella and cilia can be found on a wide range of cells such as human epithelial cells (cilia only) and are particularly predominant on protists such as *Paramecium* and *Chlamydomonas*.

A third functional class of microtubules can be found ramifying throughout the cytosol of many eukaryotic cells. They play a crucial role in maintaining the position of cellular organelles as well as serving as tracks along which organelles (e.g. ribosomes) and vesicles can be transported (Fig. 1.7 B). Motor proteins from the dynein and kinesin families, which use MgATP as a source of fuel, are used to

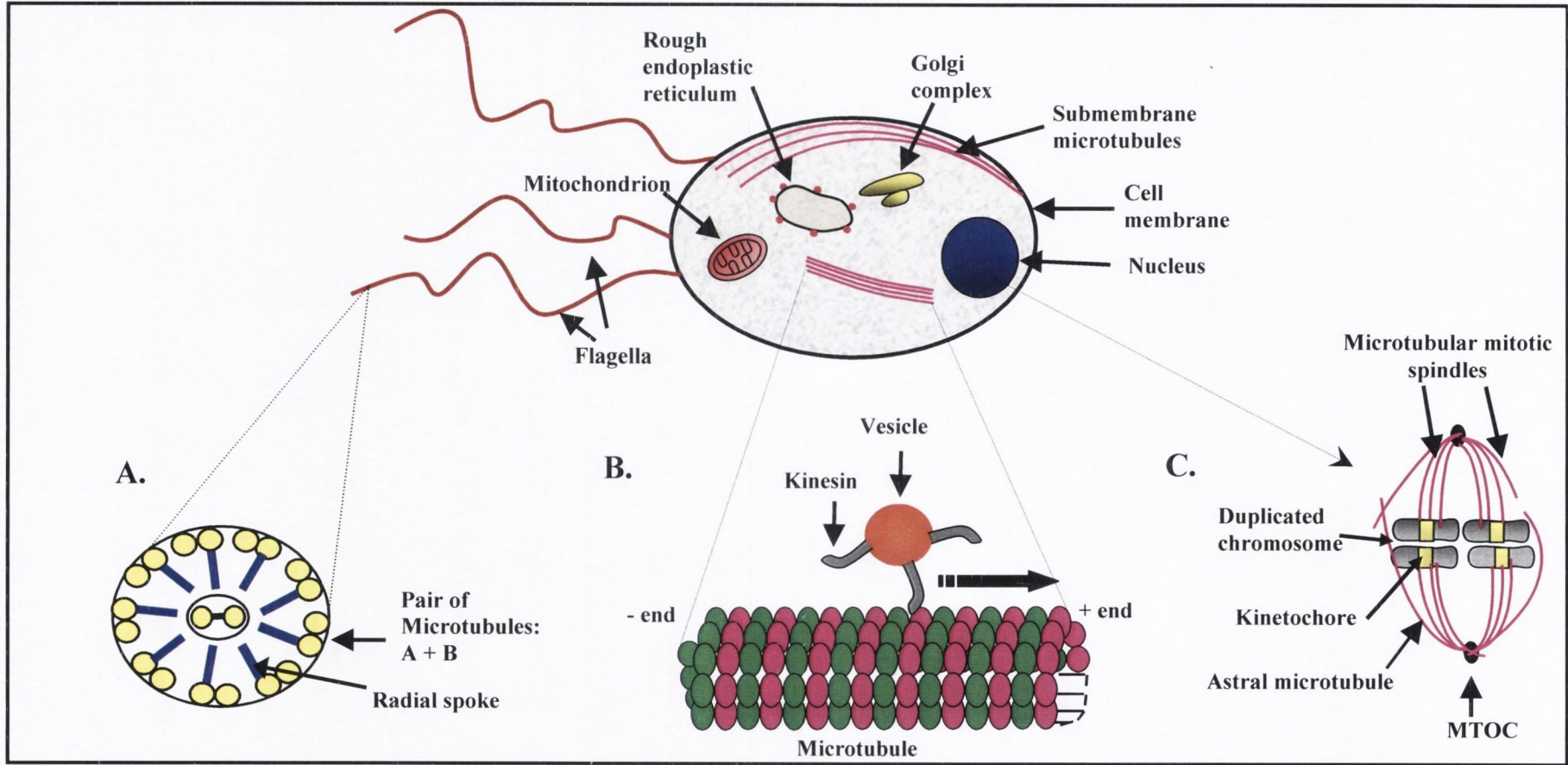


Figure 1.7. Highly schematic diagram of the organisation of microtubule-containing structures in a simple eukaryotic cell. **A.** Cross-section through a flagellum showing the 9 + 2 arrangement of microtubules. The nine peripheral doublet microtubules are termed A- and B-tubules and attached to the A-tubule is the inner and outer dynein arms that project to the next adjacent doublet (not shown) and the radial spokes that project to the central pair. **B.** Cytosolic microtubular cytoskeleton acting as a track for the kinesin-mediated transport of an intracellular vesicle. **C.** Nuclear spindle microtubules extending from MTOC to kinetochores (the points of attachment to chromosomes) during the metaphase stage of cell division. In addition, note the submembrane microtubules, which are important for cell shape (in diagram of cell).

shuttle the membranous cargo along the microtubule track, which can be minus-end or plus-end directed (Bloom, 1992). For example, microtubule-based motors are believed to be involved in the organisation of the endoplasmic reticulum membranes that are often dispersed throughout the cytosol. Moreover, newly synthesised material in the endoplasmic reticulum and the Golgi system is thought to be delivered to various cellular locations by vesicle trafficking along the microtubule tracks (Ludueña *et al*, 1995).

Finally, the submembrane microtubules comprise another major functional class of microtubules in various eukaryotic cells (Fig.1.7) and make a key contribution to the maintenance of cell shape and integrity. However, it should be noted that numerous other microtubule-containing structures can be found in the eukaryotic cell and that this brief overview just serves to highlight some of the diverse forms that can be found in even the simplest of cells.

1.2.3. Tubulin diversity

In the previous section, the conserved nature of the tubulin dimer was clearly highlighted. However, given the fact that microtubules serve a variety of cellular functions, the issue arises of whether and how the individual microtubules composed of the different tubulin heterodimers are assigned to each of these specific functions. To this end, the cell generates tubulin diversity by at least two mechanisms, namely expression of multiple isoforms of both α - and β -tubulin and by generating an extensive array of post-translational modifications.

1.2.3.1. Tubulin isotypes

Genetic and molecular techniques have revealed the expression of multiple isoforms of both α - and β -tubulin that are distinct but related proteins encoded by multigene families in a wide variety of eukaryotic cells (Cleveland *et al*, 1985). The size of the gene families ranges from small families in the fungi consisting of one or two genes for α - and β -tubulin to larger gene families in mammalian cells where about six genes can be found for each tubulin subunit (Ludueña, 1998). A number of differences between the tubulin isotypes have been found among species, which include varying expression levels and relative amounts in various tissues. The amino acid compositions of the different isotypes, however, are highly conserved, with the majority of differences located within the last 15 amino acids of the acidic C-

terminal region of both tubulin subunits.

The recognition that eukaryotic organisms can express multiple isotypes of α - and β -tubulin raises the possibility which was first noted over 28 years ago that microtubules performing different functions might be composed of these different tubulin polypeptides - the “multi-tubulin hypothesis” (Fulton, 1976). A variety of molecular, genetic and biochemical techniques have since been used in an attempt to validate this premise. Results from such experimental systems have provided evidence that different α/β -tubulin isotypes can influence microtubule structure and function but in most cases, the isoforms generally seem functionally interchangeable (Ludueña, 1998; McKean *et al*, 2001; Raff, 1994). While the biological significance of the different isotypic forms of tubulin remains a matter of intense debate, tubulin alteration by post-translational modification provides a definite mechanism of generating distinct biochemical differences within the tubulin population.

1.2.3.2. Post-translational modifications of tubulin

Both α - and β -tubulin are subject to an extensive array of post-translational modifications, which generate diversity within the tubulin population and possibly influence microtubule functioning. Indeed, for some organisms (e.g. certain protists) that express only a single set of α/β -tubulin genes they may provide the only source of tubulin variation. Most of these changes are enzymatically driven and reversible, thus providing the potential to cause rapid changes to tubulin and to generate highly dynamic subgroups within the tubulin population. Several techniques including use of specific monoclonal antibodies, isoelectric focusing and mass spectrometry have been used in the identification of post-translational modifications of the tubulin molecule (Westermann *et al*, 2003). Approximately seven known types have been identified, which will briefly be outlined here.

The first of these, acetylation, which occurs on most known α -tubulins, involves the addition of an acetyl group to a lysine residue at position 40 in the N-terminal domain (Ludueña *et al*, 1992). It occurs after microtubule assembly and probably involves diffusion of acetyltransferase (the enzyme involved in modification) down the lumen of the microtubule, as lysine 40 is located on the inside surface of the polymer (Nogales, 2000). This modification has been observed in vertebrates, arthropods and numerous protists and is believed to be associated with increased microtubule stability and possible regulation of cell motility (Westermann

et al, 2003).

With the exception of acetylation, all other known post-translational modifications occur in the divergent carboxy-terminal tubulin tails, which are believed to lie on the outside of the microtubule lattice, thus facilitating their access to modifying enzymes. One such modification that is apparently unique to tubulin is the tyrosination and detyrosination of α -tubulin. The C-terminal tyrosine residues present on a wide range of α -tubulin isoforms are removed by a tubulin tyrosine carboxypeptidase and re-added by the enzyme tubulin-tyrosine ligase (Ludueña *et al*, 1992). Tyrosine removal is associated with highly stable microtubules and may be important for the coordination of crosstalk between microtubules and different cytoskeletal elements such as intermediate filaments (Westermann *et al*, 2003). Furthermore, removal of the penultimate glutamate residue of detyrosinated α -tubulin by an as of yet unidentified enzyme leads to the formation of $\Delta 2$ -tubulin (McKean *et al*, 2001). $\Delta 2$ -tubulin has been found in microtubular structures such as the axonemes of the flagella and cilia and is unable to act as a substrate for tubulin-tyrosine ligase, therefore functioning to remove tubulin from the tyrosination cycle.

Polyglycylation, which involves the covalent attachment of a polyglycine side chain of variable length (up to 34 residues) to conserved glutamate residues located in the C-terminus of both α - and β -tubulin, is another tubulin-specific modification. Polyglycylation has been found to occur extensively in axonemal tubulins of organisms such as *Paramecium*, *Tetrahymena* and *Giardia lamblia* and plays an important role in motility, axonemal organisation and in the severing of microtubules during cytokinesis (McKean *et al*, 2001). Moreover, the same glutamate residues can also be modified by the covalent attachment of polyglutamyl side chains of variable length (up to 20 residues), a modification known as polyglutamylation. Polyglutamylation is associated with stable microtubule structures such as the axonemes of cilia and flagella and just like polyglycylation, it occurs in a diverse range of eukaryotes including a number of protists such as *Trypanosoma brucei* (Schneider *et al*, 1997) and *Toxoplasma gondii* (Plessmann *et al*, 2004). Polyglutamylation modifications are believed to function in regulation of microtubule interaction with MAPs such as Tau and the motor protein kinesin as well as aiding centriole maturation and stability (Westermann *et al*, 2003). Finally, two less reported modifications of the tubulin subunits include phosphorylation and palmitoylation, of which the latter change is believed to be implicated in the

positioning of astral microtubules of the mitotic spindle in the yeast cell (Westermann *et al*, 2003).

1.2.4. Tubulin/microtubule-drug interactions

The tubulin molecule and microtubules in general are well known targets for a wide variety of drugs. These drugs are of great interest for the insights they can provide into the functions and properties of microtubules in the cell as well as for their potential activity for the treatment of a number of human and animal diseases. Indeed anti-microtubule agents have already found use in a wide variety of medical applications, including as anthelmintic, anti-fungal, and anti-inflammatory agents as well as for use in cancer chemotherapy (Lacey, 1988). A number of assays and techniques are commonly used to validate the actions of existing and potential microtubule inhibitors at the cellular and molecular level. For example, immunofluorescent and electron microscopy are widely used to visualise the effects of such agents on the microtubular architecture in the cell (Hadfield *et al*, 2003). However, interactions that are more direct can be inferred from measuring the ability of such agents to inhibit microtubule formation *in vitro*. Drug binding can be measured using radiolabelled ligands and techniques such as fluorescent quenching, while photo-affinity labelled ligands have proved useful for locating drug-binding domains on the tubulin dimer (Wilson *et al*, 1994).

To date, three main classes of tubulin-binding drugs have been identified, which can be classified according to their binding sites, namely those that bind tubulin at the colchicine-binding site, those that bind it at the “*Vinca*” domain and those that bind it at the Taxol site (Nogales, 2000). While agents from the colchicine and “*Vinca*” domain families inhibit microtubule assembly and depolymerise microtubules, agents from the Taxol family promote microtubule assembly and stabilisation. Despite these differences, all agents are believed to interfere with the function of the mitotic spindle, leading to a loss of chromosome segregation with consequent inhibition of cell division and ultimately cell death.

1.2.4.1. Colchicine-site agents

Colchicine, a tricyclic acetylated alkaloid, produced by the meadow saffron, *Colchicum autumnale*, and by other members of the Lily family, is the classic tubulin-binding agent. It was first shown to bind to tubulin over 35 years ago

(Borisy *et al*, 1967) and has since played a key role in determining the properties and functions of microtubules in the cell. It is highly toxic to mammalian cells at sub-micromolar concentrations and blocks or delays mitosis at prometaphase (Morejohn *et al*, 1991). It binds in a non-covalent, biphasic manner (first step rapid, but weak, with the second step slower but stronger) to a single high-affinity site on the unpolymerised β -tubulin monomer (Ravelli *et al*, 2004). The site is near the monomer-monomer interface of the dimer and is largely buried in the intermediate domain of the β -subunit, although some contact between colchicine and a neighbouring loop of α -tubulin is observed (Fig. 1.8). The binding of colchicine to the unpolymerised dimer invokes movement of loop and helix structures within the β -subunit, thus providing space for the ligand and readily explaining its biphasic binding.

Colchicine acts in a concentration-dependent fashion on animal microtubules: at low concentrations (substoichiometric: less than one molecule of drug for each molecule of tubulin), it inhibits microtubule growth and dynamics, whereas at high concentrations it causes microtubule depolymerisation (Downing, 2000). Such diverse effects stem from the influence of colchicine on lateral and longitudinal contacts between the tubulin subunits in the microtubule lattice. When colchicine binds to β -tubulin, it prevents the dimer from adopting its normal straight conformation (see section 1.2.2.1), as this would result in a steric clash between bound colchicine and the α -subunit. Thus, when the curved tubulin-colchicine complex is added to the plus end of a growing microtubule, the lateral contacts between this subunit and the subunits of adjacent protofilaments fail to establish as the M-loop of the liganded tubulin is displaced by more than 9 Å (Ravelli *et al*, 2004). Hence, at low colchicine concentrations, further microtubule growth is prevented, although the polymer mass can remain preserved, if the number of missing lateral contacts remains small. However, at higher colchicine concentrations, the number of missing lateral contacts increases, leading to microtubule destabilisation and consequently disassembly.

A number of other agents, both natural (e.g. combrestatin) and synthetic (e.g. ZD6126 4) are also believed to bind at the colchicine-binding site, based on their ability competitively to inhibit colchicine binding to tubulin (Hadfield *et al*, 2003). In fact, one such agent, podophyllotoxin, has already been shown to bind at the colchicine site (Ravelli *et al*, 2004) and displays potent activity against mammalian

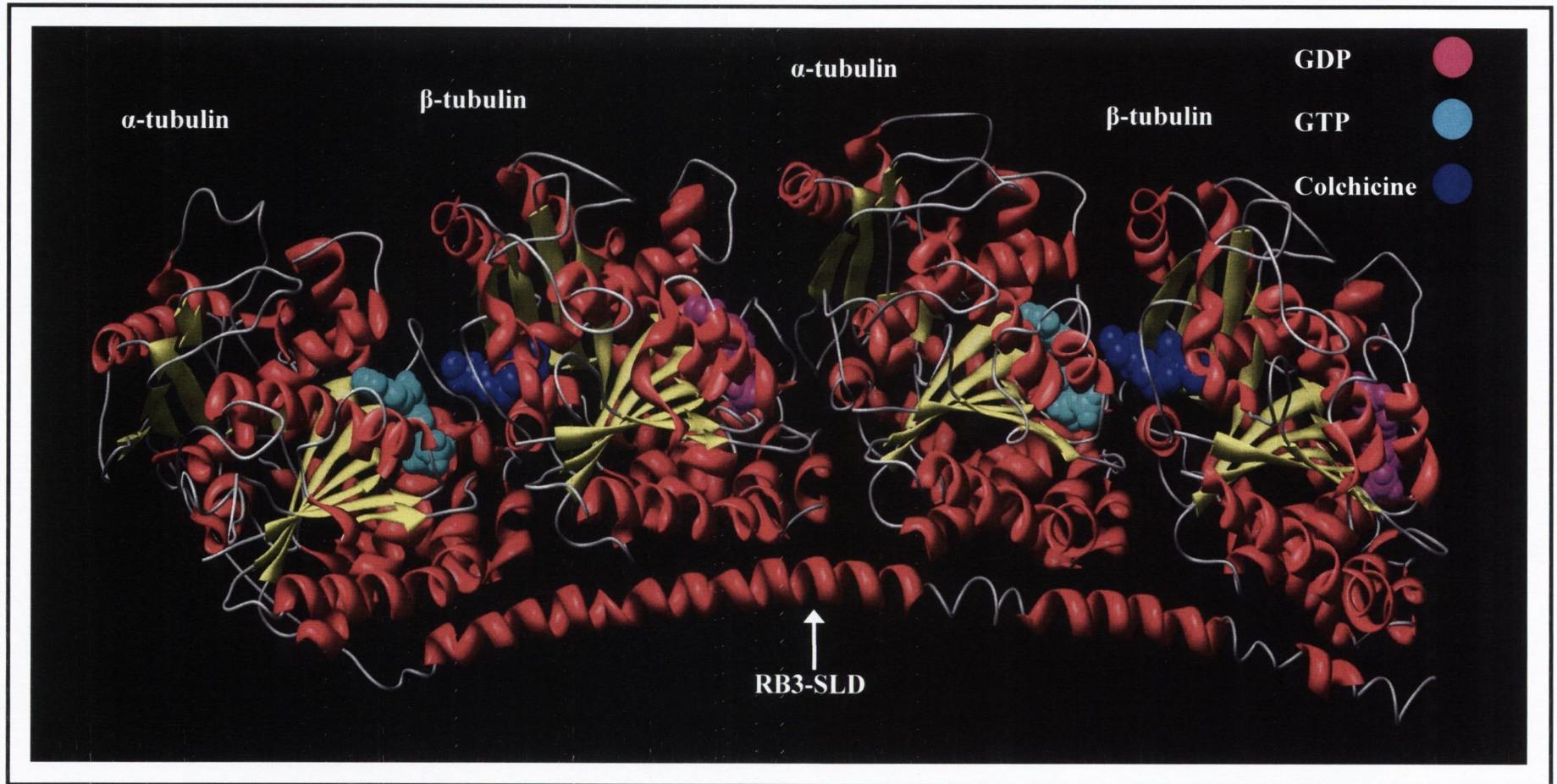


Figure 1.8. Ribbon diagram of two tubulin heterodimers complexed with colchicine and RB3-SLD. α helices are shown as red helical ribbons and β strands are shown as yellow arrows. Loop regions are shown in gray. The nucleotides (GTP, GDP) and the drug colchicine are shown as space-filling molecules as indicated. The stathmin-like domain (SLD) of RB3 is shown as indicated. Accession no. 1SA0.

cells. Interestingly, concentrations of colchicine in the micromolar to millimolar range are generally required to inhibit lower eukaryotes and various plant species. Such high concentrations can inhibit other cellular processes such as DNA synthesis and respiration that may be unrelated to microtubule function (Morejohn *et al*, 1991). Moreover, tubulin isolated from plants and protozoan parasites show little affinity for colchicine (Morejohn *et al*, 1991; Werbovetz, 2002), suggesting that significant differences exist between mammalian and plant/parasite tubulins at the colchicine site.

1.2.4.2. “*Vinca*” domain agents

The “*Vinca*” domain refers to a region on the tubulin subunits where a number of structurally highly dissimilar compounds are proposed to bind. These agents all show varying degrees of competitive inhibition of each other’s binding to tubulin and because of such differences, it has been proposed that their binding sites do not overlap completely (Downing, 1999). Vinblastine, an alkaloid obtained from the plant *Catharanthus roseus* (formerly *Vinca rosea*), is one of the most extensively studied of these “*Vinca*” domain agents and is widely used in cancer chemotherapy (Wilson, 1994). It has profound effects on both higher and lower eukaryotes, inhibiting the processes of cell division and cytokinesis. It binds rapidly, reversibly and with high affinity to tubulin *in vitro*, weakly inhibiting GTP hydrolysis and preventing microtubule assembly. At substoichiometric concentrations (in the nanomolar range), it can bind to free protofilament ends and induce dramatic effects on microtubule dynamics without causing microtubule depolymerisation (Dumontet, 2000). At higher concentrations, it binds stoichiometrically to tubulin subunits preventing their assembly and promoting microtubule depolymerisation by encouraging splaying and peeling of protofilaments at both microtubule ends, which aggregate to form vinblastine-tubulin paracrystals (Downing, 2000).

The location of the “*Vinca*”-binding domain is widely believed to be adjacent to or overlap with the N-site as “*Vinca*” domain agents can inhibit nucleotide exchange on β -tubulin (Wilson, 1994). However, photolabelling studies with a number of “*Vinca*” domain agents have revealed labelling of both tubulin subunits (Nasioulas *et al*, 1990; Sawada *et al*, 1993a), although more specific labelling of β -tubulin has also been observed. A photoreactive vinblastine analog labelled a peptide containing residues 175 - 213 of β -tubulin (Rai *et al*, 1996), while a

photoreactive rhizoxin analog labelled a β -tubulin peptide containing residues 363 - 379 (Sawada *et al*, 1993b). More recently, a photoreactive analog of dolastatin 10 labelled the amino-terminal peptide of β -tubulin (residues 2 - 31), although the specific amino acid could not be identified (Bai *et al*, 2004). Thus, as of yet the exact binding location for a “*Vinca*” domain agent on the tubulin dimer remains to be established.

1.2.4.3. Taxol-site agents

Taxol, a natural product, isolated from the pacific yew tree, *Taxus brevifolia*, is a potent inhibitor of higher and lower eukaryotic cells. It blocks mitosis at the metaphase-anaphase boundary and can lead to cell death by apoptosis (Torres *et al*, 1998). It is widely used for the treatment of breast, lung and ovarian cancer, as is its more soluble congener, Taxotere (Altmann, 2001). In contrast to colchicine and vinblastine, Taxol exerts its growth-inhibitory effects by promoting the assembly of tubulin dimers into microtubules and stabilising them against disassembly, thus suppressing microtubule dynamic behaviour (Ganesh *et al*, 2004). It binds to microtubules with an approximate stoichiometry of 1 mole of Taxol to 1 mole of tubulin dimer, although at substoichiometric concentrations it can suppress microtubule dynamics without greatly altering the polymer mass. The binding site of Taxol is in a hydrophobic pocket in the intermediate domain of β -tubulin (Fig. 1.3), situated on the luminal side of the microtubule wall (Nogales *et al*, 1998). Bound Taxol adopts a T-shaped or butterfly-like structure which permits intermolecular hydrophobic contact between the drug and β -subunit (Ganesh *et al*, 2004). A considerable number of residues are involved in these hydrophobic contacts with the aromatic rings of Taxol, especially those of the M-loop such as Pro274, Leu275 and Thr276 (Löwe *et al*, 2001). It has been proposed that the binding of Taxol to such residues acts to stabilise M-loop lateral contacts in the microtubule lattice, possibly counteracting the constraining conformational change that occurs in the β -subunit following GTP hydrolysis (see section 1.2.2.2) (Nogales, 2000). Interestingly, the equivalent pocket on α -tubulin is occupied by eight extra residues, which presumably prevent Taxol binding and possibly mimic the stabilising effect of Taxol between alpha monomers (Downing *et al*, 1999). Finally, other antimicrotubule agents such as the epothilones and sarcodictins have recently been discovered that exhibit a similar mechanism of action to Taxol and Taxotere and are believed to hold some

promise for cancer treatment (Ganesh *et al*, 2004; Amos, 2004).

1.2.4.4. Other agents

Various other classes of drug have displayed an anti-tubulin mechanism of action, but their binding sites remain to be elucidated. Among these classes are the benzimidazoles (e.g. albendazole, fenbendazole and mebendazole), which are used as anthelmintic agents (Lacey, 1988). The selective toxicity of such drugs results from their differential binding to host and helminth tubulins (Bell, 1998), although their binding site(s) have yet to be determined. Photolabelling studies with a fenbendazole derivative labelled recombinant *Haemonchus contortus* β -tubulin at residues 65 - 81 (Nare *et al*, 1996), while analysis of β -tubulin genes of benzimidazole-resistant nematodes have implicated the residue Phe200 in benzimidazole binding (Kwa *et al*, 1994). Despite their high efficacy against nematode and trematode parasites, benzimidazoles show poor activity against a range of protozoan parasites (reviewed by Werbovetz, 2002), which has hindered their development as effective antiprotozoal agents.

The dinitroaniline herbicides comprise another important class of microtubule inhibitor. They are widely used for pre-emergence weed control, producing gross morphological abnormalities in plant cells consistent with an antitubulin mechanism of action. They have little or no effect on the microtubules of mammalian cells, which has facilitated their safe use in the field (Anthony *et al*, 1999a). Dinitroanilines such as oryzalin and trifluralin have been shown to bind to plant but not animal tubulin and are believed to exert their activity by inducing net microtubule depolymerisation (Morejohn *et al*, 1991). Interestingly, dinitroanilines are also effective against a range of protozoan parasites including *Cryptosporidium parvum*, *Toxoplasma gondii*, *Leishmania major* and *Trypanosoma cruzi* (reviewed in Traub-Cseko *et al*, 2001). As in plants, the target of the dinitroanilines in protozoan parasites is believed to be tubulin. In agreement with this premise, oryzalin and a number of its analogs have been shown to inhibit the polymerisation of purified *Leishmania* tubulin *in vitro* suggesting that the selective inhibition of protozoal tubulin is possible (Werbovetz *et al*, 2003). To date, the location of the dinitroaniline binding site(s) on plant or parasite tubulins remains unknown. A number of mutations have been identified on both tubulin subunits that confer dinitroaniline resistance in plant cells (reviewed in Anthony *et al*, 1999a), but their relevance to the

antimitotic herbicide binding site remains unclear. Similarly, homology models of plant and parasite tubulins based on the crystal structure of the bovine tubulin heterodimer have facilitated the identification of a number of putative dinitroaniline-binding sites (Blume *et al*, 2003; Morrissette *et al*, 2004), yet direct experimental evidence of the correctness of these sites remains to be found.

1.3. MICROTUBULES IN *PLASMODIUM*

1.3.1. Tubulin: genes and proteins

To-date two α -tubulin (α I- (Holloway *et al*, 1989) and α II- (Holloway *et al*, 1990)), one β -tubulin (Delves *et al*, 1989, Sen *et al*, 1990, Wesseling *et al*, 1989) and one γ -tubulin (Maessen *et al*, 1993) genes from *P. falciparum*, a *P. berghei* β -tubulin gene (Belkum *et al*, 1991) and two incomplete *P. yoelii* α -tubulin genes (Akella *et al*, 1988) have been cloned and characterised. Apart from γ -tubulin, all other tubulin genes of *P. falciparum* contain two introns, which are in identical positions in α I and α II, but not β . All tubulin genes are unlinked, single copy genes in *P. falciparum*, in contrast to the multiple tubulin genes of mammalian cells or the clusters of tandemly repeated α/β -tubulin genes in other protozoan parasites such as *Trypanosoma brucei* or *Leishmania* species (Gull, 1999). By Northern blot (Delves *et al*, 1990) and microarray analysis (Le Roch *et al*, 2003) α I-, α II-, and β -tubulin-encoding transcripts have been detected in most stages of the parasite's asexual development cycle, as well as in sporozoites and sexual-stage gametocytes. While Delves and co-workers demonstrated an abundance of α I- and β -tubulin mRNA in ring and trophozoite stages (Delves *et al*, 1990), Calvo and co-workers found maximum expression of β -tubulin mRNA in the schizont stage of parasite development (Calvo *et al*, 2002). Similarly, microarray analysis has revealed maximum expression α I- and β -tubulin mRNA in the late trophozoite and early schizont stages of the parasite's asexual development cycle (Le Roch *et al*, 2003).

The two *P. falciparum* α -tubulins share ~ 94% identity at the amino acid level and both have ~ 40% identity to β -tubulin. They are also very similar to tubulins from most other organisms, with the major amino acid differences found in the last 15 residues of the C-terminal tails. For example, *P. falciparum* β -tubulin shares ~ 88 % identity with human β -tubulin, while α I- and α II-tubulins are slightly less similar to human α -tubulin, sharing ~ 83% and ~ 82%, identity, respectively. Expression of

α I- (Sinou *et al*, 1998; Read *et al*, 1993; Fowler *et al*, 2001), β - (Bell *et al*, 1995) and γ -tubulin (Fowler *et al*, 2001) at the protein level has been detected by western immunoblotting in asexual erythrocytic parasites. α I-tubulin was found to be most abundant in schizont-stage parasites, with a weak quantity detected in rings and trophozoites (Sinou *et al*, 1998), while γ -tubulin was detected in schizonts and merozoites but not trophozoite-stage parasites (Fowler *et al*, 2001). Western immunoblotting has also revealed that α II-tubulin expression is confined to the sexual stages of *P. falciparum* development and is present specifically in male gametocytes, gametes and newly formed zygotes (Rawlings *et al*, 1992). To-date, no post-translational modifications of *P. falciparum* tubulins have been reported. Immunofluorescence experiments suggested that the terminal tyrosine residue of α I-tubulin in asexual stage parasites was unmodified, while western immunoblotting indicated that lysine 40 of α I-tubulin remained unacetylated (α II-tubulin contains a glutamine residue at position 40) (Read *et al*, 1993). As of yet, native tubulin has not been purified from *P. falciparum*, thus hindering its structural, biochemical and pharmacological characterisation. Although recombinant *P. falciparum* β -tubulin was expressed in *Bacillus brevis*, it could not be purified (Bell *et al*, 1995), while the functional characterisation of partial, recombinant α I- and α II-tubulins expressed as fusion proteins in *E. coli* was not reported (Rawlings *et al*, 1992).

1.3.2. Functional classes of microtubules in *Plasmodium*

The microtubules of *Plasmodium* species have not been investigated in nearly as much detail as their mammalian counterparts. However, studies employing cell biology techniques such as electron and immunofluorescent microscopy have revealed the presence of at least three functional classes of microtubules in *Plasmodium* species, namely the mitotic microtubular spindles, the subpellicular microtubules and the axonemal microtubules (reviewed in Bell, 1998). With the recent identification of the microtubule-associated motor proteins kinesin and dynein in various stages of the parasite's asexual cycle (Fowler *et al*, 2001) it may be reasonable to assume that a cytosolic microtubular cytoskeleton may also exist for the transport of various cellular vesicles and organelles.

The mitotic microtubular spindles have been identified in exoerythrocytic (Suhrbier *et al*, 1993) and erythrocytic schizonts (Read *et al*, 1993), male gametocytes, zygotes and oocysts (Sinden *et al*, 1978) and play a pivotal role in cell

division and cytokinesis (see Fig. 1.2. for overview of stages of development of *Plasmodium* species). The spindle (actually half-spindle or hemispindle) microtubules are nucleated from a MTOC, which in most stages take the form of a centriolar plaque embedded in a pore in the nuclear membrane (Read *et al*, 1993). The nuclear membrane remains intact during the process of mitosis, except for where the centriolar plaque is located. The hemispindle is subsequently split into two daughter hemispindles during the duplication of the centriolar plaque, which then migrate along the nuclear membrane until both plaques are located in nearly opposite positions. The daughter hemispindles combine to produce the complete mitotic spindle which consists of three sets of microtubules in the case of sporogony in *P. berghei*, namely those connecting each kinetochore to either spindle pole body, those extending from pole to pole of the spindle (astral microtubules) and those that radiate from either pole to a location somewhere beyond the equatorial plane of the spindle (reviewed in Morrissette *et al*, 2002). Interestingly, the centriolar plaques do not have to be aligned directly opposite each other for the successful movement of chromosomes along the spindle microtubules in *P. falciparum* (Read *et al*, 1993). There are on average four nuclear divisions in various *Plasmodium* species and each division in the schizont does not appear to be synchronous (i.e. mitotic spindles at different stages of division can be observed in a single nucleus) (Vickerman *et al*, 1967; Canning *et al*, 1973; Read *et al*, 1993). Such asynchrony of division is in contrast to most models of mitosis in eukaryotic cells and the reasoning for its occurrence has yet to be determined. Following erythrocytic schizogony, the mitotic microtubular apparatus is reorganised into structures that are believed to assist in the separation of daughter cells (merozoites) and their organelles (Read *et al*, 1993; Morrissette *et al*, 2002). Similarly, post-mitotic microtubule-associated structures have also been observed following schizogony and sporogony in *P. berghei* and after gametogenesis in *P. yoelii* (Sinden *et al*, 1976).

A second class of functional microtubules, the subpellicular microtubules, has been identified in most stages of the parasites development cycle, including erythrocytic segmenters, extracellular merozoites, both micro- (male) and macro- (female) gametocytes as well as in the ookinete and sporozoite (Bell, 1998). In general, they extend longitudinally from the cell apex, displaying a banana-like profile (see Fig. 1.7. for schematic representation) that intimately tethers the pellicular membranes (series of flat vesicles found below the plasma membrane that

comprise the so-called internal membrane complex), providing shape, integrity and apical polarity in the parasite cell. Their arrangement can vary greatly among *Plasmodium* species both in microtubule number and in length. For example, the number of subpellicular microtubules in the merozoite of *P. falciparum* is relatively minimal, consisting of a narrow band of 2 - 3, (designated f-MAST [falciparum merozoite assemblage of subpellicular microtubules] (Fowler *et al*, 1998)) compared to the more extensive array of ~ 60 in the *Plasmodium* ookinete (Aikawa, 1967 and 1971). Despite their reduced number, *P. falciparum* subpellicular microtubules appear to play a crucial role in the transportation of micronemes to the anterior end of the merozoite, where they appear to associate with the twin rhoptries in readiness for secretion and erythrocyte invasion (Bannister *et al*, 2003). Microtubule inhibitors have previously been shown to depolymerise the f-MAST (Fowler *et al*, 1998) and prevented merozoite invasion of uninfected erythrocytes (Bejon *et al*, 1997; Fowler *et al*, 1998), possibly due to a failure in microneme trafficking. Interestingly, merozoites of other *Plasmodium* species have a greater complement of subpellicular microtubules than the minimal set of *P. falciparum* (Aikawa, 1967).

A third class of microtubules together with a number of accessory proteins are found to constitute the axoneme of the male gamete flagella, which facilitate parasite motility. They form during the process of gametogenesis, when eight axonemes of varying length which display the characteristic “9 + 2” arrangement of microtubules radiate from the cytosol of the male gametocyte (see Fig. 1.7A) (reviewed in Tilney *et al*, 1996). This process is soon followed by the release of eight motile male gametes each harbouring a single flagellum, which swim to the female gamete in the mosquito midgut to carry out fertilisation.

1.3.3. Effects of microtubule inhibitors on *Plasmodium*

As in mammalian cells, microtubule inhibitors have also played an important role in elucidating the functions of microtubules in various *Plasmodium* species and may even comprise an avenue for antimalarial chemotherapy. Their effects have mainly been studied on parasites in culture, as there have been no reports outlining the purification of native malarial parasite tubulin for use in drug-binding studies. The following is a brief outline of what is known pertaining to the effects of various classes of microtubule inhibitor on *Plasmodium* species (reviewed in Bell, 1998).

1.3.3.1. Colchicine-site agents

In contrast to mammalian cells, *Plasmodium* species are relatively insensitive to the *Colchicum* alkaloids. Colchicine has an IC₅₀ of between 10 - 13 µM against erythrocyte-stage *P. falciparum*, while the related compound Colcemid is even less potent with an IC₅₀ between 10 - 110 µM (Bell, 1998). Gametocytes of *P. falciparum* are also relatively insensitive to colchicine (Sinden *et al*, 1979), while concentrations in the high micromolar range are generally required to inhibit microgametogenesis in *P. yoelii nigeriensis* (Sinden *et al*, 1985) and the transformation of the avian malaria parasite *P. gallinaceum* zygotes into ookinetes (Kumar *et al*, 1985). In the latter study, colchicine (25 µM) treatment of the *Plasmodium* zygote resulted in microtubule depolymerisation.

Interestingly, colchicine appears to exert its inhibitory effects on the process of merozoite invasion rather than on schizont development in asexual parasites. Concentrations of colchicine as high as 10 mM had no effect on schizont development and merozoite formation while inhibition of merozoite invasion into erythrocytes occurred at concentrations between 10 µM - 1 mM (Bejon *et al*, 1997). Erythrocytes pre-incubated in colchicine and subsequently washed also had no effect on invasion. Moreover, Fowler and co-workers have confirmed that the merozoite f-MAST is the target of colchicine inhibition (Fowler *et al*, 1998). They showed that the number and length of f-MASTs were reduced in colchicine-treated merozoites, albeit at high concentrations (500 µM) and that colchicine inhibition of invasion was reduced by the Taxol-stabilisation of the f-MAST prior to colchicine exposure. Thus, despite the fact that *Colchicum* alkaloids at relevant concentrations can inhibit other cellular processes unrelated to microtubule function (section 1.2.5.1) such as protein synthesis in *P. falciparum* (Bell *et al*, 1993), it would appear that the f-MAST is the likely target of colchicine action. However, as colchicine is active in mammalian cells at submicromolar concentrations it would appear that significant differences may exist between the colchicine-binding affinities of mammalian and *P. falciparum* tubulins.

1.3.3.2. “Vinca” domain agents

The “*Vinca*” domain agents vinblastine and vincristine inhibit the growth of *P. falciparum* more potently than the *Colchicum* alkaloids. Vinblastine has an IC₅₀ of between 0.028 - 1.7 µM against asexual erythrocytic forms of *P. falciparum*, while

vincristine is even more potent with an IC_{50} of between 6 - 7 nM (Bell, 1998). However, both compounds display similar toxicity to mammalian cells, thus hindering their development as potential antimalarial agents. Vinblastine exerts its effect when added to the trophozoite stage of parasite development (Usanga *et al*, 1986) and appears to cause gross microtubule depolymerisation and loss of microtubule-containing structures in the parasite cell (Bell, 1998). Similarly, treatment of *P. yoelii nigeriensis* with vinblastine inhibited male gametogenesis and caused a loss of spindle and axonemal microtubular structures as observed by electron microscopy (Sinden *et al*, 1985). Thus, it seems as in the case of mammalian tubulin, that *Plasmodium* tubulin contains a vinblastine binding-site.

1.3.3.3. Taxol-site agents

Taxol has an IC_{50} of between 0.071 - 1.0 μ M against asexual erythrocytic forms of *P. falciparum*, while its semisynthetic derivative Taxotere is even more potent with an IC_{50} range of 3.1 - 5 nM. However, both agents display unusual dose-response curves after 48 h incubation and must be exposed to asynchronous cultures of *P. falciparum* for over 72 h to reveal their full inhibitory effects (Pouvelle *et al*, 1994; Schrével *et al*, 1994). Both agents also display antimalarial activity in animal rodent models of malaria, albeit at doses closest to the maximum tolerable (Pouvelle *et al*, 1994; Sinou *et al*, 1996). Although both agents are less toxic to some mammalian cell lines, the narrowness of the therapeutic window has prevented their development as potential antimalarial agents.

Taxol exerts its inhibitory effects when applied before parasite schizogony (i.e. ring and trophozoite stages) in contrast to Taxotere, which is most effective when applied to schizonts and segmenters, suggesting that these agents may display differential uptake kinetics. However, higher concentrations of Taxotere (> 1 μ M) prevented maturation of ring-stage parasites and the preincubation and subsequent washing of erythrocytes with the same agent inhibited parasite invasion (Schrével *et al*, 1994). The later observation suggests that parasite inhibition could result from specific interactions between the erythrocyte and Taxotere. Electron and immunofluorescent microscopy studies have revealed that both agents cause a loss of normal microtubular structures in the parasite cell, in particular the dynamic mitotic spindles, which are replaced by abnormal, thick rods of polymerised tubulin (Bell, 1998; Sinou *et al*, 1998). Similar structures have also been observed upon

application of Taxol to cultures of *P. gallinaceum* ookinetes (Kumar *et al*, 1985). Another effect of Taxol-stabilised microtubules on asexual erythrocytic parasites would appear to be in the prevention of migration of nuclear material into the daughter merozoites as well as merozoite release from the mother schizont during merogony (Taraschi *et al*, 1998). Overall, these results would suggest that *Plasmodium* tubulin probably contains a suitable Taxol-binding site.

1.3.3.4. Other agents

While a number of other microtubule inhibitors have been reported to inhibit *P. falciparum* growth, none has displayed superior or even similar levels of potency to those of the “*Vinca*” alkaloids or Taxoids. One class, however, the dinitroaniline herbicides, which includes compounds such as trifluralin, oryzalin, and pendimethalin, has displayed selective antimalarial activity at low micromolar concentrations. Trifluralin has been shown to inhibit both asexual and sexual forms of *P. falciparum* in culture in the micromolar and nanomolar range, respectively, as well as completely inhibiting the sexual development of the parasite in the mosquito midgut (Nath *et al*, 1994). In gametocytes, trifluralin (5 μ M) resulted in fragmentation and dissolution of the subpellicular microtubules with an apparent increase in microtubule diameter while in *P. falciparum* merozoites it resulted in depolymerisation of the f-MAST, albeit at much higher concentrations (0.1 - 1.0 mM) (Fowler *et al*, 1998). Moreover, depolymerisation of the f-MAST with trifluralin does not appear to affect the merozoite location of kinesin and dynein, suggesting that the motor proteins can shuttle their cargo by random diffusion (Fowler *et al*, 2001). Although dinitroanilines have also displayed antimalarial activity against *P. berghei* in culture, they failed to retain their antimalarial activity in a rodent model of malaria, possibly due to their poor solubility (Dow *et al*, 2002). However, given their selective mode of action, derivatives of the dinitroanilines with more favourable pharmacokinetic profiles and more potent antimalarial activity may yet offer hope as potentially useful antimalarial agents.

1.4. PROJECT OBJECTIVES

The potent antimalarial activity of certain classes of microtubule inhibitor demonstrates the importance of the microtubule lattice to parasite development and multiplication. Despite the conserved nature of its composite protein tubulin, there

are interspecies differences in microtubule composition and function, making it possible selectively to target parasite tubulin (Lacey, 1988).

The work documented in this thesis was undertaken to investigate whether microtubules represent a possible target for antimalarial chemotherapy. This project had three main aims:

- 1) to evaluate the antimalarial activity of certain novel and existing microtubule inhibitors and to characterise their effects at the cellular level;
- 2) to investigate the stage-dependent production and electrophoretic behaviour of tubulins in *P. falciparum*;
- 3) to characterise the functionality and drug-binding properties of recombinant forms of *P. falciparum* tubulins.

Chapter 2

Materials and Methods

2.1. CHEMICALS, REAGENTS AND INHIBITORS

Chemicals and reagents used in this project were purchased from Sigma-Aldrich (Dublin, Ireland), unless otherwise stated. All general chemicals were of analytical grade. The grade of water used was filter-sterile, double deionised (ddH₂O), and was dispensed from a Milli-Q Synthesis A10 (Millipore, Billerica, Massachusetts, USA). Dolastatin 10, auristatin PE and related compounds were provided by Prof. G. R. Pettit, Cancer Research Institute, Arizona State University, Tempe, AZ, USA. Trifluralin and derivatives were obtained from Dr Fyaz M.D. Ismail, Liverpool John Moores University, UK. RIG-plasmid was a kind gift obtained from Prof. W. G. J. Hol, University of Washington, Seattle, WA, USA. α -tub II (anti GYE) male-gamete-specific rabbit antiserum was obtained from the MR4/American Type Culture Collection, University Blvd., Manassas, VA, USA. All reagents used during electrophoresis were of electrophoresis grade, unless otherwise stated. All chemicals used for cell culture were of cell culture grade.

2.2. CULTURE OF *PLASMODIUM FALCIPARUM*

2.2.1. Routine culture

Plasmodium falciparum FCH5.C2 (chloroquine sensitive), a cloned subline of strain FCH5/Tanzania, and K1/Thailand were adapted to grow in medium containing horse serum (Bell *et al*, 1993). Both strains were maintained in continuous culture in human erythrocytes (obtained from the National Blood Centre, Dublin, as needed) at 2.5% or 5% (v/v) haematocrit, according to the method of Trager and Jensen (Trager and Jensen, 1976). Whole blood was washed weekly using a Sorvall RT6000D benchtop centrifuge (Du Pont Ltd., Stevenage, Herts, UK), by centrifuging at 1500 rpm (487.5 x g) at 4°C for 10 min, removing the buffy coat, washing twice in sterile, cold phosphate-buffered saline (PBS) (OXOID Ltd., Basingstone Hampshire, UK), and once in complete culture medium by centrifuging as before and removing the buffy coat each time. Washed erythrocytes were resuspended to 50% haematocrit in complete culture medium and stored at 4°C. A sample of washed erythrocytes was added to complete medium and incubated at 37°C for 24 hours after which Giemsa-stained smears were prepared to check for the presence of yeast or bacterial contamination. Smears were made on twin frosted microscope slides (76 x 26 mm) (Western Laboratory Service, Aldershot,

Hampshire, UK) which were stained with a 1:10 dilution of Giemsa stain (Fluka Chemie AG, Buchs, Switzerland) in Giemsa buffer (1% (w/v) Na₂HPO₄·2H₂O, 1% (w/v) KH₂PO₄). Strains were cultured routinely in complete medium, pH 7.0, which consisted of RPMI 1640 medium, supplemented with 25 mM HEPES, 0.01% (v/v) neomycin sulphate, 0.18% (w/v) sodium bicarbonate, 50 µg/ml hypoxanthine and 10% (v/v) horse serum (heat-inactivated at 56°C for 1 h). Parasites were cultured in petri dishes (Sarstedt Ltd., Driminagh, Co. Wexford) at 37°C in a candle jar with reduced O₂ tension. Parasitemia was observed by microscopic assessment of Giemsa-stained smears and routine cultures were diluted with fresh erythrocytes twice a week or as needed, and culture medium was replaced depending on parasitemia. *P. falciparum* 3D7 was cultured as outlined for the previous two strains except for the following modifications: (i) complete medium contained 5% (w/v) Albumax (Gibco, Paisley, UK) instead of horse serum and 0.002% (w/v) gentamicin instead of neomycin; (ii) human erythrocytes were pre-treated with 10% (v/v) PIGPA (0.55% (w/v) sodium pyruvate, 1.34% (w/v) inosine, 1.8% (w/v) glucose, 7.1% (w/v) disodium hydrogen phosphate, 0.07% (w/v) adenine, 0.9% (w/v) sodium chloride) at 37°C for one hour with periodic agitation and subsequently centrifuged at 1500 rpm (487.5 x g) at 4°C for 10 min before commencing washing steps with PBS and complete medium.

2.2.2. Gametocyte culture

P. falciparum NF54 was maintained in continuous culture as outlined in section 2.2.1 for FCH5.C2 and K1/Thailand. Gametocytes were generated according to the methods of Trager and Jensen (1976) and Ifediba and Vanderberg (1981). Initial asynchronous cultures (parasites predominantly in the asexual stage of development) of 2.5% parasitemia were maintained over a 10-day period with a daily change of complete medium at identical time points, without provision of fresh erythrocytes. Development of gametocyte stages over this period was monitored by microscopic evaluation of Giemsa-stained smears. Parasites which had progressed to stages I - III (day 7 of culture) and stages IV - V (day 10 of culture) of gametocyte maturation were harvested as outlined in section 2.2.4.

2.2.3. Synchronisation of cultures

Routine cultures typically consist of an asynchronous population of parasites

i.e. rings, trophozoites, schizonts, segmenters and merozoites. Parasites were synchronised using two-step sorbitol treatment (Lambros and Vanderberg, 1979) to produce eight populations, which had age ranges of approximately six hours, which covered the parasite's whole developmental cycle within the erythrocyte. Cultures to be synchronised were resuspended, centrifuged at 2000 rpm (650 x g) at room temperature for 10 min, the supernatants removed and the resulting pellets resuspended in warm filter-sterilised 5% (w/v) D (-) sorbitol (Merck, Darmstadt, Germany) and left at room-temperature for 5 min to kill trophozoite, schizont and segmenter parasites by osmotic lysis of their host erythrocytes. The suspension was centrifuged again, the resulting supernatant removed, and the pellet resuspended in warm wash medium (RPMI 1640 medium supplemented with 25 mM HEPES, 0.18% (v/v) sodium bicarbonate, 50 µg/ml hypoxanthine). The suspension was re-centrifuged and the resulting pellet resuspended in complete culture medium to 2.5% haematocrit and cultured as normal. One round of sorbitol treatment is estimated to reduce the age of the culture from 0 - 48 h to ~ 0 - 20 h post-invasion. Highly synchronised cultures were created by repeating sorbitol treatment twice, 36 hours apart, followed by parasite maturation for an additional 48, 54, and 60 hours (for rings ~ 0 - 6, 6 - 12, and 12 - 18 h post-invasion), 66, 72, and 78 hours (for trophozoites ~ 18 - 24, 24 - 30, and 30 - 36 h post-invasion) and finally 84 and 90 hours (for schizonts/segmenters ~ 36 - 42 and 42 - 48 h post-invasion) for use in microtubule inhibitor stage-specific susceptibility assays as described in section 2.4.2 and harvesting of parasites as described in section 2.2.4.

2.2.4. Harvesting of parasites

Parasites were released from erythrocytes by the saponin treatment method of Zuckerman (1967). Cultures of between 5 and 20% parasitemia, 2.5% haematocrit, were resuspended and washed twice in ice-cold PBS and pelleted by centrifugation at 2000 rpm (650 x g) at 4°C for 10 min using a Sorvall RT6000D benchtop centrifuge. Pellets were resuspended in 0.05% (w/v) saponin in ice-cold salt sodium citrate (SSC) (150 mM NaCl, 15 mM sodium citrate, pH 7.0) buffer for 20 min on ice with vigorous shaking every 5 min for 30 s to rupture erythrocyte membranes and to release parasites. Liberated parasites were pelleted by centrifugation for 15 min at 3000 rpm (975 x g) at 4°C and washed twice with ice-cold SSC to remove lysed erythrocytes. Parasite pellets were resuspended in PBS containing 9.5% (v/v)

glycerol, 1 µg/ml pepstatin A, 21 µg/ml leupeptin and 2 mM phenylmethylsulphonyl fluoride (PMSF). Parasite preparations were divided into 50 µl - 500 µl portions, snap frozen in liquid nitrogen and stored at -70°C in a freezer (Revco Ltd., Asheville, NC, USA).

2.3. PREPARATION OF FRACTIONS OF HARVESTED PARASITES

2.3.1. Preparation of whole cell extracts

Harvested parasites (gametocytes, synchronous or asynchronous populations) (see section 2.2.4.) were thawed on ice to minimise protease activity and lysed in 0.5% (w/v) Triton X-100 for 30 min on ice with agitation every 10 min to improve the release of membrane-bound proteins. Insoluble debris was removed by centrifugation for 5 min at 4°C at 14,000 rpm (18,000 x g) using a Sigma 1-15 microfuge. The resulting supernatant was clarified twice more by this process. Pellets were resuspended in PBS, pooled together and defined as the “insoluble fraction”. The final supernatant was defined as the “whole cell extract” and its protein concentration was determined by the Bradford method (see section 2.6.1).

2.3.2. Isolation of RNA

Total RNA was isolated from *P. falciparum* K1/Thailand with RNA ISOLATOR™ (Genosys Biotechnologies Inc., Cambridge, UK) according to manufacturer’s instructions. Briefly, 200 µl of frozen parasite suspension (section 2.2.4) were thawed on ice, 1 ml of RNA ISOLATOR added and the sample was homogenised for 5 min at room temperature to permit complete dissociation of nucleoprotein complexes. Phase separation was achieved by adding 0.2 ml of chloroform to the homogenate, shaking the sample gently for 15 s and incubating the sample at room temperature for 15 min. Following centrifugation at 11,500 rpm (12,000 x g) for 15 min at room temperature, the homogenate separated into a lower, red, phenol-chloroform phase, an interphase, and an upper, colourless, aqueous phase. RNA remains exclusively in the aqueous phase. The aqueous phase was transferred to a fresh tube, mixed with 0.5 ml of isopropanol, and the RNA was precipitated by centrifugation at 11,500 rpm (12,000 x g) for 10 min. The RNA pellet was washed with 75% (v/v) ethanol, centrifuged at 9000 rpm (7,500 x g) for 5 min at 4°C, the ethanol was aspirated off, and the pellet was resuspended in ddH₂O

previously treated with 0.1% (v/v) diethylpyrocarbonate (DEPC) to inhibit RNases. The quality of the isolated RNA was analysed by agarose gel electrophoresis as outlined in section 2.5.2.

2.4. ASSESSMENT OF ANTIMALARIAL ACTIVITY OF MICROTUBULE INHIBITORS

2.4.1. Inhibition of parasite proliferation assessed using the lactate dehydrogenase (pLDH) method

Effects of microtubule inhibitors on *P. falciparum* growth in culture were determined using the spectrophotometric parasite lactate dehydrogenase (pLDH) assay of Makler *et al* (1993). The assay is based on measurement of the biochemical reaction in which the parasite LDH has the ability to utilise 3-acetyl pyridine adenine dinucleotide (APAD) as a co-factor in the conversion of lactate to pyruvate. Human erythrocyte LDH is also able to use APAD, but only to a very small extent. In a typical assay, asynchronous parasite cultures of 0.8% parasitemia, 2% haematocrit were grown in complete medium containing titrations of inhibitors in 96-well flat-bottom culture plates (Sarstedt Ltd., Drimnagh, Co. Wexford) for 48 - 72 h. Dimethylsulphoxide (DMSO) (BDH Laboratory Supplies, Poole, UK) alone was diluted in culture medium and added to cultures at a similar percentage (v/v) as used for inhibitor studies as a control for the solvent in which the inhibitor stock solutions were prepared. After 48 and 72 h, 10 µl samples of parasitised erythrocytes were removed and their pLDH activities were determined by mixing the samples with 50 µl of Malstat (Flow Inc., Portland, OR, USA), which provides APAD and L-lactate substrate. pLDH is secreted by the parasites into the extracellular environment resulting in the production of pyruvate and reduced APAD. 10 µl of nitro blue tetrazolium (NBT) : phenazine ethosulfate (PES) (ratio 1 : 1 of NBT (2 mg/ml) and PES (0.1 mg/ml)), were added to each sample, forming a blue formazan product in the presence of reduced APAD that was detected using a Titertek Multiskan[®] Plus spectrophotometer (Eflab, Finland) at 650 nm. The resulting absorbance is proportional to pLDH activity, which correlates with parasite growth (Makler *et al*, 1993). Uninfected erythrocytes were used as controls to determine the background level of LDH secreted by human erythrocytes. Parasites cultured in the absence of inhibitors were used as controls for the measurement of uninhibited pLDH activity.

All inhibition assays were repeated three times in duplicate. Dose-response curves for each drug were created from the averages of absorbance readings, and the median inhibitory concentrations (IC₅₀) were determined graphically.

2.4.2. Effects of inhibitors on synchronised cultures of different initial ages

The influence of the initial age of a culture on susceptibility to microtubule inhibitors was determined using the pLDH method as outlined in section 2.4.1. Parasite cultures synchronised to produce eight populations with age ranges of ~ 6 h covering the whole parasite erythrocytic cycle (0 - 6, 6 - 12, 12 - 18, 18 - 24, 24 - 30, 30 - 36, 36 - 42, 42 - 48 [hours post-invasion as described in section 2.2.3.]) were exposed to serial two-fold dilutions of dolastatin 10 (7.8 nM - 0.01 nM), auristatin PE (125 nM - 0.24 nM), vinblastine (Sigma, Dublin) (16,000 nM - 31.25 nM) or Taxol (ICN Biomedicals Inc., Aurora, Ohio, USA) (8000 nM - 15.62 nM) in growth medium at 2.0% haematocrit and 0.8% parasitemia. After 48 h incubation, samples of parasitised erythrocytes were taken and pLDH activity was determined. All experiments were repeated three times. Dose response curves were constructed and IC₂₅, IC₅₀ and IC₇₅ were determined for the eight initial parasite ages tested.

2.4.3. Effects of inhibitors on parasite morphology

Parasite cultures synchronised to the early trophozoite stage (18 - 24 h post-invasion) were established in 24-well microculture plates at 3.0% parasitemia and 5.0% haematocrit. Cultures were treated with 4 - 8 x IC₅₀ concentrations of each inhibitor (0.8 nM dolastatin 10, 2.0 µM vinblastine, and 480 nM Taxol). Untreated cultures established in the corresponding concentration of the inhibitor vehicle DMSO were also included. Plates were incubated at 37°C and after incubation for 6, 12, 24, 30, 42 and 48 h, samples of parasitised erythrocytes were removed and used to make duplicate Giemsa-stained smears (see section 2.2.1). Smears were examined by light microscopy at 1000 X magnification using a Nikon SE microscope (The Micron Optical Co. Ltd, Co. Wexford) for obvious morphological or developmental abnormalities of parasites, and for calculating parasitemias of inhibitor-treated and control parasites. Photographs were taken with a Nikon Coolpix 950 digital camera using full auto-exposure mode and Best Shot Selection attached to a Nikon Eclipse E400 microscope (The Micron Optical Co. Ltd.).

2.4.4. Activity of inhibitors on different developmental stages

For determination of susceptibility of different stages, parasites were synchronised and grown to 6 - 12, 21 - 27, 36 - 42 h post-invasion (see section 2.2.3) and 1 ml of the cultures at 2.5% haematocrit and 2% parasitemia were exposed to inhibitors at $\sim 8 \times IC_{50}$ (see section 2.4.4) or corresponding concentrations of DMSO, for 6 h. Cultures were then washed three times in 10 ml of warm wash medium and recultured for 48 h in inhibitor-free medium, with a change of medium after 24 h. After incubation, samples of parasitised erythrocytes were removed and used to make Giemsa-stained smears as described in section 2.2.1. Slides were prepared in duplicate and the parasitemia of at least 1000 erythrocytes was counted on each slide.

2.4.5. Effects of inhibitors on mitotic microtubular structures

Analysis of *P. falciparum* tubulin-containing structures by immunofluorescent microscopy was performed by a technique developed by A. Bell (Fennell *et al*, 2003). Cultured parasites at 10 - 15% parasitemia, 5% haematocrit were exposed to inhibitors (1 nM dolastatin 10, 10 nM auristatin PE, 20 μ M vinblastine, 1 μ M Taxol, 20 μ M trifluralin, chloralin, oryzalin or amiprophos-methyl, or corresponding concentrations of DMSO alone) in 24-well dishes for 6 h. 150 μ l portions were subsequently removed into 9 volumes of warm wash medium and centrifuged at 1500 rpm (800 x g) for 5 min. Erythrocyte pellets were then resuspended in 140 μ l of wash medium. Eight-millimeter diameter windows of printed slides (Hendley, Essex, UK), were coated for 10 min with 1 mg/ml poly-L-lysine and washed twice before application of 20 μ l of fixative (4% (w/v) paraformaldehyde, 0.2% (v/v) Triton X-100 in PBS). 10 μ l of parasitised erythrocyte suspension were then mixed into each drop of fixative and slides were left for 30 min in a moist chamber at room temperature. Parasite-coated windows were then subjected to the following steps, using a capillary pipette under vacuum for changing the solutions: (1) washing 5 x 3 min in PBS; (2) blocking overnight at 4°C in 5% (v/v) goat serum in PBS; (3) probing for 1 h with primary antibody (affinity-purified rabbit antiserum to a synthetic *P. falciparum* β -tubulin peptide, as in section 2.7.9); (4) washing as in step 1; (5) probing for 1 h with secondary antibody (anti-rabbit Ig conjugated to fluorescein isothiocyanate); (6) washing as in step 1; (7) probing with the fluorescent DNA dye 4',6-diamidino-2-phenyl-indole (DAPI; 1 μ g/ml in ddH₂O); (8) washing 2 x 30 s in PBS; and (9) mounting under a coverslip with either 5.0 mg/ml n-

propylgallate, 90% (v/v) glycerol, 100 mM Tris-HCl, pH 8.0 or VECTASHIELD® (Vector Laboratories Inc., Burlingame, CA, USA). Photographs were taken with either a Nikon Coolpix 950 or DXM 1200 digital camera as outlined in section 2.4.3.

2.5. CLONING OF *P. FALCIPARUM* α I- AND β -TUBULIN GENES

2.5.1. Amplification of *P. falciparum* α I- and β -tubulin genes by reverse-transcriptase polymerase chain reaction (RT-PCR)

DNA encoding *P. falciparum* tubulin genes contains non-coding introns. So RNA was isolated from parasites to synthesise cDNA by reverse transcription. Two-stage RT-PCR was performed on total RNA previously isolated from *P. falciparum* (section 2.3.2). Firstly, cDNA synthesis was performed on ~ 2 μ g RNA in the presence of 0.01 units of oligo (dT)₁₂₋₁₈ primer (Roche Diagnostics Ltd., Lewes, East Sussex, UK), 10 mM dithiothreitol (DTT) (Roche), 0.2 mM of each dNTP (Roche), 34 units of RNAGuard (Pharmacia), 27 units of avian myeloblastosis virus (AMV) reverse transcriptase (Roche) and AMV buffer (Roche). Samples were incubated at 42°C for 45 min, followed by 5 min at 95°C to inactivate the enzyme. The second stage of RT-PCR (amplification of the cDNA) used the primers 5'-GCGGGCGCCAATGAGAGAAGTAATAAGTATCCA-3' and 5'-GCGGGATCCTAATAATCTGCTTCATATCCTTC-3' for amplifying the α I-tubulin gene and 5'-GCGGGCGCCAATGAGAGAAATTGTTCATATTCAA-3' and 5'-GCGGGATCCTTAGGCTTCTACGTCTCCTTC-3' for amplifying the β -tubulin gene. Primers for both tubulin genes were designed to incorporate *Nar*I and *Bam*HI restriction endonuclease sites into the PCR fragment at the 5' and 3' ends, respectively, to facilitate subsequent cloning into the pTrp2 expression vector (see section 2.5.4). "Hot-start" PCR was performed using ~ 3 μ g cDNA, ~ 0.4 μ M of the appropriate primers, 2.5 units of *Pfu* Turbo DNA polymerase (Stratagene, La Jolla, California, U.S.A.), 0.2 mM each of dATP, dTTP, dGTP and dCTP (Roche) and *Pfu* Turbo buffer in a Hybaid thermocycler. The programme used for PCR was: denaturation at 95°C for 5 min; followed by 28 cycles of denaturation at 95°C for 30 s, annealing at 55°C for 1 min and extension at 72°C for 3 min; with a final extension at 72°C for 7 min.

2.5.2. Visualisation of DNA by agarose gel electrophoresis

DNA preparations (PCR products, DNA base pair markers (X, XIV (Boehringer Mannheim, Mannheim, Germany)), purified plasmids, restriction enzyme-treated plasmids and PCR fragments) were examined by mixing 5 - 10 µl of sample with 1 - 2 µl of loading buffer (0.25% (w/v) bromophenol blue, 0.25% (w/v) xylene cyanol FF, 30% (v/v) glycerol, 10 mM EDTA) and running through a 1% (w/v) agarose gel prepared in tris acetate EDTA (TAE) buffer (40 mM Tris-HCl, 2 mM EDTA, 1 mM glacial acetic acid). Samples were resolved by electrophoresis at 100 V in the direction from the anode to the cathode until the desired degree of separation was achieved (as judged by visual inspection of the migration of the separating dyes). The running buffer for electrophoresis was TAE buffer. Gels were stained in ethidium bromide (1.0 µg/ml) for 15 - 30 min, rinsed in ddH₂O and the DNA was visualised and photographed by exposing the gel to ultraviolet (UV) light using an AlphaImager 2200 gel imaging system (Alpha Innotech Corporation, San Leandro, California, USA).

2.5.3. Purification of PCR products

PCR products were purified (from excess dNTP's, polymerases, salts and excess primers) by one of two kits both based on glass fibre membranes that affinity purify the DNA. For PCR products where only one band was observed from ethidium-bromide-stained gels, a High Pure™ PCR product purification kit (Roche) was used for purification of the DNA directly from the PCR sample according to manufacturer's instructions. A PerfectPrep Gel Cleanup purification kit (Eppendorf, Hamburg, Germany) was also used in certain cases for the purification of excised PCR products from agarose gels (e.g. PCR products with 3' recessed ends filled in with the Klenow fragment of DNA polymerase (see section 2.5.5)).

2.5.4. Generation of pTrp2-βTub

pTrp2 plasmid (a kind gift from Pharmacia and Upjohn, Kalamazoo, MI, USA) was isolated from *E. coli* XL-1 Blue cells (Stratagene) using a Mini Plasmid purification kit (Qiagen). Purified pTrp2 and the PCR-amplified β-tubulin gene were doubly digested with relevant restriction enzymes (*NarI* and *BamHI* for the β-tubulin gene and *ClaI* and *BamHI* for the pTrp2 plasmid). Briefly, 20 µl reactions were set up in microfuge tubes using 0.4 - 1.0 µg DNA, 20 units *BamHI*, 16 units *NarI* or 10

units *Cla*I, Buffer A (Roche) and the appropriate amount of ddH₂O to bring the reaction volumes to 20 µl. Tubes were incubated for 4 - 16 hours in a 37°C water bath, followed by purification of the digested plasmid and PCR fragment by use of High Pure™ PCR product purification kits (Roche) as outlined in section 2.5.3. The plasmid and fragment (ratio of 1 : 3) were then ligated together using 1 unit of T4 DNA Ligase (Roche) and Ligase buffer, in a 16 µl reaction volume at room temperature overnight. Competent *E. coli* XL-1 Blue cells, prepared as described in section 2.5.8, were transformed with the ligate by the heat-shock method (as in section 2.5.9) and plated out on to L-agar (5% yeast extract, 10% tryptone, 5% NaCl, 1% agar) supplemented with 100 µg/ml ampicillin and incubated overnight at 37°C. The resulting transformants were screened for the construct of interest (pTrp2-β-Tub) as outlined in section 2.5.10.

2.5.5. Generation of pET11a-αITub and pET11a-βTub

Tubulin genes were re-amplified to retain the original *Bam*HI restriction endonuclease site at the 3' end and to remove the restriction endonuclease site at the 5' end. This step facilitated cloning of a 5' blunt end / 3' sticky end PCR fragment into the pET11a plasmid that was previously digested with *Nde*I, filled in with the large (Klenow) fragment of *E. coli* DNA polymerase I, and subsequently digested with *Bam*HI. pTrp2-β-Tub served as the template in a PCR reaction to generate the insert for pET11a-βTub. Briefly, a forward primer (5'-TGAGAGAAATTGTTCA TATTCAAGCTGGCCAATG-3') and the previously designed reverse primer (5'-GCGGGATCCTTAGGCTTCTACGTCTCCTTC-3') were used to re-amplify the β-tubulin gene (reaction conditions as in section 2.5.1). The αI-tubulin gene amplified in section 2.5.1 was used as the template in a PCR reaction to provide the insert for pET11a-αITub. Forward primer (5'-TGAGAGAAGTAATAAGTATCCATGTAGG ACAAGC-3') together with the previously designed reverse primer (5'-GCGGGAT CCTTAATAATCTGCTTCATATCCTTC-3') were used to re-amplify the αI-tubulin gene (reaction conditions as in section 2.6.1.). pET11a (Novagen) was isolated from *E. coli* BL21(DE3) cells (Novagen) using a Qiagen Mini Plasmid purification kit. Purified pET11a (3 µg) was digested with 4 units of *Nde*I, in a 60 µl reaction containing restriction enzyme buffer H (Roche) at 37°C for 4 hours. The 3' recessed termini were filled in by the addition of dNTP's (0.067 mM), 4 units Klenow fragment (New England Biolabs, Inc.) and by incubating for a maximum of 15 min

in a 25°C water bath. The sample was then run through an agarose gel as outlined in section 2.5.2 and the linearised plasmid was purified from the gel as outlined in section 2.5.3. Three 20 µl reactions were set up in separate microfuge tubes containing 0.4 - 1.0 µg DNA (α I-tubulin gene, β -tubulin gene or previously linearised pET11a plasmid), 20 units *Bam*HI, Buffer A (Roche) and the appropriate amount of ddH₂O to bring the reaction volumes to 20 µl. Tubes were incubated for 4 - 16 hours in a 37°C water bath, followed by the purification of the digested plasmid and PCR fragments by use of a High Pure™ PCR product purification kit (Roche) as outlined in section 2.5.3. Each tubulin gene fragment was ligated to the digested plasmid in individual reactions using 1 unit of T4 DNA Ligase (Roche) and Ligase buffer in 16 µl volume reactions at 22°C (higher temperatures increase ligation efficiency of blunt end / sticky end PCR fragments) overnight. Competent *E. coli* XL-1 Blue cells, prepared as described in section 2.5.8, were transformed with the individual ligates by the heat-shock method (as in section 2.5.9), plated out on to L-agar containing 100 µg/ml ampicillin and incubated overnight at 37°C. The resulting transformants were screened for carriage of the constructs of interest (pET11a- α ITub and pET11a- β Tub) as described in section 2.5.10.

2.5.6. Generation of pMAL-c2X- α ITub and pMAL-c2X- β Tub

Both pMAL-c2X- α ITub and pMAL-c2X- β Tub constructs were generated as part of an undergraduate 4th year project by E. Dempsey under my supervision. The objective was to express recombinant *P. falciparum* tubulins as fusions to maltose binding protein (MBP) in the hope that they would be more soluble than the authentic polypeptides. Briefly, both tubulin genes were amplified by PCR with primers that allowed subsequent cloning into the pMAL-c2X vector (New England Biolabs, Hertfordshire, UK), using reaction conditions as described in section 2.5.1, and pET11a- α ITub or pET11a- β Tub as templates. *E. coli* TB1 (New England Biolabs) was used as the recipient strain for the pMAL-c2X- α ITub and pMAL-c2X- β Tub constructs.

2.5.7. Recovery of DNA by ethanol precipitation

Sample DNA was concentrated by mixing with a 1/10 volume of 3 M sodium acetate (pH 5.5) and 2 volumes of absolute ethanol and incubating at -70°C for 30 min - 1 h. DNA was then precipitated by centrifugation at 11,500 rpm (12,000 x g)

for 10 min, the supernatant was removed and the resulting pellet washed with 200 μ l of 70% ethanol. The sample was re-centrifuged as before, the supernatant removed, and the DNA pellet was dried at 37°C for \sim 1 h, and resuspended in an appropriate volume of ddH₂O.

2.5.8. Preparation of competent *E. coli* cells

A single colony from the desired strain of *E. coli* was used to inoculate 20 ml of L-broth and grown overnight with agitation at 200 rpm at 37°C. Five ml of overnight culture were used to inoculate 400 ml of fresh L-broth in a 2-litre baffled flask and the bacteria were then grown at 37°C with agitation at 200 rpm until they had an absorbance reading at 600 nm (A_{600}) of \sim 0.4. Cells were decanted into two 250 ml GSA Sorvall containers and were chilled on ice for \sim 20 min. Cells were pelleted by centrifugation at 4000 rpm (2600 \times g) for 10 min at 4°C in a Sorvall RC-50 centrifuge (Du Pont Ltd., Stevenage, Herts, UK). The supernatant was decanted and each pellet was gently resuspended in 30 ml of ice-cold sterile CaCl₂ solution (60 mM CaCl₂, 10 mM PIPES pH 7.6, 15% (v/v) glycerol). Cells were pelleted as before and were resuspended in 100 ml of ice-cold CaCl₂ (100 mM) and incubated on ice for 1 hour. Cells were re-pelleted and resuspended in 20 ml of ice-cold CaCl₂ solution, divided among pre-chilled sterile eppendorf tubes (200 - 500 μ l volumes), snap frozen in liquid nitrogen and relocated to a - 70°C freezer for storage.

2.5.9. Transformation of competent *E. coli* strains

Competent *E. coli* cells were transformed using the heat-shock method as described by Maniatis *et al* (1982). To separate cloning from protein expression experiments, *E. coli* strain XL-1 Blue cells were used for transformations involving DNA manipulations only (e.g. screening of transformants (section 2.5.10)). For protein expression experiments, strains used for transformation were as recommended by the suppliers of the expression plasmids. The transformation technique involved thawing the competent cells on ice for 30 min and mixing them with 2 - 16 μ l of ligation mixture or expression plasmid alone in a sterile eppendorf tube. Samples were incubated on ice for 30 min, heat-shocked in a 43°C water bath for 2 min and placed back on ice for a further two min. One ml of pre-warmed L-broth was added to the samples, which were then incubated in a 37°C water bath for 1 hour. After incubation, 100 μ l volumes of each sample were plated in duplicate on

L-agar/ampicillin and incubated overnight at 37°C. The remaining cells in the transformation mixture were pelleted by centrifugation at 10,000 rpm (11,950 x g) for 2 min at room temperature and most of the resulting L-broth was removed except for ~ 100 µl. The pellet was then resuspended in the excess L-broth and plated in duplicate on L-agar plates as previously outlined. The later step was included so to obtain the maximum possible number of transformants. Cells transformed with vector alone served as positive controls, while cells transformed with vector alone, but previously digested with the appropriate restriction enzyme(s) and left unligated, served as negative controls.

2.5.10. Screening of transformants

Putative transformants obtained after 12 - 16 h growth on L-agar supplemented with the appropriate antibiotic were screened for the construct of interest by a number of techniques. All of the methods involved the replica-plating of colonies onto fresh L-agar plates supplemented with the appropriate antibiotic and the use of the rest of the colony for the screening procedure. DNA sequence analysis was carried out by the Advanced Biotechnology Centre, Imperial College London, UK, on identified clones to confirm that the construct had the correct DNA sequence.

2.5.10.1. Screening by small-scale plasmid isolation

Putative transformants along with controls (cells hosting plasmid alone) were used to inoculate 2 ml of L-broth supplemented with the appropriate antibiotic in a test tube. Cultures were grown overnight at 37°C with agitation at 200 rpm. Overnight cultures were transferred to eppendorf tubes and cells were pelleted by centrifugation at 14,000 rpm (18,000 x g) for 5 min (all centrifugation steps carried out at room temperature). The supernatants were discarded and pellets were resuspended in 100 µl of a glucose solution (50 mM glucose, 10 mM Tris-HCl, 1 mM EDTA, pH 8.0). Two hundred µl of freshly prepared lysis solution (200 mM NaOH, 1% SDS) were added and tubes were gently mixed by inversion and incubated on ice for 5 min. Following incubation, 300 µl of a potassium acetate solution (4 M potassium acetate, 2 M acetic acid) were added, mixed and incubated on ice for 5 min. The tubes were then centrifuged for 5 min at 14,000 rpm (18,000 x g) and the resulting supernatants were transferred to fresh tubes. After adding 1 ml of absolute ethanol, the tubes were mixed and left on ice for 5 min. The DNA was

then pelleted by centrifugation at 14,000 rpm (18,000 x g) for 10 min, the supernatants discarded and the pellets washed in 500 µl of 70% ethanol. All traces of ethanol were removed and the pellets were left to dry in a 37°C incubator for 1 hour. The pellets were resuspended in 50 µl ddH₂O containing 0.01 µg RNase A, and 15 µl of each sample were loaded directly onto an agarose gel and treated as outlined in section 2.5.2. Following ethidium bromide staining, constructs of interest were identified by their slower migration through the gel than vector alone.

2.5.10.2. Rapid colony screening

Colonies were emulsified in 16 µl lysis buffer (0.67% (v/v) SDS, 130 mM NaOH, 6x loading buffer (see section 2.6.2.)) in eppendorf tubes before adding 3 µl of a potassium acetate formate solution (3 M potassium acetate, 1.8 M formic acid). Tubes were centrifuged for 4 min at 12,000 rpm (13,000 x g) to pellet cellular debris and 10 - 15 µl of the resulting supernatants were loaded directly onto an agarose gel and treated as outlined in section 2.5.2. Following ethidium bromide staining, constructs of interest were identified by their apparent slower migration through the gel than vector alone.

2.5.10.3. Screening by restriction endonuclease digestion

The presence of the insert (tubulin gene) in the construct of interest was investigated by the ability of restriction endonucleases, for which specific recognition sites had been introduced, to linearise the putative recombinant plasmid. Putative transformants were used to inoculate 3 - 6 ml of L-broth supplemented with the appropriate antibiotic in a test tube and cultures were grown overnight at 37°C with agitation at 200 rpm. Putative recombinant plasmids were obtained from cultures by purification using either a Qiagen Mini plasmid purification kit or a FastPrep Mini Plasmid purification kit (Eppendorf AG, Hamburg, Germany). Restriction endonuclease digestion was carried out using the relevant enzymes as described in section 2.5.5. The size of the linearised putative recombinant plasmid and plasmid alone (control) was assessed by electrophoresis through an agarose gel as outlined in section 2.5.2. If the putative recombinant plasmid contained an insert, a known size difference between it and plasmid alone was expected to be observed.

2.5.10.4. Screening by PCR

PCR was performed on recombinant plasmids obtained from putative transformants to confirm the presence of the insert (tubulin genes). Recombinant plasmids were obtained as outlined in section 2.5.10.3. and used as the templates in PCR (conditions as in section 2.5.1) together with primers specific for regions upstream and downstream of the cloned gene.

2.6. PROTEIN QUANTIFICATION AND ANALYSIS

2.6.1. Quantification of protein concentration by the Bradford assay

Protein concentration was determined using the colorimetric assay of Bradford (1976), which is based on quantitating the binding of a dye, Coomassie Brilliant Blue G250, to the protein of interest. Protein amounts in experimental samples are determined with reference to a BSA standard curve. The assay involved diluting from a filter-sterile stock solution of 0.5 mg/ml BSA to 15.0, 12.5, 10.0, 7.5, 5.0, 2.5 and 1.0 µg/ml in a final volume of 100 µl in PBS. Experimental samples used for protein quantification were also diluted in PBS to a final volume of 100 µl. One ml of Bradford reagent (0.01% (w/v) Coomassie Brilliant Blue G-250, 0.25% (v/v) ethanol and 10% (v/v) orthophosphoric acid) was added to experimental samples and BSA standards, with vortexing to ensure sufficient mixing. Samples and standards were incubated at room temperature for 20 min and absorbances determined at 595 nm in a Shimadzu UV-1601PC spectrophotometer (Shimadzu Scientific Instruments, Inc., Columbia, MD, USA).

2.6.2. SDS-polyacrylamide gel electrophoresis (SDS-PAGE)

Protein samples were electrophoretically separated by SDS-PAGE according to the method of Laemmli (1970). For maximum resolution of the proteins of interest 10% (w/v) acrylamide mini-gels were generally used. Glassware used was first cleaned with 70% (v/v) methylated spirits. Separating gels consisted of 0.375 M Tris-HCl, pH 8.8; 10% (v/v) acrylamide/bisacrylamide (37.5:1.0) (Protogel, National Diagnostics, Hull, UK); 0.1% (v/v) SDS; 0.06% (v/v) ammonium persulphate (APS) and 0.05% (v/v) N, N, N', N'-tetramethyl-ethylenediamine (TEMED). Stacking gels consisted of 0.125 M Tris-HCl, pH 6.8; 4% (v/v) acrylamide/bisacrylamide (ratio as above); 0.1% (v/v) SDS; 0.1% (v/v) APS; and 0.1% (v/v) TEMED. Mini-gel glass plates were clamped together, the separating gel was poured to ~ 1.5 cm

from the top of the plates and overlaid with water-saturated iso-butanol for one hour. After polymerisation, the gel was washed with ddH₂O, dried with Whatman paper and the stacking gel was poured on top of the separating gel. A comb was inserted, and the gel was left to polymerise for 30 min. Samples were solubilised in an equal volume of 2x reducing SDS sample loading buffer (0.125 M Tris-HCl, pH 6.8, 2.3% (v/v) SDS, 10% (v/v) glycerol, 10% (v/v) 2-mercaptoethanol and 0.009% (w/v) bromophenol blue as a tracking dye), heated to 90 - 100°C for 10 min, cooled to room temperature, then centrifuged at 10,000 rpm (9,000 x g) for 10 s before being loaded on the gel. A combination of proteins of known molecular weight (New England Biolabs, Hertfordshire, UK) were loaded on each gel as reference standards (Table 2.1 and 2.2). The protein samples (0.2 - 20 µl) were resolved at 100 V through the stacking gel, followed by 147 V through the separating gel, using an EC105 power supply pack (E-C Apparatus Corp., Holbrook, New York, USA) until the sample tracking dye reached the bottom. Running buffer consisted of 0.30% (w/v) Tris-HCl, 1.44% (w/v) glycine and 0.1% (w/v) SDS.

Commercial SDS preparations specially purified (>99% pure) for electrophoresis have previously been shown not to achieve efficient separation of tubulin subunits. Better separation is achieved if impure SDS preparations are used (impurities include other long-chain alkyl sulfates) (Best, *et al*, 1981, Stephens, 1998). SDS-PAGE was also carried out as previously outlined except for the following modifications: (i) the source of SDS used in the running buffer, sample loading buffer, separating and stacking gels was of low grade and contained the contaminants myristyl sulfate (C₁₄) (~ 29%; based on the purity of the SDS preparation being 95% pure total alkyl sulfate) and cetyl sulfate (C₁₆) (~ 6%) (Sigma-Aldrich); (ii) separating gels of varying pH value (pH 8.25, pH 8.75 and pH 9.25) were also used to improve the separation of the tubulin subunits.

2.6.3. Visualisation of protein samples on polyacrylamide gels

SDS-PAGE gels were stained with 20 - 25 ml of Coomassie blue reagent (0.15% (w/v) Coomassie Brilliant Blue R250 (PhioBio, Fisons Scientific Equipment, Loughborough, UK), 45% (v/v) methanol (BDH), 10% (v/v) glacial acetic acid (BDH), filtered to remove undissolved components) for 2 - 4 hours, followed by destaining with 20% (v/v) methanol, 7.5% (v/v) glacial acetic acid until the background was clear. Detection and visualisation of small amounts of protein

Table 2.1. Standard Broad Range molecular weight protein markers.

Protein	Source	MW (Da)
Myosin.....	rabbit muscle.....	212,000
^a MBP- β -galactosidase.....	<i>E. coli</i>	158,194
β -Galactosidase.....	<i>E. coli</i>	116,351
Phosphorylase <i>b</i>	rabbit muscle.....	97,184
Serum albumin.....	bovine.....	66,409
Glutamic dehydrogenase.....	bovine liver.....	55,561
MBP2.....	<i>E. coli</i>	42,710
Lactate dehydrogenase M.....	porcine muscle.....	36,487
Triosephosphate isomerase.....	rabbit muscle.....	26,625
Trypsin inhibitor.....	soybean.....	20,040
Lysozyme.....	chicken egg white.....	14,313
Aprotinin.....	bovine lung.....	6,517
Insulin A, B chain.....	bovine pancreas.....	2,340

^aMBP: Maltose binding protein

Table 2.2. Prestained Broad Range molecular weight protein markers.

Protein	Source	MW (Da)
MBP- β -galactosidase.....	<i>E. coli</i>	175,000
MBP-paramyosin.....	<i>E. coli</i>	83,000
Glutamic dehydrogenase.....	bovine liver.....	62,000
Aldolase.....	rabbit muscle.....	47,500
Triosephosphate isomerase.....	rabbit muscle.....	32,500
β -Lactoglobulin A.....	bovine milk.....	25,000
Lysozyme.....	chicken egg white.....	16,500
Aprotinin.....	bovine lung.....	6,500

required the use of silver staining (Ansorge, 1985). Gels were incubated in solutions in the following order: (1) 50% (v/v) methanol for 10 min; (2) 10% (v/v) ethanol, 5% (v/v) glacial acetic acid for 10 min; (3) 0.06% (w/v) potassium permanganate for 5 min; (4) 0.1% (w/v) potassium carbonate for 5 min; (5) 3 x 10 min washes in ddH₂O; (6) 0.1% silver nitrate for 10 min; (7) 2 x 15 s washes in ddH₂O; (8) 2% (w/v) potassium carbonate, 0.015% formaldehyde until desired colour was obtained; (9) 1% (v/v) glacial acetic acid for 5 min to complete staining; and (10) finally the gel was stored in ddH₂O. Gels were photographed with the Alphaimager 2200 (Alpha Innotech Corp.) and dried onto cellophane (Bio-Rad Laboratories, Hercules, CA, USA).

2.6.4. Precipitation of protein with trichloroacetic acid (TCA)

TCA precipitation was used to concentrate samples removed from dilute proteins fractions collected after ion-exchange and affinity chromatography procedures (see section 2.7.7 and 2.7.8) prior to analysis by SDS-PAGE. Protein samples were mixed with an equal volume of ice-cold 25% (w/v) TCA, incubated on ice for 5 min and centrifuged at 12,000 rpm (18,000 x g) for 5 min at room temperature. The supernatant was removed and the protein pellet was resuspended in 15 - 20 µl SDS loading buffer (62.5 mM Tris-HCl pH 6.8, 1.15% (v/v) SDS, 5.0% (v/v) glycerol, 5.0% (v/v) 2-mercaptoethanol and 0.005% (w/v) bromophenol blue as a tracking dye). If the protein sample turned yellow upon addition of SDS loading buffer, the pH was neutralised by the addition of 2 - 3 crystals of Tris base. Samples were boiled for 10 min before loading on SDS-PAGE gels as outlined in section 2.6.2.

2.6.5. Western immunoblotting

After electrophoresis (section 2.6.2), unstained polyacrylamide gels were soaked in transfer buffer (1.44% (w/v) glycine, 0.30% (w/v) Tris-HCl, pH 8.3, 20% (v/v) methanol) and sandwiched with polyvinylidene difluoride (PVDF) membrane (Roche Diagnostics GmbH, Mannheim, Germany) previously treated in 100% (v/v) methanol for 5 s. The gel-membrane sandwich was then inserted into a blotting tank with ~ 1 l transfer buffer and transferred for 1 hour at 100 V, with an ice block present to keep the tank from over-heating. After transfer, the blot was blocked in 5% (w/v) skimmed milk in Towbin's buffer (10 mM Tris-HCl, pH 7.4, 0.9% (w/v)

NaCl) overnight with shaking. Primary antibodies used were diluted to a final concentration of between 1 : 400 - 1 : 15,000 in 3% (w/v) skimmed milk in Towbin's buffer, and applied to the blocked membrane for 2 h. The blot was washed 3 - 10 times for 25 min in Towbin's buffer with 0.05% (v/v) Tween 20. These steps were repeated for the secondary antibody, which in all cases was goat-anti-rabbit immunoglobulin-peroxidase (GARIG-PO) diluted to a final working concentration of 1 : 2000. Bands were detected using a chemiluminescence system (Roche) according to the manufacturer's instructions in a darkroom with use of safety lights. The blot was exposed to X-OMAT UV film (Kodak, Dublin) for the desired length of time prior to passage through a Kodak X-OMAT 1000 automatic developer which involved automatic carriage of X-ray film through Industrex developer (Kodak) for 30 s, washing in ddH₂O for 30 s and passage through Industrex fixative (Kodak) for 30 s. The film was air-dried and photographed using an Alphaimager 2200 (Alpha Innotech Corp.).

2.6.6. Stripping and re-probing PVDF membranes

Antibodies were stripped off previously used membranes by heating the blot at 60°C for 30 min in a stripping solution (62.5 mM Tris-HCl, pH 6.8, 2% (v/v) SDS, 100 mM 2-mercaptoethanol). The blot was washed three times in Towbin's/Tween solution (see section 2.6.5) for 10 min. After blocking with 3% (w/v) skimmed milk, the membrane was probed with the appropriate primary antibody and developed as outlined in section 2.6.5.

2.7. RECOMBINANT TUBULIN PRODUCTION, PURIFICATION AND REFOLDING

2.7.1. Expression studies with pTrp2-βtub construct

A number of different strains of *E. coli* including XL-1-Blue, JM101, and TOP3 were assessed for recombinant β-tubulin production from plasmid pTrp2-βtub. A single colony harbouring the construct (or vector alone which served as the negative control) was grown at 37°C to an A₆₀₀ = 0.8 with agitation at 200 rpm in L-broth/ampicillin with 1 mg/ml tryptophan to repress promoter activity. To induce recombinant gene expression by tryptophan starvation, the cells were pelleted by centrifugation at 3000 rpm (975 x g), washed in M9 minimal salts medium containing 100 µg/ml ampicillin, 6 mg/ml glucose, 0.1% acid hydrolysed casein

amino acids and 1 µg/ml vitamin B1 (thiamine) and cultured for a further 1 - 3 hours. Approximately equal numbers of cells were harvested by centrifugation at 11,500 rpm (12,000 x g) for 10 min at 4°C in a Sigma 1 - 15 microfuge. The pellets were either used immediately or frozen at - 20°C. They were resuspended in 50 µl PBS and mixed with 50 µl SDS loading buffer (see section 2.6.2) and 6 µl samples were analysed by SDS-PAGE (see section 2.6.2). Production of recombinant protein from the colony harbouring the construct of interest was assessed by comparing its protein profile after Coomassie blue staining of SDS-PAGE gels (see section 2.6.3) or by Western Immunoblotting (see section 2.6.5) with that of a colony harbouring the vector alone.

2.7.2. Expression studies with pET11a-tubulin constructs

A single colony of *E. coli* BL21(DE3) (Novagen) harbouring the construct of interest (or vector alone) was grown at 37°C with agitation at 200 rpm to $A_{600} = 0.6 - 1.0$ and stored overnight at 4°C. On the following day, the cells were pelleted by centrifugation at 11,500 rpm (12,000 x g) for 1 min at room temperature and resuspended in L-broth, which was used to inoculate fresh L-broth/ampicillin in baffled flasks. Cultures were grown at 30 - 37°C with agitation at 200 rpm to an $A_{600} = 0.5 - 0.7$ and gene expression was induced by the addition of 0.3 - 1.0 mM (filter-sterilised) isopropylthiogalactopyranoside (IPTG) (Melford Laboratories, U.K.). The culture was incubated for a further 2 - 3 hours after which the cells were harvested by centrifugation at 7900 rpm (7,000 x g) for 10 min at 4°C in a Sorvall RC50 Plus centrifuge using a GSA rotor. Pellets were either used immediately or frozen at - 20°C. Production of recombinant protein by the colony harbouring the construct of interest was assessed as outlined in section 2.7.1.

2.7.3. Determination of recombinant protein solubility

The solubility of recombinant tubulins was assessed by the method of Williams *et al* (1991). Pellets obtained as outlined in section 2.7.2 were resuspended in 150 µl of lysis buffer (50 mM Tris-HCl, pH 8.0, 2 mM EDTA, 100 µg/ml lysozyme (added immediately before use)), incubated for 15 min in a 30°C water bath and sonicated twice for 10 s on ice using a Soniprep 150 MSE sonicator (Sanyo, Dublin). Samples were centrifuged at 14,000 rpm (18,000 x g) and supernatants removed to fresh tubes and mixed with 150 µl of 2x SDS loading

buffer: these were the soluble protein extracts. Pellets were resuspended in 300 μ l 2x SDS loading buffer: these were the insoluble protein extracts. Ten μ l amounts of the soluble and insoluble extracts were analysed by SDS-PAGE (see section 2.6.2). Solubility of the recombinant tubulins was visually assessed after Coomassie blue staining of SDS-PAGE gels (see section 2.6.3) by the presence or absence of the induced protein in the soluble and insoluble fractions. Although the pellets were contaminated with some soluble proteins, the absence of an induced protein in the soluble fraction is generally a reliable indicator of insolubility.

2.7.4. *E. coli* cell lysis and purification of inclusion bodies containing recombinant protein

Bacterial pellets (from section 2.7.2) were resuspended in ice-cold lysis buffer (50 mM Tris-HCl, pH 8.0, 1 mM EDTA, 200 μ g/ml lysozyme, 3 μ g/ml DNase I) by gentle vortexing and pipetting action. Cells were lysed by 2 - 3 passages through a French Press at a pressure of 2000 psi and examined using a Nikon Optiphot microscope (The Micron Company) by phase-contrast illumination to examine the extent of cell lysis. Following clarification of the lysate by centrifugation at 17,000 rpm (35,000 x g) in a Sorvall RC50 Plus centrifuge using an SS-34 rotor for 1 h at 4°C, the soluble supernatant was decanted and recombinant tubulin in the form of inclusion bodies was recovered in the pellet. Pellets were resuspended in wash buffer (50 mM Tris-HCl, pH 8.0, 10 mM EDTA, 100 mM NaCl and 0.5% (v/v) Triton-X-100) to remove cell wall proteins, outer membrane material and soluble proteins adsorbed onto the inclusion bodies and re-pelleted by centrifugation at 10,000 rpm (11,950 x g) for 10 min at 4°C. The washing step was repeated twice more and finally the purified inclusion bodies were recovered in the pellet.

2.7.5. Solubilisation of inclusion bodies and renaturation of tubulin

Inclusion bodies were solubilised and renatured by the urea-alkaline method as described by Marston (1987) and Lubega *et al* (1993). Isolated inclusion bodies were solubilised in 50 mM Tris-HCl pH 8.0, 1mM EDTA, 50 mM NaCl, 8 M urea by gentle stirring for 1 h at room temperature, to give an approximate final protein concentration of 1 mg/ml. Using a peristaltic pump the solubilised recombinant tubulin was added in a dropwise fashion to the refolding buffer (50 mM KH₂PO₄, 1

mM EDTA, 50 mM NaCl, pH 10.7) with constant stirring and incubated for 30 min (final protein concentration $\sim 50 \mu\text{g/ml}$) at room temperature. The pH was then adjusted to 8.0 with 4 M HCl and the incubation continued for a further 30 min. Protein aggregates were pelleted by centrifugation at 10,000 rpm (12,000 x g) at 4°C for 10 min in a Sorvall RC50 Plus centrifuge using an SS-34 rotor and the resulting supernatant was concentrated to 1/3 of its original volume using an Amicon centrifugal filter with a molecular weight cut-off point of 30,000 Da (Millipore). The concentrate was diluted 3 fold with G-PEM-G buffer (1 mM GTP, 80 mM PIPES-NaOH, pH 6.9, 1 mM EGTA, 1 mM MgCl₂, 10% (v/v) glycerol) and re-concentrated to one-third its volume. This cycle of concentration and re-dilution was repeated twice more. The sample was then ultracentrifuged at 24,000 rpm (100,000 x g) using a Beckman L8-M ultracentrifuge (Beckman Instruments Inc. Harbour Boulevard, CA, USA) with a Beckman SW40 Ti rotor for 1 h at 4°C to pellet any remaining aggregated tubulin. The sample was concentrated with an Amicon centrifugal filter to a final protein concentration of $\geq 5\text{mg/ml}$ as determined by the method of Bradford (see section 2.6.1). Recombinant tubulin was divided into pre-chilled eppendorf tubes, snap frozen in liquid nitrogen and stored at - 70°C.

2.7.6. Expression studies with pMaL-c2X-tubulin constructs

Recombinant proteins were produced by inoculating L-broth/ampicillin in baffled flasks, with overnight cultures of the strain of *E. coli* harbouring the construct of interest, and grown at 37°C with agitation at 200 rpm to an $A_{600} = \sim 0.5$. Recombinant gene expression was induced for by the addition of 0.35 mM IPTG and the culture was incubated for a further 2 - 3 hours. Cells were harvested by centrifugation at 6500 rpm (7,000 x g) for 10 min at 4°C in a Sorvall RC50 Plus centrifuge using either a GSA or GS3 rotor. Pellets were either used immediately or frozen at - 20°C. Production of recombinant protein by the colony harbouring the construct of interest was assessed as outlined in section 2.7.1. Cells were lysed by French Press as outlined in section 2.7.4. except an alternative Tris buffer (20 mM Tris-HCl, 200 mM NaCl, 1mM EDTA, pH 7.4, filter-sterilised) supplemented with Complete Mini Protease inhibitor tablets (Roche) was used to resuspend the pellet. Solubility of the recombinant tubulin fusion proteins was determined as outlined in section 2.7.3.

2.7.7. Amylose affinity chromatography

Amylose resin (New England Biolabs, MA, USA) was dispensed into a 2 x 10 cm column (BioRad) and equilibrated with >15 column volumes of amylose column buffer (20 mM Tris-HCl, 200 mM NaCl, 1 mM EDTA, pH 7.4 and filter-sterilised). Soluble lysate (see section 2.7.6.) was applied to the column at a flow rate of 1 ml/min using a peristaltic pump and the resin was washed with ≥ 15 column volumes of amylose column buffer at a flow rate of 2 ml/min. Bound proteins were eluted by washing the resin with 4 - 5 column volumes of amylose elution buffer (amylose column buffer supplemented with 10 mM maltose, pH 7.4 and filter sterilised) at a flow rate of 2 ml/min. Eluted proteins were concentrated to a volume of 5 - 10 ml using an Amicon filter device with a molecular weight cut-off of 50,000 Da (Millipore). The resin was regenerated by washing with 3 column volumes of ddH₂O, 3 column volumes of 0.1% (v/v) SDS, 1 column volume of ddH₂O, 3 column volumes of amylose column buffer and finally 3 column volumes of 20% (v/v) ethanol.

2.7.8. Ion-exchange chromatography

A cationic-exchange column (HiTrap Mono Q) (Amersham Pharmacia, Pollards wood, Bucks, UK) was attached to a FPLC machine (Amersham Pharmacia), washed with high-salt buffer (20 mM Tris-HCl, pH 8.0, 1 M NaCl, filter-sterilised), pre-eluted with and equilibrated with low-salt buffer (20 mM Tris-HCl, pH 8.0, filter-sterilised). Concentrated protein eluate (see section 2.7.7) was diluted 10-fold with low-salt buffer and applied to the column at a flow rate of 2 ml/min. The resin was washed with low-salt buffer at a flow rate of 2 ml/min until a base line was reached on the chart recorder. Bound proteins were eluted over an NaCl gradient of 0 - 100% using high-salt buffer and collected automatically with a fraction collector. Fractions were analysed by Coomassie staining of SDS-PAGE gels (see sections 2.6.2 and 2.6.3) and relevant fractions were pooled and concentrated using an Amicon centrifugal filter. Buffer exchange and ultracentrifugation was performed on the concentrate as outlined in section 2.7.5, followed by a concentration step and subsequent storage of the recombinant proteins at -70°C.

2.7.9. Purification of antibodies specific to *P. falciparum* tubulins

Antibodies to *P. falciparum* β -tubulin were purified from a crude rabbit immune serum by affinity chromatography as outlined by Bell *et al* (1995). Briefly, Affigel 15 (Bio-Rad) coupled to a synthetic peptide (GEFEEEEGDVEA: corresponding to the C-terminal residues of *P. falciparum* β -tubulin) was poured into a 1.0 x 10 cm column (Bio-Rad), pre-eluted with Affigel elution buffer (100 mM sodium citrate, pH 2.5) and equilibrated with >9 column volumes of Affigel column buffer (PBS, 100 mM NaCl, pH 7.4) to give a bed volume of ~ 900 μ l. One ml of the rabbit immune serum raised against the β -peptide was applied to the column, left for ~ 30 min and the column was washed with >20 column volumes of Affigel column buffer. Bound β -tubulin specific antibodies were eluted by washing the resin with 1 - 2 column volumes of Affigel elution buffer. Fractions containing eluted β -tubulin antibodies were neutralised with 8 M NaOH, pooled and concentrated with a Centricon centrifugal filter with a molecular weight cut-off of 10,000 Da (Millipore). Antibodies specific to *P. falciparum* α I-tubulin were also raised in a rabbit to a synthetic peptide (AEGEDEGYEADY: corresponding to the C-terminal residues of *P. falciparum* α I-tubulin) (Bell, A - personal communication) and used directly as a crude serum in experimentation. Antibodies specific to *P. falciparum* α II-tubulin were obtained from the MR4/American Type Culture Collection.

2.8. FUNCTIONAL ANALYSIS OF RECOMBINANT *P. FALCIPARUM* TUBULINS

2.8.1. Tubulin co-sedimentation assay

To determine if recombinant tubulins could polymerise to form microtubules or co-polymerise with bovine brain tubulin, a technique was developed based on the methods of Lubega *et al* (1993), Oxberry *et al* (2001) and Yaffe *et al* (1988). Bovine brain tubulin (Cytoskeleton Inc., Denver, CO, USA), which consists of > 99% pure tubulin (α - β -tubulin dimers only, no detectable MAPS) and polymerises readily to form microtubules, was used as a positive control.

2.8.1.1. Sedimentation of bovine brain tubulin alone

Assay conditions for positive control involved incubating ~ 24 μ M bovine brain tubulin in G-PEM-G buffer (as in section 2.7.5, except that the GTP

concentration used was 2 mM) in the presence or absence of 30 μ M Taxol on ice for 30 min in sterile microfuge tubes to depolymerise any polymeric tubulin. Tubes were then transferred to a 37°C water bath and incubated for 45 min - 1 h to promote polymerisation. Samples were then gently overlaid on prewarmed (\sim 37°C) 60% (v/v) glycerol cushions in PEM buffer (80 mM PIPES-NaOH, pH 6.9, 1 mM EGTA, 1 mM MgCl₂) in sterile microfuge tubes. Microtubules were pelleted by the method of Kumar (1981) through the glycerol cushion by centrifugation at 19,000 rpm (40,000 x g) at 37°C in a Sorvall RC50 Plus centrifuge using an SS-34 rotor with specially fitted Sorvall 408 adaptor cones. Supernatant and cushion fractions were removed to fresh eppendorf tubes containing equal volumes of 2x SDS loading buffer (see section 2.6.2) and pellets were carefully rinsed with warm (\sim 37°C) G-PEM-G buffer and re-centrifuged as previously outlined. The washing step was repeated 2 - 3 times to ensure removal of unpolymerised contaminants adhering to the pellet and the sides of the tubes. The pellets were resuspended in known volumes of SDS loading buffer (usually 2 - 4 volumes less than the supernatant/cushion/2x SDS loading buffer samples) and samples were heated to 90 - 100°C for 10 min, cooled to room temperature, centrifuged at 10,000 rpm (9,000 x g) for 10 s, then loaded on a SDS gel as previously outlined in section 2.6.2. Equal proportions (for example if the total supernatant/cushion fraction was 100 μ l and the total pellet fraction 50 μ l, then 2 μ l of supernatant/cushion fraction and 1 μ l of pellet fraction were loaded) of the supernatant/cushion fraction and the pellet fraction were electrophoretically separated by SDS-PAGE and visually assessed after Coomassie blue staining (see section 2.6.3) to observe the extent of microtubule formation. Protein found in the supernatant/cushion fraction corresponded to unpolymerised tubulin, while tubulin found in the pellet fraction corresponded to polymerised microtubules. The extent of microtubule formation was therefore quantified by densitometry using a GS-800 Densitometer (Bio-Rad) by calculating the relative amounts of tubulin in the supernatant/cushion and pellet fractions.

Assay conditions for the negative control involved incubating \sim 24 μ M bovine brain tubulin in G-PEM-G buffer in the presence of 20 μ M vinblastine (which is inhibitory to microtubule formation) instead of Taxol and assessing the extent of microtubule formation as previously outlined. A second negative control involved incubating \sim 24 μ M bovine brain tubulin in G-PEM-G buffer in the absence of Taxol and proceeding with the assay as outlined with the exception that the reaction

temperature remained at 4°C throughout (temperatures > 4°C are usually required for microtubule formation).

2.8.1.2. Sedimentation of bovine brain tubulin in the presence of other proteins

The assay involved examining the ability of recombinant *P. falciparum* α I- or β -tubulin fusion proteins or BSA or MBP as negative controls to co-polymerise with bovine brain tubulin in a dose-dependent manner. Assay conditions were as follows: 24 μ M bovine brain tubulin + 12 μ M test protein (ratio of monomers 1 : 1), 16 μ M bovine brain tubulin + 16 μ M test protein (ratio of monomers 1 : 2) or 12 μ M bovine brain tubulin + 18 μ M test protein (ratio of monomers 1 : 3). These mixtures were assayed as outlined in section 2.8.1.1 in the presence of 30 μ M Taxol. Negative controls included the same set of assays with the omission of bovine brain tubulin, performed simultaneously, to determine background levels of test protein adhering to the reaction tubes. Levels of test protein observed in the pellet fractions of the mixtures with bovine brain tubulin were compared with the negative controls (test protein alone) and quantified by densitometry as previously outlined (see section 2.8.1.1). As MBP was found to migrate in SDS-PAGE gels at an apparent size similar to bovine brain tubulin, western immunoblotting (section 2.6.5) was used to compare the amounts of MBP in the bovine brain tubulin-containing and bovine brain tubulin-free pellet fractions.

2.8.1.3. Sedimentation of recombinant MBP α I- and MBP β -tubulin fusions combined

Assay conditions for the formation of recombinant *P. falciparum* microtubules were as outlined in section 2.8.1.1 except that bovine brain tubulin was replaced with both recombinant tubulin fusions to give a final tubulin concentration of ~ 24 μ M (~ 12 μ M of each monomer). MBP- α I-tubulin and MBP- β -tubulin alone served as negative controls and microtubule formation was assessed as outlined in section 2.8.1.1.

2.8.2. Turbidimetric assay of microtubule polymerisation

To establish if refolded recombinant *P. falciparum* tubulins or recombinant tubulin fusion proteins could polymerise to form microtubules in the absence of bovine tubulin, a light-scattering assay was adapted from the methods of Algaier *et*

al (1988) and Oxberry *et al* (2001). Bovine brain tubulin (Cytoskeleton Inc.) was used as a positive control. The polymerisation was assessed using a “precool” system, in which all components were mixed at 4°C and assembly was initiated by adding the cold solution to a cuvette at 37°C. Bovine brain tubulin at 2.5 - 20 µM in G-PEM-G buffer (see section 2.5.4; except that the GTP concentration used was 1 - 2 mM) was incubated on ice for 30 min in the presence or absence of 30 µM Taxol. Microtubule assembly was initiated by adding the solution to a prewarmed quartz cuvette (2 mm width and 10 mm light path) and measuring the changes in turbidity at 10 - 30 s intervals for 1 hour at 350 nm at 37°C using a Shimadzu UV-1601PC spectrophotometer (Shimadzu Scientific Instruments, Inc.) with a thermostated multicell holder. At a wavelength of 350 nm, the scattering of light by polymerised microtubules causes an increase in absorbance. An increase in absorbance (A_{350}) of 1.0 is approximately equal to a polymer mass of 5 mg/ml (Cytoskeleton Inc., 2004).

Formation of microtubules from a mixture of refolded recombinant α I- and β -tubulins was assessed using final tubulin concentrations from 10 - 60 µM in the presence or absence of 20 - 40 µM Taxol and 1 - 4 mM GTP. For recombinant MBP- α I- and MBP- β -tubulin fusions, final concentrations tested in the assay ranged from 0.5 - 40 µM, in the presence of 30 µM Taxol and 2 mM GTP.

2.9. STAGE-DEPENDENT PRODUCTION AND ELECTROPHORETIC BEHAVIOUR OF TUBULINS IN *P. FALCIPARUM*

2.9.1. Investigation of the “ α / β inversion” of *P. falciparum* tubulins

Tubulin subunit migration in SDS-PAGE has been shown to be somewhat anomalous. Conventionally α -tubulin is the slower and β -tubulin is the faster migrating species during SDS-PAGE. Reversed order of electrophoretic migration of the two subunits is termed the “ α/β inversion”. The behaviour of *P. falciparum* native and recombinant tubulins in this respect was investigated by methods of Best *et al* (1981), Clayton *et al* (1980), Delgado *et al* (1991), and Suprenant (1985). Briefly, electrophoretic behaviour of tubulins from *P. falciparum* whole cell extracts (see section 2.3.1), *E. coli*-produced recombinant *P. falciparum* tubulins (2 - 3 µg of α I and β) (see section 2.7) and bovine brain (2 - 3 µg) were examined by SDS-PAGE with variations in the grade of SDS used and the pH of the separating gels (see sections 2.6.2). Migration of tubulin subunits was visualised after Coomassie blue

staining of SDS-PAGE gels (see section 2.6.3) or by western immunoblotting (see section 2.6.5) and the gels and blots were photographed with Alphaimager 2200 (Alpha Innotech Corp.).

2.9.2. Stage-specific expression and quantitation of *P. falciparum* α I- and β -tubulin during the intra-erythrocytic cycle

Quantification of α I- and β -tubulin expression during the asexual erythrocytic cycle of *P. falciparum* was carried out by a method adapted from that of Gavigan *et al* (2003). Briefly, synchronised parasites (see section 2.2.3) which included rings (6 -12 h post invasion), trophozoites (18 - 24 h post-invasion), and schizonts (36 - 42 h post-invasion) were harvested (see section 2.2.4), detergent-lysed (as in section 2.3.1) and protein concentrations of resulting whole cell extracts and solubilised pellets were determined by the method of Bradford (section 2.6.1). Whole cell extracts (8 - 10 μ g) from each stage of development, solubilised pellets (~ 2 - 3 μ g), and recombinant *P. falciparum* α I- and β -tubulins (1 - 5 ng) (see section 2.7) were electrophoretically separated by SDS-PAGE as outlined in section 2.6.2 and subjected to western immunoblotting with relevant antibodies as outlined in section 2.6.5. Bands on the resulting blots were quantified by densitometry using a GS-800 Densitometer (Bio-Rad) and comparison of the values obtained for synchronised parasite stages with those for recombinant tubulin standards gave an approximate quantitation of α I and β -tubulin present in whole cell extracts from the various stages. Results were correlated with previously published data on the transcription profiles of *P. falciparum* tubulin genes during the asexual stages of parasite development (De Risi Lab Transcriptome database site / PlasmoDB <http://plasmodb.org/>) using the accession codes, PF10180w, PFD1050w and PF10_0084.

2.9.3. Investigation of α II-tubulin expression in asexual stages of *P. falciparum* erythrocytic development

Previous reports have suggested that α II-tubulin expression at the protein level in *P. falciparum* is confined to male sexual-stage parasites (Rawlings *et al*, 1992). Data from the De Risi Lab Transcriptome database site (section 2.9.2) and previous reports (Delves *et al*, 1990) show that the α II-tubulin gene is also transcribed in asexual parasites, suggesting that a low level of expression of α II-

tubulin protein may exist outside of male sexual-stage parasites. To examine this possibility, synchronised parasites (see section 2.2.3) which included rings (6 - 12 h post invasion), trophozoites (18 - 24 h post-invasion), schizonts (42 - 48 h post-invasion) and gametocytes (~ stages III - IV) were harvested (see section 2.2.4), detergent lysed (as in section 2.3.1) and protein concentrations of resulting whole cell extracts and solubilised pellets were determined by the method of Bradford (section 2.6.1). Whole cell extracts (25 µg) from each stage, solubilised pellets (~ 2 - 3 µg) for asexual stages, ~ 25 µg for gametocytes stages III - V), and *P. falciparum* recombinant α I-tubulin (25 - 500 ng) were electrophoretically separated by SDS-PAGE as outlined in section 2.6.2 and subjected to western immunoblotting as outlined in section 2.6.5, with a 1/3000 dilution of α -tub II (anti-GYE) male-gamete specific antibody (MR4/American Type Culture Collection) which served as the primary antibody. Expression of α II-tubulin was also assessed in an asynchronous population of *P. falciparum* by immunofluorescent microscopy as outlined in section 2.4.5 with a 1/200 - 1/500 dilution of α -tub II (anti-GYE) as primary antibody.

2.10. INVESTIGATION OF THE DINITROANILINE BINDING SITE ON *P. FALCIPARUM* TUBULINS

2.10.1. Investigation of the interaction of [¹⁴C] trifluralin with recombinant *P. falciparum* tubulin fusion proteins

To determine if [¹⁴C] trifluralin could bind to *P. falciparum* recombinant tubulin fusions (see section 2.7), a study adapted from Hess *et al* (1977) was undertaken. 5.8 µM [¹⁴C] trifluralin (sp. act. 16.8 mCi / mmol) alone or in the presence of ~ 8.7 µM protein (MBP- α I-tubulin fusion, MBP- β -tubulin fusion, MBP alone, or bovine brain α/β tubulin (Cytoskeleton Inc.)) in G-PEM-G buffer were incubated for 1 h in a 37°C water bath and subsequently cooled on ice for ~ 20 min. Free trifluralin (low-molecular weight component) was separated from trifluralin that had become bound to the proteins (high-molecular weight component) by gel filtration (Sephadex G-100, Sigma-Aldrich, prepared according to manufacturers instructions) at 4°C on a 6.2 x 1-cm column (Pharmacia) prepared fresh for each assay. The void volume of the column (fraction 2) was determined by elution of Blue Dextran 2000 (mol. wt. 2,000,000) (Pharmacia). The protein-trifluralin mixture was eluted from the column with column buffer (10 mM PIPES-NaOH, pH 6.9, 10

mM MgCl₂, 100 mM NaCl, 0.1 mM GTP) and 1-ml fractions were collected at a rate of 1 drop per 15 seconds. Fractions were divided into two: fraction A (250 µl) was used for protein determination by the Bradford method as outlined in section 2.6.1 and fraction B (750 µl) was mixed with 3 ml of scintillation cocktail (EcoLite, ICN Biomedicals Inc., Aurora, Ohio, USA) and radioactivity was counted in a liquid scintillation spectrometer (Packard Tri-Carb model 2100TR). The absolute amounts of radioactivity (dpm) were determined using a [¹⁴C] internal standard.

2.10.2. Sequence alignments

The amino acid sequences of α - and β -tubulins from a number of higher plants (sensitive to dinitroaniline herbicides) and various mammals (generally resistant to dinitroanilines) were aligned independently using ClustalW 1.8 (Higgins *et al*, 1996). Amino acid sequences were obtained from the Pubmed Entrez database (<http://www.ncbi.nlm.nih.gov/entrez>) and accession numbers are outlined in Table 2.3. From the alignments, representative plant and animal α - and β -tubulin sequences were determined. Subsequently these sequences were aligned to the amino acid sequences of *P. falciparum* α I- and β -tubulins (see Table 2.3.) using ClustalW 1.8. From the resulting alignments, residues which were identical or deemed to be similar in plant and *P. falciparum* tubulins but different in mammalian tubulins were highlighted. Such differences were categorised as being conserved, semi-conserved or non-conserved, depending on the amino acids involved.

2.10.3. Molecular modeling of *P. falciparum* tubulins

The 3-dimensional structure of the α - β tubulin heterodimer from bovine brain was previously obtained by electron crystallography of zinc-induced tubulin sheets stabilized with Taxol (Nogales *et al*, 1998). *P. falciparum* and bovine brain α - and β -tubulins share ~ 83% and ~ 87% identity at the amino acid level, respectively, making the crystal structure of the bovine brain tubulin heterodimer a suitable template for homology modeling of *P. falciparum* tubulins. *P. falciparum* α I- and β -tubulin subunits (accession nos. X15979 and X16075, respectively) were modeled independently using the co-ordinates of the α - and β -tubulin subunits of the bovine crystal structure (PDB (<http://www.rcsb.org/pdb/>) No. 1JFF) as templates. Homology modelling was performed using the Insight II, Biopolymer and Discover software from Accelrys (San Diego, CA, USA), running on a Silicon Graphics O₂

Table 2.3. Tubulin sequences used in alignment studies.

<u>α-tubulin</u>	<u>accession no.</u>	<u>β-tubulin</u>	<u>accession no.</u>
<u>Plants</u>		<u>Plants</u>	
<i>Zea mays</i> (Maize)		<i>Arabidopsis thaliana</i>	
Isotype 1.....	L27815	Isotype 2.....	M84700
Isotype 2.....	X15704	Isotype 4.....	M21415
<i>Eleusine indica</i> (Goosegrass)		<i>Lupinus albus</i> (White lupine).....	
Isotype 1.....	AF008120		X70184
Isotype 3.....	AF008122	<i>Zea mays</i>	
<i>Arabidopsis thaliana</i> (Thale cress)		Isotype 1.....	AF059287
Isotype 1.....	M17189	Isotype 2.....	X52879
Isotype 2.....	M84696	<i>Oryza sativa</i> (Rice)	
Isotype 4.....	M84697	Isotype 1.....	X79367
Isotype 6.....	M84699	Isotype 2.....	X79368
<i>Pisum sativum</i> (Garden pea).....		<i>Pisum sativum</i>	
	U12589	Isotype 1.....	X54844
<i>Prunus dulcis</i> (Almond).....		<i>Glycine max</i> (Soybean).....	
	X67162		X60216
<u>Mammals</u>		<u>Mammals</u>	
<i>Sus scrofa</i> (Pig).....		<i>Sus scrofa</i>	
	P02550		PO2554
<i>Rattus norvegicus</i> (Rat).....		<i>Rattus norvegicus</i>	
	J00797		AB011679
<i>Mus musculus</i> (Mouse).....		<i>Mus musculus</i>	
	BC083120	Isotype 3.....	NM_011655
<i>Homo sapiens</i> (Human)		<i>Homo sapiens</i>	
Isotype 1.....	NM_006000	Isotype 1.....	AF141349
Isotype 2.....	NM_006001	Isotype 2.....	NM_006088
Isotype 4.....	NM_00600	Isotype 4.....	NM_006086
<i>Cricetulus griseus</i>		Isotype 5.....	NM_178014
(Chinese hamster).....	AY173017	<i>P. falciparum</i>	
<u><i>P. falciparum</i></u>		<u><i>P. falciparum</i></u>	
Strains: K1/Thailand.....	X15979	Strains: K1/Thailand.....	X16075
3D7a1.....	PF10180w	FCR-3/Gambia.....	M28398
		NF54.....	M31205
		3D7.....	PF10-0084

workstation. The models of *P. falciparum* tubulins generated were then modified using the computer programme Rotamers (Insight II software), which invoked re-positioning of atoms that were in energetically unsuitable positions. The formal charge was adjusted to zero by the addition of H atoms or –OH groups to the N- and C- termini of both monomers to correct for unbalanced charges as a result of the Rotamers programme and subjected to ~ 1000 rounds of energy minimisation refinement with the DISCOVER programme (Accelrys, San Diego, U.S.A.). Modeled α - and β -tubulin subunits were superimposed individually on the bovine heterodimer and combined to form the *P. falciparum* $\alpha\beta$ heterodimer model. The dimeric model was energy-minimised using DISCOVER to allow for appropriate inter-monomeric contacts. GTP, GDP, and Taxol were excluded from the model. The N-terminal methionines of both monomers and the C termini of α -tubulin (amino acid positions 442 - 447) and β -tubulin (amino acid positions 428 - 457) were not included in the model, because they were not resolved in the bovine tubulin structure (Nogales *et al*, 1998). In addition, residues in the N-loop region (amino acid positions 35 - 60) of α -tubulin were built in very weak density and were included for completeness in the original bovine model, but were disregarded in later refinements (Löwe *et al*, 2001). A recent report suggests that the N-loop region may play a role in forming the dinitroaniline-binding site on the tubulin dimer of *Toxoplasma gondii* (Morrissette *et al*, 2004). To model this segment accurately, the protein database (PDB) (Berman *et al*, 2000) was searched with the sequence of this section using the software BLAST (Altschul *et al*, 1990), but no similar structures were identified. The bacterial cell-division protein FtsZ, which has a similar three-dimensional structure to α - and β -tubulin (Löwe *et al*, 1998), was also investigated for the presence of an N-loop region, which was found not to be present. The omitted N-loop structure (residues Gln35 - Lys60) of the *P. falciparum* α I-tubulin model was designed by using the related bovine β -tubulin N-loop region (1JFFB). The appropriate N-loop region from bovine β -tubulin was extracted and used for homology modeling of the *P. falciparum* α I-tubulin N-loop region using Insight II software as outlined previously. The modeled N-loop was then adjusted to fit onto the modeled *P. falciparum* α -tubulin monomer using a best fit-approach. The modeled N-loop and α -monomer were subjected to energy minimisation using the DISCOVER programme as previously outlined. Coordinates and interactive views of the *P. falciparum* α I- β -tubulin heterodimer model with and without the N-loop

structure were made accessible to the Chimera protein structure visualisation tool (<http://www.cgl.ucsf.edu/chimera/>) for future manipulations.

2.10.4. Identification of a putative trifluralin-binding site

In section 2.10.2, residues were identified that were identical or similar in plant and *P. falciparum* tubulins but different in mammalian tubulins. These residues were subsequently mapped onto the *P. falciparum* dimeric tubulin model. The *P. falciparum* tubulin model was then investigated for any potential trifluralin-binding domains using the highlighted residues as a starting point. The molecular structure of trifluralin was built using the Biopolymer software. The potential trifluralin-binding domains identified were assessed by manual docking of the configured trifluralin molecule into the putative sites and comparing the docking process on the same region in the bovine tubulin model. The autodock programme, Monte Carlo (Insight II software), was also used to complement the manual docking procedures. Energy-refinement of any ligand-receptor complexes identified was invoked in each case to lessen the number of negative contacts. The putative site identified was made accessible for viewing by the Chimera tool.

Chapter 3

Antimalarial Activity and Mechanisms of Action of the Dolastatin/Auristatin Family of Compounds

3.1. INTRODUCTION

Microtubules of *P. falciparum* have previously been identified as a potential target for antimalarial chemotherapy (Bell, 1998; Taraschi *et al*, 1998). Their crucial role in cell division coupled with the ability of drugs that interact with tubulin to interfere with the cell cycle have already made microtubules a successful target for applications that include fungicides (Hollomon *et al*, 1998), anticancer drugs (Altmann, 2001; Kavallins *et al*, 2001) and anthelmintic agents (Lacey, 1988).

A number of microtubule inhibitors have been shown to inhibit *P. falciparum* sexual and asexual forms of development apparently by interfering with the tubulin/microtubule system of the parasite (Bejon *et al*, 1997; Bell, 1998; Dieckmann *et al*, 1989; Fowler *et al*, 1998; Kaidoh *et al*, 1995; Schrével *et al*, 1994; Sinou *et al*, 1996; Sinou *et al*, 1998; Taraschi *et al*, 1998; Usanga *et al*, 1986). While many of these compounds have proved useful in elucidating the roles of microtubules throughout the various developmental stages of *P. falciparum*, their potential medical use is hindered by their toxicity to mammalian cells, probably resulting from the high level of amino acid conservation between *P. falciparum* and mammalian tubulins. Nonetheless, results from the “*Vinca*” alkaloid and taxoid groups indicate it is possible to have higher potency against cultured parasites than host cells (Bell, 1998). This coupled with the success of benzimidazole anthelmintics, whose potency results from a differential binding to host and parasite tubulin (Lacey, 1988), implies that microtubule inhibitors could be discovered or fashioned into antimalarial drugs with low host toxicity, possibly as a result of fine differences in tubulin structure, or different rates of drug uptake.

In light of the excellent but unselective antimalarial activity of the microtubule inhibitor dolastatin 10 (IC₅₀ 100 pM) (Bell, A, personal communication), the rationale of the work reported in this chapter was to: (1) investigate the antimalarial activity of a number of synthetic derivatives of dolastatin 10, the auristatins, and from the data obtained to compare the orders of activity of the series against parasite and mammalian cells to determine whether a compound with striking selectivity for parasite over mammalian cells could be identified; and (2) to characterise the morphological and cellular effects of dolastatin 10 and related peptides on intra-erythrocytic *P. falciparum* growth in comparison with other classes of microtubule inhibitor. This characterisation involved: (i) investigation of the stage-specific sensitivities of *P. falciparum* cultures; (ii) analysis of the effects of

inhibitors on parasite maturation and morphology; (iii) inhibitor reversibility studies; and finally (iv) investigation of the effects of inhibitors on mitotic microtubular and nuclear structures in the parasite.

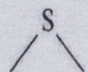
3.2. RESULTS

3.2.1. Growth inhibition of cultured *P. falciparum* by microtubule inhibitors

3.2.1.1. Dolastatin 10

Dolastatin 10, a pseudopeptide isolated from the shell-less mollusc *Dolabella auricularia* found in the Indian Ocean, inhibited *P. falciparum* grown asynchronously in culture, as measured by the pLDH method outlined in section 2.4.1 (Bell, A, personal communication; Fennell *et al*, 2003) with an IC₅₀ (concentration of drug required to inhibit parasite growth by 50%) of 100 pM after 72 h incubation. Unfortunately, dolastatin 10 also displays a similar degree of potency against a number of mammalian cell lines (see Table 3.1) preventing its subsequent progression as a potential antimalarial agent. It was also noted that the determination of an IC₅₀ value for dolastatin 10 after 48 h incubation was problematic due to the presence of a “plateau” of partial inhibition (~ 50 - 70% inhibition) over a very extensive drug concentration range between ~ 250 pM and ~ 8 µM (Bell, A, personal communication; Fennell *et al*, 2003). The lack of a clear sigmoidal-concentration effect relationship as seen with most potent antimalarials (Makler *et al*, 1993) is an unusual phenomenon, but one that has been previously reported with another potent microtubule inhibitor Taxotere (Schrével *et al*, 1994). After 72 h incubation the level of the plateau was reduced to 80 - 90% inhibition over the same drug concentration range. Only after incubation periods of 96 h was the biphasic effect completely eliminated and a single sigmoidal curve obtained. Consequently it would appear that one part of the asynchronous population of parasites used in these assays was more susceptible to inhibition than the other. Furthermore, the disappearance of the plateau upon longer exposure times suggests that the two populations may differ in age at the start of the experiment and that different stages are responding to the agents in different ways i.e. some are inhibited after 48 h drug exposure and some are not.

Table 3.1. Inhibitory effects on growth of *P. falciparum* and mammalian cells (various lines) by dolastatin 10 and derivatives

Compound	Substituent groups				IC ₅₀ <i>P. falciparum</i> (nM)	IC ₅₀ mammalian (nM) ^d			
	R1	R2	R3	R4		P388	ASU ^a	NCI ^b	L1210
Dolastatin 10	N(Me) ₂	<i>i</i> -Pr	<i>i</i> -Pr	CH(CH ₂ Ph)2-thiazolyl	0.1 ^c	0.059	0.0077	0.12	0.5
Auristatin PE	N(Me) ₂	<i>i</i> -Pr	<i>i</i> -Pr	CH ₂ CH ₂ Ph	2 ^c	–	0.01	0.49	0.6
Auristatin PYE	N(Me) ₂	<i>i</i> -Pr	<i>i</i> -Pr	CH ₂ CH ₂ (2-pyridyl)	4.6	1.0	0.01	0.85	5
Auristatin C	N(Me) ₂	<i>i</i> -Pr	<i>i</i> -Pr	CH ₂ CH ₂ Ph(<i>p</i> -Cl)	90	7.5	<0.006	0.76	3
GRP18112	N(Me) ₂	<i>i</i> -Pr	<i>i</i> -Pr	CH(CO ₂ Me)CH ₂ Ph	5.2	88	<0.13	0.44	5
GRP18290	N(Me) ₂	<i>i</i> -Pr	<i>i</i> -Pr		0.34	<0.11	–	–	–
Auristatin M	N(Me) ₂	<i>i</i> -Pr	<i>i</i> -Pr	CH(CH ₂ Ph)CONHC=N-N=CPh	1.9	0.52	<0.13	0.4	6
GRP18158	N(Me) ₂	<i>i</i> -Pr	<i>i</i> -Pr	CH(CO ₂ Me)CH ₂ CH ₂ SMe	9	0.42	–	–	–
Auristatin MQ	N(Me) ₂	<i>i</i> -Pr	CH ₂ <i>i</i> -Pr	CH(CH ₂ CH ₂ SMe)CONH(3-quinolyl)	38	0.31	<0.061	1.6	3
Auristatin PAC	N(Me) ₂	<i>i</i> -Pr	CH ₂ <i>i</i> -Pr	CH(CH ₂ Ph)CONHPh(<i>p</i> -Cl)	9	0.0029	0.011	1.8	0.5
GRP18183	[CH ₂] ₃ NHC(NHCO ₂ CH ₂ Ph) NCO ₂ CH ₂ Ph	NHCO ₂ CH ₂ Ph	<i>i</i> -Pr	CH(CO ₂ Me) [CH ₂] ₃ NHCO ₂ CH ₂ Ph	240	–	800	–	600

^aGeometric means for the Arizona State University cell line panel (Pettit *et al.*, 1995 and 1998) (n=6).

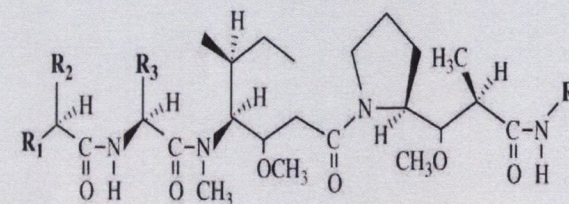
^bGeometric means for the US National Cancer Institute cell line panel (n=60).

^cData - Bell, A, personal communication.

–, not determined.

^dData - Pettit, G, personal communication.

i-Pr = iso-propyl
Ph = phenyl



3.2.1.2. Auristatins

In view of the excellent antimalarial potency of the archetype compound, dolastatin 10, the antimalarial activities of a number of its synthetic derivatives, the auristatins, were investigated. The rationale was to explore the possibility that from the derivative series, an agent might be identified which retains or exceeds the antimalarial activity of the parent drug, while exhibiting a prominent selectivity for parasite cells over those of various mammalian cell lines. Compounds of the auristatin series were observed to have varying potencies, with IC_{50} values between 340 pM and 240 nM (Table 3.1), with no compound displaying superior activity to dolastatin 10. GRP18290 was the most active of the derivatives tested with a 72 h IC_{50} of 340 pM. It also displayed the presence of a “plateau” of partial inhibition (~ 50 - 70% inhibition) in 48 h dose-response curves as seen with the dolastatins, over a wide drug concentration range from ~ 1 nM to ~ 400 nM. Following 72 h exposure, the plateau was reduced to ~ 90% inhibition compared to control growth over the same drug concentration range (Fig. 3.1 a). Biphasic dose response curves were also evident with the majority of compounds tested from the auristatin series (data not shown). Interestingly, as seen with auristatin PE (Fig. 3.1 b) (Bell, A - personal communication; Fennell *et al*, 2003), the plateau effect for most of the derivatives initiated at a drug concentration of ~ 1 - 70 nM and extended frequently into the micromolar range of drug concentrations tested. It was also observed, for dolastatin 10 and auristatin PE, that the dose response curve for 48 h inhibition turns from partial (latter section of plateau effect) to complete inhibition at roughly the same drug concentration (between 10 and 100 μ M), despite the varying width of plateau (Bell, A - personal communication; Fennell *et al*, 2003). The data suggested that this class of microtubule inhibitor was equally active against a low-affinity target in the micromolar concentration range but activity fluctuated greatly (IC_{50} values of 100 pM - 240 nM) against a separate high-affinity target in the sub-nanomolar to nanomolar concentration range. The presence of two putative targets of varying affinity for the dolastatin/auristatin series also appears for the structurally-unrelated microtubule inhibitors vinblastine (Fig. 3.2) (72 h IC_{50} , 250 nM; 48 and 72 h plateaux from ~ 500 nM to 16 μ M) and Taxol (Fig. 3.2) (72 h IC_{50} , 60 nM; 48 h plateau from ~ 100 nM to 8 μ M) (Bell, personal communication; Fennell *et al*, 2003).

Analysis of results from mammalian cell lines showed closer potency of dolastatin 10 and auristatin PE and less difference in potency between the dolastatins

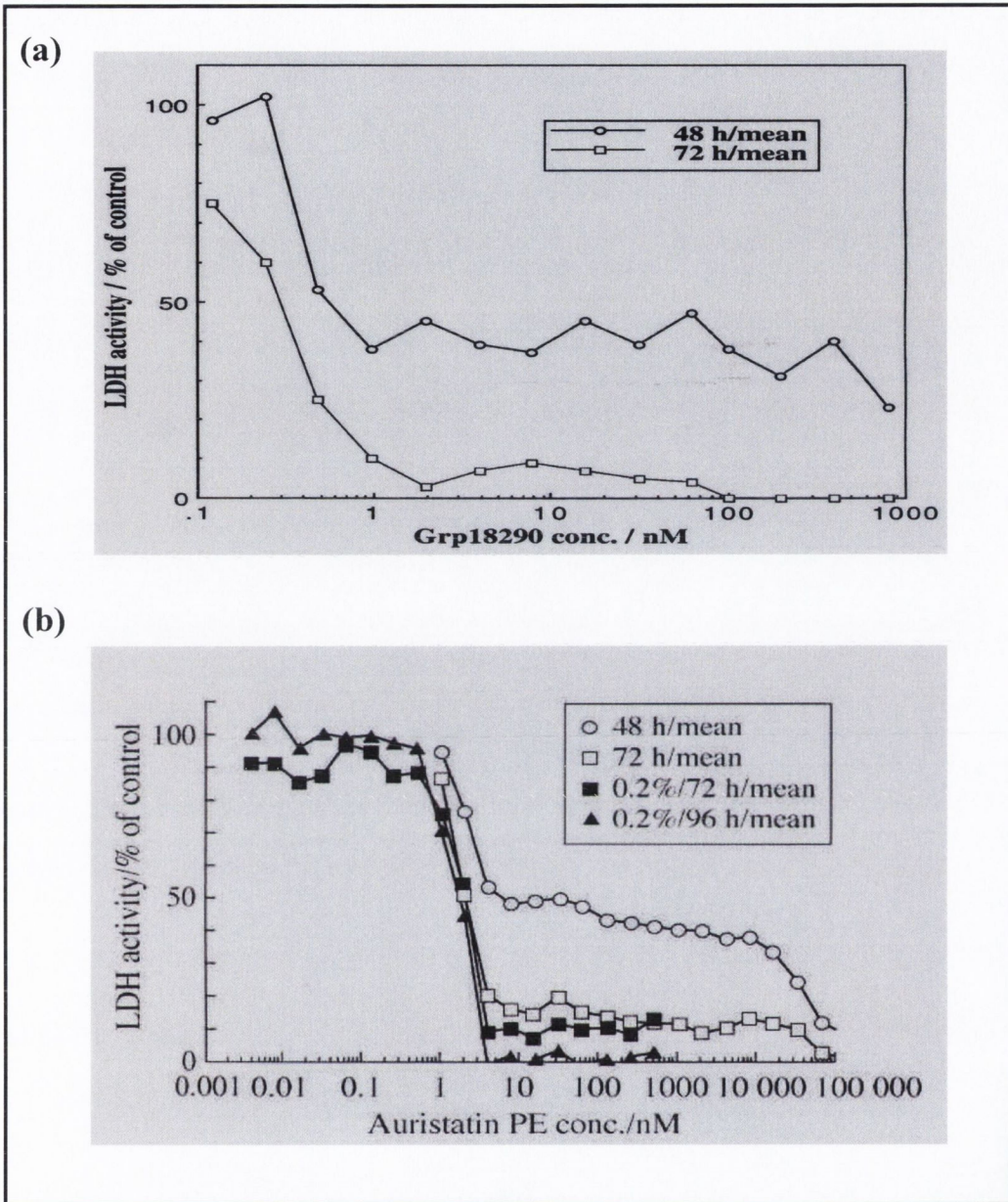


Figure 3.1. Susceptibilities of asynchronous cultures to GRP18290 (a), and auristatin PE (b), as measured by the pLDH method. Geometric mean values of four to eight determinations after 48 h (circles) and 72 h (squares) are shown; the initial parasitemias were 0.8%. In (b), mean values after 72 h (black squares) and 96 h (black triangles) are shown for initial parasitemias of 0.2%. Data in (b) are from Fennell *et al* (2003).

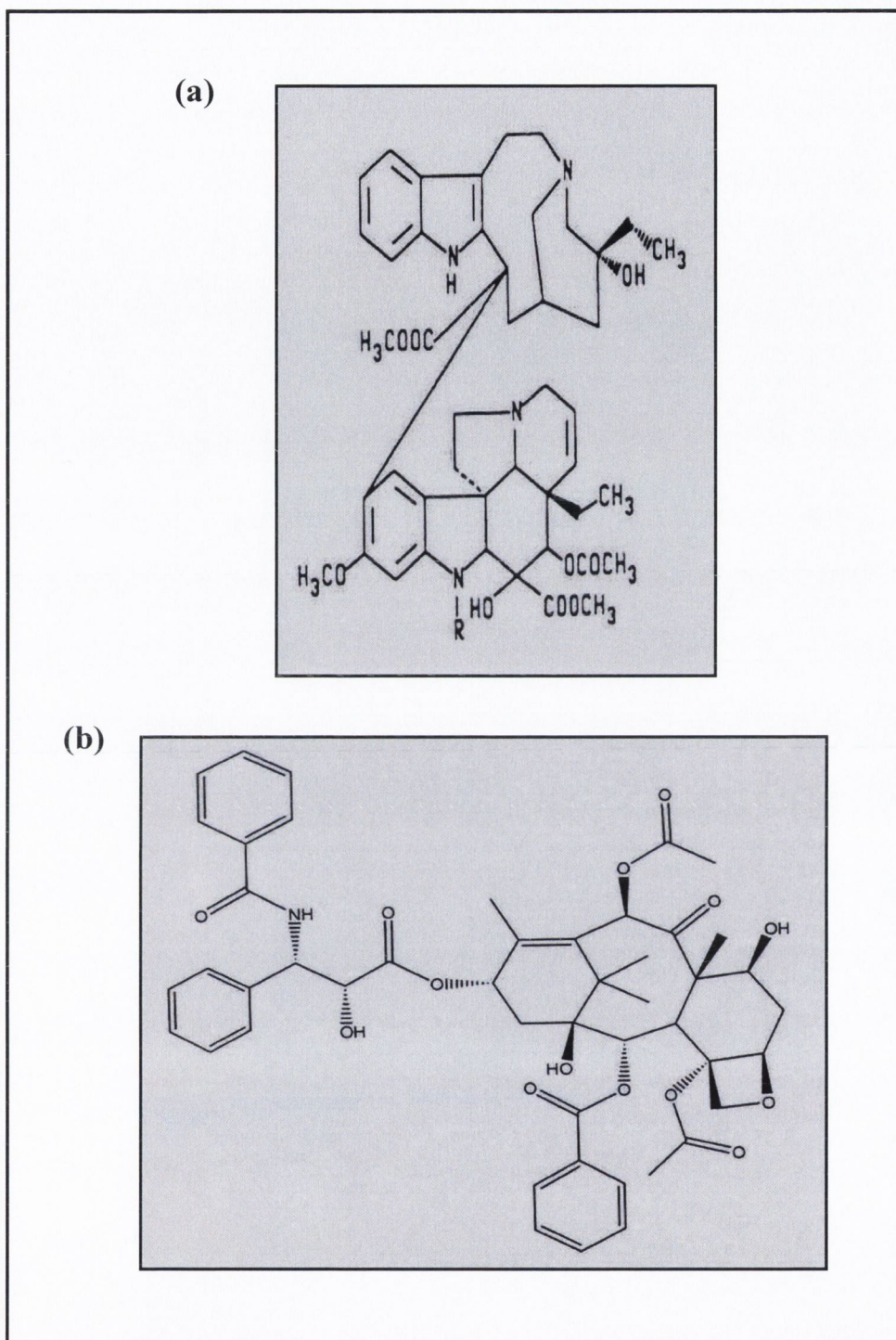


Figure 3.2. Chemical structures of vinblastine (a) and Taxol (b) used in this study. Note in the case of (a) R = CH₃.

(Poncet, 1999) than is apparent here against *P. falciparum*. However, none of the dolastatin structural modifications were found to result in significantly stronger antimalarial than antimammalian cell activity. A structure-activity relationship (SAR) for the dolastatin/auristatin series of compounds based on the data presented in Table 3.1 for antimalarial activity relative to mammalian cell toxicity revealed: (i) merit exists in having the heterocyclic side chain extensions at position R4 in GRP18290 and dolastatin 10 over that in auristatin PE; (ii) the chlorophenyl group in auristatin C results in lower activity than a phenyl (auristatin PE) or pyridyl (auristatin PYE); and (iii) the additional CH₂ in auristatin MQ at position R3 confers a shortcoming in activity relative to GRP18158.

3.2.2. Stage-specific sensitivities of *P. falciparum* to microtubule inhibitors

The purpose of this experiment was two-fold: (i) to determine at which point during the parasite's erythrocytic cycle addition of dolastatin 10/auristatin PE caused maximum inhibition of parasite growth and (ii) to explain the plateau effect.

As demonstrated in section 3.2.1 the biphasic dose-response curves of the dolastatin/auristatin series imply that two individual populations of parasites were present with differing susceptibilities, but that the less susceptible population disappears upon longer exposure to inhibitors, as shown by the disappearance of the plateau. However, it is also worth remembering that a lag period may exist as the drug infiltrates the parasite cell to its site of action and takes full effect, so although parasites may be at the stage most susceptible to inhibition, they may not be exposed to sufficient concentrations of inhibitor to impede their subsequent progression through the erythrocytic cycle.

To test this hypothesis, parasite cultures were synchronised to produce eight populations with age ranges of ~ 6 h, which covered the parasite's whole intra-erythrocytic developmental cycle. Then inhibitor susceptibilities for 48 h exposure were determined for each of these populations. The data in Table 3.2 clearly indicate that application of dolastatin 10 or auristatin PE at different time points in the parasite's intra-erythrocytic cycle results in different inhibition profiles. Cultures initially aged 0 -6, 6 - 12, 12 - 18 and 42 - 48 h post-invasion at the start of exposure were found to be highly resistant at the inhibitor concentrations tested. In contrast, cultures aged 18 - 24, 24 - 30 and 30 - 36 h post-invasion at the start of exposure were found to be extremely susceptible at the inhibitor concentrations tested,

Table 3.2. Susceptibilities of synchronous cultures of different initial ages upon 48 h exposure to inhibitors.

Age of culture (h post-invasion)	Dolastatin 10			Auristatin PE			Vinblastine			Taxol		
	IC ₂₅ (nM)	IC ₅₀ (nM)	IC ₇₅ (nM)	IC ₂₅ (nM)	IC ₅₀ (nM)	IC ₇₅ (nM)	IC ₂₅ (nM)	IC ₅₀ (nM)	IC ₇₅ (nM)	IC ₂₅ (nM)	IC ₅₀ (nM)	IC ₇₅ (nM)
0-6	>7.8	>7.8	>7.8	>125	>125	>125	>16000	>16000	>16000	>8000	>8000	>8000
6-12	>7.8	>7.8	>7.8	>125	>125	>125	>16000	>16000	>16000	>8000	>8000	>8000
12-18	>7.8	>7.8	>7.8	3	>125	>125	ND ^a	>10000	>16000	2000	>8000	>8000
18-24	0.06	0.1	0.2	2	4	7	30	50	100	20	40	80
24-30	0.03	0.07	ND ^a	2	3	10	<31	<31	40	20	40	90
30-36	0.08	0.1	0.2	2	4	10	<31	<31	40	30	80	200
36-42	0.09	0.1	>7.8	3	4	>125	40	50	>16000	50	200	>8000
42-48	>7.8	>7.8	>7.8	>125	>125	>125	5000	>16000	>16000	>8000	>8000	>8000

^aND, not determined; plateau near this level of inhibition.

displaying dose-response curves (data not shown) similar to those obtained with asynchronous cultures after 72 h incubation with auristatin PE (see Fig. 3.1). Populations aged 36 - 42 h post-invasion at the start of exposure were found to display susceptibilities intermediate between the previous two extremes. These differences were found in spite of the fact that all of the cultures were exposed to inhibitor for the same 48 h total. Therefore, dolastatin 10 and auristatin PE appear to display their most intoxicating effect when initially applied at the trophozoite / early schizont stage of asexual parasite development.

3.2.3. Effects of inhibitors on parasite maturation and morphology

Assays were established with parasite cultures synchronised to the early trophozoite stage (18 - 24 h post-invasion) i.e. the initial age most susceptible to dolastatin 10 and auristatin PE in the 48-h experiments, to see what effects these inhibitors had on the intra-erythrocytic development of the parasites. They were exposed to dolastatin 10 and auristatin PE and examined for obvious morphological abnormalities or developmental irregularities by Giemsa-stained smears as outlined in section 2.4.3. The results presented in Fig. 3.3 (a) indicated the following: (i) in untreated controls, parasites continued their intra-erythrocytic development through the schizont and segmenter stages of development to subsequently re-invade new erythrocytes and cause an increase in parasitemia; and (ii) in dolastatin-10-treated cultures, parasites also appeared to be able to progress to the schizont stage of maturity. However, at subsequent time points, when new rings /trophozoites were emerging in untreated controls, schizonts were seen to persist in drug-treated cultures with an ensuing plunge in parasitemia, suggesting the inhibitors were obstructing late maturation of intra-erythrocytic forms of the parasite. Similar effects were observed with both Taxol and vinblastine (Fig. 3.3 a). This developmental delay, which materialises in the arrest of the parasite at the schizont stage, correlates well with similar reports from other classes of microtubule inhibitors such as taxoids (Sinou *et al*, 1996). It was also observed that some of the developmentally-delayed schizonts appeared distorted or irregular in morphology compared to untreated controls (Fig. 3.3 b and c). This deformation of the typical morphology of schizont-stage parasites was also apparent for Taxol- and vinblastine-treated cultures (data not shown). It was also noted that the characteristic appearance of mature schizonts with well-defined merozoite structures was rarely observed in dolastatin 10-treated cultures.

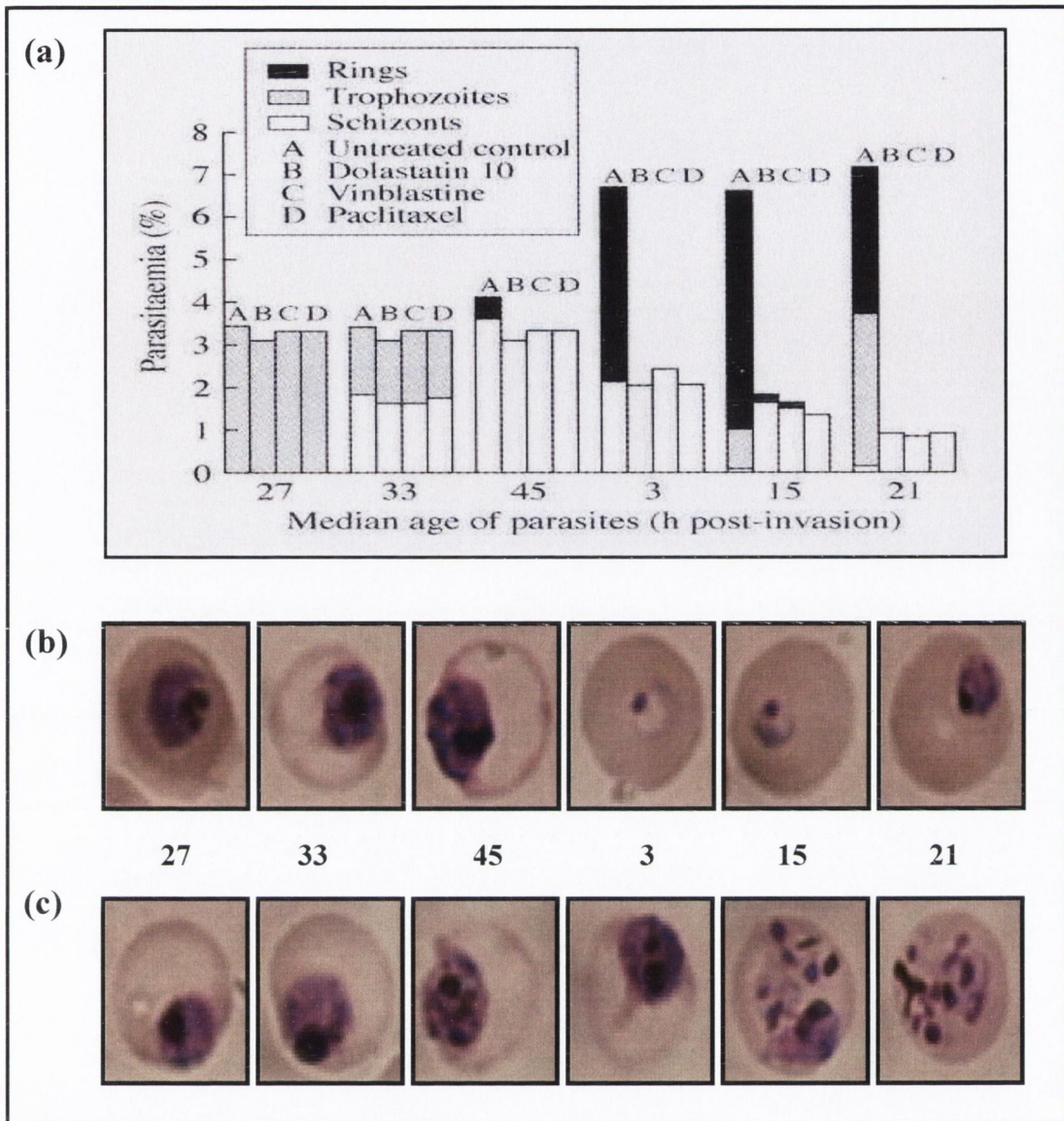


Figure 3.3. Development of parasites in the presence of inhibitors. (a) Cultures of 18 - 24 h post-invasion were exposed to no inhibitor, or 0.8 nM, 2.0 μ M or 480 nM, respectively, of dolastatin 10, vinblastine, or Taxol as indicated, and smears were counted at 6 or 12 h intervals, as described in section 2.4.3. The ages of parasites shown on the x-axis are averages over an \sim 6 h range. The data are those of a representative experiment. (b), (c) Morphology of parasites. Cultures were treated as described above, and the microscopic appearance of parasitised erythrocytes in Giemsa-stained smears was photographed. The numbers indicate the median ages of the parasites in hours post-invasion. The parasites shown are representative of those examined. (b) no inhibitor, (c) 0.8 nM dolastatin 10.

The only forms seen were as illustrated in Fig. 3.3 (c) or were exoerythrocytic parasite remnants.

3.2.4. Stage-dependent susceptibility and inhibitor reversibility studies

The stage-dependent susceptibility of *P. falciparum* to short exposures (6 h) of dolastatin 10 and auristatin PE was evaluated by subjecting ring-infected (6 - 12 h post-invasion), trophozoite infected (21 - 27 h post-invasion) and schizont-infected (36 - 42 h post-invasion) erythrocytes to various concentrations of dolastatin 10 and auristatin PE. At the end of the incubation period, cultures were carefully washed and recultured for 48 h in inhibitor-free medium. The results in Fig. 3.4 reveal that the susceptibility of *P. falciparum* towards dolastatin 10 and auristatin PE differed according to its particular erythrocytic stage of development. The progression of ring forms was unaffected at inhibitor concentrations equivalent to 8x (Fig. 3.4) and 80x (data not shown) IC₅₀. The development of trophozoite forms pulsed for 6 h with 8x IC₅₀ dolastatin 10 or auristatin PE resulted in ~ 60% inhibition compared to controls, suggesting that these drugs had the ability to penetrate trophozoite cells within the 6 h incubation period. The schizont stage appeared to be the most sensitive, with inhibition of ~ 90% and 86% of parasite development by dolastatin 10- and auristatin PE-pulsed cultures, respectively. This result suggests that the inhibitors can readily infiltrate the parasitised erythrocytes at this stage of development and correlates well with the previous observation of activity of both dolastatin 10 and auristatin PE on the schizont stage of parasite development (see section 3.2.4). A similar profile of stage-dependent killing was seen with Taxol and vinblastine (Fig. 3.4). Thus, a 6-h pulse of dolastatin 10 at a concentration as low as 0.8 nM appears to be sufficient to block parasite maturation when the exposure is just before or during the period of parasite division (schizogony).

3.2.5. Effects of inhibitors on mitotic microtubular structures

Results up to now have indicated that dolastatin 10 and auristatin PE appear to interact with a high-affinity target in the nanomolar range in parasite cultures aged 18 - 42 h post-invasion, with an apparent primary effect on schizogony. As the primary target of dolastatin 10 and auristatin PE in mammalian cells has previously been found to be microtubules (Poncet, 1999), the effects of both compounds on *P. falciparum* tubulin-containing structures was explored by immunofluorescent

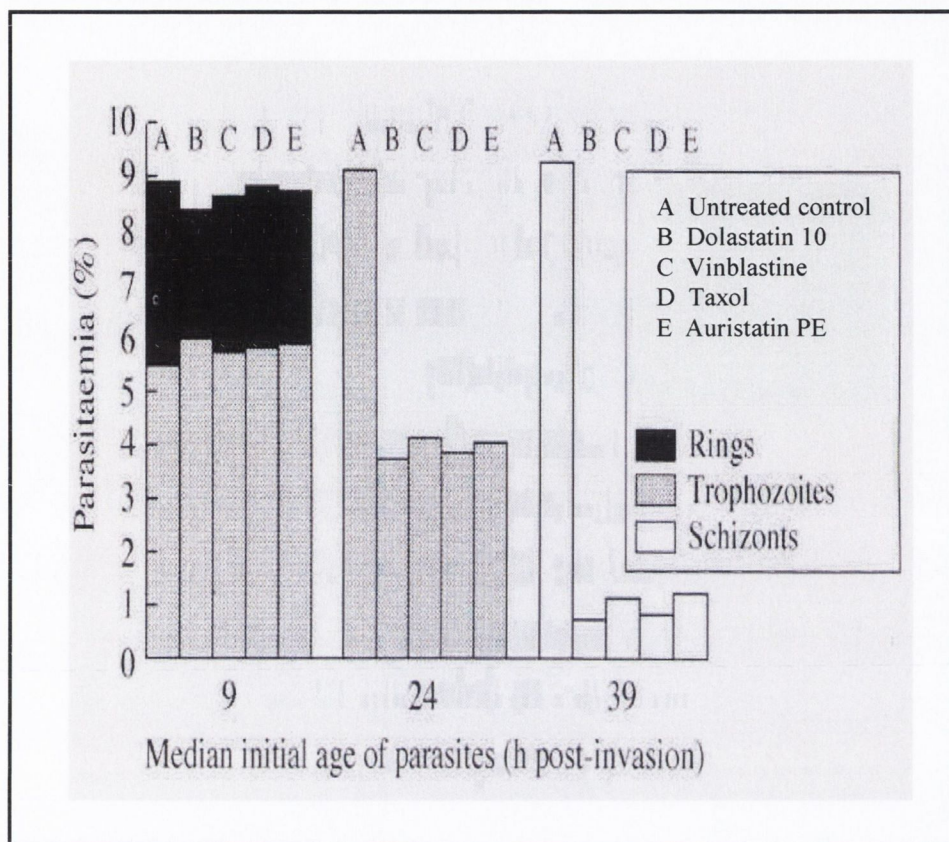


Figure 3.4. Effects of microtubule inhibitors on different developmental stages. Cultures synchronised to the ring stage (6 - 12 h post-invasion), trophozoite stage (21 - 27 h) and schizont stage (36 - 42 h) were each incubated for 6 h in the presence of no inhibitor or 0.8 nM, 2.0 μ M, 480 nM or 16 nM of dolastatin 10, vinblastine, Taxol or auristatin PE, respectively, as indicated. The cells were then washed, recultured for 48 h in inhibitor free medium, and finally examined on Giemsa-stained smears; the parasitemias obtained at this time are indicated on the y-axis. The ages of parasites shown on the x-axis are averages over the \sim 6 h range at the beginning of the experiment. The data shown are from a single, representative experiment.

microscopy (see section 2.4.5). Using asynchronous, inhibitor-free control cultures, mitotic and post-mitotic microtubular structures were observed which consisted of mitotic spindles and microtubule-organising centres (MTOC's) (Fig 3.5 a). The nuclear material (stained with DAPI) was organised at the ends of the mitotic spindles as expected. The presence of ~ 5 nuclear bodies in both parasites suggested that they were undergoing schizogony. Similar tubulin-containing structures in malarial parasites have previously been reported by Fowler *et al* (1998) and Read *et al* (1993). Treatment of asynchronous cultures with dolastatin 10 or auristatin PE resulted in the loss of typical tubulin-containing mitotic structures and caused non-specific tubulin staining, over the total area of the parasite cell, with the exception of the haemozoin granules (Fig. 3.5 b and c, respectively). The labelling of the nuclear DNA with DAPI showed nuclei which appeared more irregular in size and shape than those in control cells, sometimes appearing in grape-like clusters, which implied that the inhibitors were causing a block on nuclear division, but possibly not DNA synthesis. Similar redistribution of microtubule-containing structures in a diffuse manner over the parasite cell apparently indicating gross microtubule depolymerisation coupled with an apparent partially-segmented nuclear mass brightly stained with DAPI was observed upon exposure of parasites to vinblastine (Fig. 3.5 d). In fact the effects of the structurally-unrelated inhibitors vinblastine and dolastatin 10 / auristatin PE were impossible to distinguish except in that their effective concentrations differed. The effects were dissimilar to those of Taxol, which resulted in accumulation of thick elongated rods of tubulin in place of the normal structures (Fig. 3.5 e). These microtubules that extended from a centriolar plaque, appeared much longer and thicker than those observed in control cells. Although some nuclear division was observed (possibly parasites in late stages of erythrocytic development that escaped the actions of the drug) most nuclear partition appeared to be prevented leading to non-segmented nuclei which were brightly stained with DAPI (Fig. 3.5 e).

To gauge the action of these agents more quantitatively, cultures were synchronised to the trophozoite stage (27 - 33 h post-invasion) and exposed to inhibitors for 6 h, after which most of the control parasites had entered schizogony. The numbers of parasites containing normal and irregular mitotic structures were counted (Table 3.3; these data were obtained by undergraduate student S. Carolan). The results showed that both dolastatin 10 and auristatin PE caused a complete loss

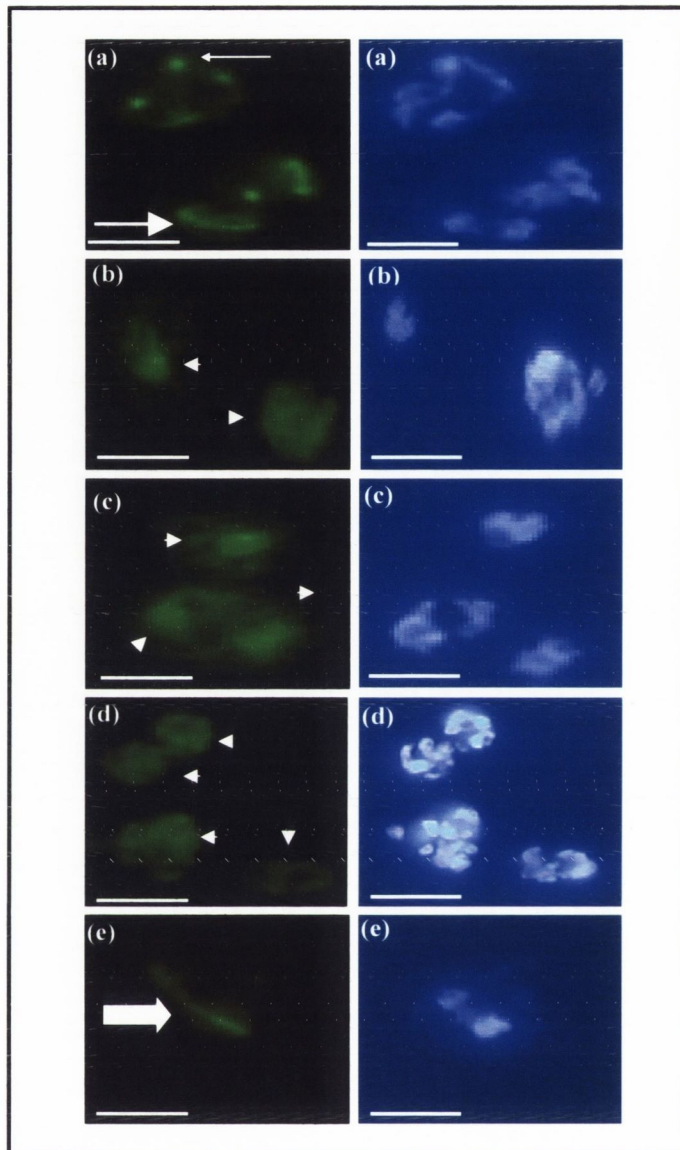


Figure 3.5. Mitotic microtubular structures of cultured parasites viewed by immunofluorescence using antibodies to *P. falciparum* β -tubulin (visualised with FITC, left) and DAPI nuclear stain (right). (a) Untreated parasites: note microtubule-organising centres (small arrow) and hemispindles (large arrow); (b) treated with 1 nM dolastatin 10: note diffuse staining (arrowheads) and loss of normal structures; (c) treated with 10 nM auristatin PE; (d) treated with 20 μ M vinblastine; (e) treated with 1 μ M Taxol: note thick rod of tubulin (block arrow) and loss of normal structures. In all cases exposure to inhibitor was for 6 h. Scale bars are 4 μ m.

Table 3.3. Quantitative analysis of effects of inhibitors on mitotic microtubular structures^a

Agent (conc.)	MTOCs ^b	Hemispindles	MTOC + Hemispindles	Total normal	Diffusely stained ^c	Fragmented ^d	Rods ^e	Other abnormal	Total abnormal
None	31	9	10	50	0	0	0	0	0
Dolastatin 10 (1 nM)	0	0	0	0	7	41	0	2	50
Auristatin PE (10 nM)	0	0	0	0	9	41	0	0	50
Vinblastine (20 µM)	1	0	0	1	4	45	0	0	49
Taxol (1 µM)	0	1	0	1	0	2	46	1	49

^a Cultures were synchronised to the trophozoite stage (27 - 33 h post-invasion) and exposed to inhibitors or solvent alone in 24-well microplates for 6 h, after which most control parasites had entered schizogony (data not shown). For each treatment, 50 parasites were examined by immunofluorescence microscopy as described in section 2.4.5, and the numbers containing normal and various abnormal structures are indicated.

^b MTOC, microtubule organising centre/centriolar plaque.

^c Fluorescence evenly distributed throughout cytosol.

^d Fluorescence in a fragmented pattern throughout the cytosol

^e Fluorescence arranged in rod-like structures much thicker than normal hemispindles.

Data obtained by Carolan, S. (Fennell *et al*, 2003).

of typical mitotic microtubular structures. A similar profile of abnormal tubulin-containing structures was observed upon treatment with vinblastine but treatment with Taxol gave very distinct lesions. The results outlined here and in the previous sections are clearly consistent with the premise that the inhibitors disrupt cell division in the malarial parasite.

3.3. DISCUSSION

Studies to date with microtubule inhibitors of the “*Vinca*” alkaloid and taxoid groups and both drug-resistant and sensitive strains of *P. falciparum* have indicated that potent growth-inhibitory activity can be observed (Bell, 1998). To continue such explorations into the effects of microtubule inhibitors on *P. falciparum*, the antimalarial activities of the marine organism-derived peptide dolastatin 10 and a number of its synthetic derivatives were investigated. Results presented in this chapter and elsewhere (Fennell *et al*, 2003) indicated that dolastatin 10 was a more potent inhibitor of *P. falciparum* than any other previously described microtubule inhibitor, with a median inhibitory concentration (IC₅₀) of 10⁻¹⁰ M. Such activity is superior to that of established anti-malarial drugs such as chloroquine (IC₅₀ ~ 2 nM), mefloquine (IC₅₀ ~ 32 nM) and halofantrine (IC₅₀ ~ 450 pM) (Geary *et al*, 1989). Unfortunately, as dolastatin 10 displayed approximately equi-potent activity against various mammalian cell lines and *P. falciparum*, its progression as an antimalarial agent for clinical development is not merited.

However, in view of the excellent antimalarial activity of dolastatin 10, a number of synthetic peptides, the auristatins, which were shown to be less potent to mammalian cells, were examined to see whether an agent with marked selectivity for parasite over mammalian cells could be identified. Although inhibitor concentrations required to hamper *P. falciparum* and mammalian cell proliferation were not the same, none of the agents tested had sufficient selectivity for the parasite to be advanced as future antimalarials. The compounds were shown to have various antimalarial potencies, with GRP18290, the heterocyclic derivative of dolastatin 10, which also contains a similar sulphur containing thiazole moiety, being the most potent (IC₅₀ 340 pM). The agent GRP18183 which was the most structurally diverse derivative, resulted in the lowest measurable inhibition of parasite growth (IC₅₀ 240 nM) of the agents tested, possibly due to the presence of bulky substituent groups

which may have delayed diffusion of the agent across erythrocytic and parasitic membranes. Overall results indicated that the closer structurally the derivative was to dolastatin 10, the better the inhibition of *P. falciparum*.

Perhaps the testing of such a (with one exception) potent series of anti-cancer agents for selective antimalarial activity made a difficult goal on this occasion. Dolastatin 10 has been shown to be one of the most potent anti-cancer drugs ever found (Pettit *et al*, 1998; Hadfield *et al*, 2003) and is currently in Phase II human cancer clinical trials which is being carried out by the US National Cancer Institute (Poncet, 1999). Nevertheless, this chapter describes the most extensive structure-antimalarial activity study ever carried out on microtubule inhibitors. In addition, a number of interesting cellular and morphological observations were made on the effects of these agents on *P. falciparum* which contributed to the overall premise that such agents act primarily on the mitotic apparatus of the schizont stage of parasite development.

One such effect was the unusual biphasic-dose response curve obtained after 48 h incubation of the dolastatin 10/auristatin series with asynchronous populations of *P. falciparum*. Similar dose response curve profiles have also been reported in the treatment of *Plasmodium* spp.-infected erythrocytes in culture by Taxotere (Schrével *et al*, 1994). These profiles are in contrast to the typical sigmoidal curves obtained with the majority of drugs used for antimalarial chemotherapy (Makler *et al*, 1993). It appears that the plateau phenomenon seems to be a common feature of microtubule inhibitors from structurally-unrelated classes and likely results from the presence of two distinct populations of parasites in asynchronous cultures with differing susceptibilities.

In keeping with this premise, the biphasic dose response curves formed from treatment of asynchronous parasites with dolastatin 10 and auristatin PE were also found to reflect differing sensitivities of parasite asexual stages to this class of microtubule inhibitor (see Fig. 3.6). It is also important to note the high levels of resistance displayed by parasites aged 0 - 18 h post-invasion to all inhibitors tested. These parasites presumably progress to and become arrested in the schizont stage, but remain to some extent metabolically active, making their detection as viable parasites still possible. pLDH activity in viable schizonts could also compensate for those that are metabolically inactive and therefore result in a similar growth readout as ring-stage parasites in the control which are known to contain lower pLDH

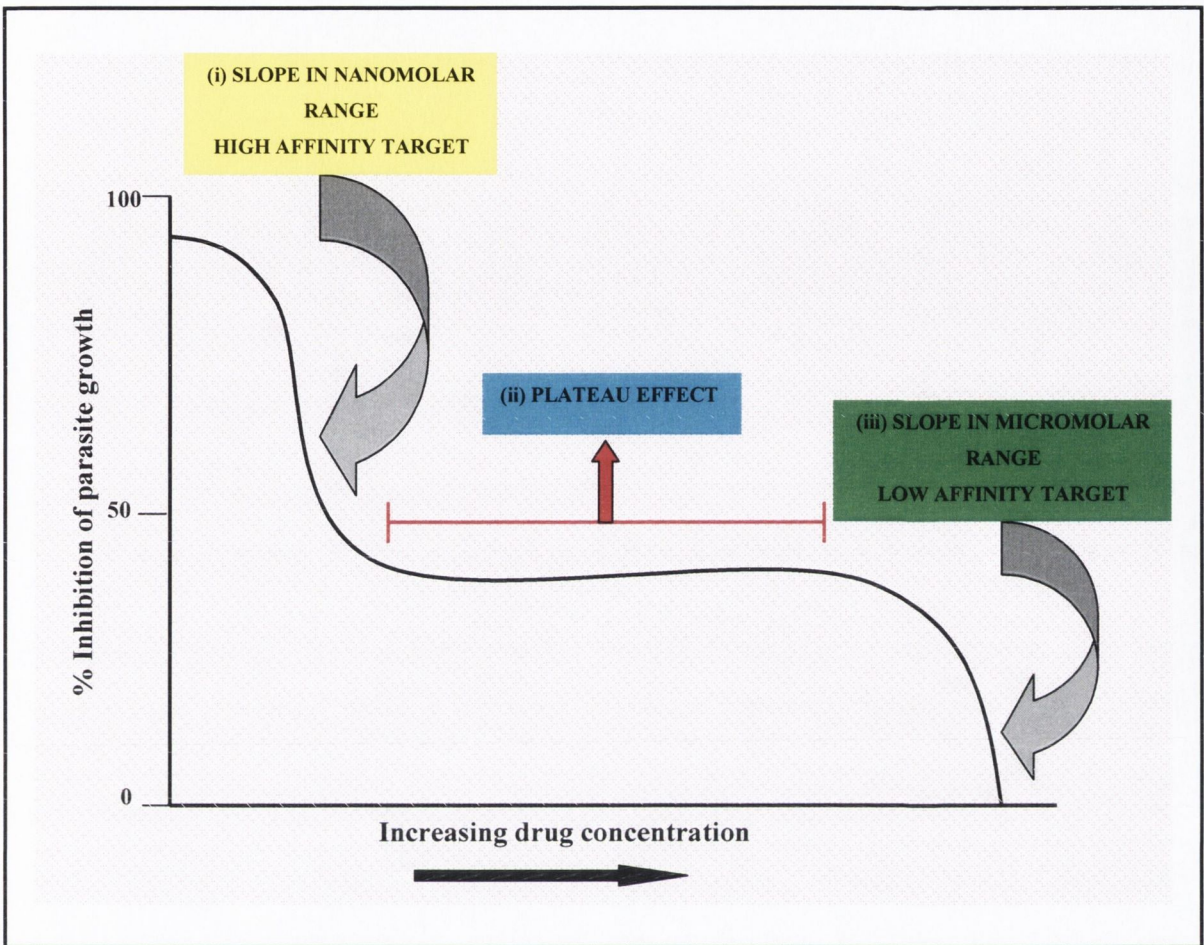


Figure 3.6. Proposed model for the typical biphasic dose-response curves observed after 48 h treatment of asynchronous cultures of *P. falciparum* with dolastatin 10 and auristatin PE.

(i) A high-affinity target exists that can be inhibited in parasite-infected erythrocytes which are initially 18 - 42 h post invasion in the nanomolar range of drug concentrations. (ii) A plateau effect observed after 48 h exposures of asynchronous cultures is most likely due to the presence of a subpopulation of parasites (~ 0 - 18 h post-invasion) not in the age range most appropriate for complete inhibition at the drug concentrations tested and parasites aged ~ 42 - 48 h post-invasion, presumably corresponding to post-mitotic, mature schizont stages which escape the actions of the inhibitors, indicating a stage-specific effect of the agents predominantly on parasite division. (iii) A putative low affinity target may exist in parasite-infected erythrocytes which are initially 0 - 18 h post invasion and is probably inhibited in the micromolar range of drug concentration.

activity per parasite than schizonts (Basco *et al*, 1995). Only after the control parasites had moved into the more metabolically-active trophozoite stage, with its higher pLDH levels, and the arrested schizonts had presumably become no longer viable, would inhibitory effects have become more apparent. Similarly, the plateau effect observed in Taxotere-treated cultures of *P. falciparum* appeared to be caused by the varying susceptibility of two distinct populations of parasites (Schrével *et al*, 1994). Schrével and co-workers reasoned that the first slope in the nanomolar range corresponds to effects on targets in erythrocytes infected with schizonts, albeit more mature, correlates well with our findings. However, the proposal that in addition to rings (0 - 4 h post- invasion), trophozoites (20 - 24 h post-invasion) also contribute to the formation of the plateau effect is slightly different from our interpretation and may reflect the fact that trophozoite development / inhibition in the presence of Taxotere was only assessed for 20 h. Perhaps if this period of incubation was extended for a further 22 - 28 h (total 42 - 48 h) inhibition of trophozoites in the nanomolar range may be realised and their relevance to the formation of the plateau effect would become more apparent.

Such stage-specific actions of microtubule inhibitors have also been reported for the compounds Taxol (Pouvelle *et al*, 1994) and vinblastine (Usanga *et al*, 1986). Taxol (1 μ M) added to *P. falciparum*-infected erythrocytes aged 0 - 30 h post-invasion displayed potent antimalarial activity, while addition to parasites aged 40 h post-invasion had no effect in preventing new ring formation in culture or *in vivo* at an equivalent time point in mice infected with *Plasmodium chabaudi adami* with a single injection of Taxol at 150mg/m². Similarly, vinblastine primarily inhibits parasite development when added at the trophozoite stage of parasite development (Usanga *et al*, 1986, Table 3.2). Thus, it appears crucial that the parasite must be exposed to inhibitor from the beginning of parasite replication in order for inhibition to be achieved. However, results from Schrével *et al* (1994) suggested that late schizonts/segmenters (44 - 48 h post-invasion) were highly susceptible to Taxotere at concentrations as low as 1 - 10 nM. This could be the result of more rapid uptake of Taxotere compared with Taxol and the dolastatin series, or slight differences in the length of asexual cycles of the parasite strains used in the different experiments.

Based on the idea that members of the dolastatin 10/auristatin series act primarily on the schizont stage of parasite development, maturation/morphology and drug pulse/reversibility experiments were performed. From maturation assays,

parasites 18 - 24 h post-invasion exposed to inhibitors were found to be arrested in the schizont stage (Fig. 3.3a). The majority of these schizonts appeared immature and deficient in the characteristic array of merozoites normally associated with parasites of this age. The reason for this may be comprehended from electron microscopy studies which have previously shown that certain microtubule inhibitors can prevent merozoite morphogenesis and formation by preventing the migration of chromosomes along the nuclear microtubules into the merozoites (Taraschi *et al*, 1998). Inhibition of spindle microtubule formation by vinblastine has also been reported for erythrocytic schizonts of *P. yoelii nigeriensis* (Sinden *et al*, 1985) which could presumably interfere with merozoite formation in the parasite. This could also prove to be the case for dolastatin 10-treated cultures, although the effects of this inhibitor on parasite tubulins would likely be more similar to those of vinblastine as opposed to the polymerisation-promoting effects of Taxol. The failure of parasites to produce mitotic spindles and thus nascent infectious merozoites could be a likely basis for the antimalarial action of dolastatin 10.

In a series of drug-pulse experiments (Fig. 3.4), schizonts were found to be more susceptible to irreversible inhibition upon short term-exposure to dolastatin 10 or auristatin PE than trophozoites, which in turn were more susceptible than rings. This finding possibly mirrors the fact that the concentration of tubulins is lowest in rings, higher in trophozoites and highest in schizonts (see section 5.2.1). In addition, the dynamic nature of parasite tubulins in the schizont stage, which is going through an active process of depolymerisation and polymerisation involved in spindle formation/nuclear division and merozoite morphogenesis, possibly makes this stage more susceptible to inhibition by such agents (Morrissette and Sibley, 2002). It is also possible that the ring-stage parasites are less permeable to the inhibitors and that is the reason that higher doses are necessary to increase their sensitivity, as observed with Taxotere (Schrével *et al*, 1994).

Although it appears clear that the microtubule inhibitors, dolastatin 10 and auristatin PE, can block parasite maturation and consequently prevent re-invasion of erythrocytes, one of the questions that still remains is, what actually kills the arrested schizont? Microscopic examination of such developmentally delayed schizonts showed morphology that was strikingly distorted compared to control parasites (Fig. 3.3 b and c). Such microtubule damage in mammalian cells caused by Taxol and dolastatin 10 is known to induce the process of apoptosis (Torres and Horwitz, 1998;

Poncet, 1999). A wide range of apoptotic markers in the *Plasmodium spp.* have also recently been reported. For example chromatin condensation, externalisation of phosphatidylserine, morphological changes such as cell shrinkage and membrane blebbing, DNA fragmentation and caspase-like activity have all been detected in *P. berghei* undergoing the transition from zygotes to ookinetes (Al-Olayan *et al*, 2002). So the different cellular responses that occur in mammalian cells to microtubule inhibitor disruption, such as those of the apoptotic cascade may also occur in *Plasmodium spp.* While the putative cell death machinery of *Plasmodium spp.* may vary significantly from mammalian cells it does seem increasingly possible that exposure to inhibitors such as dolastatin 10 may result in eventual parasite death from an apoptosis-like process.

It was also noted that the effects of dolastatin 10 and auristatin PE were comparable to those of vinblastine in four respects: (i) the presence of a “plateau” of partial inhibition in 48 h dose-response curves using asynchronous parasites, which departed upon longer incubation (Fig. 3.2); (ii) a primary mode of action against the schizont stage of asexual parasite development (Fig. 3.4) (iii) arrested development during schizogony, resulting in a decrease in overall parasitemia (Fig. 3.3); and (iv) the loss of typical mitotic microtubular structures and their replacement by diffuse or fragmented tubulin labelling (Fig. 3.5). This last observation provides evidence for an interaction between dolastatin 10/auristatin PE and the microtubules of *P. falciparum* and suggests the failure of parasites to maintain their characteristic mitotic architecture in the presence of such agents, which is crucial to cell functioning, could be a likely reason for the antimalarial action of dolastatin 10.

The previous similarities outlined are not unexpected as dolastatin 10 and vinblastine are proposed to bind in the same region on mammalian tubulin termed the “*Vinca*” domain (Hadfield *et al*, 2003) which could also hold true for *P. falciparum* tubulins. Dolastatin 10 has also been shown to inhibit noncompetitively the binding of “*Vinca*” alkaloids to β -tubulin by a proposed mechanism of steric interference and also prevents nucleotide (GTP) hydrolysis and exchange during microtubule polymerisation (Poncet, 1999). Recently, the amino-terminal peptide (amino acid residues 2 - 31) of mammalian β -tubulin was photoaffinity labelled by dolastatin 10, suggesting these residues formed part of the dolastatin 10 binding site (Bai *et al*, 2004). A proposed model of the dolastatin 10 binding site on the mammalian tubulin dimer is shown in Fig. 3.7 (a). The fact that dolastatin 10 is equally potent to

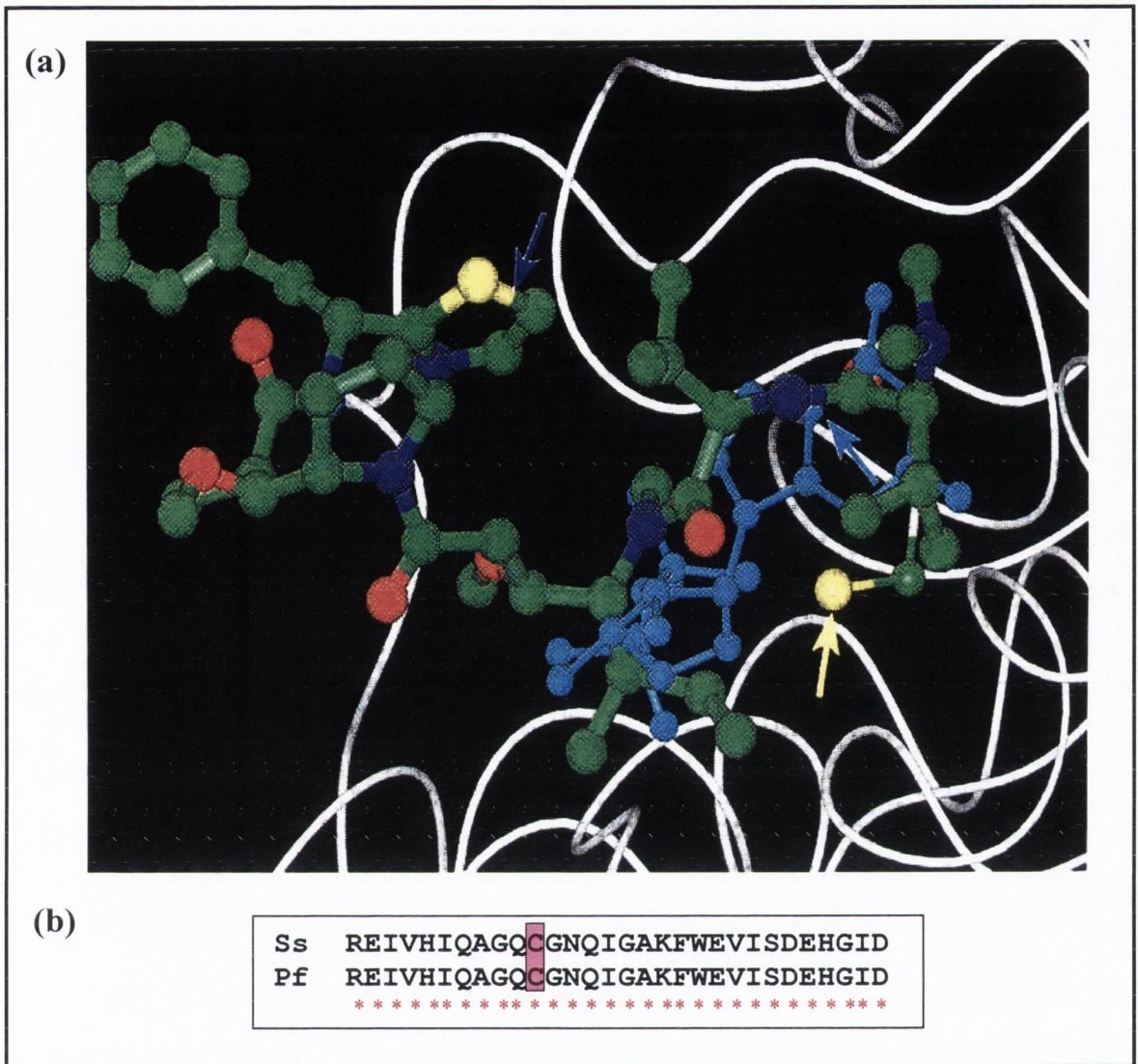


Figure 3.7. (a) Proposed + end binding site for dolastatin 10 on mammalian β -tubulin. The polypeptide backbone of β -tubulin is shown in white, along with atomic models (hydrogen atoms not shown) of GDP, dolastatin 10, and the cysteine-12-side chain. The atoms of GDP are shown in light blue, whereas in dolastatin 10 and the cysteine-12 side chain carbon atoms are shown in green, sulphur in yellow, oxygen in red, and nitrogen in purple. The yellow arrow indicates the cysteine-12 sulfur atom, the light blue arrow the C-5 atom of GDP, and the purple arrow the thiazole ring of dolastatin 10 [adapted from Bai *et al*, 2004] **(b) Clustal alignment of *Sus scrofa* (Ss) and *P. falciparum* (Pf) amino-terminal β -tubulin residues.** Letters represent amino acids spanning residues 2 - 31 (left to right), asterisks indicate amino acid identity, and boxed residue in pink illustrates conserved nature of cysteine amino acid involved in putative covalent bond formation between radiolabelled dolastatin 10 and mammalian tubulin.

mammalian and *P. falciparum* cells would tend to imply that the binding site on the tubulin dimer of both organisms for this agent is probably conserved. A sequence alignment of the amino terminal peptides of β -tubulins of the two organisms confirms this suggestion (Fig. 3.7 b). This would appear to verify that agents targeting the dolastatin 10-binding site hold insufficient promise for selective antimalarial activity. However, little in-depth molecular information currently exists pertaining to the interaction between other “*Vinca*” domain agents and mammalian tubulin. Therefore, it is possible that differences between *P. falciparum* and host tubulin may exist that could be exploited for the discovery of parasite-biased ligands. This together with the potent activity of “*Vinca*” domain agents most likely merits their continued investigation as potential antimalarial agents.

In summary, the studies of this chapter demonstrate the high antimalarial potency of dolastatin 10/auristatin series, the differences in order of activity in this series against *P. falciparum* and mammalian cells, the primary mode of action of the agents against the schizont stage and the apparent vinblastine-like action of dolastatin 10 and auristatin PE on nuclear division and mitotic microtubules of the parasite.

Chapter 4

Recombinant Expression, Purification and Functional Analysis of *P. falciparum* Tubulins

4.1. INTRODUCTION

The investigation of the effects of compounds on *P. falciparum* microtubular architecture, such as those described in chapter 3, is one of the few methods available to elucidate the roles of microtubules in the development and multiplication of malarial parasites. The majority of biochemical work pertaining to purified tubulin from protozoan parasites has been performed with kinetoplastids such as *T. brucei brucei* (Macrae *et al*, 1990) and *L. mexicana amazonensis* (Werbovets *et al*, 1999). Tubulins represent one of the major (if not the major) protein types of several kinetoplastid parasites and can account for > 10% of cellular protein (Bell, 1998). The purification of tubulin from microtubule-rich parasites is normally accomplished by procedures that rely on the ability of tubulin to assemble at 37°C in the presence of GTP and Mg²⁺ to form microtubules and to disassemble at 4°C in the presence of calcium ions to regenerate α/β -tubulin heterodimers. Successive cycles of assembly and disassembly allow purification of native tubulin by differential centrifugation, since microtubular tubulin but not free dimers can be sedimented at 40,000 x g within one hour (Shelanski *et al*, 1973). However, this cycling method requires a “critical concentration” of tubulin for assembly, and is difficult to achieve with tubulin-poor cell types, like *P. falciparum*. Thus, structural, functional, biochemical and drug-binding studies of *P. falciparum* microtubules *in vitro* have been prevented due to difficulties in obtaining high numbers of parasites from culture and the corresponding problems in obtaining sufficient amounts of purified native tubulin.

To circumvent the problems associated with the purification of native *P. falciparum* tubulin, cloning of tubulin genes coupled with heterologous expression offers a potential route to produce large amounts of α/β -tubulins. However, the use of a eukaryotic expression system such as *Pichia pastoris* could entail contamination with endogenous host tubulins, while cell-free transcription-translation systems result in minute (pmol) quantities of recombinant tubulins (Yaffe *et al*, 1988). Up until recently, tubulins produced in various prokaryotic systems were deemed either assembly-incompetent (Yaffe *et al*, 1988) or difficult to purify (Bell *et al*, 1995). In addition, it has been suggested that tubulins need to interact with eukaryotic chaperonins to attain their correct three-dimensional structures (Cowan *et al*, 1998; Gao *et al*, 1993; Tian *et al*, 1997).

However, a number of recent reports have documented the expression, purification and in some cases functional characterisation of tubulins from various

organisms produced in *E. coli* (see Table 4.1). In view of these findings, an attempt to generate sufficient quantities of *P. falciparum* tubulins for functional and drug-binding studies by this route was undertaken. This chapter describes the amplification and cloning of *P. falciparum* α I- and β -tubulin genes, their expression in *E. coli* and the purification of their products to apparent homogeneity. The functional analysis of the purified recombinant tubulins is also described. Drug-binding studies using these recombinant tubulins are described in chapter 6.

4.2. RESULTS

4.2.1. Amplification of *P. falciparum* α I- and β -tubulin genes

To-date, two α -tubulin (designated α I and α II) (Holloway *et al*, 1989, 1990) and one β -tubulin (Delves *et al*, 1989; Sen *et al*, 1990; Wesseling *et al*, 1989) genes from *P. falciparum* have been cloned and sequenced. Subsequent to their identification, the complete genome sequence of *P. falciparum* clone 3D7 has been determined (Gardner *et al*, 2002). Analysis of this genome database further verifies the existence of just two genes encoding α -tubulin and a single gene encoding β -tubulin (data not shown). Moreover, their expression has been reported to be developmentally regulated (Delves *et al*, 1990). α I- and β - tubulin expression is observed in both asexual and sexual stages of parasite growth, while α II expression is reported to be confined to the sexual stage of *P. falciparum* development (Rawlings *et al*, 1992). As the majority of research throughout this project has centred on asexual forms of parasite development, it was decided to focus the recombinant tubulin studies exclusively on *P. falciparum* α I- and β - tubulin genes and their corresponding products.

Genomic DNA encoding *P. falciparum* α I- and β -tubulin contains two non-coding introns in each gene (see Fig. 4.1 and 4.2). Therefore, total RNA was isolated from parasites and cDNA synthesised by reverse transcription as outlined in section 2.5.1. This cDNA, only containing coding exons, formed the template for the successful PCR amplification of the α I and β -tubulin fragments at the expected sizes of 1.36 kb and 1.34 kb, respectively (Fig. 4.3). In addition, both tubulin genes were amplified so as to incorporate *Nar*I and *Bam*HI restriction endonuclease sites into the PCR fragments at the 5' and 3' ends, respectively, to facilitate subsequent cloning into the pTrp2 expression vector.

Table 4.1. Overview of approaches previously used to produce recombinant tubulins in *E. coli*

Source of gene(s)	Tubulin monomer(s)	Vector/Fusion partner	Solubility	Yield	Refolding method	Functionality and assay used	Drug/protein binding	Reference
<i>Trypanosoma brucei</i>	$\alpha\beta$	pOTS/none	Insoluble	7-10 mg/l	None	ND	ND	Wu <i>et al</i> (1987)
<i>Homo sapiens</i>	α	pKK223-3/none	Soluble	20-100 pmol/30 μ l <i>in vitro</i> in <i>E.coli</i> lysates	None	No: coassembly with bovine tubulin	ND	Yaffe <i>et al</i> (1988)
<i>Haemonchus contortus</i>	β	pTrp2/none	Insoluble	>10 mg/l	Urea-alkaline	Yes: co-polymerisation with native <i>H. contortus</i> and bovine tubulin	[³ H]mebendazole	Lubega <i>et al</i> (1993)
<i>Rhynchosporium secalis</i>	β	pMAL-c2X/MBP	Soluble	75% total protein	None	ND	[¹⁴ C]carbendazim [¹⁴ C]diethonfencarb	*Hollomon <i>et al</i> (1998)
<i>Reticulomyxa filosa</i>	$\alpha\beta$	pKK223-3/none	Soluble	5-10 mg/l	None	Yes: co-polymerisation with bovine tubulin	ND	Linder <i>et al</i> (1998)
<i>Tetrahymena pyriformis</i>	$\alpha\beta$	pGEX-2T/GST	Soluble	ND	None	ND	Elongation factor 1 α (EF-1 α)	Nakazawa <i>et al</i> (1999)
<i>Neurospora crassa</i>	β	pET-32a(+)/S-Tag	Soluble	10 mg/l	None	ND	ND	*Yoshida <i>et al</i> (1999)
<i>Haemonchus contortus</i>	$\alpha\beta$	pTrp2/none	Insoluble	1.5-3.5 mg/l	Urea-alkaline	Yes: electron microscopy and turbidity assays	Albendazole [¹⁴ C]mebendazole	Oxberry <i>et al</i> (2001a, b)
<i>Mus musculus</i>	$\alpha\beta$	pET11a/none	Insoluble	ND	Chaperonin mediated	Yes: sedimentation and electron microscopy	ND	Shah <i>et al</i> (2001)
Chicken	β	pGEX-4T1/GST	Soluble	ND	None	ND	Inner centromere protein (INCENP)	Wheatley <i>et al</i> (2001)
<i>Euplotes focardii</i>	β	pET11a/none	Insoluble	ND	Chaperonin mediated	ND	ND	Pucciarelli <i>et al</i> (2002)
<i>Giardia duodenalis</i>	$\alpha\beta$	pMAL-c2X/MBP	Soluble	40-50 mg/l	None	Yes: dimerisation and turbidity assays	Variety of benzimidazoles	*MacDonald <i>et al</i> (2003 and 2004)
<i>Cryptosporidium parvum</i>	$\alpha\beta$	pMAL-c2X/MBP	Soluble	40-45 mg/l	None	Yes: dimerisation and turbidity assays	Variety of benzimidazoles	*MacDonald <i>et al</i> (2003 and 2004)
<i>Encephalitozoon intestinalis</i>	$\alpha\beta$	pMAL-c2X/MBP	Soluble	35-40 mg/l	None	Yes: dimerisation and turbidity assays	Variety of benzimidazoles	*MacDonald <i>et al</i> (2003 and 2004)

*additional constructs used for recombinant tubulin expression can also be found in these references.

ND: Not determined.

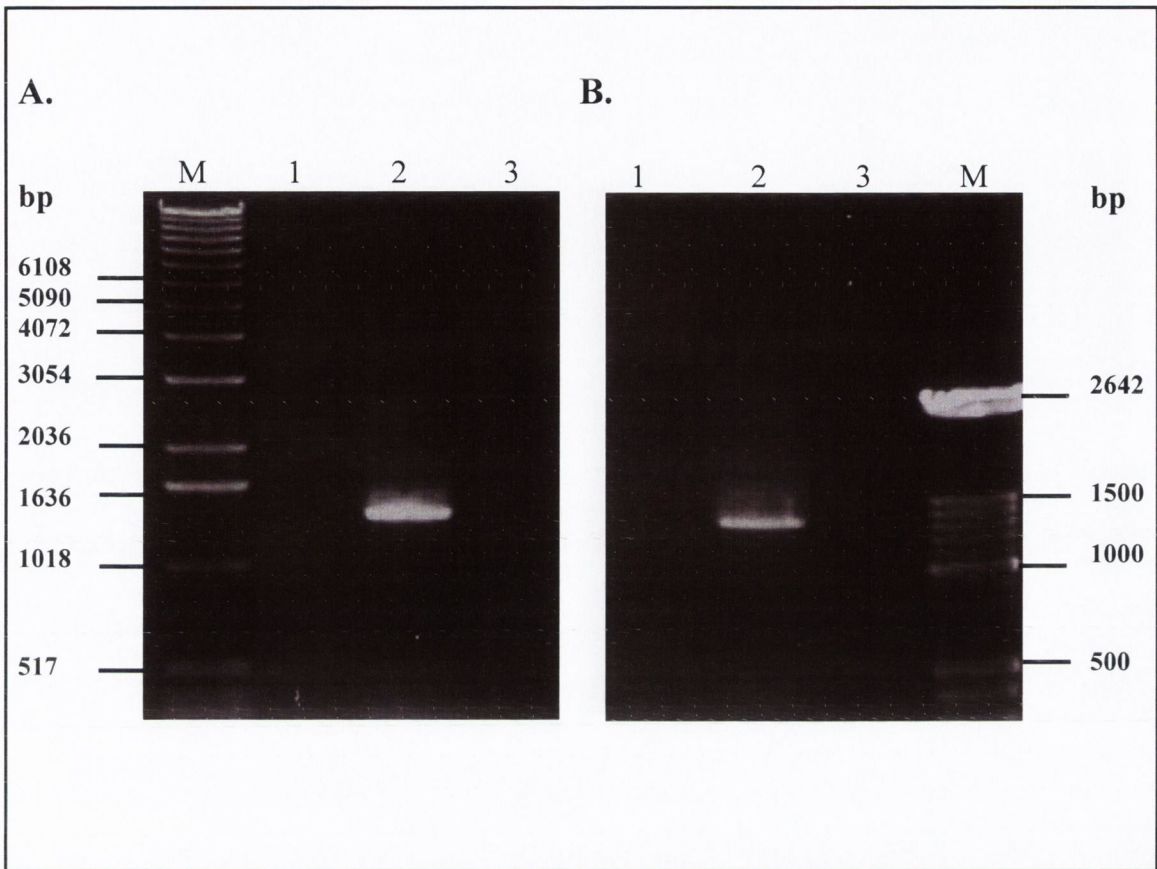


Figure 4.3. Amplification of *P. falciparum* α I- and β -tubulin cDNA. Total RNA isolated from *P. falciparum* was used to generate cDNA with an oligo(dT)₁₂₋₁₈ primer. This cDNA was then subjected to PCR using primers based on the sequences of the α I- and β -tubulin genes, and 6 μ l of each 50 μ l reaction were run through 1% (w/v) agarose gels, stained with ethidium bromide and visualised under UV light. **A.** Lanes 1 and 3 correspond to controls (1 = absence of RNA, 3 = absence of reverse transcriptase). Lane 2 contains the 1.36 kb α I-tubulin fragment. **B.** Lanes 1 and 3 correspond to controls (1 = absence of RNA, 3 = absence of reverse transcriptase). Lane 2 contains the 1.34 kb β -tubulin fragment. M = DNA ladder (sizes indicated in base pairs).

4.2.2. Recombinant production of *P. falciparum* α I- and β -tubulin

A number of approaches were used throughout this chapter in an attempt to obtain functional recombinant *P. falciparum* tubulins, which necessitated various cloning strategies. The plasmids constructed during the course of this study are outlined in Table 4.2.

4.2.2.1. Generation of β -tubulin using pTrp2

Our initial approach to generate recombinant *P. falciparum* tubulins was based on the methods of Lubega *et al* (1993) and Oxberry *et al* (2001) (see Table 4.1) who successfully expressed, purified, refolded and characterised recombinant *H. contortus* tubulins. The rationale was to produce recombinant tubulins as native proteins, eliminating possible conformational interferences induced by fusion tags. The expression vector pTrp2, which allows expression of a heterologous gene without the formation of a translational fusion (Olsen *et al*, 1989), was chosen to direct expression of *P. falciparum* recombinant tubulins. The PCR-amplified β -tubulin gene (Fig. 4.3 B), which included *NarI* and *BamHI* restriction endonuclease sites at the 5' and 3' ends, respectively, was inserted into the *ClaI* and *BamHI* restriction sites within the multiple cloning site (MCS) of pTrp2, and transformed into *E. coli* XL1-Blue. Transformants were selected based on pTrp2-encoded resistance to ampicillin. To check for ampicillin-resistant colonies harbouring the construct of interest (i.e. pTrp2 with inserted β -tubulin fragment [pTrp2- β Tub]) rather than parent vector alone, both PCR and restriction endonuclease analyses were performed on plasmids purified from ampicillin-resistant colonies (Fig. 4.4). These methods assisted in the recognition of a clone harbouring pTrp2- β Tub. DNA sequencing of purified plasmid from this clone verified the presence of the correct β -tubulin gene.

E. coli were then grown in minimal medium under tryptophan-starvation conditions to induce expression of unfused β -tubulin from pTrp2- β Tub. However, no expression of the recombinant tubulin was detected by SDS-PAGE (see Fig 4.5 A). Nevertheless, expression was detected by western immunoblotting using antibodies specific to *P. falciparum* β -tubulin, and the apparent size of the recombinant β -tubulin was \sim 49 kDa, which corresponds well with its predicted size of 49,758 kDa (Delves *et al*, 1989) (Fig. 4.5 B). In addition, the bacterially-expressed *P. falciparum* β -tubulin displayed differing migratory behaviour on SDS-PAGE gels to the

Table 4.2. Plasmid constructs used in this study.

Plasmid	Parent vector	Host strain/genotype	Protein	Comments
pTrp2-βTub	pTrp2	XL1-Blue/ <i>recA1 endA1 gyrA96 thi-1 hsdR17 supE44 relA1 lac</i> [F' <i>proAB lacI^ΔZΔM15 Tn10</i> (Tet ^r)] ^c JM101/ <i>SupE thi-1 Δ(lac-proAB)</i> [F' <i>traD36 proAB lacI^ΔZΔM15</i>] TOPP3/ Rif ^r [F' <i>proAB lacI^ΔZΔM15 Tn10</i> (Tet ^r) (Kan ^r)]	β-tubulin	β-tubulin non-fusion. Low yield, detected by western blot only.
pET11a-αITub	pET11a	BL21(DE3)/ <i>E.coli B F⁻ dcm ompT hsdS(r_B⁻ m_B⁻) gal λ(DE3)</i>	αI-tubulin	αI-tubulin non-fusion. Solubility dependent on temperature of induction.
pET11a-βTub	pET11a	BL21(DE3)/ <i>E.coli B F⁻ dcm ompT hsdS(r_B⁻ m_B⁻) gal λ(DE3)</i>	β-tubulin	β-tubulin non-fusion.
pMAL-c2X-αITub	pMAL-c2X	TB1/ JM83 <i>hsdR</i>	MBP-αI-tubulin	MBP fused to N-terminus of αI-tubulin. Soluble.
pMAL-c2X-βTub	pMAL-c2X	TB1/ JM83 <i>hsdR</i>	MBP-β-tubulin	MBP fused to N-terminus of β-tubulin. Soluble.
pMAL-c2X	pMAL-c2X	TB1/ JM83 <i>hsdR</i>	MBP	MBP alone. Negative control in assays.

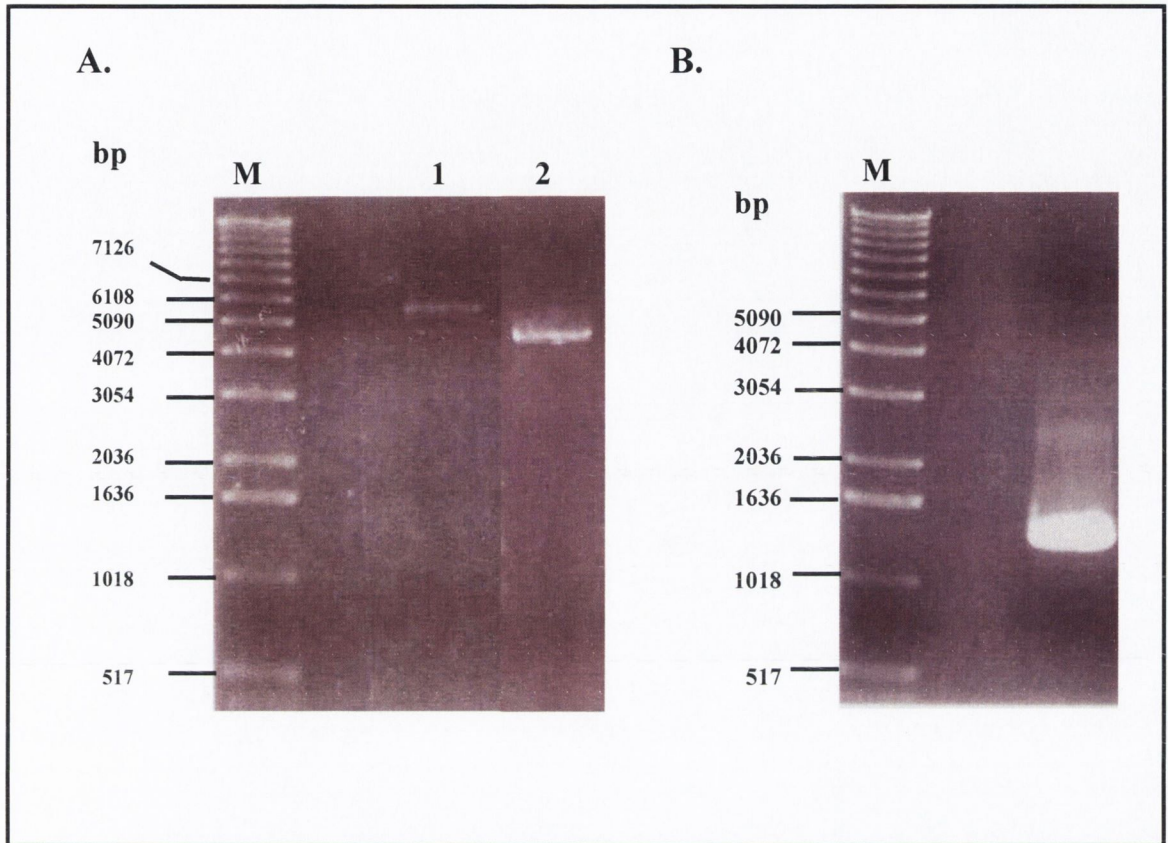


Figure 4.4. Analysis of the clone pTrp2- β Tub. Plasmid purified from ampicillin-resistant *E. coli* colonies was subjected to restriction endonuclease or PCR analysis, resolved through 1% (w/v) agarose gels, stained with ethidium bromide and visualised under UV light. **A.** pTrp2- β Tub (lane 1, ~ 40 ng) and pTrp2 alone (lane 2 ~ 80 ng) were linearised with *Eco*RI, and their apparent sizes were compared (pTrp2 = ~ 4.2 kb, pTrp2- β Tub = ~ 5.5 kb). **B.** PCR amplification of cloned β -tubulin gene. M = DNA ladder (sizes indicated in base pairs).

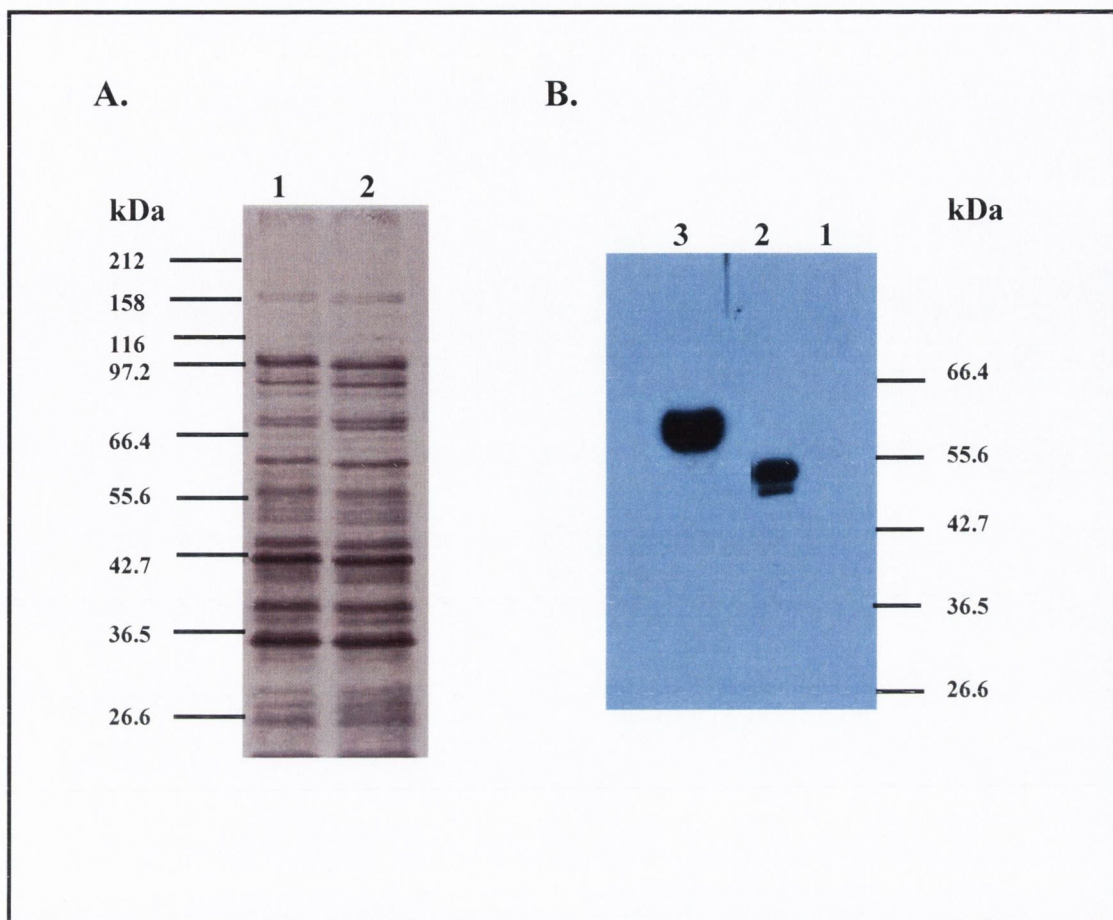


Figure 4.5. Analysis of production of β -tubulin from *E. coli* containing the pTrp2- β Tub plasmid. Cells were grown in minimal medium at 37°C under tryptophan-starvation conditions for 3 h, harvested, lysed by boiling in SDS-loading buffer and run through SDS- 10% PAGE gels. The gel was either **A.** stained in Coomassie Blue, destained and visualised under white light or **B.** transferred to PVDF membrane, and probed with *P. falciparum*-specific β -tubulin antibodies as described in section 2.6.5. Lanes 1 contains the lysate of cells containing the parental vector pTrp2. Lanes 2 contains an equal volume of lysate from cells containing the construct pTrp2- β Tub. Lane 3 corresponds to native *P. falciparum* extract (~ 25 μ g). The running positions of molecular weight markers (M) (sizes indicated in kDa) are shown on the left for A and right for B.

corresponding protein from *P. falciparum* extracts. Native *P. falciparum* β -tubulin migrated at ~ 57 kDa (Fig. 4.5 B), suggesting the possible presence of post-translational modifications on parasite tubulin.

As functional and drug-binding studies generally require relatively large quantities of tubulin (> 0.5 mg per sample) (Lacey, 1988), a number of efforts were made to boost expression of recombinant β -tubulin. Seeing that *E. coli* strains differ in their ability to support high-level expression of cloned genes (Kaytes *et al*, 1986), the pTrp2- β Tub construct was transformed into TOPP3 and JM101 strains of *E. coli* (see Table 4.2 for genotypes). The *Ptrp* promoter was induced under tryptophan-starvation conditions as before, yet recombinant β -tubulin remained detectable by western immunoblotting only (data not shown). Neither growth at lower temperatures (25 - 30 °C rather than 37°C) nor longer induction periods (4 - 12 h instead of 3 h) increased expression of β -tubulin (data not shown).

It has previously been documented that the overexpression of *P. falciparum* genes in *E. coli* can be problematic (Baca *et al*, 2000). Even though *E. coli* and *P. falciparum* use the same genetic code, the preferential use of a number of codons is generally different between the two (Baca *et al*, 2000) (Table 4.3). This codon bias is believed to result in translational stalling, whereby *E. coli* presumably runs out of specific tRNAs to incorporate their cognate amino acids into the recombinant protein, resulting in reduced or failed expression of recombinant *P. falciparum* proteins. In addition, the effects of the codon bias are believed to be of elevated significance when a run of consecutive rare codons occurs near the N-terminus of the coding sequence (Kurland *et al*, 1996). A number of plasmids (RIG, Baca *et al*, 2000; pRARE, www.novagen.com) which encode for tRNAs recognizing codons preferentially used by *P. falciparum* and other eukaryotic organisms have recently been developed to help overcome potential codon-bias problems and to facilitate increased yields of recombinant protein. The RIG plasmid includes the genes that encode for three tRNAs which recognize the codons AGA/AGG (arginine), ATA (isoleucine) and GGA (glycine). In addition to these four tRNAs, the pRARE plasmid includes genes that encode for the tRNAs that recognize the codons CUA (leucine) and CCC (proline). However it is important to note that codons recognized by RIG or pRARE-encoded tRNAs are not the only codons for which *P. falciparum* displays a preference to over *E. coli* (Table 4.3).

To understand whether codon bias played a role in the observed low-level

Table 4.3. Comparative codon usage by *E. coli* and *P. falciparum*.

Amino Acid	Codon	<i>E. coli</i> [*]		<i>P. falciparum</i> [*]	
		1000/ ^a	% usage ^b	1000/ ^a	% usage ^b
Arginine	AGA	2.1	3.8	15.9	60.5 ^c
	AGG	1.2	2.2	4.3	16.4
	CGA	3.5	6.3	2.4	9.1
	CGC	22.0	39.9 ^c	0.4	1.5
	CGG	5.4	9.8	0.3	1.1
	CGU	21.0	38.0	3.0	11.4
Glycine	GGA	7.9	10.8	12.7	44.2 ^c
	GGC	29.4	40.2 ^c	1.3	4.5
	GGU	24.9	34.0	11.9	41.5
	GGG	11.0	15.0	2.8	9.8
Isoleucine	AUA	4.3	7.2	49.9	54.2 ^c
	AUC	25.0	41.9	6.3	6.8
	AUU	30.4	50.9 ^c	35.9	39.0
Leucine	CUA	3.9	3.7	6.0	7.9
	CUC	11.0	10.3	1.8	2.4
	CUG	52.8	49.7 ^c	1.4	1.9
	CUU	11.0	10.3	8.7	11.5
	UUA	13.9	13.1	47.4	62.6 ^c
	UUG	13.7	12.9	10.4	13.7
Proline	CCA	8.5	19.2	9.2	46.0 ^c
	CCC	5.5	12.4	2.0	10.0
	CCG	23.3	52.6 ^c	0.9	4.5
	CCU	7.0	15.8	7.9	39.5

^{*} Table compiled from data available at <http://www.kazusa.or.jp/codon/> using *P. falciparum* 3D7 and *E. coli* K12 as sample strains.

^a Number of times this codon occurs per 1000 codons.

^b Usage of this codon in respect to all other codons which code for the same amino acid

^c Favoured codon.

Codons coloured red represent those for which the RIG plasmid was engineered to encode tRNA's. In addition to those colored red, pRARE plasmid also encodes for those coloured blue.

expression of *P. falciparum* β -tubulin (and possibly α I-tubulin) in *E. coli* we examined the coding sequence of both tubulin genes for the presence of rare codons. α I- and β - tubulin were found to contain $\sim 10.4\%$ and 8.54% respectively, of the codons that match those for which RIG encodes tRNA's (Fig. 4.6 B i - ii). It was also noted that one doublet of consecutive rare codons was identified close to the N-terminus of both tubulin gene sequences. Thus, in an effort to increase expression of β -tubulin, *E. coli* was co-transformed with pTrp2- β Tub and RIG. Co-transformants were selected on the basis of ampicillin and chloramphenicol resistance (RIG carries a gene for chloramphenicol resistance) and transformants were induced for overexpression of β -tubulin by tryptophan starvation as previously outlined. However, no expression of recombinant β -tubulin was detectable by Coomassie blue staining (Fig. 4.6 A). Thus, due to the apparent inability of pTrp2 to support high levels of expression of recombinant *P. falciparum* β -tubulin, it was decided to subclone and clone the β - and α - tubulin genes, respectively, into alternative vectors.

4.2.2.2. Generation of α I- and β -tubulin using pET11a

The expression vector selected to replace pTrp2 was pET11a (www.novagen.com). Unlike systems based on *E. coli* promoters (e.g. *lac*, *trp*, *tac*), the pET system uses the strong bacteriophage T7 promoter to direct expression of target genes with or without transcriptional fusion to vector-encoded sequence. The MCS of pET11a contains an *Nde*I site which is available for cloning into the AUG start codon at the 5'-end of the insert coding sequence. A C-terminal fusion can be avoided by including a translational stop codon in the insert. Target genes are initially cloned using *E. coli* hosts that do not contain the T7 RNA polymerase gene, therefore eliminating plasmid instability caused by production of proteins which may be toxic to the host cell. To initiate protein expression, the construct of interest is transferred into a host containing a chromosomal copy of the T7 RNA polymerase gene and expression is induced by addition of IPTG to the bacterial culture.

The strategy used to facilitate cloning of α I- and β -tubulin genes into the pET11a vector is outlined in Fig 4.7. The resulting putative constructs pET11a- α ITub and pET11a- β Tub were then used to transform *E. coli* XL-1-Blue. Plasmids were isolated from ampicillin-resistant transformants and checked for the presence of α I- and β - tubulin genes by PCR, restriction endonuclease analysis and DNA sequencing. These approaches led to the confirmation of clones harbouring the

A(i).

ATG **AGA** GAA GTA **ATA** AGT ATC CAT GTA **GGA** CAA GCT GGT ATC CAA GTT **GGA** AAT GCT TGC TGG GAA TTG
 TTT TGC **CTA** GAG CAT **GGA ATA** CAG **CCC** GAT GGT CAA ATG **CCC** TCT GAC AAG GCT TCT **AGA** GCT AAT GAT
 GAT GCT TTT AAT ACA TTC TTT TCA GAA ACG GGG GCA **GGA** AAA CAT GTA CCA CGT TGT GTT TTT GTC GAT
 TTA GAG CCA ACC GTT GTT GAT GAA GTC **AGA** ACA **GGA** ACT TAT CGT CAA TTA TTT CAT CCT GAA CAA TTA
ATA TCA **GGA** AAA GAA GAT GCT GCC AAC AAT TTT GCT **AGA GGA** CAC TAT ACA ATC GGT AAA GAA GTT **ATA**
 GAT GTA TGT TTG GAC **AGA** ATT **AGA** AAA TTA GCT GAT AAC TGT ACC GGT TTA CAA **GGA** TTT TTA ATG TTC
 AGC GCA GTT **GGA** GGT GGA ACA GGT AGT **GGA** TTT GGT TGT TTA ATG TTA GAA **AGA** TTA TCC GTT GAT TAT
GGA AAG AAA TCC AAA CTG AAT TTT TGC TGT TGG CCA TCA CCT CAA GTT TCA ACT GCT GTA GTT GAA CCA
 TAC AAT TCA GTT TTG TCT ACT CAT TCA TTA TTA GAA CAT ACT GAT GTA GCA **ATA** ATG CTT GAT AAC GAA
 GCT **ATA** TAT GAT **ATA** TGC **AGA AGA** AAT TTA GAT ATT GAA **AGA** CCA ACA TAT ACT AAT TTA AAT **AGA** TTG
 ATT GCT CAA GTT ATT TCT TCC TTA ACA GCA TCT TTA **AGA** TTT GAT GGT GCT TTA AAT GTT GAT GTA ACA
 GAA TTC CAA ACC AAC TTA GTA CCA TAC CCT CGT ATT CAT TTT ATG TTA TCT TCA TAT GCT CCA GTT GTT
 AGT GCT GAA AAA GCA AAC GAT GCT GAA CAA TTG TCC GTT TCT GAA ATT ACC AAC TCA GCA TTC GAA CCA GCA
 AAT ATG ATG GCA AAA TGT GAT CCG **AGA** CAT **GGA** AAA TAT ATG GCT TGT TGT TTA ATG TAT **AGA** GGT GAT
 GTA GTA CCA AAG GAT GTG AAC GCA GCT GTT GCT ACC **ATA** AAA ACA AAA **AGA** ACC ATT CAA TTT GTT GAC
 TGG TGT CCT ACT GGT TTT AAA TGT GGT **ATA** AAT TAT CAA CCA CCA ACT GTT GTA CCA **GGA GGA** GAT TTA
 GCC AAA GTT AGT **AGA** GGT AAT TGT ATG ATC AGC AAT TCA ACA GCA ATT GCA GAA ATG TTC TCA **AGA** ATG
 GAT CAA AAA TTT GAT TTA ATG TAT GCA AAA **AGA** GCT TTC GTT CAT TGG TAT GTA GGT GAA GGT ATG **GAA**
 GAA **GGA** GAA TTT AGT GAA GCT **AGA** GAA GAT TTG GCC GCC TTA GAA AAA GAT TAT GAA GAG GTA **GGA** ATT
 GAA TCC AAT GAA GCA GAA **GGA** GAA GAT GAA **GGA** TAT GAA GCA GAT TAT TAA

A(ii).

ATG **AGA** GAA ATT GTT CAT ATT CAA GCT GGC CAA TGT **GGA** AAT CAA **ATA** GGT GCA AAG TTT TGG GAA GTC
 ATT TCT GAT GAG CAT **GGA ATA** GAT CCA AGT GGT ACC TAT TGT GGG GAC AGT GAC TTA CAG TTA GAA **AGA**
 GTT GAC GTT TTT TAC AAC GAA GCA ACA **GGA** GGT **AGA** TAT GTT CCA **AGA** GCT **ATA** **AGA** GCT **ATA** GAT GAC TTG GAA
 CCT GGT ACT ATG GAT AGT GTT CGT GCT GGC **CCC** TTT GGT CAA TTA TTT CGT CCA GAT AAT TTT GTG TTT
 GGT CAA ACA GGT GCA **GGA** AAT AAT TGG GCT AAA **GGA** CAT TAT ACT GAA GGT GCT GAA TTG **ATA** GAT GCA
 GTT TTA GAT GTC GTT **AGA** AAA GAA GCA GAA GGT TGT GAT TGT TTA CAA **GGA** TTT CAG ATT ACT CAT TCA
 TTA GGT GGT GGT ACA GGT AGT GGT ATG GGT ACT TTG TTG ATT AGT AAA **ATA AGA** GAG GAG TAT CCT GAT
 CGT ATT ATG GAA ACA TTT TCT GTA TTT CCA TCA CCA AAA GTT TCT GAT ACT GTT TCT GAT TTT GAA CCA TAT AAT
 GCT ACA TTA TCA GTT CAT CAG TTG GTT GAA AAT GCT GAT GAA GTT CAA GTT ATC GAT AAT GAA GCT TTA
 TAT GAC **ATA** TGT TTT **AGG** ACT CTT AAA TTA ACA ACA CCA ACA TAT **GGA** GAT TTA AAT CAC CTT GTA TCA
 GCT GCA ATG TCA GGT GTA ACC TGT TCG TTA **AGA** TTT CCT GGT CAA CTT AAC AGT GAC TTA **AGA** AAA TTA
 GCT GTT AAT TTG ATC CCA TTC CCA CGT TTA CAT TTC TTT ATG ATC GGG TTT GCT CTT TTA ACT AGT **AGA**
 GGC AGT CAA CAA TAC **AGA** GCC TTA ACT GTG CCG GAG TTA ACA CAA CAA ATG TTC GAC GCA AAA AAT ATG
 ATG TGC GCA AGT GAT CCA **AGA** CAT **GGA AGA** TAT TTA ACG GCA TGT GCT ATG TTT **AGA GGA AGA** ATG TCC
 ACA AAG GAA GTT GAC GAA CAA ATG TTA AAC GTT CAA AAT AAA AAC TCA TCT TAT TTT GTC GAA TGG ATT
 CCT CAC AAC ACA AAA TCA AGT GTT TGT GAT ATT CCA CCT AAG **GGA** TTA AAA ATG GCT TTT ACT TTT GTA
GGA AAC TCA ACC GCC ATT CAA GAA ATG TTT AAA **AGA** GTT TCT GAT CAA TTT ACT GCT ATG TTT **AGA AGA**
 AAA GCC TTT TTG CAC TGG TAC ACC **GGA** GAA GGT ATG GAC GAG ATG GAA TTT ACA GAA GCT GAA TCA AAT
 ATG AAT GAT TTA GTT TCA GAA TAT CAA CAA TAT CAA GAT GCT ACA GCA GAA GAG GAA **GGA** GAA TTT GAA
 GAA GAA GAA **GGA** GAC GTA GAA GCC TAA

B

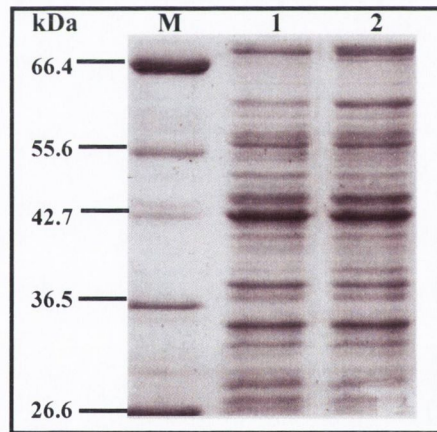


Figure 4.6. Effect of the RIG plasmid on overproduction of P β -tubulin. **A.** The nucleotide sequences (exons only) of *P. falciparum* α I- (Ai) and β - (Aii) tubulins is shown with the codons recognised by tRNA's encoded by the RIG plasmid illustrated in colour: red codons correspond to those for which the RIG plasmid was generated to encode tRNA's; blue codons represent additional rare codons recognised by the pRARE plasmid. Boxed coloured codons indicate those occurring in doublets or triplets throughout both tubulin gene sequences. **B.** Lack of effect of RIG plasmid on overexpression of β -tubulin. Equal volumes of *E. coli* lysates co-transformed with RIG-plasmid and either pTrp2 (Lane 1), or pTrp2- β Tub (Lane 2), both induced by tryptophan starvation, were resolved through SDS- 10% PAGE gels, stained with Coomassie Blue, destained and visualised under white light. The running positions of molecular weight markers (M) in kDa are shown on the left.

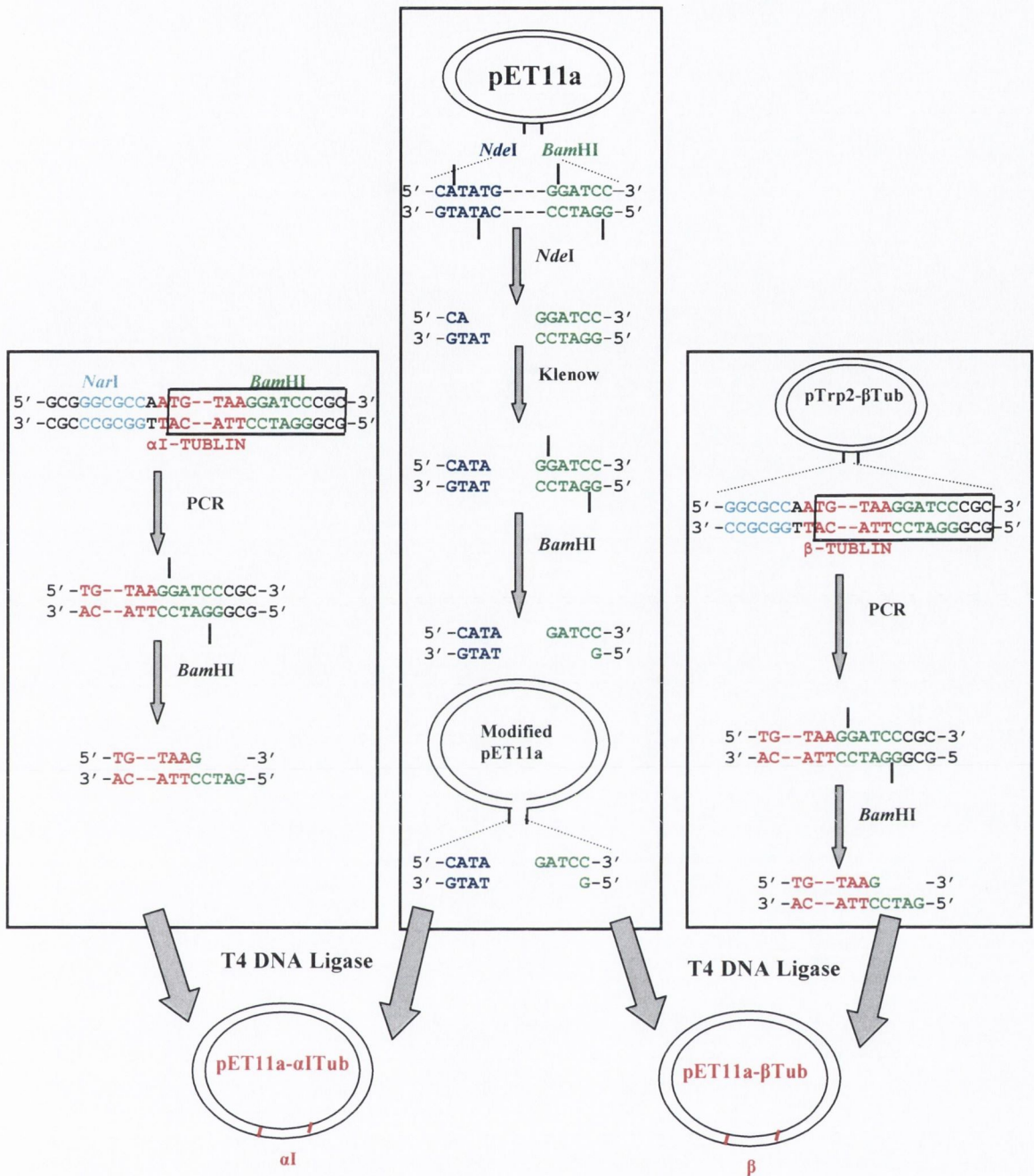


Figure 4.7. Cloning of *P. falciparum* tubulin genes into the expression vector pET11a. The α I- and β -tubulin genes were re-amplified so to incorporate a *Bam*HI site only at their 3' ends (box denotes region to be amplified by PCR) as described in section 2.5.5 (which also contains the details of primers used). After digestion with this endonuclease, fragments with 5' blunt ends and 3' sticky ends were created. The vector pET11a was digested with *Nde*I, made blunt with the large (Klenow) fragment of DNA polymerase I, and digested with *Bam*HI. The digested fragments and vector were ligated using T4 DNA ligase. Restriction sites are denoted by green, dark blue and light blue coloured nucleotides and labelled, and sites of cleavage are shown by vertical lines. Only start (ATG) and stop (TAA) codons (indicated in red) are shown for both tubulin genes, with dashes representing omitted codons.

constructs of interest (Fig 4.8, data not shown for β -tubulin). Both constructs were then used to transform *E. coli* BL21 (DE3), a strain deficient in both *lon* and *ompT* proteases, for recombinant tubulin expression studies.

IPTG-induction of the resulting clones (pET11a- α Tub and pET11a- β Tub) resulted in the overproduction of both recombinant tubulins, as judged by SDS-PAGE (Fig 4.9). The relative mobility of bands through SDS-PAGE gels representing recombinant α I- and β -tubulin were found to be ~ 53 kDa and ~ 57 kDa, respectively. The predicted molecular weights of *P. falciparum* α I- and β -tubulins are 50,297 and 49,758, respectively (Holloway *et al*, 1989; Delves *et al*, 1989). Hence, an apparent size discrepancy of ~ 7 kDa exists between the predicted size of native and recombinant *P. falciparum* β -tubulin. However, as observed in Fig. 4.10, the bacterially-expressed *P. falciparum* tubulins showed the same migratory behaviour on SDS-PAGE gels as the corresponding tubulins from parasite extracts. Additionally, use of *P. falciparum* specific α I/ β tubulin antibodies showed that the C-terminal residues, to which they were raised (see section 2.7.9), were present in the bacterially-expressed material. Therefore, *P. falciparum* tubulins were most likely expressed as full-length proteins in *E. coli* cells. However, the reason for the size difference (~ 8 kDa) between the recombinant β -tubulins expressed with the pTrp2 and pET11a vectors remains unclear. The size difference may be due to the presence of loop or secondary structures in cloned β -tubulin gene mRNA transcripts arising from the pTrp2- β Tub vector during induction of gene expression, resulting in their possible incomplete translation and hence reduced β -tubulin protein size. The size difference, however, is unlikely to be related to post-translational modifications of the recombinant β -tubulin molecules as *E. coli* generally lacks the cellular organelles to carry out such modifications (Marston, 1987). It is also important to note that conventionally α -tubulin is the slower and β -tubulin the faster migrating species during SDS-PAGE (Stephens, 1998). However, *P. falciparum* native and recombinant tubulins display a reversed order of electrophoretic mobility (“tubulin inversion”: see chapter 5).

To establish whether the recombinant tubulins had been produced in a soluble or insoluble form, *E. coli* cells used for expression were lysed, separated into pellet and supernatant fractions as described in section 2.7.3 and analysed by SDS-PAGE. Upon induction at 37°C, the majority of the expressed tubulins were insoluble and formed inclusion bodies (Fig. 4.10 A, lanes 5 - 6). The presence of inclusion bodies

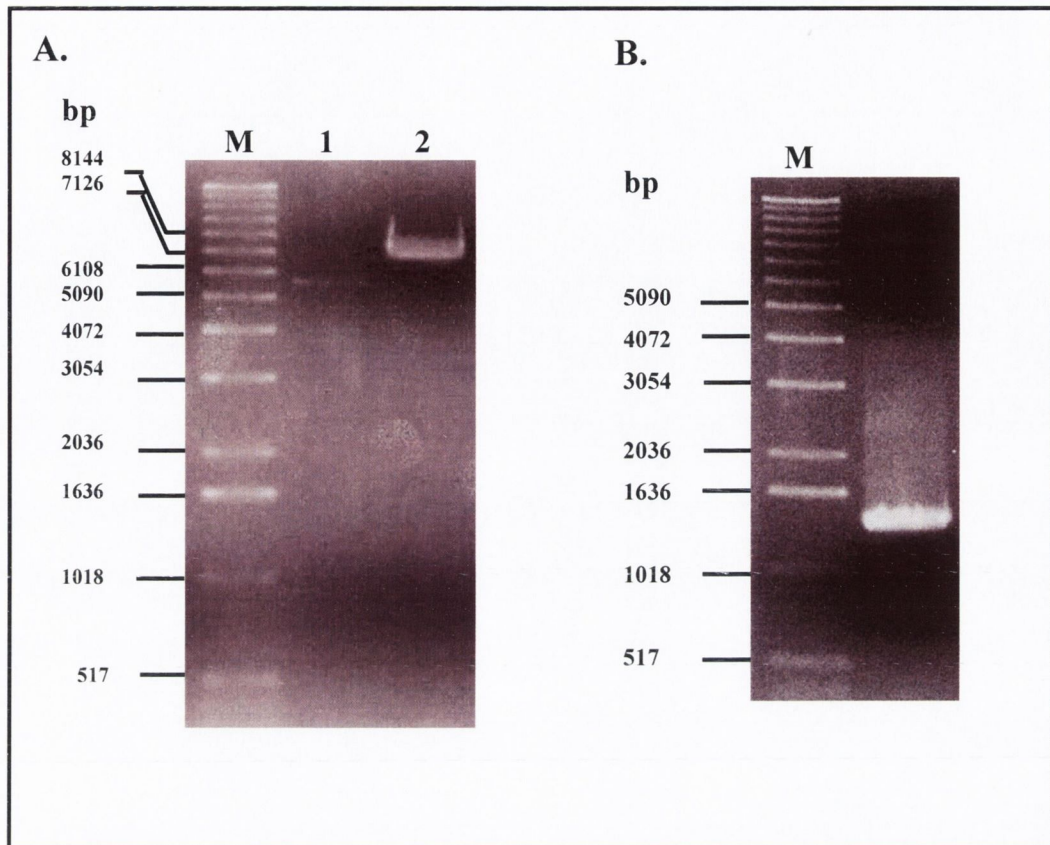


Figure 4.8. Analysis of the clone pET11a- α ITub. Plasmid purified from ampicillin-resistant *E. coli* colonies was subjected to restriction endonuclease or PCR analysis, run through 1% (w/v) agarose gels, stained with ethidium bromide and visualised under UV light. **A.** pET11a only (lane 1, ~ 40 ng) and pET11a- α ITub (lane 2 ~ 350 ng) were linearised with the endonuclease *ClaI* and their apparent sizes were compared (pET11a = ~ 5.68 kb, pET11a- α ITub = ~ 7.04 kb). **B.** PCR amplification of cloned α I-tubulin gene. M = DNA ladder (sizes indicated in base pairs).

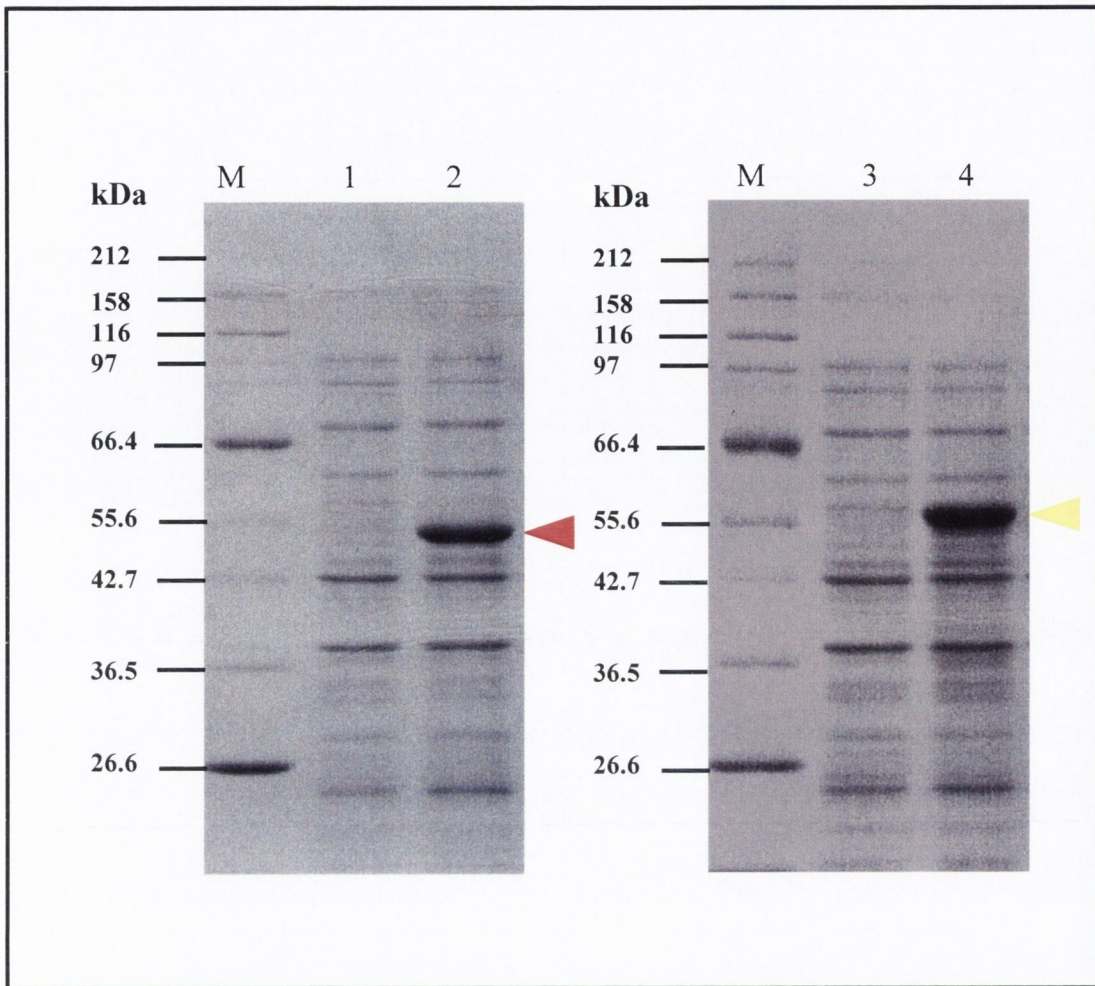


Figure 4.9. Expression of *P. falciparum* α I- and β - tubulin in *E. coli*. Equal volumes of lysates of *E. coli*, transformed with pET11a (lanes 1 and 3, induced with 1 mM IPTG) or either pET11a- α I-Tub (lane 2) or pET11a- β -Tub (lane 4) both induced with 1 mM IPTG, were resolved by SDS-PAGE (10%), stained with Coomassie Blue, destained and visualised under white light. The red and yellow arrow-heads indicate recombinant α I- and β - tubulin, respectively. M = molecular weight markers (sizes indicated in kDa).

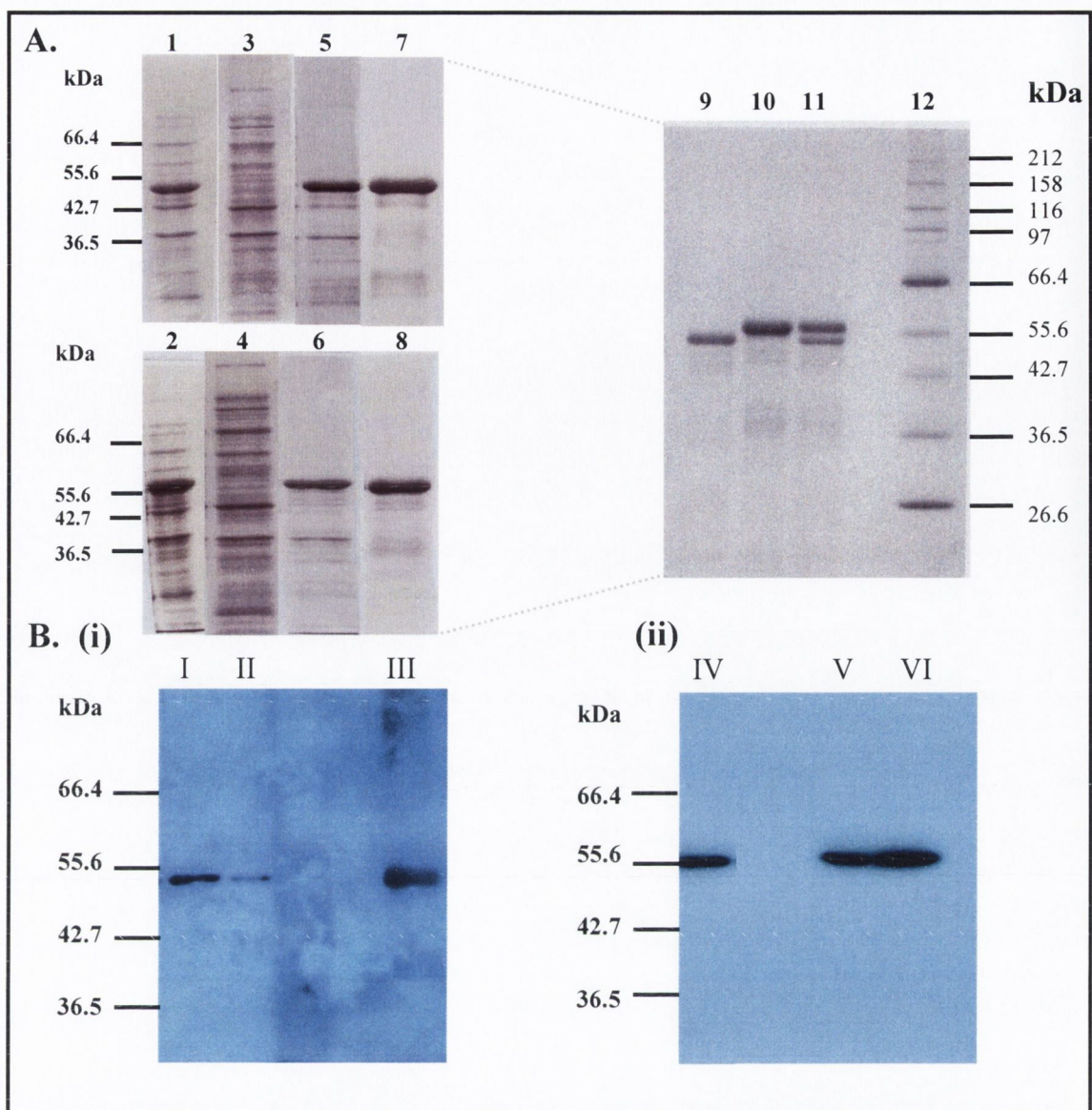


Figure 4.10. Purification of *P. falciparum* α I- and β -tubulin overexpressed in *E. coli*. **A.** Proteins were separated by SDS-PAGE (10%) and stained with Coomassie Blue. Lanes: 1 and 2, crude extracts from *E. coli* cells expressing α I- and β - tubulin, respectively, prior to purification; 3 and 4 soluble fractions of the cell lysates; 5 and 6, insoluble fractions of the cell lysates, 7 and 8, pellets recovered after detergent extraction and solubilisation in urea; 9, 10, 11 tubulins after renaturation by the urea/alkaline method (lane 9 = 4.5 μ g α I-tubulin, lane 10 = 7.5 μ g β -tubulin and lane 11 = 2.2 μ g α I-tubulin + 3.75 μ g β -tubulin); 12, molecular weight markers (M) (sizes indicated in kDa) **B.** 5 ng of purified recombinant α I- (lane III) and β - (lane IV) tubulin and parasite extracts (lanes I, II, V and VI) were resolved by SDS-PAGE, transferred to PVDF membrane and probed with antibodies specific to *P. falciparum* (i) α -tubulin and (ii) β -tubulin. The running positions of molecular weight markers are shown in kDa on the left of each immunoblot.

within the bacterial cells was also confirmed by phase-contrast microscopy (data not shown). However, at an induction temperature of ≤ 30 °C recombinant α I-tubulin was also found in the soluble supernatant fraction (data not shown), and was a major band in the *E. coli* lysate as viewed by SDS-PAGE (experiment not performed for β -tubulin). However, expected difficulties in purifying sufficient native tubulins from the soluble fraction encouraged us to attempt to purify and renature the relatively pure and highly abundant recombinant tubulins from the insoluble fraction as outlined by Lubega *et al* (1993) and Oxberry *et al* (2001).

Recombinant α I- and β -tubulin in the form of inclusion bodies were released from *E. coli* cells by both enzymatic (lysozyme) and mechanical disruption. The relatively high specific density of the tubulin-containing inclusion bodies facilitated their subsequent purification from the soluble components of the *E. coli* cell lysate by centrifugation at moderate rotor speeds (major purification step) (Fig 4.10 A, lanes 3, 4, 5 and 6). After centrifugation the pellet was washed with buffer containing a low concentration of Triton-X-100 to remove contaminants that may have adsorbed onto the hydrophobic inclusion bodies during processing (Fig 4.10 A, lanes 7 and 8). The washed inclusion bodies were resuspended in the denaturant urea and the solubilised tubulins were refolded by dilution with alkaline buffer and a shift to physiological pH in an effort to obtain biologically-active protein (Fig 4.10 A, lanes 9 and 10). To slow down the aggregation process, refolding was carried out using low protein concentrations, in the range 10 - 50 μ g / ml. Although some protein aggregation occurred during this process (visually detected), the majority of the recombinant tubulins appeared to remain in solution. The final yield was \sim 20 - 30 mg of either α I- or β -tubulin per 1 l of cell culture. Prior to discussion of functional analysis, the following section outlines the expression and purification of recombinant *P. falciparum* tubulins as soluble fusion proteins.

4.2.2.3. Generation of MBP- α I-tubulin and MBP- β -tubulin

During the course of this project, a number of reports outlining the expression of soluble, assembly-competent eukaryotic tubulin(s) in *E. coli*, containing various N-terminal peptide and protein tags to facilitate their subsequent purification, became available (see Table 4.1). In addition to characterising refolded recombinant tubulins, we also endeavoured to generate soluble, recombinant *P. falciparum* tubulin fusion proteins, with a view to removing the fusion partner by

site-directed protease treatment. This study was carried out as part of an undergraduate project by E. Dempsey under my supervision. The vector pMAL-c2x (www.neb.com) was chosen to direct expression of the recombinant tubulin fusion proteins. The MCS of this vector is positioned adjacent to the 3' end of the *E. coli malE* gene, which is under the control of the *Ptac* promoter. IPTG induction of *Ptac* results in expression of maltose-binding protein (MBP) and genes cloned in frame within the MCS are expressed with MBP fused to the N-terminus of the cloned target protein. MBP's affinity for amylose allows for purification of the fusion protein by affinity chromatography.

Briefly, both tubulin genes were amplified by PCR with primers that allowed subsequent cloning into pMAL-c2X, using pET11a- α Tub and pET11a- β Tub as the templates. The identity of the resulting constructs, pMAL-c2X- α Tub and pMAL-c2X- β Tub was confirmed by PCR, restriction endonuclease analysis and DNA sequencing (Dempsey, A - personal communication). All cloning and expression studies were carried out using *E. coli* TB1, a strain that lacks endogenous MBP (see Table 4.2).

IPTG induction of the resulting clones resulted in the over-production of both recombinant tubulin fusion proteins as judged by SDS-PAGE (Fig. 4.11). The apparent sizes of MBP- α I-tubulin and MBP- β -tubulin as judged by their relative motilities through SDS-PAGE gels were 95,500 and 99,500, respectively (molecular weight of MBP = 42,500). Thus, the α/β -tubulin inversion described in section 4.2.2.2 was also apparent for MBP-tubulin fusions. The identity of the recombinant tubulin fusions was also confirmed by western immunoblotting using antibodies specific to *P. falciparum* α I- and β -tubulins (data not shown).

The solubility of recombinant *P. falciparum* tubulin fusions was investigated as outlined in section 2.7.3. Upon induction at 37°C, both MBP- α I- and MBP- β -tubulin were found in the soluble fraction of *E. coli* lysates (Dempsey, E - personal communication). Therefore it would appear that the addition of the fusion partner MBP helps recombinant *P. falciparum* tubulins to overcome their lower cytoplasmic solubility (see Fig. 4.10) and circumvent inclusion body formation. Consequently, refolding of the tubulin fusions was not required and affinity chromatography using an amylose resin and ion-exchange chromatography was performed to purify MBP- α I- and MBP- β -tubulins to near homogeneity (Fig. 4.11). Although treatment of both tubulin fusions with factor X_a (a protease whose recognition site is incorporated

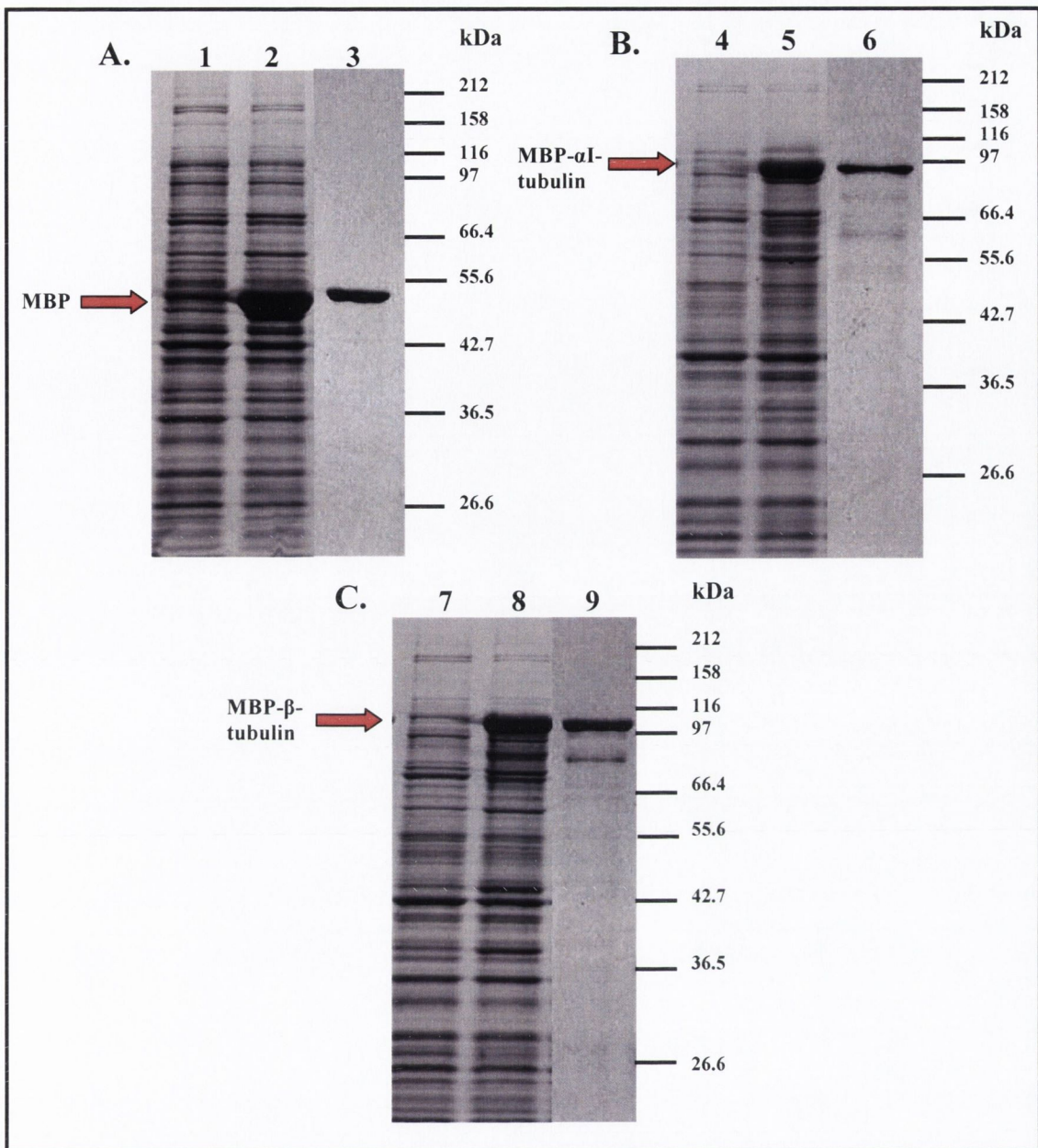


Figure 4.11. Recombinant production and purification of *P. falciparum* α I- and β -tubulins as MBP-fusion proteins under optimised conditions. *E. coli* cells transformed with the construct of interest were induced for recombinant protein production with 0.35 mM IPTG and equal volumes of resulting *E. coli* lysates were resolved by SDS-PAGE (10%) and stained with Coomassie Blue: **A.** pMAL-c2X uninduced [lane 1], induced [lane 2]; **B.** pMAL-c2X- α ITub uninduced [lane 4], induced [lane 5]; **C.** pMAL-c2X- β Tub uninduced [lane 7], induced [lane 8]. Recombinant proteins were then purified from the *E. coli* soluble supernatant extracts to near homogeneity by affinity and ion-exchange chromatography [lane 3 = $\sim 3 \mu\text{g}$ MBP; lane 6 = $\sim 2 \mu\text{g}$ MBP α I-tubulin; and lane 9 = $\sim 3 \mu\text{g}$ MBP β -tubulin]. The running positions of molecular weight markers are shown in kDa on the right of each gel.

immediately upstream of the MCS of pMAL-c2X, facilitating the removal of the MBP partner from the fusion protein) resulted in the removal of the MBP-tag from MBP- α I- and MBP- β -tubulins, various other bands (apparent sizes < 50 kDa) were also observed after cleavage (data not shown). This suggested the recombinant tubulins were susceptible to secondary activity of factor X_a. However, based on the successful drug-binding studies with the recombinant MBP- β -tubulin fusion of *R. secalis* (Hollomon *et al*, 1998; see Table 4.1) and the ability of green fluorescent protein (GFP)-tagged tubulins to co-polymerise with native intracellular eukaryotic tubulins (Rusan *et al*, 2001), it was decided to use both *P. falciparum* recombinant tubulins fusions for functional (section 4.2.3) and drug-binding studies (section 6.2.5).

4.2.3. Functional analysis of recombinant *P. falciparum* tubulins

4.2.3.1. Turbidimetric assay of the polymerisation of recombinant tubulin monomers

To investigate if refolded recombinant *P. falciparum* tubulins or tubulin fusion proteins could polymerise to form microtubules, a light-scattering assay adapted from the methods of Algaier *et al* (1988) and Oxberry *et al* (2001) was employed. This assay monitors the ability of the α/β -tubulin heterodimers to polymerise to form microtubules *in vitro*, which is approximated by the absorbance of the polymerised protein at 350 nm in a spectrophotometer (Lacey, 1988). The presence of GTP, glycerol, DMSO, a Ca²⁺ chelator (usually EGTA), and magnesium ions and / or a physiological temperature of 37 °C at a pH 6.4 - 7.0 are known to promote the assembly of tubulin into microtubules, while the presence of calcium ions and a temperature of 4°C trigger disassembly of microtubules into tubulin heterodimers. Microtubule-stabilising agents such as Taxol and Taxotere have also been shown to induce polymerisation of tubulin in the absence of polymerisation promoters such as glycerol and to stabilise microtubules against calcium- and cold-induced depolymerisation (Mooberry *et al*, 1999).

As a positive control for microtubule formation, bovine brain α/β tubulin was polymerised as outlined in section 2.8.2 (Fig 4.12). A typical profile was observed consisting of a lag of ~ 2 - 3 min followed by a linear increase in absorbance and finally a plateau after ~ 15 min. However, studies with refolded recombinant *P. falciparum* tubulins failed to give a similar profile. Various modifications of the

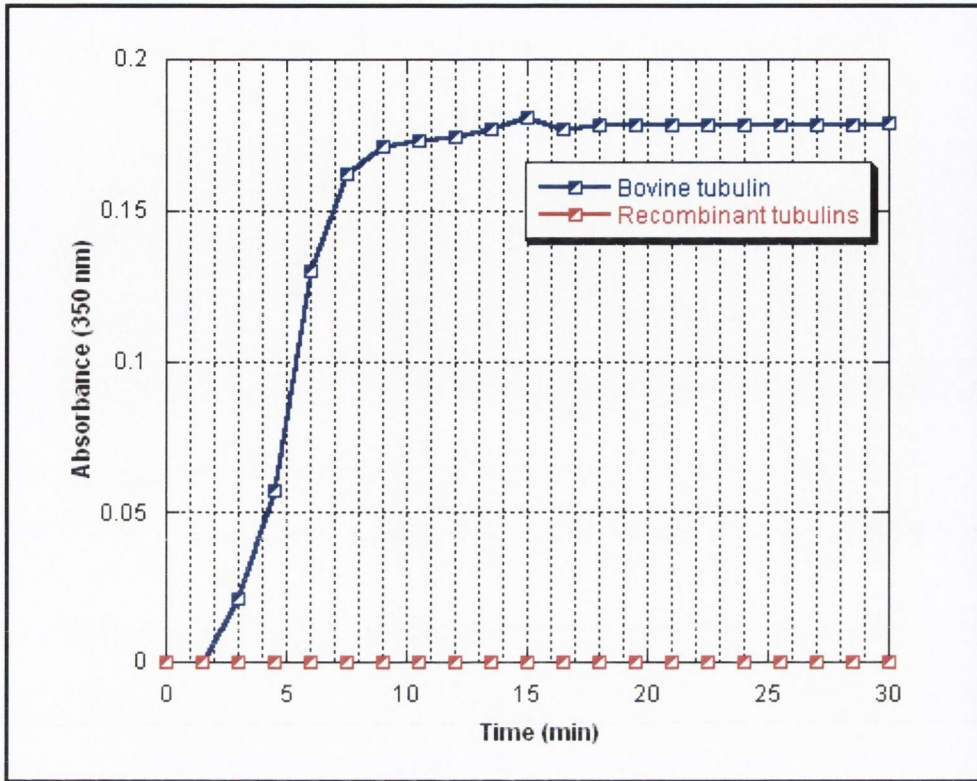


Figure 4.12. Turbidimetric analysis of bovine brain tubulin and recombinant *P. falciparum* tubulin polymerisation. Bovine brain tubulin ($\sim 12 \mu\text{M}$) or recombinant *P. falciparum* α I- and β -tubulins ($\sim 10 \mu\text{M}$ of each monomer) in the presence of $30 \mu\text{M}$ Taxol were placed in a quartz cuvette at 37°C as described in section 2.8.2. Tubulin polymerisation was observed by measuring the absorbance of the solution ($A_{350 \text{ nm}}$) over a 30 min period.

technique, including variation of the final concentrations of tubulin (10 - 60 μ M), Taxol (20 - 40 μ M) and GTP (1 - 4 mM) failed to generate an increase in absorbance (A_{350}), suggesting that the tubulin monomers or dimers were incapable of polymerising to form microtubules. This result implies that either or both recombinant tubulins had remained in a predominantly non-functional form after attempts at refolding. Unfortunately, recombinant tubulin fusions also failed to polymerise to form microtubules in this assay, possibly due to the presence of the MBP tag on one or both monomers. As all modifications of this assay had apparently failed to generate microtubules from recombinant *P. falciparum* tubulins, we decided to investigate the ability of the individual monomers to co-polymerise with polymerisation-competent bovine brain tubulin by the classic sedimentation assay.

4.2.3.2. Co-polymerisation studies of recombinant tubulins with bovine brain tubulin as assessed by sedimentation assay

The amino acid sequences of both α - and β -tubulins are highly conserved throughout eukaryotes (Ludueña *et al*, 1992) (see Figs. 6.4 - 6.7). Consequently, tubulin isolated from bovine brain tissue is very similar to tubulin isolated from most other eukaryotic sources. This fact results in the technical benefit that bovine tubulin can be used both intracellularly and *in vitro* for co-polymerisation experiments with tubulins from evolutionarily diverse sources. For example, *Physarum polycephalum* tubulin injected into mammalian cells was incorporated into host cell microtubules arranged in interphase arrays and mitotic spindles (Prescott *et al*, 1989). Similarly, recombinant tubulins from *R. filosa* (Linder *et al* 1998), *H. contortus* (Lubega *et al*, 1993) and hamster and chicken (Phadtare *et al*, 1994) were also integrated into the microtubules of bovine brain tubulin *in vitro* as assessed by the classical sedimentation assay. Based on the accomplishments of these groups, we decided to employ similar methods to investigate the ability of recombinant MBP- α I- and MBP- β - tubulin to co-polymerise with bovine brain tubulin. In addition, it was noted that the presence of the MBP-tag may potentially interfere with the functionality of both recombinant monomers. However, the ability of green fluorescent protein (GFP, size range 25 - 30 kDa) tagged-tubulins to co-polymerise with native intracellular eukaryotic tubulins (Rusan *et al*, 2001) suggested that tagged recombinant *P. falciparum* tubulins may still have the ability to co-polymerise with bovine brain tubulin.

The sedimentation technique involves the polymerisation of tubulin to form microtubules, which are then separated from unpolymerised tubulin heterodimers by centrifuging the protein through a microtubule-stabilising buffer. Unpolymerised contaminants adhering to the pellet are removed by washing and the extent of microtubule formation is assessed by comparing the amounts of tubulin in the pellet and supernatant/cushion fractions by SDS-PAGE and densitometry. As a positive control for microtubule formation, bovine brain tubulin was polymerised as outlined in section 2.8.1.1. From Fig. 4.13 (A, B, and E) it can be observed that nearly 1.5-fold more tubulin was found in the pellet fraction (polymerised tubulin) when Taxol was included in the polymerisation process. Thus, Taxol was included in all co-polymerisation assays to obtain the maximum yield of microtubules. As a negative control for the polymerisation process, low temperatures (4°C) resulted in the prevention of microtubule formation (Fig 4.13 C). Similarly, incubation with vinblastine (an inhibitor of microtubule formation) reduced the extent of tubulin incorporation into microtubules as seen by the increased amount of tubulin in the soluble unpolymerised fraction compared to the pellet (polymerised) fraction (3.7-fold difference - Fig 4.13 E).

Using bovine brain tubulin as a source of assembly-competent tubulin, we investigated the ability of MBP- α I-tubulin to co-polymerise with the bovine $\alpha\beta$ -tubulin heterodimer in a dose-dependent fashion. MBP- α I-tubulin alone was also subjected to the same polymerisation conditions so to determine non-specific sedimentation of the recombinant tubulin. From Fig. 4.14 (A, B, C and E), it was observed that as the ratio of recombinant MBP- α I-tubulin monomers to bovine tubulin α -monomers was increased a corresponding increase in the incorporation of recombinant tubulin into the microtubule pellet was found. When the ratio of recombinant α monomers to bovine α monomers was $\sim 3 : 1$, up to 25.5-fold more recombinant tubulin was found in the pellet fraction than in the control (Fig 4.14 E). These results suggested that recombinant MBP- α I-tubulin was capable of co-polymerising with bovine brain tubulin. It was noted in all assays that the majority of the recombinant tubulin remained in the supernatant fraction (unpolymerised) (Fig 4.14 D). This result is unsurprising as it can be assumed that bovine tubulin would be preferentially incorporated into the microtubules in preference to *P. falciparum* tubulin. However, it does seem apparent that MBP- α I-tubulin may have been folded correctly during synthesis in *E. coli* and is capable of being incorporated into bovine

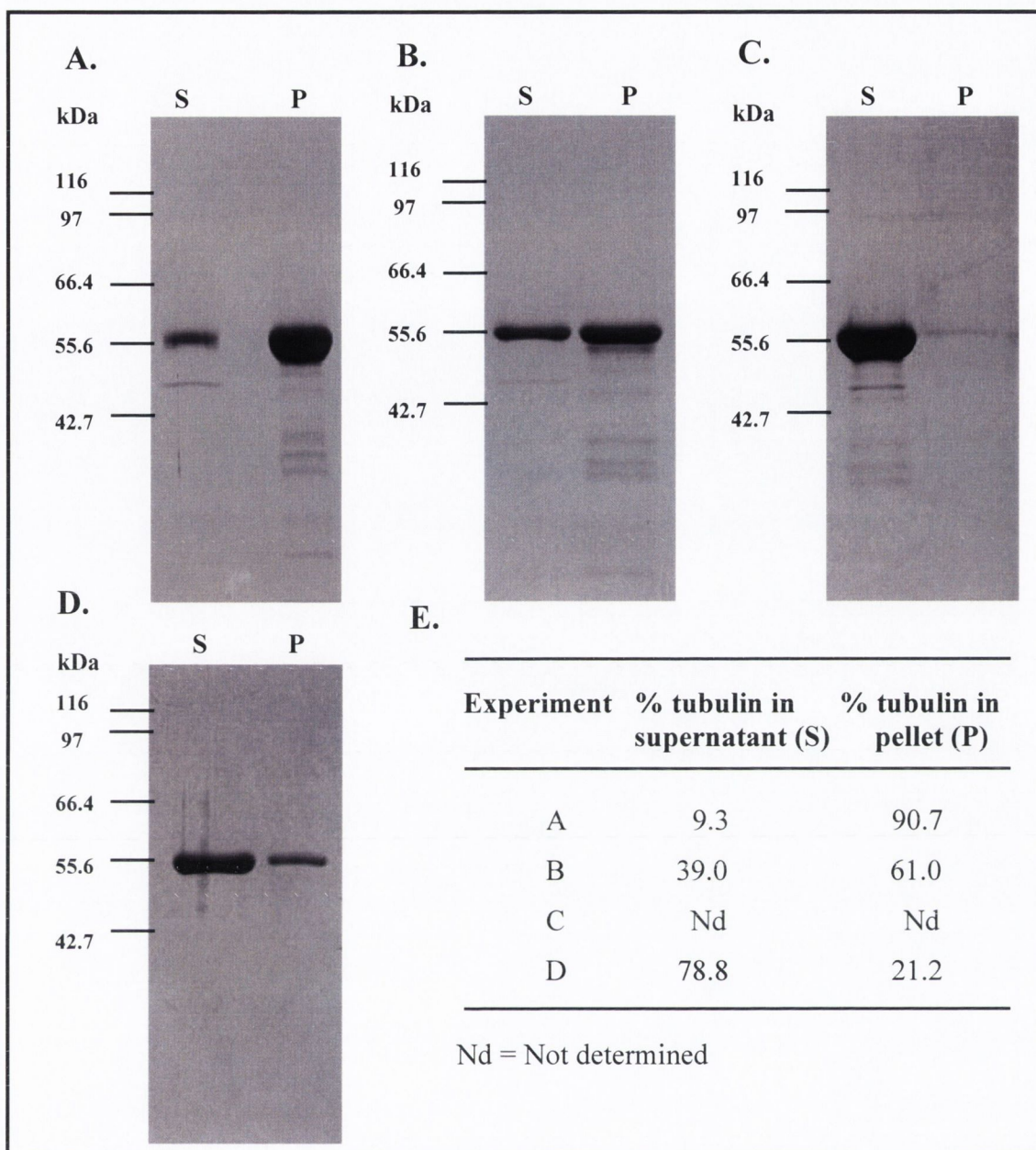


Figure 4.13. Analysis of bovine brain tubulin polymerisation by the sedimentation assay. Tubulin (~ 22 μ M) was incubated at: 37°C in the presence of 30 μ M Taxol [A]; 37°C in the absence of Taxol [B]; 4°C in the absence of Taxol [C]; and 37°C in the presence of 20 μ M vinblastine [D], for 1 h. Following centrifugation of the samples through a glycerol cushion, the resulting supernatants (S) and pellets (P) were resuspended in SDS-loading buffer and equal proportions of both fractions were resolved by SDS-PAGE (10%), stained with Coomassie Blue, destained and visualised under white light. The extent of microtubule formation was quantified by densitometry and the relative amounts of tubulin in the supernatant/cushion and pellet fractions were determined and expressed as an overall percentage value [E]. The running positions of molecular weight markers are shown in kDa on the left of each gel. The data shown are from single, representative experiments.

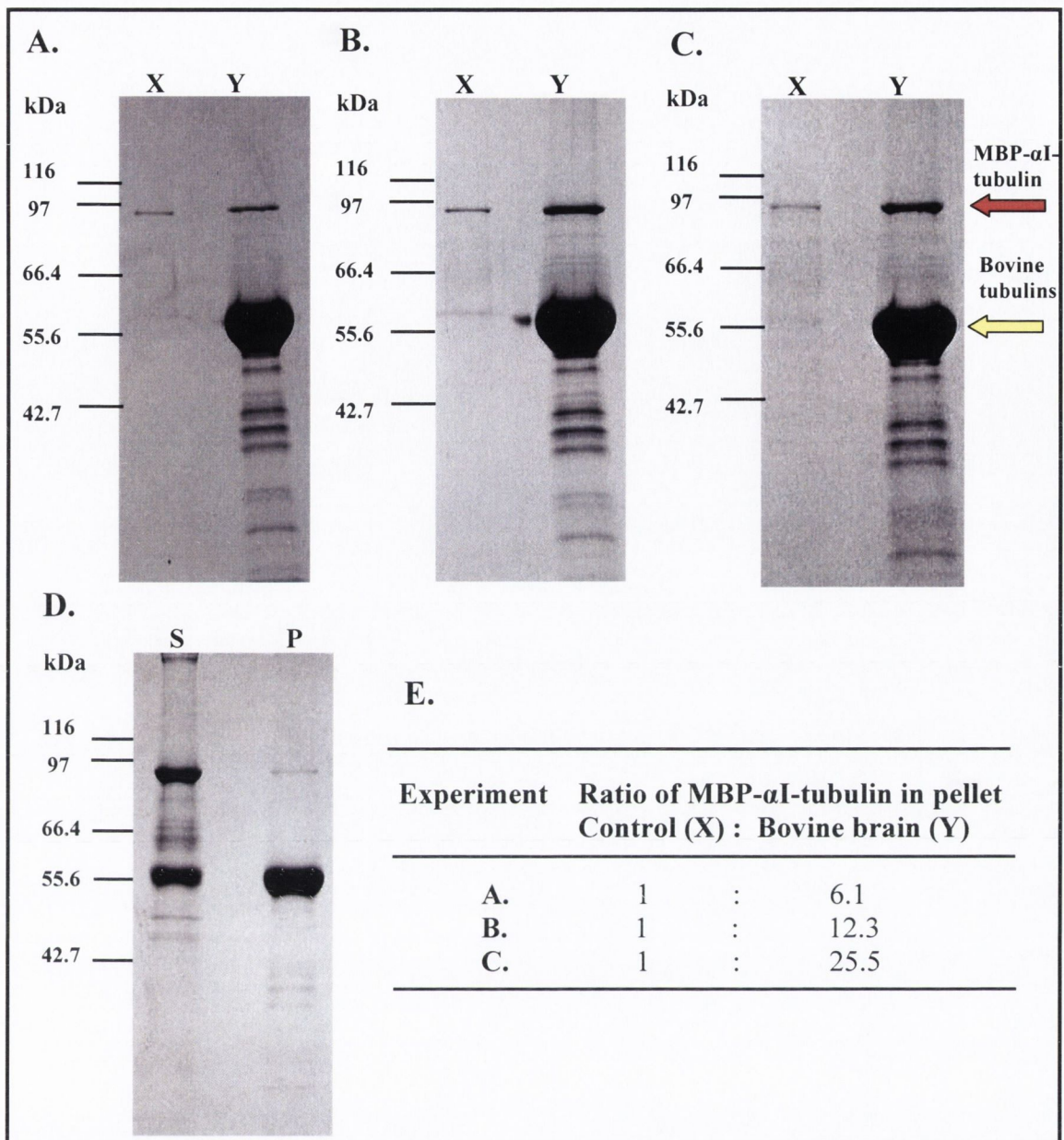


Figure 4.14. Analysis of the dose-dependent co-polymerisation of MBP- α I-tubulin with bovine brain tubulin. Various concentrations of bovine brain tubulin and MBP- α I-tubulin: [A] ($\sim 24 + 12 \mu\text{M}$, respectively) [or in terms of amounts $\sim 100 \mu\text{g} + 47 \mu\text{g}$, respectively]; [B] ($\sim 16 + 16 \mu\text{M}$) [$\sim 100 \mu\text{g} + 94 \mu\text{g}$]; [C] ($\sim 12 + 18 \mu\text{M}$) [$\sim 100 \mu\text{g} + 141 \mu\text{g}$] or MBP α I-tubulin alone (same concentrations), were incubated at 37°C in the presence of $30 \mu\text{M}$ Taxol and centrifuged through a glycerol cushion. Resulting supernatants and pellets were resuspended in SDS-loading buffer and equal proportions from the pellet fractions of the control (MBP- α I-tubulin alone) (X) and bovine brain tubulin + MBP- α I-tubulin mixture (Y) were resolved by SDS-PAGE (10%), and stained with Coomassie Blue. [D] Equal proportions from the supernatant (S) and pellet (P) fractions for experiment A only (MBP- α I-tubulin + bovine brain tubulin) is also shown. The extent of MBP- α I-tubulin incorporation into polymerised bovine brain tubulin for experiments A, B, and C was quantified by densitometry and expressed as a ratio value [E]. The running positions of molecular weight markers are shown in kDa on the left of each gel. The data shown are from single, representative experiments.

microtubules.

To eliminate the possibility that recombinant MBP- α I-tubulin found in the microtubule fraction was due to non-specific entrapment within the bovine tubulin pellet, a similar set of experiments was performed using BSA instead of MBP- α I-tubulin (Fig. 4.15). In all experiments performed, the amounts of BSA observed in the pellet fraction of polymerised tubulin were never greater than the levels in the control (BSA alone). This suggests that MBP α I-tubulin found in the pellet fractions of polymerised bovine tubulin more than likely corresponds to co-polymerised tubulin rather than non-specific binding.

Similarly, to ensure co-polymerisation of MBP- α I-tubulin with bovine tubulin was not due to the fusion-tag MBP, co-polymerisation experiments were performed with bovine tubulin and MBP alone (Fig 4.16). As MBP was observed to migrate similarly to bovine tubulins on SDS-PAGE (10%), western blotting was performed using anti- MBP as the primary antibody to determine the levels of MBP in the pellet

and supernatant fractions. As in the case of BSA, the amounts of MBP observed in the pellet fraction of polymerised tubulin were never substantially greater than the levels in the control (MBP alone). Thus, the ability of recombinant α I-tubulin fusion to co-polymerise with bovine tubulin would appear to be independent of its fusion partner, MBP.

We also investigated the ability of MBP- β -tubulin fusion to co-polymerise with bovine tubulin in a dose-dependent manner. From Fig. 4.17 (A and E) it initially appeared as if the recombinant tubulin fusion could co-sediment with bovine tubulin. However, increasing the ratio of *P. falciparum* β -tubulin monomer to bovine β -tubulin monomer failed to result in a corresponding increase in the incorporation of recombinant tubulin into the microtubule pellet (Fig. 4.14 B, C and E). These results would suggest that recombinant MBP- β -tubulin is incapable of co-assembling efficiently with bovine tubulin. The reason for this is unclear, given the fact that MBP- α I-tubulin prepared in a similar way appears to be capable of co-polymerising with the same source of tubulin, and may be related to its fusion partner MBP.

Attempts to form microtubules from both recombinant tubulin fusion proteins by the sedimentation assay also proved to be unsuccessful. The relative amounts of both recombinant fusion proteins in the pellet fraction were similar to controls with each fusion protein alone (data not shown). However, the apparent ability of MBP-

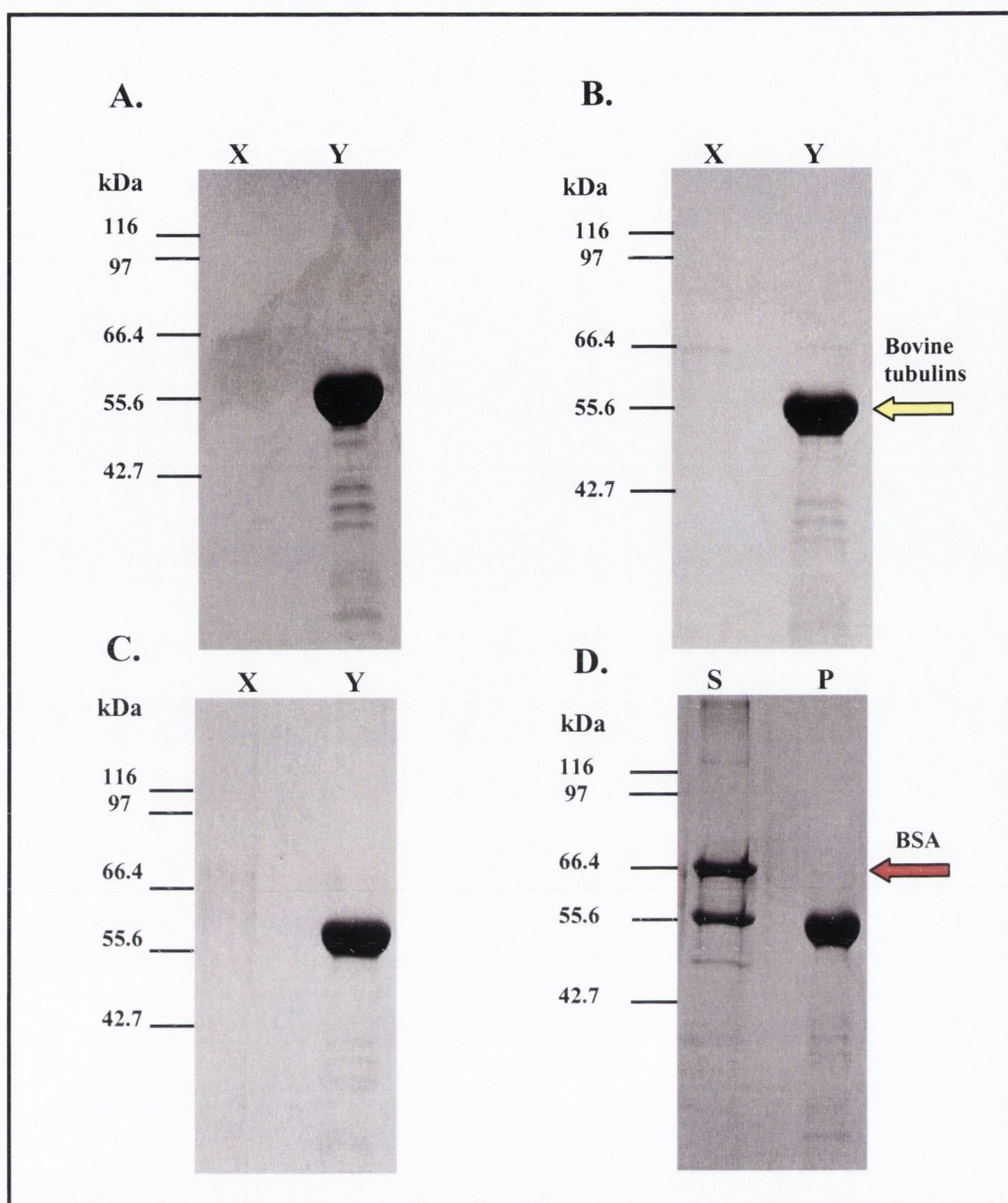


Figure 4.15. Analysis of the dose-dependent co-polymerisation of BSA with bovine brain tubulin. Various concentrations of bovine brain tubulin and BSA: [A] ($\sim 24 + 12 \mu\text{M}$, respectively) [or in terms of amounts $\sim 100 \mu\text{g} + 33 \mu\text{g}$, respectively]; [B] ($\sim 16 + 16 \mu\text{M}$) [$\sim 100 \mu\text{g} + 65 \mu\text{g}$]; [C] ($\sim 12 + 18 \mu\text{M}$) [$\sim 100 \mu\text{g} + 98 \mu\text{g}$] or BSA alone (same concentrations), were incubated at 37°C in the presence of $30 \mu\text{M}$ Taxol and centrifuged through a glycerol cushion. Resulting supernatants and pellets were resuspended in SDS-loading buffer and equal proportions from the pellet fractions of BSA alone (X) and bovine brain tubulin + BSA mixture (Y) were resolved by SDS-PAGE (10%), and stained with Coomassie Blue. [D] Equal proportions from the supernatant (S) and pellet (P) fractions for experiment A only (BSA + bovine brain tubulin) is also shown. The extent of BSA incorporation into polymerised bovine brain tubulin for experiments A, B, and C could not be quantified by densitometry. The running positions of molecular weight markers are shown in kDa on the left of each gel. The data shown are from single, representative experiments.

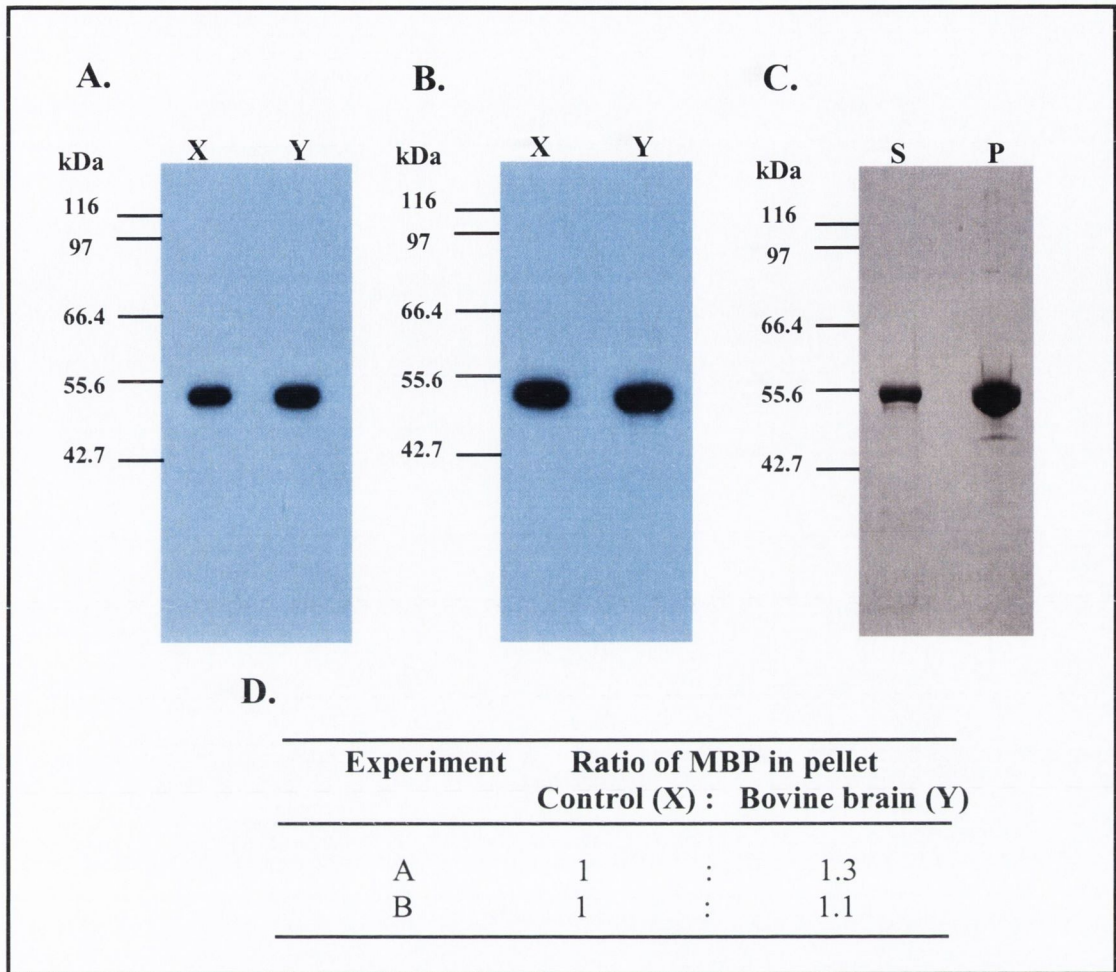


Figure 4.16. Analysis of the dose-dependent co-polymerisation of MBP with bovine brain tubulin. Various concentrations of bovine brain tubulin and MBP: [A] (~ 24 + 12 μ M, respectively) [or in terms of amounts ~ 100 μ g + 25 μ g, respectively]; [B] (~ 16 + 16 μ M) [~ 100 μ g + 50 μ g]; or MBP alone (same concentrations), were incubated at 37°C in the presence of 30 μ M Taxol and centrifuged through a glycerol cushion. Resulting supernatants and pellets were resuspended in SDS-loading buffer and equal proportions from the pellet fractions of MBP alone (X) and bovine brain tubulin + MBP mixture (Y) were resolved by SDS-PAGE (10%), transferred to PVDF membrane, and probed with anti-MBP antibody. [C] Equal proportions from the supernatant (S) and pellet (P) fractions for experiment A only (MBP + bovine brain tubulin) were also resolved by SDS-PAGE (10%), and stained with Coomassie Blue. The extent of MBP incorporation into polymerised bovine brain tubulin for experiments A and B was quantified by densitometry and expressed as a ratio value [D]. The running positions of molecular weight markers are shown in kDa on the left of each gel. The data shown are from single, representative experiments.

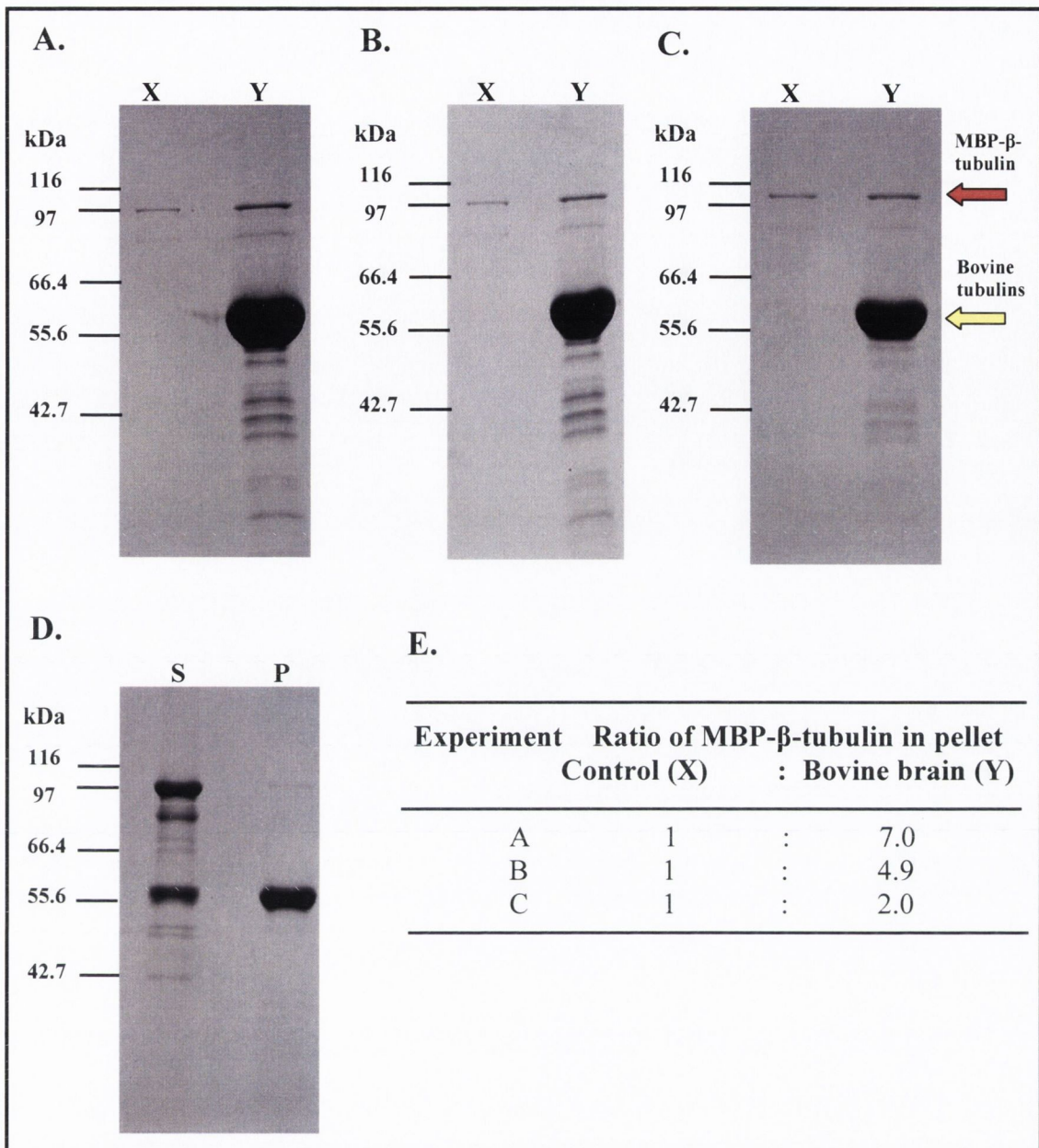


Figure 4.17. Analysis of the dose-dependent co-polymerisation of MBP-β-tubulin with bovine brain tubulin. Various concentrations of bovine brain tubulin and MBP-β-tubulin: [A] (~ 24 + 12 μM, respectively) [or in terms of amounts ~ 100 μg + 49 μg, respectively]; [B] (~ 16 + 16 μM) [~ 100 μg + 98 μg]; [C] (~ 12 + 18 μM) [~ 100 μg + 147 μg] or MBP-β-tubulin alone (same concentrations), were incubated at 37°C in the presence of 30 μM Taxol and centrifuged through a glycerol cushion. Resulting supernatants and pellets were resuspended in SDS-loading buffer and equal proportions from the pellet fractions of the control (MBP-β-tubulin alone) (X) and bovine brain tubulin + MBP-β-tubulin mixture (Y) were resolved by SDS-PAGE (10%), and stained with Coomassie Blue. [D] Equal proportions from the supernatant (S) and pellet (P) fractions for experiment A only (MBP-β-tubulin + bovine brain tubulin) is also shown. The extent of MBP-β-tubulin incorporation into polymerised bovine brain tubulin for experiments A, B, and C was quantified by densitometry and expressed as a ratio value [E]. The running positions of molecular weight markers are shown in kDa on the left of each gel. The data shown are from single, representative experiments.

α I-tubulin to co-polymerise with bovine tubulin and the results from numerous studies in Table 4.1 would suggest that in general, eukaryotic tubulins expressed in the soluble form in *E. coli* are often capable of yielding properly-folded functional tubulins.

4.3. DISCUSSION

In-depth studies of *P. falciparum* tubulin biochemistry have been hampered by the low levels of tubulin in this parasite and the lack of a method for the purification of native *P. falciparum* tubulins. Consequently, the aim of the work described in this chapter was to clone and express the α I- and β -tubulin genes of *P. falciparum* in *E. coli* as a means of providing sufficient amounts of purified tubulins for functional, structural and drug-binding studies.

Analysis of the genome sequence of *P. falciparum* clone 3D7 indicated the existence of two α -tubulin genes, designated α I (located on chromosome 9) and α II (located on chromosome 4) and one β -tubulin gene (located on chromosome 10). Similar findings have also been reported with *P. falciparum* K1/Thailand (Delves *et al*, 1989 and Holloway *et al*, 1989), *P. falciparum* FCR-3/Gambia (Sen *et al*, 1990) and *P. falciparum* NF54 (Wesseling *et al*, 1989). This is in contrast to various other protozoan parasites, which often contain multiple tubulin genes arranged in tandemly repeated, separated α - and β - clusters as in *Leishmania* spp. (Landfear *et al*, 1983), or in alternating α - β repeats, as in the trypanosomes (Schneider *et al*, 1987). As expression of α II-tubulin at the protein level has been reported to be confined to the male gametocyte stage of *P. falciparum* development (Rawlings *et al*, 1992), we decided to confine our cloning and recombinant expression studies to the α I- and β -tubulin genes, which are expressed throughout the parasite's developmental cycle.

The genome sequence of *P. falciparum* is the most A + T-rich genome sequenced to date (Gardner *et al*, 2002). This high A + T content has been reported to make difficult the amplification of *P. falciparum* DNA under standard reaction conditions (Su *et al*, 1996). Despite this concern, both α I- and β -tubulin genes were successfully amplified by RT-PCR at the expected sizes of 1.34 and 1.36 kb, respectively. Our initial strategy was then to clone and overexpress both tubulin genes in *E. coli* based on the work of Prichard and co-workers, who successfully expressed and characterised *H. contortus* recombinant tubulins (Lubega *et al*, 1993; see Table 4.1). The rationale was to produce unfused recombinant tubulins as

inclusion bodies to facilitate their subsequent purification, and then to refold the tubulins *in vitro* for use in functional and drug-binding studies. However, use of the pTrp2 vector failed to generate sufficient amounts of recombinant β -tubulin for such studies. Both modification of expression conditions and use of a plasmid (RIG) carrying the genes for rare-codon tRNAs which had been identified in relative abundance throughout both tubulin genes ($\sim 10.4\%$ and 8.54% of total codons in α I- and β -tubulin genes, respectively) failed to increase levels of tubulin expression.

These expression problems were overcome by use of an alternative vector, pET11a, to direct overproduction of both recombinant tubulins to satisfactory levels. The explanation for the superior expression of recombinant tubulins directed by the pET11a vector over that of pTrp2 is uncertain but may be related to a difference in promoter strength. The identity of both recombinant tubulins was confirmed by western immunoblotting using antibodies specific to *P. falciparum* α I- and β -tubulins. The relative mobilities of both recombinant and native parasite tubulins (~ 53 kDa for α I-tubulin and ~ 57 kDa for β -tubulin) through SDS-PAGE gels was deemed unusual, as conventionally, the α -subunit is the slower migrating species and the β -subunit is the faster migrating species in higher eukaryotes (Delgado *et al*, 1991). However, a similar reversal in the relative migration of α - and β -tubulins has been reported in a number of unicellular organisms such as *T. pyriformis* (Nakazaw *et al*, 1999), *R. filosa* (Linder *et al*, 1997) and *Naegleria gruberi* (Shea *et al*, 1987), highlighting an electrophoretic difference between some metazoan and protozoan tubulins. The apparently similar mobilities of native and recombinant *P. falciparum* tubulins also suggested that any post-translational modifications of parasite native tubulins were not significant enough to alter the migratory behaviour of parasite tubulins through SDS-PAGE gels.

The tubulins produced by the pET system were insoluble upon IPTG induction of the T7 promoter at 37°C . This was not unusual as the expression of foreign proteins at high levels often results in the formation of inclusion bodies composed of insoluble aggregates of the expressed protein (Marston, 1987). However, lowering the induction temperature to 30°C resulted in the production of some soluble recombinant α I-tubulin (data not shown). Reduction of temperature during recombinant protein expression has previously been demonstrated to correspond with a lowering of the rate of protein synthesis within the *E. coli* cell, allowing for an increase in the amount of soluble protein expressed (Schein *et al*,

1988). Due to the perceived difficulties in purifying untagged recombinant tubulins from the complex mixture of proteins present in the *E. coli* cytosol, we decided to purify and refold the tubulin-containing inclusion bodies based on previously published procedures. However, it is important to note that although the amount of tubulin in the soluble protein extract of *E. coli* was not quantified, the protein band corresponding to α I-tubulin was the most prominent band observed. If the same level of soluble recombinant β -tubulin could be obtained it may be possible to purify both tubulins by the temperature-dependent *in vitro* assembly-disassembly technique of Shelanski *et al* (1973). For this technique to be successful a minimum concentration of recombinant tubulins in the soluble *E. coli* lysates would have to be present ($> 1\text{mg/ml}$) for the initial polymerisation step at 37°C (Ikeda *et al*, 1976). However, possible problems with proteases at this temperature may require a purification step prior to use of the assembly-disassembly technique.

The insoluble, recombinant tubulins were purified to near-homogeneity by differential centrifugation and detergent extraction (see Fig. 4.10) and dissolved and renatured by the urea/alkaline method of Marston (1987). Although most published methods advocate the use of dialysis to eliminate the denaturing agent during refolding, this method was avoided as dialysis exposes the protein solution to a decreasing denaturant gradient over a few hours. Thus proteins will remain exposed for an extended period of time to an intermediate denaturant concentration where they are not yet folded but no longer denatured and extremely prone to aggregation. In addition, different proteins require different conditions for folding into biologically active protein and searching for these conditions can be a long and futile task. As Lubega *et al* (1993) successfully used the dilution method to refold *H. contortus* recombinant tubulins, it seemed practical that this method might also be applied to recombinant *P. falciparum* tubulins.

Unfortunately, the refolded recombinant monomers failed to assemble to form microtubules under all conditions tested. This suggested that either or both tubulin monomers had misfolded and possibly aggregated during the refolding process. It could also be possible that despite using sufficient quantities of tubulin for polymerisation studies that the final concentrations of tubulin monomers that folded correctly were insufficient to equal the critical concentration of tubulin required to form microtubules. Despite the success of Lubega *et al* (1993) our results would appear to agree with the observations of other groups that unfolded tubulin

whether obtained by biochemical isolation from tissue or by expression in a bacterial host, cannot be readily folded or refolded by the methods normally employed with other proteins, such as dilution or dialysis (Andreu *et al*, 2002; Guha *et al*, 1997; Shah *et al*, 2001; Wu *et al*, 1987). Recent reports suggest that the use of rabbit reticulocyte lysates (RRL), enriched in tubulin folding machinery, is a more successful method for the *in vitro* refolding of bacterially-expressed tubulins (Shah *et al*, 2001; Pucciarelli *et al*, 2002). This system employs use of the cytoplasmic chaperonin CCT and several cofactors in the RRL, which appear correctly to fold denatured tubulin chains when they are rapidly diluted into it from solution in urea. Analysis of the primary structure of *P. falciparum* β -tubulin confirms the presence of the CCT-binding motifs, which have previously been characterised for bovine tubulin (Llorca *et al*, 2001; data not shown). Perhaps this system may prove to be a more successful *in vitro* refolding technique for recombinant *P. falciparum* tubulins than that of dilution.

As studies with refolded tubulins failed to generate functional protein, we also endeavoured to characterise recombinant *P. falciparum* tubulins produced as soluble fusion proteins. Expression with the N-terminal fusion MBP was found to enhance the solubility of both tubulin monomers at induction temperatures of 37°C. This may be due to the chaperone-like qualities that have been attributed to MBP when fused at the N-terminus of recombinant proteins, assisting in correct protein folding and forming biologically active proteins (Kapust *et al*, 1999; Sachdev *et al*, 1998). Apart from improved solubility, the MBP-tag also offered the advantage of purifying the recombinant tubulin fusion proteins by affinity chromatography. However, problems were encountered during the cleavage of MBP from the chimeric protein using the site-specific protease factor X_a. Although removal of the MBP-tag was achieved, a number of additional bands besides full-length recombinant tubulin were observed on SDS-PAGE gels after the cleavage step, which were subsequently inseparable by ion-exchange chromatography (data not shown). No site-specific cleavage site for factor X_a was identified from analysis of amino acid sequences of both tubulin proteins, suggesting that the chimeric proteins were susceptible to non-specific secondary activity of factor X_a. Tubulin fusions incubated in the absence of factor X_a under the same reaction conditions were found to remain intact, suggesting that host proteases had not co-purified with the recombinant tubulin fusions (data not shown). Related cleavage problems have also been reported with other MBP-tubulin

fusion proteins. Removal of the MBP-tag from *Rhynchosporium secalis* β -tubulin was unsuccessful, as the factor X_a site was believed to be buried within the structure of the chimeric protein (Holloman *et al*, 1998). However Macdonald *et al* (2003; 2004) have reported the successful removal of both GST and MBP tags from a range of recombinant protozoan tubulins (see Table 4.1). Perhaps the use of an alternative vector for expressing recombinant tubulins from the pMAL-c2 series such as pMAL-c2E or pMAL-c2G, which include a sequence coding for the recognition sites of alternative specific proteases, namely Enterokinase and Genenase I, respectively, may allow for improved removal of the MBP tag from *P. falciparum* recombinant tubulins.

Despite our unsuccessful efforts to remove the MBP-tag from the tubulin fusion protein, we investigated the ability of both tubulin fusions to co-polymerise with assembly-competent bovine brain tubulin. Interestingly, MBP- α I-tubulin was found to co-polymerise in a dose-dependent fashion with this evolutionarily diverse source of tubulin as indicated by the sedimentation assay (Fig. 4.14). Similar assays using BSA and MBP as negative controls indicated that the observed co-polymerisation was specific. However, MBP- β -tubulin failed to co-assemble efficiently, indicating the MBP-tag may be inhibitory to the functional activity of recombinant β -tubulin but apparently not α -tubulin. These results in conjunction with those of Macdonald *et al* (2003 and 2004) and Linder *et al*, (1998) (see Table 4.1) suggest that soluble recombinant tubulins expressed in *E. coli* can be correctly folded and incorporated into functional microtubules.

The apparent ability of a tubulin fusion protein to be incorporated into microtubules has been also realised with GFP-tagged tubulins in a wide range of eukaryotic cells (Rusan *et al*, 2001). Furthermore, incorporation of *P. polycephalum* tubulin into the microtubules of mammalian cells was able to endow the injected cells with novel properties (Prescott *et al*, 1989). For example resistance to colchicine-induced microtubule depolymerisation, a characteristic of *Physarum* tubulin, was conferred on injected mammalian cells, which are normally very sensitive to this antimitotic agent. It would therefore be of interest to investigate the ability of recombinant *P. falciparum* MBP- α I-tubulin fusion to bequeath such novel properties on bovine tubulin *in vitro*. For example, the resistance of bovine tubulin to the depolymerising effects of dinitroaniline antimitotic herbicides has been well documented (Chan *et al*, 1990; Morejohn *et al*, 1991). However, the microtubules of

P. falciparum have been shown to be susceptible to this class of agent (Fowler *et al*, 1998; Kaidoh *et al*, 1995; chapter 6), although the binding site has yet to be identified (see section 6.2.5). Ligands from the dinitroaniline class are proposed to exert their microtubule depolymerising activity by binding to tubulin heterodimers in the cytoplasm. As the herbicide-tubulin complex is added to the emergent microtubule, further growth of the microtubule ceases (Anthony *et al*, 1999a). Therefore, using either the sedimentation or turbidimetric assay, it would be of interest to investigate the ability of MBP α I-tubulin to confer dinitroaniline sensitivity upon bovine tubulin. Since our results showed that co-polymerisation assays resulted in microtubules primarily composed of bovine tubulin, it might be argued that not enough recombinant tubulin would be incorporated to induce such effects. However, microtubule inhibitors have been shown to inhibit the polymerisation of tubulin into microtubules *in vitro* at drug concentrations far below the concentration of tubulin in solution. For example, vinblastine acts substoichiometrically by binding to the ends of the microtubules (Wilson *et al*, 1976). Therefore, there may be sufficient amounts of recombinant MBP- α I-tubulin-herbicide complex incorporated into the bovine microtubules to exert a net microtubule depolymerising effect and this idea merits investigation.

In summary, I have reported for the first time, high-level expression and purification of both soluble and insoluble forms of *P. falciparum* tubulins in *E. coli* and their partial characterisation. Although refolded recombinant tubulins failed to polymerise into microtubule structures, results that are more favourable were achieved with α I-tubulin expressed as a soluble fusion protein, which was capable of co-polymerising with bovine brain tubulin. Thus, we have opened up a route for future structure-function and biochemical studies of *P. falciparum* tubulins, which up until now has been prevented by the inability to purify these proteins direct from the parasite.

Chapter 5

Stage-Dependent Production and Electrophoretic Behaviour of Tubulins in *P. falciparum*

5.1. INTRODUCTION

The developmental cycle of the malarial parasite, *P. falciparum*, consists of numerous nuclear divisions and cellular differentiations involving various microtubular structures (Bell, 1998). Expression of the α/β -tubulin heterodimer, an integral component of such structures, is developmentally regulated in the parasite (Delves *et al*, 1990; Le Roch *et al* 2003). The α I- and β -tubulin genes appear to be transcribed to varying degrees during both asexual and sexual erythrocytic stages. Transcription of the α II-tubulin gene has also been reported in both stages; however, expression at the protein level has been reported to be confined to male gametocyte stages only (Rawlings *et al*, 1992). While a wealth of data exists on tubulin gene expression in the various stages of parasite development, information pertaining to the corresponding levels of tubulin proteins in such stages is lacking. This is in contrast to certain other protozoan parasites, where for example tubulin has been shown to be the major protein expressed in the insect stages of growth of *L. mexicana* (Fong *et al*, 1981), *T. brucei* (MacRae *et al*, 1990) and *Crithidia fasciculata* (Russell *et al*, 1984).

In addition, a number of differences in electrophoretic behaviour, immunological reactivity and drug binding have been observed between the tubulins of protozoa such as those listed above and metazoa, suggesting that significant structural differences exist between the tubulins from these species (Anthony *et al*, 1999a; Morejohn *et al*, 1991). For example, the α -tubulins of a wide range of protozoa have been reported to migrate faster than their β -tubulins during SDS-PAGE, in contrast to the migratory behaviour of vertebrate tubulins (Clayton *et al*, 1980, and Suprenant, 1985). We have also reported the existence of a similar phenomenon displayed by recombinant and native *P. falciparum* tubulins as described in chapter 4. This α/β inversion phenomenon appears to occur in a distinct group of organisms and it has been suggested that this inversion under specific electrophoretic conditions might be a property common to most protists (Delgado *et al*, 1991).

In view of the lack of reports on various properties of *P. falciparum* tubulins, this chapter describes the quantification of the relative amounts of α I- and β -tubulin expressed in the asexual stages of *P. falciparum* development. We also report the analysis of α II-tubulin expression in the asexual stages of parasite growth as well as a comprehensive analysis of the apparent electrophoretic mobilities of recombinant

and native *P. falciparum* tubulins in comparison with vertebrate (bovine brain) tubulin.

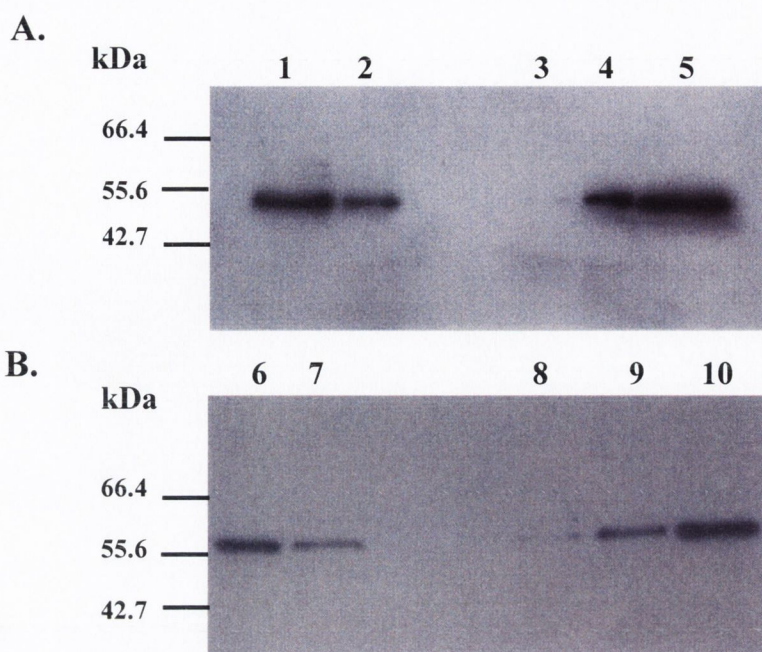
5.2. RESULTS

5.2.1. Quantification of α I- and β -tubulin production in asexual erythrocytic stages of *P. falciparum* development

Although immunofluorescent and electron microscopic analyses have identified microtubules in various stages of the *P. falciparum* asexual cycle (Read *et al*, 1993; Bannister *et al*, 1995), no information pertaining to the actual levels of tubulin expressed in such stages currently exists. In response to this deficit, we attempted to quantify α I- and β - tubulin expression in the ring (6 - 12 h, post invasion), trophozoite (18 - 24 h, post-invasion) and schizont (36 - 42 h, post-invasion) stages of intra-erythrocytic parasite development. The relative amounts of α I- and β -tubulin expressed in whole parasite extracts of these various stages were compared to known amounts of purified recombinant α I- and β -tubulin (see chapter 4) by western immunoblotting and quantified by densitometry (Fig 5.1).

The results indicated that the two tubulin monomers were present at roughly equal levels in all stages examined. During the first part of the parasite erythrocytic cycle (ring stage, 6 - 12 h post invasion), a small quantity of tubulin was detected, which represented < 0.03% of proteins in whole cell extracts of ring-stage parasites. While increased levels of tubulin were observed in the trophozoite stage, highest expression was detected in the schizont stage, with α I/ β -tubulin together comprising up to 0.25% of proteins in whole-cell extracts of schizont-stage parasites (Fig 5.1).

Results obtained for tubulin expression were then correlated to the data obtained from the malaria transcriptome database (<http://www.plasmodb.org>; Le Roch *et al*, 2003) which outlined the transcription profiles of α I- and β -tubulin genes during the *P. falciparum* development cycle (Fig 5.2). From the Scripps/GNF malaria array, transcription of both α I- and β -tubulin genes appeared to be lowest in the ring-stage parasites and highest in early schizonts with maximum expression occurring at 34 h and 31 h post-invasion for α I- and β -tubulin genes, respectively (data not shown). Thus, our data on the production of both tubulins at the protein level throughout the asexual cycle would appear to correlate well with data on their corresponding expression at the mRNA level.



C.

Stage (h-post invasion)	Microtubular structures present	~ % α I-tubulin ^a	~ % β -tubulin ^a
Ring (6 - 12)	n.o.	<0.03	<0.02
Trophozoite (18 - 24)	n.o.	0.03	0.02
Schizont (36 - 42)	Spindle and spindle associated-microtubules ^b Subpellicular ^b	0.13	0.12

^aTubulin present as a % whole cell protein.

^bPreviously confirmed in this stage by immunofluorescence and electron microscopy (Bell, 1998).
n.o. none observed.

Figure 5.1. Stage-specific quantitation of *P. falciparum* α I- and β -tubulin expression during the asexual erythrocytic cycle. Western blots of SDS-10% polyacrylamide gels probed with antibodies to either *P. falciparum* α I-tubulin (**A**) or β -tubulin (**B**). Lanes: 1 - 2, 5 ng and 1 ng, respectively, of unfused recombinant α I-tubulin; lanes 3 - 5, 10 μ g of ring, trophozoite and schizont stage proteins, respectively; lanes 6 - 7, 5 ng and 1 ng, respectively of unfused recombinant β -tubulin; lanes 8 - 10, 8 μ g of ring, trophozoite and schizont stage proteins, respectively. The running positions of molecular weight markers are shown in kDa on the left of each immunoblot. (**C**) The relative amounts of tubulins in parasite stages were quantitated by densitometry using recombinant tubulins as standards and the values obtained are shown as % values of the protein contents of whole cell extracts.

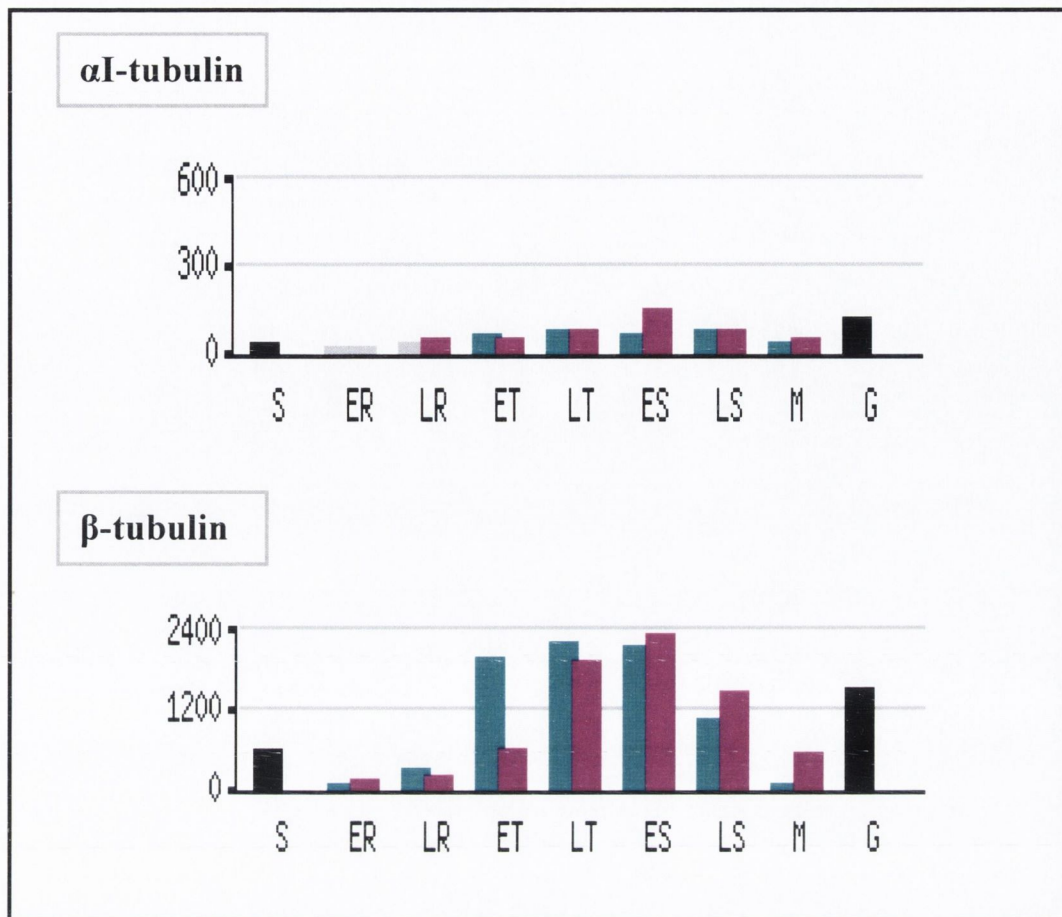


Figure 5.2. The transcription profile of α I- and β -tubulin genes in the development cycle of *P. falciparum* as determined by the Scripps/GNF malaria array. Total RNA extracted from *P. falciparum* developmental stages synchronised by either sorbitol (denoted light green; black for gametocytes and sporozoites) or temperature (denoted pink), were labelled by a strand-specific technique and hybridised to a custom-made, high-density oligonucleotide array, designed using the *P. falciparum* genome nucleotide sequence. Probes attached to the array corresponded to at least 5159 *P. falciparum* genes, which were used to compute gene expression levels from hybridisation experiments by means of a match-only integral distribution algorithm (MOID). Abbreviations on the x-axis: ER = early rings, LR = late rings, ET = early trophozoites, LT = late trophozoites, ES = early schizonts, LS = late schizonts, M = merozoites, S = sporozoites and G = gametocytes. Values on the y-axis correspond to Affymetrix MOID expression value normalised by experiment. Stages coloured gray are below confidence threshold. Adapted from <http://plasmodb.org> and Le Roch *et al* (2003).

5.2.2. Analysis of α II-tubulin expression in *P. falciparum* asexual stages

The two α -tubulin genes (α I and α II) of *P. falciparum*, which share 94 % identity at the amino acid level, have been reported to be expressed in a stage-specific manner in the growth cycle of the parasite. While α I-tubulin expression is found in most stages of parasite growth, α II-tubulin is reported to be confined to the sexual stages of *P. falciparum* development and is present specifically in male gametocytes, gametes and newly formed zygotes (Rawlings *et al*, 1992). In addition, ultrastructural studies located α II-tubulin in the microgametocyte axoneme, suggesting a role for this molecule in motility. These observations were made by use of a monoclonal antibody (IgM mAb, 5E7) raised against purified *P. falciparum* gametes and zygotes. While this antibody specifically recognised α II-tubulin in male gametes of the avian parasite, *Plasmodium gallinaceum*, no reactivity was detected with asexual parasites (Rawlings *et al*, 1992).

Despite the apparent stage-specificity of α II-tubulin, its expression at the mRNA level appears to occur throughout the developmental cycle. Initial observations by Delves *et al* (1990) indicated that the α II-tubulin gene was predominantly expressed in gametocyte forms, although low levels of α II-tubulin gene transcripts were detected in ring and trophozoite stages. More recently, microarray studies on the transcription profiles of parasite genes (Le Roch *et al*, 2003) have indicated the transcription of α II-tubulin in both asexual and sexual stages (see Fig. 5.3 A). While the predominance of α II-tubulin in gametocyte stages of parasite development is undoubted, in light of the transcriptomics data we decided to investigate possible presence of low levels of α II-tubulin in asexual stages.

This study was instigated by immunofluorescent microscopy using a rabbit antiserum raised against the α II-tubulin carboxy-terminal sequence. This antiserum has been reported to detect α II-tubulin in *P. falciparum* male gametocytes and gametes but not females or asexual stages (Guinet *et al*, 1996). However, using asynchronous, asexual cultures, mitotic and post-mitotic microtubular structures were observed (Fig. 5.3 B) with the nuclear material stained with DAPI conforming closely to the shape of the mitotic apparatus. The presence of sharply defined nuclei in both multi-nucleate parasites stained with DAPI also suggested parasites were undergoing the process of mitosis. Similar tubulin-containing structures in malarial parasites were observed in Figs. 3.6. and 6.3 using antibodies specific to *P. falciparum* β -tubulin. While this result would indicate the presence of α II-tubulin in

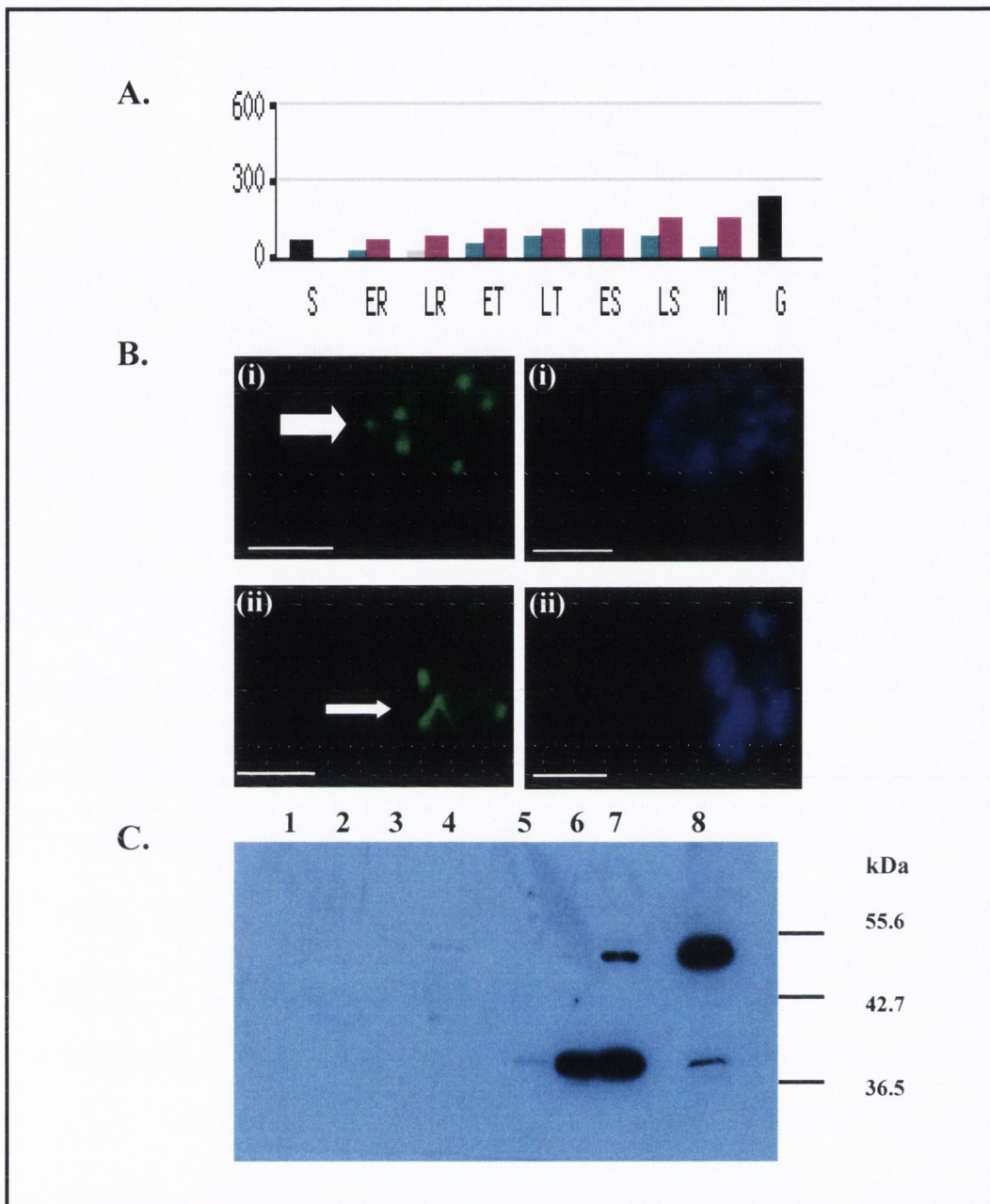


Figure 5.3. Analysis of α II-tubulin expression at the mRNA and protein level in asexual stages of *P. falciparum*. **A.** The transcription profile of the α II-tubulin gene in the development cycle of *P. falciparum* as determined by the Scripps/GNF malaria array (methodology and abbreviations are as indicated in Fig 5.2). **B.** Two examples of mitotic microtubular structures of cultured parasites viewed by immunofluorescence using antibodies to *P. falciparum* α II-tubulin (left) and DAPI nuclear stain (right). Note: microtubule-organising centres (large arrow) and hemispindle (small arrow). Scale denoted by bar = 4 μ m. **C.** Western blot of SDS-10% polyacrylamide gel probed with anti- α II-tubulin. Lanes: 1 - 4, 25 ng, 50 ng, 200 ng and 500 ng, respectively of recombinant α I-tubulin; lanes 5 - 8, 25 μ g of ring, trophozoite, schizont and gametocyte stage extracts, respectively. The running positions of molecular weight markers are shown in kDa on the right of the immunoblot.

parasite asexual stages, we cannot rule out the possibility that α II-tubulin antibodies may be cross-reacting with epitopes of α I-tubulin under the conditions used for immunofluorescence.

In response to this difficulty, we also analysed extracts of asexual and sexual parasites for α II-tubulin by western immunoblotting using recombinant α I-tubulin (see chapter 4) as a negative control. From Fig. 5.3 (c) little or no cross-reaction was observed between anti- α II-tubulin and recombinant α I-tubulin, even at protein amounts as high as 500 ng. While no full-length α II-tubulin was detected in ring or trophozoite stages, a band was observed in schizont extracts at ~ 53 kDa, which is the approximate expected size of α II-tubulin. A major band was also observed at a similar size in *P. falciparum* gametocyte extracts, as expected. It is important to note that gametocyte extracts resolved by SDS-PAGE in Fig 5.3 were obtained from solubilising the insoluble gametocyte pellet, which resulted after detergent (Triton X-100) lysis. The supernatant or soluble fraction was found to lack α II-tubulin (data not shown) indicating the apparent Triton X-100-insoluble nature of α II-tubulin. In addition, an unidentified band was also detected on blots migrating at ~ 38 kDa in both asexual and gametocyte extracts, indicating possible breakdown of α II-tubulin by native proteases during the lysis procedure.

The presence of α II-tubulin in the schizont (and possibly trophozoite) stage implies that α II-tubulin exists in asexual parasites albeit at a lower level than in gametocytes. However, as the schizont extracts used in blotting studies were found to contain $\sim 0.12\%$ gametocytes out of a total of 4000 parasite forms counted, we cannot rule out that the band observed represents α II-tubulin originating from such sources. Nonetheless, if the band at ~ 38 kDa is a breakdown product of α II-tubulin it would appear unlikely that the low numbers of contaminating gametocytes could make bands of that intensity. Thus, these studies would appear to suggest that low levels of α II-tubulin expression possibly exists in asexual parasites.

5.2.3. Investigation of the α/β -inversion of *P. falciparum* recombinant and native tubulins

The two subunits of tubulin were originally labelled by Bryan *et al* (1971) as α - and β -tubulin, who assigned the α -subunit as the slower and the β -subunit as the faster migrating species during SDS-PAGE. This nomenclature of tubulin subunits has since been adopted and used to identify tubulins from a range of eukaryotic

organisms. However, as described in chapter 4, native and recombinant *P. falciparum* tubulin subunits display an apparently reversed order of electrophoretic mobility. A similar phenomenon has also been observed with tubulins from a number of lower eukaryotes and plant species (see section 5.3).

It has previously been established that the α/β inversion of tubulins may depend on the grade of SDS used in electrophoresis (Best *et al*, 1981; Stephens, 1998), the presence of urea in the separating gels (Clayton *et al*, 1980) or variations in the pH of the separating gel (Suprenant *et al*, 1985). High-grade SDS has been reported to result in poor separation of tubulin subunits, while tubulin separation was accentuated by hexadecyl and tetradecyl sulfate contaminants in commercial SDS preparations. Similarly, by lowering the pH of the separating gel from pH 9.25 to pH 8.25, separation of tubulins was observed. Thus, using specific electrophoretic conditions, we attempted to characterise the electrophoretic behaviour of native and recombinant *P. falciparum* tubulins in comparison with vertebrate (bovine brain) tubulins.

Using high-grade SDS (with no detectable long-chain alkyl sulfates) and separating gels of pH 8.25 - 9.25, native and recombinant *P. falciparum* α I- and α II-tubulins were consistently resolved from β -tubulin, in contrast to the tubulin subunits of bovine brain (Fig. 5.4 A - C). In addition, under all conditions tested, the inversion in migration of parasite tubulins remained evident albeit less markedly at pH 9.25.

However, when low-grade SDS (see section 2.6.2) was used in gels and buffers for electrophoresis, parasite and vertebrate tubulins displayed different electrophoretic behaviour (Fig 5.5 A - C). As the pH of the separating gel increased, a corresponding increase in the resolution of the α/β tubulin subunits of bovine brain became apparent. The opposite effect was observed with parasite tubulins. The higher the pH of the separating gel, the closer the parasite tubulins migrated to each other. Again, under all conditions tested, parasite tubulins constantly displayed a reversed order of electrophoretic mobility.

5.3. DISCUSSION

The primary goals of the work described in this chapter were to investigate features of tubulin expression in the *P. falciparum* development cycle and to characterise the unusual electrophoretic behaviour of parasite tubulin. This may form

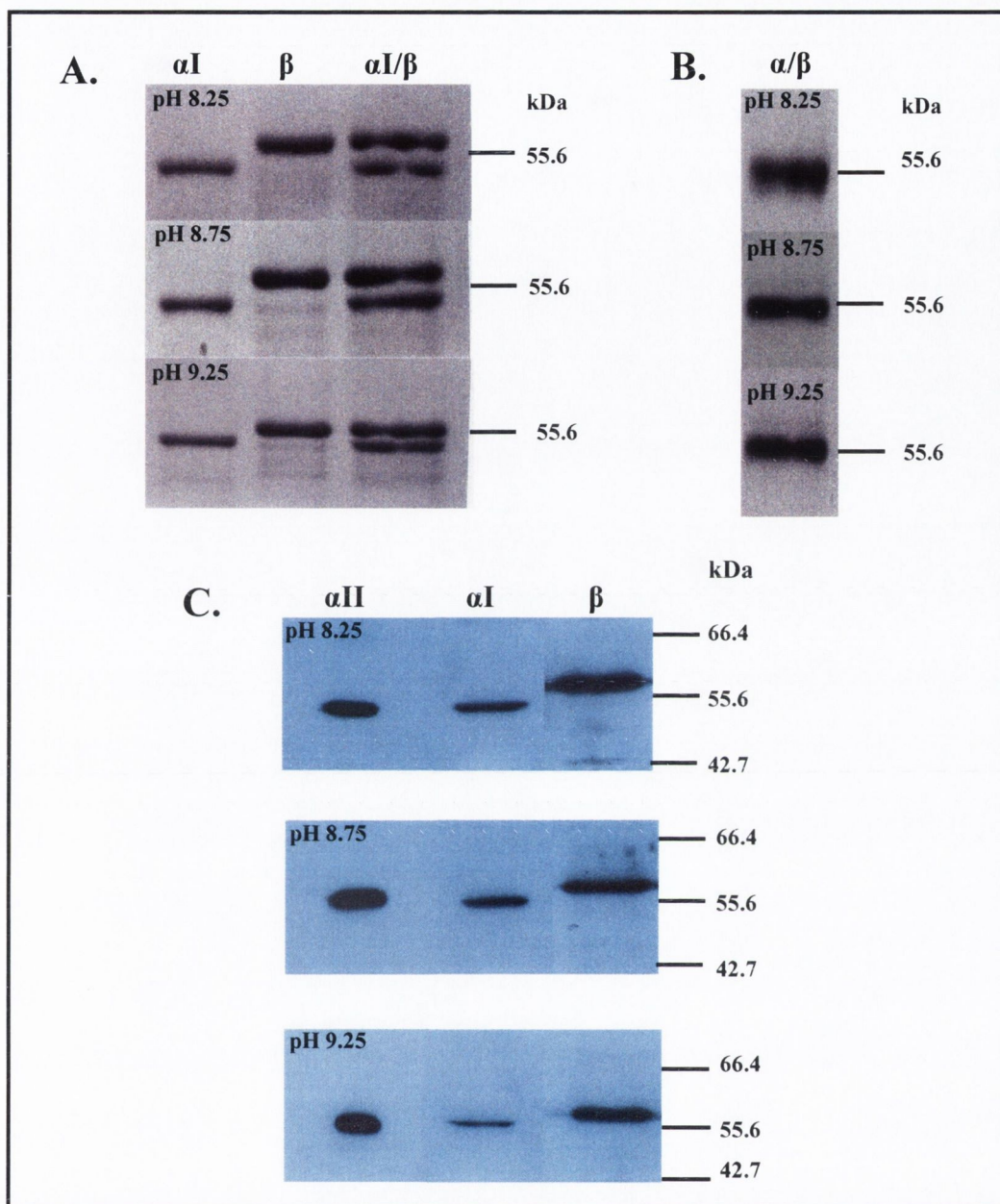


Figure 5.4. pH effects on tubulin separation in high-grade SDS-PAGE. (A) The migration of recombinant *P. falciparum* tubulins (~ 2 μ g; denoted αI , β , and $\alpha I/\beta$) was compared to (B) bovine brain tubulin (~ 2 μ g; denoted α/β) simultaneously on three separate Coomassie Blue stained gels where the pH of the separating gel was increased from 8.25 to 9.25 (as indicated). (C) Western blots of SDS-10% polyacrylamide gels of either *P. falciparum* gametocyte extracts probed with antibodies to αII -tubulin (denoted αII) or asynchronous asexual parasite extracts probed with anti- αI -tubulin or anti- β -tubulin antibodies, respectively (denoted αI and β). The running positions of molecular weight markers are shown in kDa on the right of each gel and immunoblot.

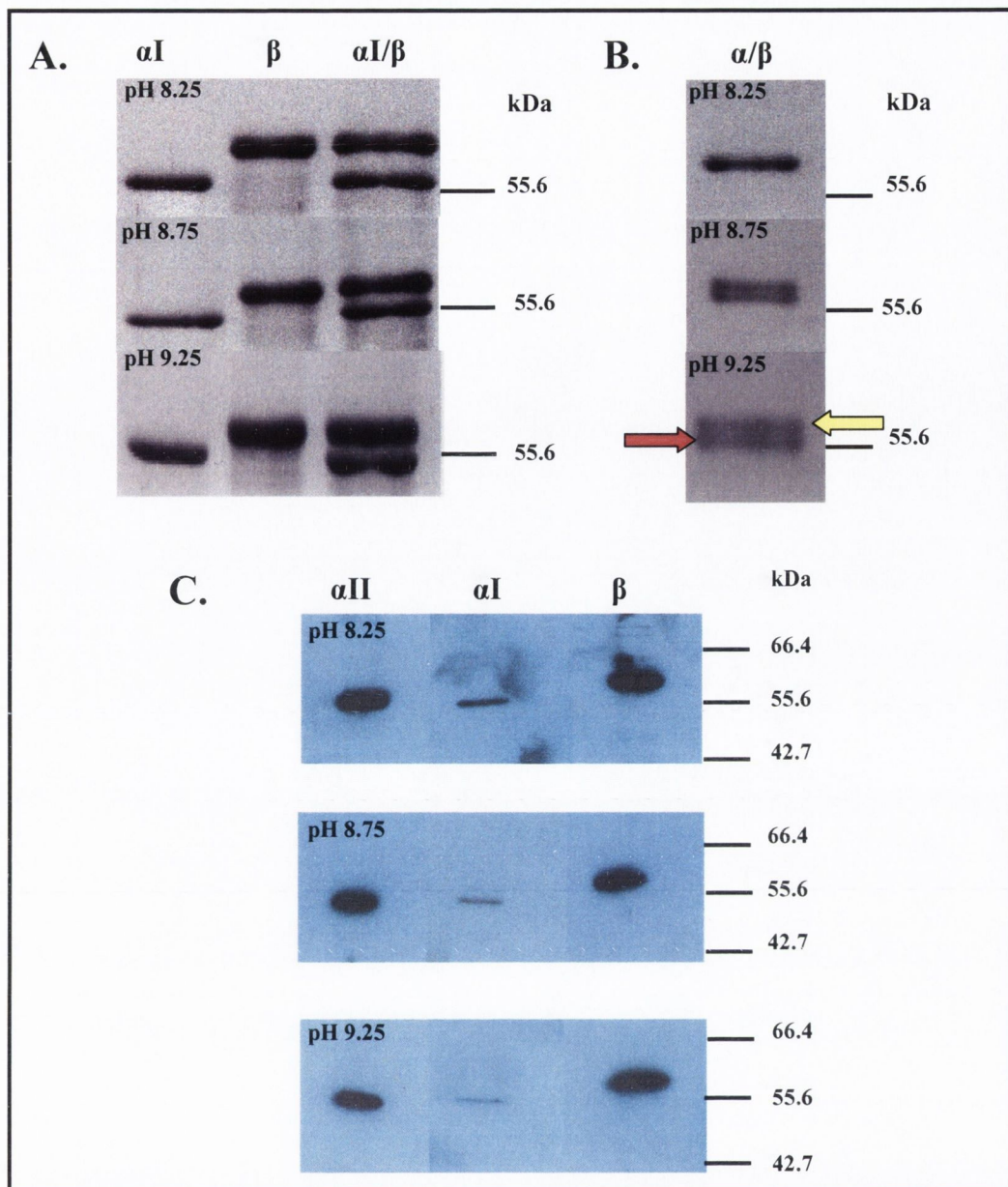


Figure 5.5. pH effects on tubulin separation in low-grade SDS-PAGE. (A) The migration of recombinant *P. falciparum* tubulins (~ 2 μ g; denoted αI , β and $\alpha I/\beta$) was compared to (B) bovine brain tubulin (~ 2 μ g; denoted α/β : yellow arrow presumably indicates the α subunit and red arrow the β subunit) simultaneously on three separate Coomassie Blue stained gels where the pH of the separating gel was increased from 8.25 to 9.25 (as indicated). (C) Western blots of SDS-10% polyacrylamide gels of either *P. falciparum* gametocyte extracts probed with antibodies to αII -tubulin (denoted αII) or asynchronous asexual parasite extracts probed with anti- αI -tubulin or anti- β -tubulin antibodies, respectively (denoted αI and β). The running positions of molecular weight markers are shown in kDa on the right of each gel and immunoblot.

the basis for future attempts to purify tubulins directly from the parasite.

In contrast to some other protozoan parasites, purification of *P. falciparum* tubulins has not so far been possible owing to the relative scarcity of these proteins in the parasite cell. To substantiate this premise, a combination of western blotting and densitometry techniques were used to quantify the levels of α I- and β -tubulin in various stages of the parasite's asexual cycle. Ring-stage parasites (6 - 12 h post-invasion) were found to contain a minute quantity of α I- and β -tubulin (< 0.03% of protein) which may represent the remnants of the f-MAST used by the merozoite during its invasion of an erythrocyte (Bannister *et al*, 2003). In contrast, a considerable increase in the rate of tubulin synthesis appeared to take place at and/or before the stage associated with cell division (schizonts, 38 - 44 h post-invasion) as tubulin was estimated to represent ~ 0.25% of schizont-stage proteins. Therefore, the schizont stage requires a high amount of tubulin, probably for the formation of both the mitotic spindle microtubules and subsequently the microtubular cytoskeleton of the new merozoites. In addition, trophozoites (18 - 24 h post invasion) were found to contain more tubulin (~ 0.03% of trophozoite stage proteins) than ring-stage parasites. This quantity of tubulin presumably corresponds to a cellular pool of free dimers as no microtubular structures have yet been identified in this stage of parasite growth. However, it could also represent in part a limited array of cytoplasmic microtubules, which may be implicated in intracellular transport in the parasite cell. Moreover, indirect evidence for the existence of such a set of microtubules comes from the identification of the microtubule-associated motor protein kinesin in all stages of parasite intra-erythrocytic development (Fowler *et al*, 2001).

To substantiate our results for the profile of tubulin production in the parasite's asexual cycle, we looked at the published transcription profiles of both tubulin genes in the corresponding stages (Fig 5.2). Transcription of α I- and β -tubulin genes appears to be lowest in rings and highest in late trophozoites/early schizonts as determined by Le Roch *et al* (2003), in agreement with their expression at the protein level. Moreover, these results suggest that the mRNA is turned over quickly as both tubulin protein production and mRNA expression levels peak in the schizont stage. In addition, our results also indicated the relatively equal production of both tubulin subunits in all parasite stages examined, as occurs in other organisms.

The amount of tubulin determined in the schizont stage of *P. falciparum* development is considerably less (at least a 40-fold difference) than that found in the

protozoan parasites *L. mexicana* (Fong *et al*, 1981), *T. brucei* (MacRae *et al*, 1990) and *Crithidia fasciculata* (Russell *et al*, 1984) where tubulin represents > 10% of cellular protein. Although *P. falciparum* asexual stages contain similar functional classes of microtubules to these parasites, namely mitotic and suppellicular microtubules, differences in tubulin concentrations can be accounted for by the more extensive array of subpellicular microtubules distributed throughout the kinetoplastid cell (Gull, 1999). Perhaps, sexual stages of *P. falciparum* development, which contain a third class of microtubules in the axonemes and flagella of the motile microgametes and therefore possibly greater quantities of tubulin, may hold more promise for the extraction of native tubulin directly from the parasite.

In view of the recent transcriptomic data outlining the expression of the α II-tubulin gene throughout the parasite's growth cycle, we decided to re-examine the stage-specificity of α II-tubulin expression in asexual parasites. Western immunoblotting demonstrated the presence of α II-tubulin in schizont-stage parasites, albeit at lower levels than sexual stage gametocytes. Similarly, immunofluorescent microscopy also demonstrated the apparent presence of α II-tubulin in the mitotic apparatus of asexual parasites. However, this result is open to doubt due to the possible cross-reaction between anti- α II-tubulin antibodies with native epitopes of α I-tubulin under conditions used for immunofluorescence (see Fig. 5.6). Thus, while our results indicate the likely production of small amounts of α II-tubulin in asexual stage parasites, this remains to be definitively proven. Perhaps, the use of parasite preparations free of contaminating gametocytes obtained by use of a Percoll gradient which facilitates the efficient separation of different parasite forms (Delves *et al*, 1990) or use of an additional antibody designed against α II-tubulin (see Fig. 5.6) would allow for more definitive answers.

In view of the inconclusive support for α II-tubulin expression in *P. falciparum* asexual stages, the cellular fate of mRNA transcripts of α II tubulin remains unresolved. Studies from various higher eukaryotes have shown that synthesis of α - and β -tubulin is autoregulated at the translational level (Cleveland *et al*, 1981). Reports suggest that a cellular factor, believed to be unassembled tubulin, interacts with the N-terminal peptide of newly-synthesised tubulin subunits emerging from the ribosome, resulting in a destabilisation of polysome-bound tubulin mRNA and a corresponding inhibition of tubulin synthesis. Perhaps a similar mechanism exists in asexual stages of *P. falciparum*, whereby low intracellular levels of

A.

α I MREVISIHVQAGIQVGNACWELFCLEHGIQPDGQMPSDKASRANDDAFNTFFSETGAG
 α II MREVISIHVQAGIQIGIACWELFCLEHGIQPDGQMPSDQVVAGGDDAFNTFFSETGAG

 α I KHVPRCVFVDLEPTVVDEVRTGTYRQLFHPEQLISGKEDAANNFARGHYTIGKEVIDVC
 α II KHVPRCVFVDLEPTVVDEVRTGTYRQLFHPEQLISGKEDAANNFARGHYTIGKEIVDVC

 α I LDRIRKLADNCTGLQGFLMFSAVGGGTGSGFGCLMLERLSVDYGKKSCLNFCCWSPSQV
 α II LDRVRKLADNCTGLQGFLMFNAVGGGTGSLGCLLLERLAIDYGKKSCLNFCSWSPSQV

 α I STAVVEPYNSVLSHSLLEHTDVAIMLDNEAIYDICRRNLDIERPTYTNLNRLIAQVIS
 α II STAVVEPYNSVLSHSLLEHTDVAIMLDNEAIYDICKKNLDIERPTYTNLNRLIAQVIS

 α I SLTASLRFDGALNVDVTEFQTNLVPYPRIHFMLSSYAPVVSAAEKAYHEQLSVSEITNSA
 α II SLTASLRFDGALNVDVTEFQTNLVPYPRIHFMLSSYAPIISAAEKAYHEQLSVSEITNSA

 α I FEPANMMAKCDPRHGKYMCCCLMYRGDVVVKDVNAAVATIKTKRTIQFVDWCPTGFKCG
 α II FEPASMMAKCDPRHGKYMCCCLMYRGDVVVKDVNAAVATIKTKRSIQFVDWCPTGFKCG

 α I INYQPPTVVPGGDLAKVMRAVCMISNSTAIAEVFSRMDQKFDLMYAKRAVFVHWYVGEGM
 α II INYQPPTVVPGGDLAKVMRAVCMISNSTAIAEVFSRMDQKFDLMYAKRAVFVHWYVGEGM

 α I EEGEFSEAREDLAALEKDYEEVGGIESNEAEGEDEGYEADY
 α II EEGEFSEAREDLAALEKDYEEVGGIESNDGEGEDEGYE

B.

Protist	Reference	Plant	Reference
* <i>Chlamydomonas reinhardtii</i>	Jarvik <i>et al</i> (1980)	Mung bean	Mizuno <i>et al</i> (1985)
<i>Crithidia fasciculata</i>	Russell <i>et al</i> (1984)	<i>Daucus carota</i>	Cyr <i>et al</i> (1987)
<i>Euplotes eurytomus</i>	Delgado <i>et al</i> (1991)	<i>Phaseolus vulgaris</i>	Hussey <i>et al</i> (1985)
* <i>Naegleria gruberi</i>	Shea <i>et al</i> (1987)	*Paul's scarlet rose	Morejohn <i>et al</i> (1982)
<i>Oxytrichia nova</i>	Delgado <i>et al</i> (1991)		
<i>Paramecium tetraurelia</i>	Adoutte <i>et al</i> (1984)		
<i>Physarum polycephalum</i>	Clayton <i>et al</i> (1980)		
<i>Reticulomyxa filosa</i>	Linder <i>et al</i> (1997)		
<i>Tetrahymena thermophila</i>	Suprenant <i>et al</i> (1985)		
<i>Tetrahymena pyriformis</i>	Barahona <i>et al</i> (1988)		
* <i>Toxoplasma gondii</i>	Plessmann <i>et al</i> (2004)		
* <i>Trypanosoma brucei</i>	Schneider <i>et al</i> (1987)		

*Display sensitivity to dinitroaniline herbicides

Figure 5.6. Tubulin diversity in *P. falciparum*, plants and various protist organisms. **A.** Comparison of the predicted amino acid sequences of *P. falciparum* α I-tubulin (α I) and α II-tubulin (α II). Residues highlighted red indicate differences between α -tubulins. Yellow box indicates COOH-terminal sequence of α II-tubulin used in generating a rabbit antiserum containing anti- α II-tubulin antibodies (Guinet *et al*, 1996). Gray box indicates an additional region of significant difference between the two proteins. **B.** List of various protists and plant species, which exhibit an α/β inversion of their tubulin subunits relative to that of vertebrates.

unpolymerised α II-tubulin (as possibly observed in Fig. 5.3 c) destabilise polysome bound α II-RNA transcripts and subsequently prevent their ensuing translation. Alternatively, protein degradation or other post-translational mechanisms may also prevent accumulation of α II-tubulin in asexual parasites. Thus, a number of questions clearly remain unanswered regarding α II-tubulin expression at the mRNA and protein level in asexual stages of *P. falciparum* and merit further investigation.

The amino acid sequences of the tubulins have remained conserved during evolution to quite a remarkable extent. Nevertheless, a number of biochemical differences have been observed in tubulins from plants/protists and vertebrates. The microtubules in some plants and some protists have shown resistance to several microtubule inhibitors such as colchicine which are commonly used to disrupt animal microtubules (Morejohn *et al*, 1991). Similarly, antimitotic herbicides which have no effect on mammalian microtubules display inhibitory activity on the microtubules of plants and protists (Anthony *et al*, 1999a). Numerous other studies have revealed additional diversity between the tubulins of these groups including variations in electrophoretic mobility, immunological differences and differing peptide-mapping patterns (Morejohn *et al*, 1991).

Of particular importance to the work reported in this chapter is the observation that plant/protist and animal tubulins differ in the rate of electrophoretic migration of their α/β -tubulin subunits in denaturing gel systems. Electrophoretic separation of *P. falciparum* native and recombinant tubulins on standard one-dimensional Laemmli SDS gels showed that both parasite α I- and α II-tubulin migrated faster than the β -tubulin subunit. Neither the grade of SDS used or variation in the pH of the separating gel prevented the increased mobility of parasite α -tubulin. In addition, the migration of *P. falciparum* and bovine brain tubulins upon simultaneous electrophoresis on the same gel displayed clear differences. While parasite tubulins were resolved under all conditions, vertebrate tubulin separation was only effected when low-grade SDS was used in gels and electrophoresis buffers.

This α/β inversion of the tubulins was first described in *Physarum polycephalum* and has now been extended to a wide range of protists and plant species (see Figure 5.6). However, the reason for it remains unclear. It has been suggested that the migratory inversion may be due to post-translational modifications (Barahona *et al*, 1988), but this is unlikely as recombinant *P. falciparum* and *Tetrahymena pyriformis* (Nakazawa *et al*, 1999) tubulins, which more than likely

lack such modifications, also display this inversion phenomenon. Similarly, recombinant vertebrate tubulins retain the same apparent migration as their native equivalents (Shah *et al*, 2001). For whatever reason, the variation in electrophoretic mobilities of tubulin subunits of *P. falciparum*/protists and plant species with those of vertebrates coupled with differences in drug-binding and antibody-cross reactivity reflect interesting structural differences between the tubulins.

Chapter 6

Antimalarial Activity and Mechanisms of Action of Dinitroaniline and Phosphorothioamidate Herbicides

6.1. INTRODUCTION

We saw in chapter 3 the high antimalarial potency that can be achieved with the dolastatin/auristatin class of microtubule inhibitors but no agent with marked selectivity for parasite over mammalian cells was identified. The only class of microtubule inhibitors which has shown selective toxicity for malarial parasites to date is the dinitroaniline class of herbicides. Compounds from this class have shown modest antimalarial activity in culture with IC_{50} values between 0.67 - 16 μ M (Dow *et al*, 2002; Fowler *et al*, 1998; Nath *et al*, 1992). However, IC_{50} values for various mammalian cell lines are typically $\geq 50 \mu$ M (Chan *et al*, 1990; Stokkermans *et al*, 1996; Werbovets *et al*, 2003), underlining the potential of antimetabolic herbicides as a source of selective and potent antimalarial agents.

As in a wide range of plant types, the target of these herbicides in certain protozoan parasites also appears to be tubulins (Morejohn *et al*, 1991; Hugdahl *et al*, 1993). The dinitroaniline, trifluralin, has been shown to bind specifically to partially-purified *Leishmania mexicana amazonensis* tubulin (Chan *et al*, 1990) and prevent its *in vitro* polymerisation (Chan, *et al* 1991). In *P. falciparum* gametocytes, trifluralin resulted in fragmentation and complete dissolution of the sub-pellicular microtubule complex (Kaidoh *et al*, 1995). The lack of any discernible effect of trifluralin or oryzalin on microtubules in mammalian cells at concentrations up to 100 μ M (Hugdahl *et al*, 1993; Kaidoh *et al*, 1995) indicates the likely absence of a dinitroaniline-binding site on mammalian tubulin.

Although the antimalarial activity of dinitroanilines has been known for some time, there have been few subsequent reports on the antimalarial mechanism of action of these compounds in the parasite, none using purified *P. falciparum* tubulin, and none at all with other classes of antimetabolic herbicides. In view of this deficit, this chapter describes the antimalarial activity and cellular effects of a number of synthetic derivatives of the dinitroaniline lead compounds trifluralin and chloralin, the structurally unrelated phosphorothioamidate herbicide, amiprofos-methyl, and the *N*-phenyl-carbamate herbicide, chloroprotham (Fig. 6.1). Additionally, in an attempt to comprehend features of tubulin structure that might make *P. falciparum* susceptible to such antimetabolic herbicides we have: (i) identified amino acid residues from a number of sequence alignments that are conserved in *P. falciparum* and dinitroaniline-sensitive plant tubulins but different in dinitroaniline-resistant mammalian tubulins and mapped them onto a homology model of the *P. falciparum*

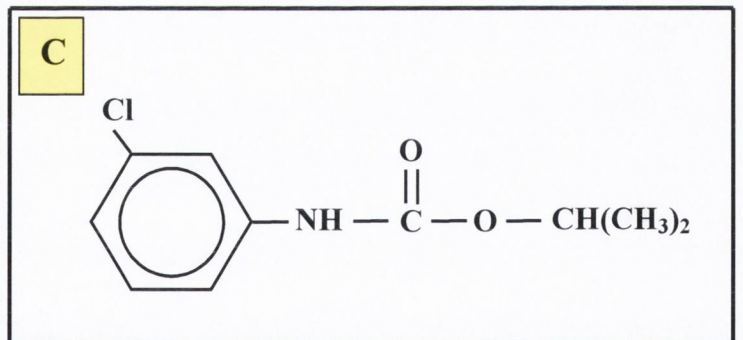
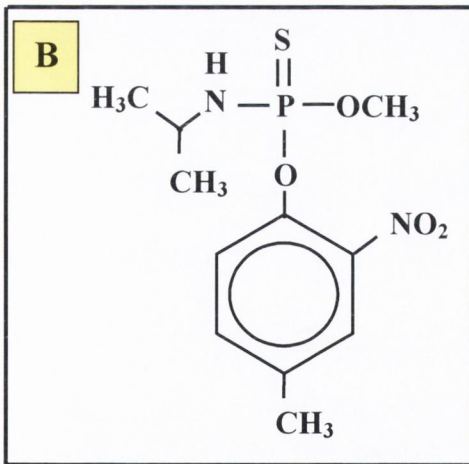
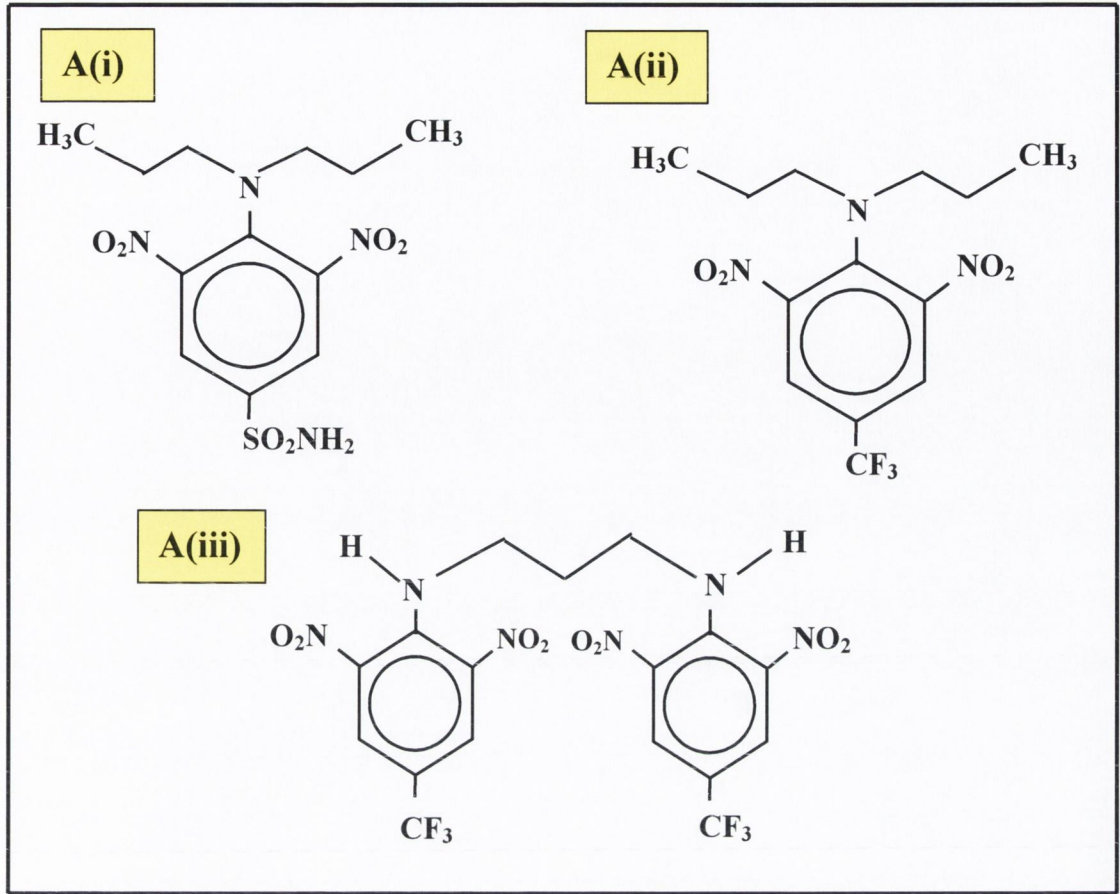


Figure 6.1. Chemical structures of (A) the dinitroaniline herbicides (i) oryzalin, (ii) trifluralin and its synthetic derivative (iii) RBO48; (B) the phosphorothioamidate herbicide amiprofos-methyl; and (C) the *N*-phenyl carbamate herbicide chloropropham.

tubulin dimer, in an attempt to identify a dinitroaniline binding site; and (ii) investigated the molecular interaction of recombinant *P. falciparum* tubulin fusion proteins with a radiolabelled form of trifluralin.

6.2. RESULTS

6.2.1. Growth inhibition of cultured *P. falciparum* by antimetabolic herbicides

6.2.1.1. Dinitroanilines

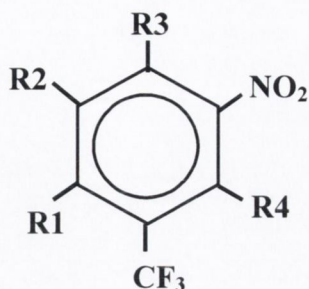
Previously published IC₅₀ values for the dinitroaniline compound chloralin against *Leishmania* promastigotes in culture have suggested it to be 100 times more active than trifluralin (Callahan *et al.*, 1996). This observation also raises the possibility of developing modified derivatives of dinitroanilines that display more potent protozoal activity. For these reasons, chloralin and a number of synthetic derivatives obtained from Dr FMD Ismail (see Table 6.1) were evaluated for their ability to inhibit chloroquine-sensitive and -resistant strains of *P. falciparum* grown asynchronously in culture, as measured by the pLDH method outlined in section 2.3.1. Chloralin was seen to display modest antimalarial activity against both strains (IC₅₀ 5 - 6.5 µM) and was less effective than trifluralin (IC₅₀ 2.9 - 3.3 µM) (see Table 6.1). The derivative RAK2 had similar activity to chloralin, while activity was eliminated by the removal of the nitro group of chloralin (RAK3) and was not restored by the extra Cl group in RAK4 (see Table 6.1(a)). The presence of the nitro groups, which have been suggested to display strong electron-withdrawing ability (Callahan *et al.*, 1996), appears fundamental to the antimalarial activity of chloralin and its analogs tested here. The compounds oryzalin (Fig. 6.1) (IC₅₀ 6.2 µM) and RBO48 which consists of two trifluralin-like moieties linked together, displayed no advantage in terms of potency over that of trifluralin (see Table 6.1). All inhibitors that had antimalarial activity displayed typical sigmoidal dose-response curves after 48 h incubation (data not shown) in contrast to the biphasic dose-response curves observed with other classes of microtubule inhibitors such as the dolastatin 10/auristatin series (see section 3.2.1).

6.2.1.2. Phosphorothioamidate and *N*-phenyl carbamate herbicides

To broaden the spectrum of antimetabolic herbicides tested against cultured *P.*

Table 6.1. Inhibitory effects on growth of *P. falciparum* by dinitroaniline herbicides and derivatives.

(a)



Compound	Substituent groups				72h IC ₅₀ <i>P. falciparum</i> (μM)	
	R1	R2	R3	R4	FCH5.C2	K1/Thailand
Chloralin	-	NO ₂	Cl	-	5.9	6.4
RAK2	-	NO ₂	-	Cl	7.8	5.5
RAK3	-	-	Cl	-	>64 [‡]	>64 [‡]
RAK4	Cl	-	Cl	-	>64 [‡]	>64 [‡]

(b)

Compound	72 h IC ₅₀ <i>P. falciparum</i> (μM)	
	FCH5.C2	K1/Thailand
Trifluralin [*]	2.7 [‡]	3.2 [†]
RBO48 [*]	4.9	3.8 [*]

* See Fig 6.1 for chemical structures

(a) Chloralin and a number of synthetic derivatives.

(b) Trifluralin and the synthetic derivative RBO48.

* different from chloralin at p<0.05, Student's t-test.

† different from chloralin at p<0.01, Student's t-test.

‡ different from chloralin at p<0.001, Student's t-test.

falciparum, amiprofos-methyl (APM) (see Fig. 6.1), a phosphorothioamidate herbicide, which disrupts microtubule assembly and cell division in plants but not mammals (Bajer *et al*, 1986; Morejohn *et al*, 1984; Murthy *et al*, 1994) was examined for antimalarial activity. APM was found to display modest antimalarial activity with a 72 h IC₅₀ value of ~ 3.5 µM. This level of inhibition is equivalent to that displayed by compounds from the dinitroaniline class. It has been suggested that these two chemically distinct classes of anti-mitotic herbicide bind to the same receptor site(s) in plant cells (Ellis *et al*, 1994) and this may also hold true for *P. falciparum*. APM displayed only a very slight plateau of partial inhibition in the 48-h dose response curve (Fig. 6.2).

Chloroprotham, which belongs to the third chemical class of antimitotic herbicides, the *N*-phenyl carbamates, was also tested for its effects on *P. falciparum* growth. At concentrations as high as 128 µM, no inhibition was observed (data not shown). The absence of any nitro groups on chloroprotham (see Fig. 6.1), which are common to the chemical structures of dinitroaniline and phosphorothioamidate herbicides, may be the basis for the lack of antimalarial activity of this compound. The fact that chloroprotham can inhibit some plant but not animal tubulin polymerisation *in vitro* (Morejohn *et al*, 1991) yet lacks antimalarial activity suggests that plant tubulin may possess a unique binding site for this compound.

6.2.2. Effects of herbicides on mitotic microtubular structures

As the primary target of dinitroanilines and phosphorothioamidates in plant cells has been shown to be tubulin (Morejohn *et al*, 1991; Murthy *et al*, 1994), effects of both classes of herbicide on *P. falciparum* tubulin-containing structures were explored by immunofluorescent microscopy as outlined in section 2.4.5. Asynchronous cultures in the absence of microtubule inhibitor displayed mitotic and post-mitotic microtubular structures (Fig. 6.3 (a)) similar to those observed in section 3.2.5. Cultures in the presence of trifluralin, chloralin and oryzalin revealed a breakdown of normal hemispindles and microtubule-organising centres and their replacement by discrete particles or speckles of tubulin labelling throughout the entire area of the parasite cell with the exception of the haemozoin granules (Fig. 6.3 (b - d)). This effect is dissimilar to the polymerisation-promoting effects of Taxol (see Fig. 3.6 (e)) and may reflect gross depolymerisation of parasite microtubules, but in a manner different to that of the “*Vinca*” domain agents vinblastine and

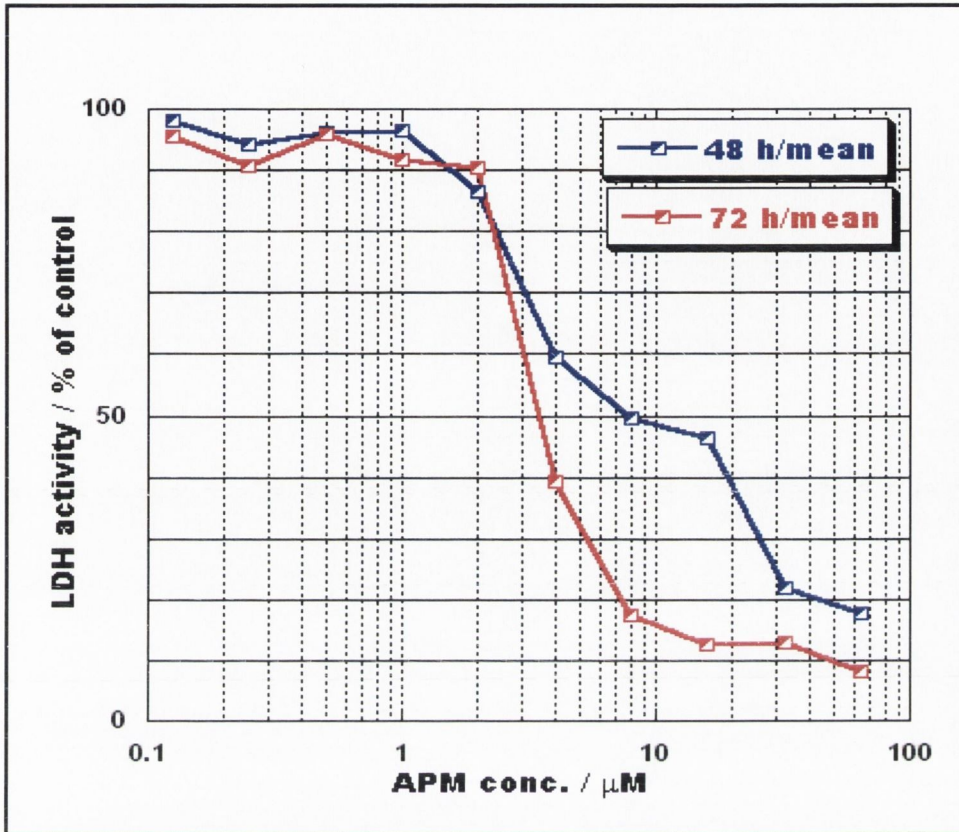


Figure 6.2. Inhibition of the growth of *P. falciparum* in culture by the phosphorothioamidate herbicide amiprofos-methyl. Graph represents parasite growth at 48 and 72 h following exposure to inhibitor. Data points represent the mean values recorded for three experimental determinations.

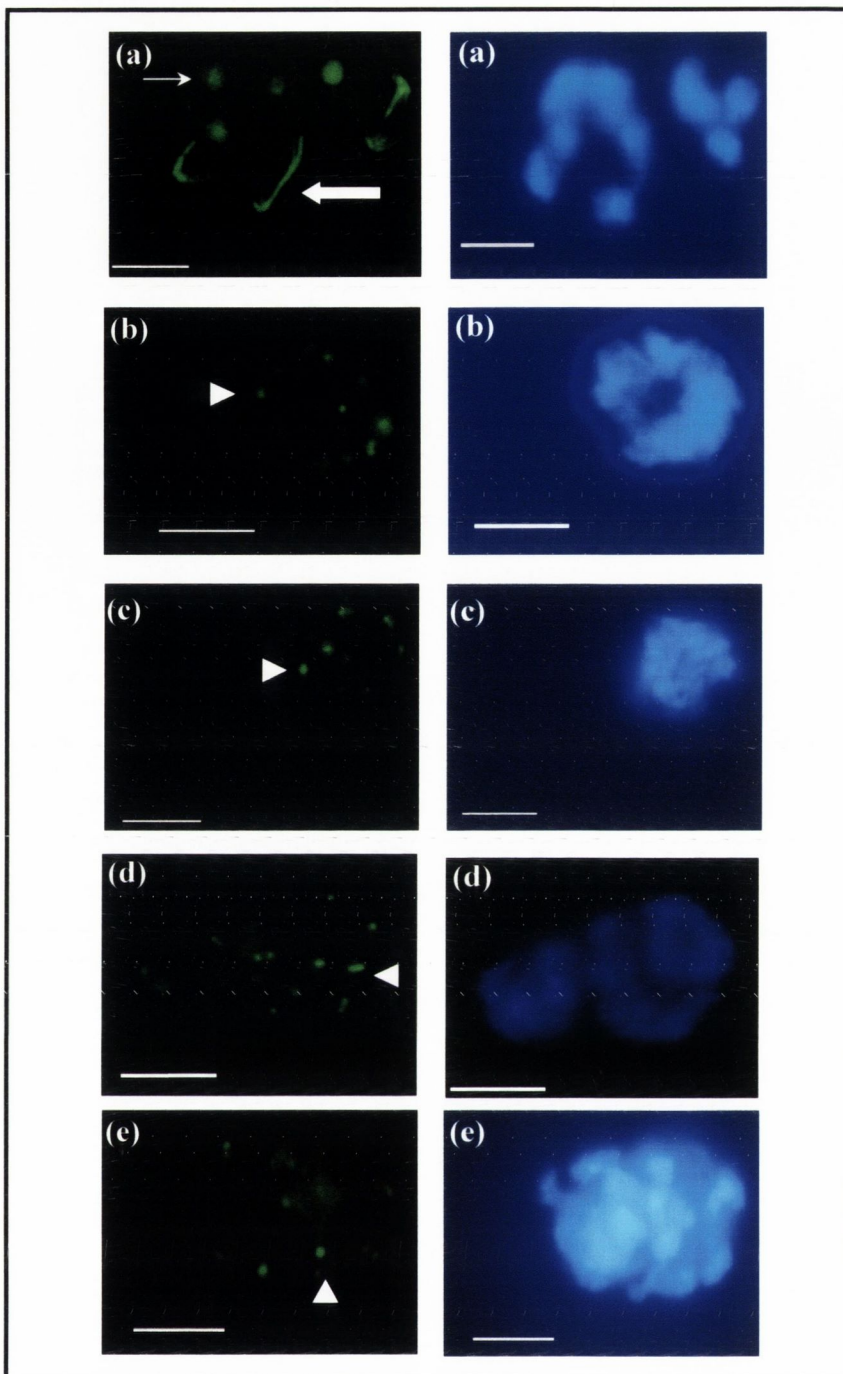


Figure 6.3. Mitotic microtubular structures of cultured parasites viewed by immunofluorescence using antibodies to *P. falciparum* β -tubulin (left) and DAPI nuclear stain (right). (a) Untreated parasites: note microtubule-organising centres (small arrow) and hemispindles (large arrow); (b) treated with 20 μ M trifluralin: note dots of tubulin fluorescence (arrowheads) and loss of normal structures; (c) treated with 20 μ M chloralalin; (d) treated with 20 μ M oryzalin; (e) treated with 20 μ M amiprophos-methyl. In all cases, exposure to inhibitor was for 6 h. Scale bars are 4 μ m.

dolastatin 10 (see Fig. 3.6 (b - d)). The reason for this uncertain, but indicates a different mechanism of microtubule disruption to that of known inhibitors. An equivalent effect was also observed with amiprofos-methyl (Fig. 6.3 (e)). In addition, nuclear material of control parasites often appeared segmented and well-defined (Fig. 6.3 (a)) in contrast to herbicide-treated parasites in which the nuclear material usually appeared as a single mass brightly stained with DAPI (Fig. 6.3 (b - e)), suggesting a block on nuclear division in the parasite.

The action of these antimitotic herbicides was determined more quantitatively by a similar method outlined in section 3.2.5 and the results clearly indicated that both classes of antimitotic herbicide clearly caused a complete loss of typical mitotic microtubular structures (Table 6.2). The results suggest that microtubule inhibitors from different chemical classes can have an extensive array of effects on *P. falciparum* tubulin-containing structures.

6.2.3. Investigation of the interaction of [¹⁴C] trifluralin with recombinant *P. falciparum* tubulin fusion proteins

In view of the disassembly-like effects of trifluralin on microtubules of asexual (see Fig. 6.3) and sexual-stage parasites (Kaidoh *et al*, 1995), we investigated the molecular interaction of recombinant *P. falciparum* tubulin fusion proteins with a radiolabelled form of trifluralin. Binding was measured by the gel-filtration method outlined in section 2.10.1. For the control experiment ([¹⁴C]trifluralin alone) a peak of radioactivity was observed in fraction 6 (669.48 ± 75.17 dpm) with little or no radioactivity detected in fractions 1 - 4 (see Fig. 6.4 a). However, in binding studies with recombinant *P. falciparum* αI- and β-tubulin fusion proteins (either alone or mixed together) a peak of radioactivity was observed not only in fraction 6 (unbound trifluralin) but also in fraction 2, which contained the eluted recombinant tubulins (see Fig. 6.4 b - d). The [¹⁴C]trifluralin bound to MBP-αI (1437.00 ± 136.07 dpm for 195.87 ± 3.54 μg protein), MBP-β (1580.03 ± 242.40 dpm for 199.63 ± 4.91 μg protein) and the MBP-αI/MBP-β mixture (1462.43 ± 122.11 dpm for 202.67 ± 4.68 μg protein) consistently in three separate experiments for each assay. It was also noted that the peak of unbound [¹⁴C]trifluralin in fraction 6 in binding studies contained a higher count of radioactivity (dpm) than in the control experiments ([¹⁴C]trifluralin alone). A related phenomenon was observed by

Table 6.2. Quantitative analysis of effects of inhibitors on mitotic microtubular structures^a

Agent (conc.)	MTOCs ^b	Hemispindles	MTOCs + Hemispindles	Total normal	Diffusely stained ^c	Fragmented ^d	Dot/ Rods ^e	Particle ^f	Other abnormal	Total abnormal
None	25	8	17	50	0	0	0	0	0	0
Vinblastine (20 µM)	1	0	0	1	6	42	0	0	1	49
Taxol (1 µM)	1	0	0	1	0	2	45	0	2	49
Trifluralin (20 µM)	0	0	0	0	2	0	0	47	1	50
Chloralrin (20 µM)	0	0	0	0	1	0	0	48	1	50
Oryzalin (20 µM)	0	2	0	2	2	0	0	46	0	48
Amiprophos-methyl (20 µM)	0	0	0	0	0	0	0	49	1	50

^aCultures were synchronised to the trophozoite stage (27-33 h post-invasion) and exposed to inhibitors or solvent alone in 24-well microplates for 6 h, after which most control parasites had entered schizogony (data not shown). For each treatment, 50 parasites were examined by immunofluorescence microscopy as described in section 2.4.7, and the numbers containing normal and various abnormal structures are indicated.

^bMTOC, microtubule organising centre/centriolar plaque.

^cFluorescence evenly distributed throughout cytosol.

^dFluorescence in a fragmented pattern throughout the cytosol.

^eFluorescence arranged in rod-like structures much thicker than normal hemispindles.

^fFluorescence arranged in dot-like particles, smaller than normal MTOCs.

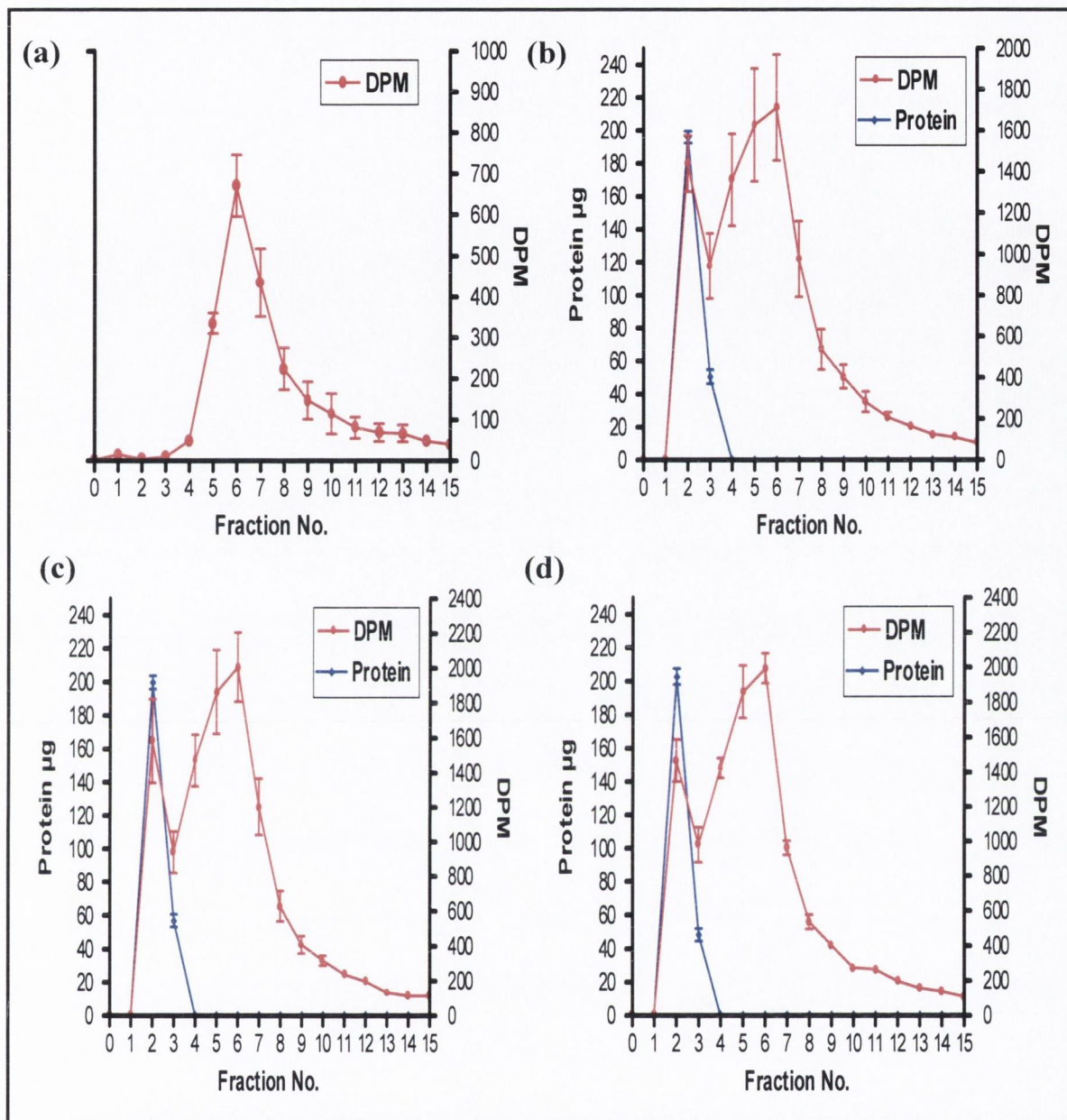


Figure 6.4. Assay of $[^{14}\text{C}]$ trifluralin binding to recombinant *P. falciparum* tubulin fusion proteins. (a) $[^{14}\text{C}]$ trifluralin (5.8 μM) alone or in the presence of 8.7 μM recombinant (b) MBP- α I-tubulin fusion, (c) MBP- β -tubulin fusion or (d) MBP- α I-/ β -tubulin fusion mixture, were incubated at 37°C for 1 h. The mixtures were cooled to 4°C and separated by gel filtration. Collected fractions were divided and assayed for protein (left ordinate) and radioactivity (right ordinate). Data points represent the mean values recorded for three experimental determinations for each assay, and vertical error bars represent the SEMs. No error bars are shown where they would not extend past the point.

Hess *et al* (1977) and may reflect a differing chromatographic effect of [¹⁴C]trifluralin with the gel substrate in control and binding experiments.

To confirm the specificity of trifluralin binding to *P. falciparum* recombinant tubulin fusion proteins, the interactions of [¹⁴C] trifluralin with MBP alone and bovine brain tubulin were studied. Comparing Figs. 6.4 (a) and 6.5 (a) a similar elution profile of [¹⁴C]trifluralin in samples incubated with and without MBP was observed. A small amount of radioactivity was detected in fraction 2 (41.15 ± 5.98 dpm) for 95.63 ± 4.14 μ g of MBP (Fig. 6.5). This radioactive count was $\sim 35 - 38$ fold less than that observed for the recombinant tubulin fusions, indicating that the binding demonstrated in Fig. 6.4 was specific for the tubulin parts of the fusion proteins. Furthermore, the peak representing unbound trifluralin in fraction 6 of the MBP-binding assay had a similar radioactive count (594.40 ± 46.34 dpm) to that of the control (669.48 ± 75.17 dpm). For binding studies with bovine brain tubulin a reduced amount of radioactivity (261.57 ± 4.21 dpm) was found to co-elute with the protein (211.2 ± 9.90 μ g) compared with the counts obtained with *P. falciparum* recombinant tubulin fusion proteins mentioned earlier. This level of binding was 6 - 6.5 fold less than that observed for the recombinant tubulin fusion proteins, indicating a higher affinity of [¹⁴C]trifluralin for recombinant *P. falciparum* tubulins than bovine brain tubulin under the assay conditions.

6.2.4. Investigation of the dinitroaniline binding site(s) on *P. falciparum* tubulins

6.2.4.1. Sequence alignments

The cellular (section 6.2.2) and molecular (section 6.2.3) data described here suggests that tubulins are the targets for dinitroanilines in asexual *P. falciparum*. However, the binding site(s) on *P. falciparum* tubulin for dinitroanilines has not yet been identified. In response to this, a tubulin sequence alignment and homology model approach was developed in an effort to understand features of tubulin structure that may make *P. falciparum* and a number of plants, but not mammals, susceptible to anti-mitotic herbicides.

The first stage of this approach involved aligning a number of dinitroaniline-sensitive plant and dinitroaniline-resistant animal tubulins independently (as outlined in section 2.10.1) to identify representative α - and β -tubulin sequences for each

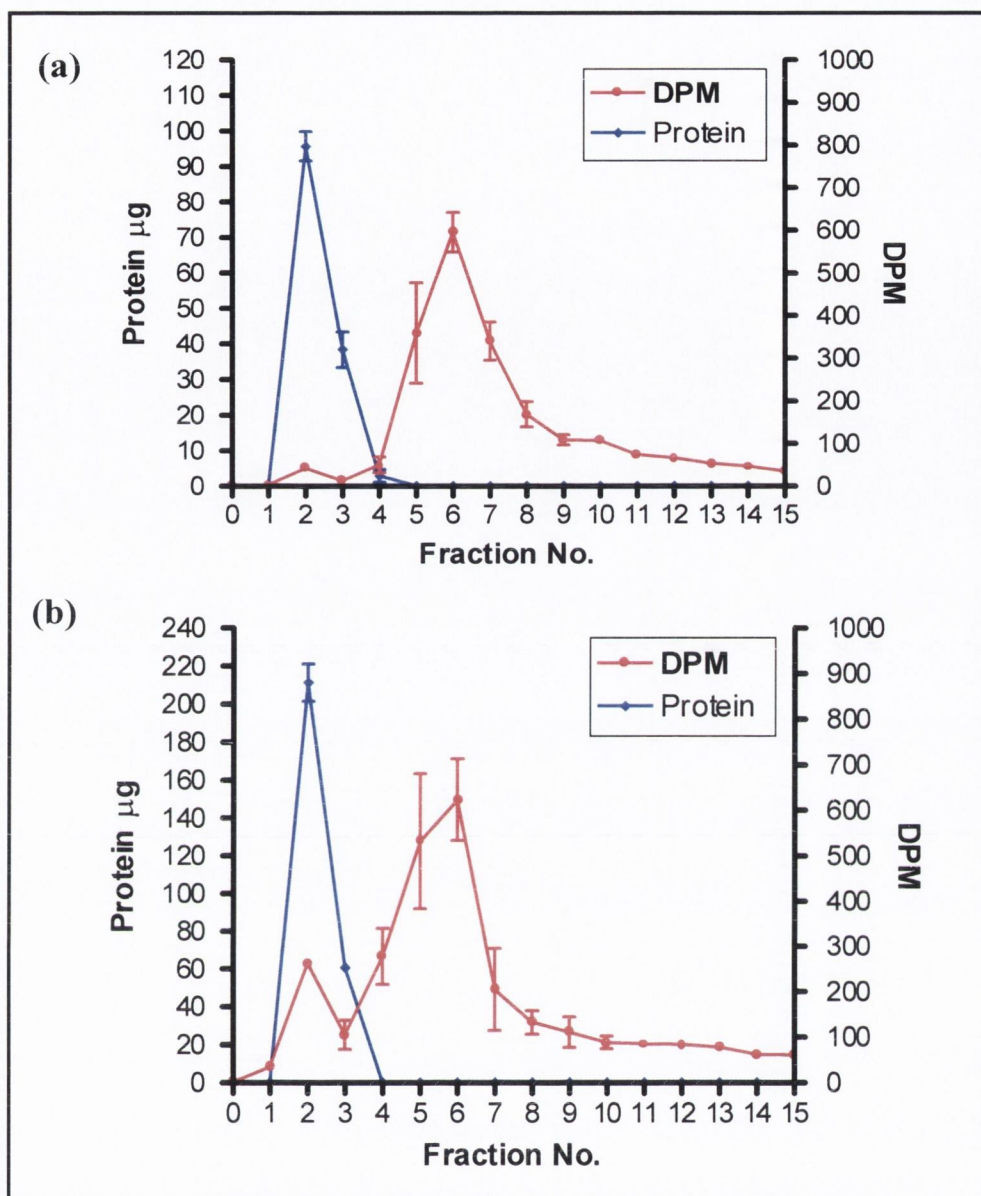


Figure 6.5. Assay of [^{14}C]trifluralin binding to maltose binding protein (MBP) and bovine brain tubulin. [^{14}C]trifluralin ($5.8\ \mu\text{M}$) in the presence of $8.7\ \mu\text{M}$ of either (a) MBP, or (b) bovine brain tubulin was incubated at 37°C for 1 h. The mixture was cooled to 4°C and separated by gel filtration. Collected fractions were divided and assayed for protein (left ordinate) and radioactivity (right ordinate). Data points represent the mean values recorded for three experimental determinations for (a) and two for (b), and vertical error bars represent the SEMs. No error bars are shown where they would not extend past the point.

Zm1	MRECI SIHIGQAGIQVGNACWELYCLEHGIQADGQMPGDKTI GGGDDAFNTFFSETGAGKHVPRAVFDLEPTVIDEVRT	80
Zm2	MRECI SIHIGQAGIQVGNACWELYCLEHGIQADGQMPGDKTI GGGDDAFNTFFSETGAGKHVPRAVFDLEPTVIDEVRT	80
Ei1*	MRECI SIHIGQAGIQVGNACWELYCLEHGIQADGQMPGDKTI GGGDDAFNTFFSETGAGKHVPRAVFDLEPTVIDEVRT	80
Ps1	MRECI SIHIGQAGIQVGNACWELYCLEHGIQPDGQMPGDKTVGGDDAFNTFFSETGAGKHVPRAVFDLEPTVIDEVRT	80
At6	MRECI SIHIGQAGIQVGNACWELYCLEHGIQPDGQMPGDKTVGGDDAFNTFFSETGAGKHVPRAVFDLEPTVIDEVRT	80
Pd1	MRECI SIHIGQAGIQVGNACWELYCLEHGIQPDGQMPGDKTVGGDDAFNTFFSETGAGKHVPRAVFDLEPTVIDEVRT	80
At2	MRECI SIHIGQAGIQVGNACWELYCLEHGIQPDGQMP SDKTVGGDDAFNTFFSETGAGKHVPRAVFDLEPTVIDEVRT	80
At4	MRECI SIHIGQAGIQVGNACWELYCLEHGIQPDGQMP SDKTVGGDDAFNTFFSETGAGKHVPRAVFDLEPTVIDEVRT	80
Ei3	MREI I SIHIGQAGIQVGNACWELYCLEHGI E PDGTPM S D T S V G V A H D A F N T F F S E T G S G K H V P R A I F V D L E P T V I D E V R T	80
At1	MREI I SIHIGQAGIQVGN S C W E L Y C L E H G I Q P D G M P S D T T V G V A H D A F N T F F S E T G A G K H V P R A V F D L E P T V I D E V R T	80
Zm1	GTYRQLFHPEQLISGKEDAANNFARGHYTIGKEIVDLCLDRIRKLADNCTGLQGFLVFNNAVGGGTGSLGSLLLERLSVD	160
Zm2	GTYRQLFHPEQLISGKEDAANNFARGHYTIGKEIVDLCLDRIRKLADNCTGLQGFLVFNNAVGGGTGSLGSLLLERLSVD	160
Ei1	GTYRQLFHPEQLISGKEDAANNFARGHYTIGKEIVDLCLDRIRKLADNCTGLQGFLVFNNAVGGGTGSLGSLLLERLSVD	160
Ps1	G A Y R Q L F H P E Q L I S G K E D A A N N F A R G H Y T I G K E I V D L C L D R I R K L A D N C T G L Q G F L V F N A V G G G T G S L G S L L L E R L S V D	160
At6	GTYRQLFHPEQLISGKEDAANNFARGHYTIGKEIVDLCLDRIRKLADNCTGLQGFLVFNNAVGGGTGSLGSLLLERLSVD	160
Pd1	GTYRQLFHPEQLISGKEDAANNFARGHYTIGKEIVDLCLDRIRKLADNCTGLQGFLVFNNAVGGGTGSLGSLLLERLSVD	160
At2	GTYRQLFHPEQLISGKEDAANNFARGHYTIGKEIVDLCLDRIRKLADNCTGLQGFLVFNNAVGGGTGSLGSLLLERLSVD	160
At4	GTYRQLFHPEQLISGKEDAANNFARGHYTIGKEIVDLCLDRIRKLADNCTGLQGFLVFNNAVGGGTGSLGSLLLERLSVD	160
Ei3	G S Y R Q L F H P E Q L I S G K E D A A N N F A R G H Y T V G K E I V D L C L D R V R K L A D N C T G L Q G F L V F N A V G G G T G S L G S L L L E R L S V D	160
At1	GTYRQLFHPEQLISGKEDAANNFARGHYT V G K E I V D L C L D R V R K L A D N C T G L Q G F L V F N A V G G G T G S L G S L L L E R L S V D	160
Zm1	YGKSKLGFVYVSPQVSTSVVEPYNSVLSVTHSLEHTDVAILLDNEAIYDICRRSLDIERPTYTNLNRVLSQVSISSLTA	240
Zm2	YGKSKLGFVYVSPQVSTSVVEPYNSVLSVTHSLEHTDVAILLDNEAIYDICRRSLDIERPTYTNLNRVLSQVSISSLTA	240
Ei1	YGKSKLGFVYVSPQVSTSVVEPYNSVLSVTHSLEHTDVAILLDNEAIYDICRRSLDIERPTYTNLNRVLSQVSISSLTA	240
Ps1	YGKSKLGFVYVSPQVSTSVVEPYNSVLSVTHSLEHTDVAILLDNEAIYDICRRSLDIERPTYTNLNRVLSQVSISSLTA	240
At6	YGKSKLGFVYVSPQVSTSVVEPYNSVLSVTHSLEHTD V S I L L D N E A I Y D I C R R S L D I E R P T Y T N L N R V L S Q V S I S S L T A	240
Pd1	YGKSKLGFVYVSPQVSTSVVEPYNSVLSVTHSLEHTDVAILLDNEAIYDICRRSLDIERPTYTNLNRVLSQVSISSLTA	240
At2	YGKSKLGFVYVSPQVSTSVVEPYNSVLSVTHSLEHTD V S I L L D N E A I Y D I C R R S L D I E R P T Y T N L N R V L S Q V S I S S L T A	240
At4	YGKSKLGFVYVSPQVSTSVVEPYNSVLSVTHSLEHTD V S I L L D N E A I Y D I C R R S L S I E R P T Y T N L N R V L S Q V S I S S L T A	240
Ei3	Y G K K S K L G F T I Y P S P Q V S T A V V E P Y N S V L S V T H S L L E H T D V A V L L D N E A I Y D I C R R S L D I E R P T Y T N L N R L I S Q I I S S L T T	240
At1	Y G K K S K L G F T I Y P S P Q V S T A V V E P Y N S V L S V T H S L L E H T D V A V L L D N E A I Y D I C R R S L D I E R P T Y T N L N R L I S Q I I S S L T T	240
Zm1	SLRFDGALNVDVNEFQTNLVYPRIHFMLSSYAPVISA EKAYHEQLSVAEITNSAFEPSSMMAKCDPRHGKYMACCLMYR	320
Zm2	SLRFDGALNVDVNEFQTNLVYPRIHFMLSSYAPVISA EKAYHEQLSVAEITNSAFEPSSMMAKCDPRHGKYMACCLMYR	320
Ei1	SLRFDGALNVDVNEFQTNLVYPRIHFMLSSYAPVISA EKAYHEQLSVAEITNSAFEPSSMMAKCDPRHGKYMACCLMYR	320
Ps1	SLRFDGALNVDVTEFQTNLVYPRIHFMLSSYAPVISA EKAYHEQLSVAEITNSAFEPSSMMAKCDPRHGKYMACCLMYR	320
At6	SLRFDGALNVDVTEFQTNLVYPRIHFMLSSYAPVISA EKAFHEQLSVAEITNSAFEPSSMMAKCDPRHGKYMACCLMYR	320
Pd1	SLRFDGALNVDVTEFQTNLVYPRIHFMLSSYAPVISA EKAYHEQLSVAEITNSAFEPSSMMAKCDPRHGKYMACCLMYR	320
At2	SLRFDGALNVDVTEFQTNLVYPRIHFMLSSYAPVISA EKAFHEQLSVAEITNSAFEPSSMMAKCDPRHGKYMACCLMYR	320
At4	SLRFDGALNVDVTEFQTNLVYPRIHFMLSSYAPVISA EKAFHEQLSVAEITNSAFEPSSMMAKCDPRHGKYMACCLMYR	320
Ei3	SLRFDGA I NVDVTEFQTNLVYPRIHFMLSSYAPVISA EKAYHEQLS V P E I T N A V F E P S S M M A K C D P R H G K Y M A C C L M Y R	320
At1	SLRFDGA I NVD I T E F Q T N L V P Y P R I H F M L S S Y A P V I S A A K A Y H E Q L S V P E I T N A V F E P A S M M A K C D P R H G K Y M A C C L M Y R	320
Zm1	GDVVPKDVNAAVATIKTKRTIQFVDWCPTGFKCGINYQPPSVVPGDDLAKVQRAVCMISNSTSVVEVFSRIDHKFDLMYA	400
Zm2	GDVVPKDVNAAVATIKTKRTIQFVDWCPTGFKCGINYQPPSVVPGDDLAKVQRAVCMISNSTSVVEVFSRIDHKFDLMYA	400
Ei1	GDVVPKDVNAAVATIKTKRTIQFVDWCPTGFKCGINYQPPSVVPGDDLAKVQRAVCMISNSTSVVEVFSRIDHKFDLMYA	400
Ps1	GDVVPKDVNAAVATIKTKRTIQFVDWCPTGFKCGINYQPPPTVVPGGDLAKVQRAVCMISNSTSVAEVFSRIDHKFDLMYA	400
At6	GDVVPKDVNAAVGTIKTKRTIQFVDWCPTGFKCGINYQPPPTVVPGGDLAKVQRAVCMISNSTSVAEVFSRIDHKFDLMYA	400
Pd1	GDVVPKDVNAAVATIKTKRTIQFVDWCPTGFKCGINYQPPPTVVPGGDLAKVQRAVCMISNSTSVAEVFSRIDHKFDLMYA	400
At2	GDVVPKDVNAAVGTIKTKRTIQFVDWCPTGFKCGINYQPPPTVVPGGDLAKVQRAVCMISNSTSVAEVFSRIDHKFDLMYA	400
At4	GDVVPKDVNAAVGTIKTKRTIQFVDWCPTGFKCGINYQPPPTVVPGGDLAKVQRAVCMISNSTSVAEVFSRIDHKFDLMYA	400
Ei3	GDVVPKDVNAAVATIKTKRT V Q F V D W C P T G F K C G I N Y Q P P S V V P G G D L A K V Q R A V C M I S N N T A V A E V F S R I D H K F D L M Y A	400
At1	GDVVPKDVNAAVGTIKTKRT V Q F V D W C P T G F K C G I N Y Q P P T V V P G G D L A K V Q R A V C M I S N N T A V A E V F S R I D H K F D L M Y A	400
Zm1	KRAFVHWYVGEGMEEGEFSEAREDLAALEKDYEEVGAEFDEGEDG-EGDEY	451
Zm2	KRAFVHWYVGEGMEEGEFSEAREDLAALEKDYEEVGAEFDEEGEDG-DGDEY	451
Ei1	KRAFVHWYVGEGMEEGEFSEAREDLAALEKDYEEVGAEFDEEGEDG-EGDEY	451
Ps1	KRAFVHWYVGEGMEEGEFSEAREDLAALEKDYEEVGAEFSGDGGDDGLGEEY	452
At6	KRAFVHWYVGEGMEEGEFSEAREDLAALEKDYEEVGAE--GGDEDEGEY	452
Pd1	KRAFVHWYVGEGMEEGEFSEAREDLAALEKDYEEVGAE S A E G E D D -- E G D D Y	450
At2	KRAFVHWYVGEGMEEGEFSEAREDLAALEKDYEEVGAE--GGDEDEGEY	450
At4	KRAFVHWYVGEGMEEGEFSEAREDLAALEKDYEEVGAE--GGDEDEGEY	450
Ei3	KRAFVHWYVGEGMEEGEFSEAREDLAALEKDYEEVGAE--GGDEDEGEDEY	450
At1	KRAFVHWYVGEGMEEGEFSEAREDLAALEKDYEEVGAE--GGDEDEGEDEY	450

Amino acid colour:

Conserved

Semi-conserved

Non-conserved

Figure 6.6. Comparison of the amino acid sequences of the α -tubulins of dinitroaniline-sensitive plants. Shown are the sequences for *Zea mays* (Zm), *Eleusine indica* (Ei), *Pisum sativum* (Ps), *Prunus dulcis* (Pd) and *Arabidopsis thaliana* (At) (number following name corresponds to α -tubulin isotype); accession numbers are as in Table 2.3. Colouring indicates amino acid differences in the plant types relative to the most common residue at each position. **E. indica* 1 was the chosen representative α -tubulin sequence.

At2*	MREILHIQGGQCGNQIGAKFWEVVC	A	E	H	G	I	D	P	T	G	R	T	G	S	D	L	Q	L	E	R	I	N	V	Y	N	E	A	S	C	G	R	F	V	P	R	A	V	L	M	D	L	E	P	G	T	M	S	L	R	S	G	P	80													
Zm1	MREILHIQGGQCGNQIGAKFWEVVC	A	E	H	G	I	D	A	T	G	R	Y	G	G	S	D	L	Q	L	E	R	V	N	V	Y	N	E	A	S	C	G	R	F	V	P	R	A	V	L	M	D	L	E	P	G	T	M	S	V	R	S	G	P	80												
La1	MREILHIQGGQCGNQIGAKFWEVVC	A	E	H	G	I	D	T	G	R	Y	G	G	D	N	E	L	Q	L	E	R	V	N	V	Y	N	E	A	S	C	G	R	F	V	P	R	A	V	L	M	D	L	E	P	G	T	M	S	I	R	S	G	P	80												
Ps1	MRQILHIQGGQCGNQIGAKFWEVVC	A	E	H	G	I	D	P	T	G	R	T	G	S	D	L	Q	L	E	R	I	D	V	Y	N	E	A	S	G	G	R	V	P	R	A	V	L	M	D	L	E	P	G	T	M	S	I	R	S	G	P	80														
At4	MREILHIQGGQCGNQIGAKFWEVVC	A	E	H	G	I	D	H	T	G	Y	V	G	S	D	L	Q	L	E	R	I	D	V	Y	N	E	A	S	G	G	K	Y	V	P	R	A	V	L	M	D	L	E	P	G	T	M	S	L	R	S	G	P	80													
Os2	MREILHIQGGQCGNQIGAKFWEVVC	A	E	H	G	I	D	H	T	G	K	Y	S	G	S	D	L	Q	L	V	R	I	N	V	Y	N	E	A	S	G	G	R	V	P	R	A	V	L	M	D	L	E	P	G	T	S	D	S	V	R	S	G	P	80												
Zm2	MREILHIQGGQCGNQIGAKFWEVVC	A	E	H	G	I	D	P	T	G	R	Y	M	G	T	S	D	V	Q	L	E	R	V	N	V	Y	N	E	A	S	C	G	R	F	V	P	R	A	V	L	M	D	L	E	P	G	T	M	A	V	R	T	G	P	80											
Os1	MREILHIQGGQCGNQIGAKFWEVVC	A	E	H	G	I	D	P	T	G	R	Y	T	G	N	S	D	L	Q	L	E	R	V	N	V	Y	N	E	A	S	C	G	R	F	V	P	R	A	V	L	M	D	L	E	P	G	T	M	S	V	R	T	G	P	80											
Dc1	MREILHIQGGQCGNQIGAKFWEVVC	A	E	H	G	I	D	P	T	G	Q	V	L	S	E	S	D	L	Q	L	R	I	N	V	Y	N	E	A	S	G	G	R	V	P	R	A	V	L	M	D	L	E	P	G	T	M	S	V	K	T	G	P	80													
Gm1	MREILHVQAGQCGNQIGAKFWEVVC	A	E	H	G	I	D	A	T	G	N	Y	V	G	N	F	H	L	Q	L	E	R	V	N	V	Y	N	E	A	S	G	G	R	V	P	R	A	V	L	M	D	L	E	P	G	T	M	S	L	R	S	G	P	80												
At2	YGQIFRPDNFVFGQSGAGNNWAKGHY	T	E	G	A	E	L	I	D	S	V	L	D	V	V	R	K	E	A	E	N	C	D	C	L	Q	G	F	Q	V	C	H	S	L	G	G	T	G	S	G	M	G	T	L	L	I	S	K	I	R	E	E	Y	P	160											
Zm1	YGQIFRPDNFVFGQSGAGNNWAKGHY	T	E	G	A	E	L	I	D	S	V	L	D	V	V	R	K	E	A	E	N	C	D	C	L	Q	G	F	Q	V	C	H	S	L	G	G	T	G	S	A	M	G	T	L	L	I	S	K	I	R	E	E	Y	P	160											
La1	YGQIFRPDNFVFGQSGAGNNWAKGHY	T	E	G	A	E	L	I	D	S	V	L	D	V	V	R	K	E	A	E	N	C	D	C	L	Q	G	F	Q	V	C	H	S	L	G	G	T	G	S	G	M	G	T	L	L	I	S	K	I	R	E	E	Y	P	160											
Ps1	YGQIFRPDNFVFGQSGAGNNWAKGHY	T	E	G	A	E	L	I	D	S	V	L	D	V	V	R	K	E	A	E	N	C	D	C	L	Q	G	F	Q	V	C	H	S	L	G	G	T	G	S	G	M	G	T	L	L	I	S	K	I	R	E	E	Y	P	160											
At4	FGQIFRPDNFVFGQSGAGNNWAKGHY	T	E	G	A	E	L	I	D	S	V	L	D	V	V	R	K	E	A	E	N	C	D	C	L	Q	G	F	Q	V	C	H	S	L	G	G	T	G	S	L	G	G	T	G	S	G	M	G	T	L	L	I	S	K	I	R	E	E	Y	P	160					
Os2	YGQIFRPDNFVFGQSGAGNNWAKGHY	T	E	G	A	E	L	I	D	S	V	L	D	V	V	R	K	E	A	E	N	C	D	C	L	Q	G	F	Q	V	C	H	S	L	G	G	T	G	S	G	M	G	T	L	L	I	S	K	I	R	E	E	Y	P	160											
Zm2	YGQIFRPDNFVFGQSGAGNNWAKGHY	T	E	G	A	E	L	I	D	S	V	L	D	V	V	R	K	E	A	E	N	C	D	C	L	Q	G	F	Q	V	C	H	S	L	G	G	T	G	S	G	M	G	T	L	L	I	S	K	I	R	E	E	Y	P	160											
Os1	YGQIFRPDNFVFGQSGAGNNWAKGHY	T	E	G	A	E	L	I	D	S	V	L	D	V	V	R	K	E	A	E	N	C	D	C	L	Q	G	F	Q	V	C	H	S	L	G	G	T	G	S	L	G	G	T	G	S	G	M	G	T	L	L	I	S	K	I	R	E	E	Y	P	160					
Dc1	HGQIFRPDNFVFGQSGAGNNWAKGHY	T	E	G	A	E	L	I	D	S	V	L	D	V	V	R	K	E	A	E	N	C	E	C	L	Q	G	F	Q	V	C	H	S	L	G	G	T	G	S	L	G	G	T	G	S	G	M	G	T	L	L	I	S	K	I	R	E	E	Y	P	160					
Gm1	FGKIFRPDNFVFGQSGAGNNWAKGHY	T	E	G	A	E	L	I	D	S	V	L	D	V	V	R	K	E	A	E	N	C	D	C	L	Q	G	F	Q	V	C	H	S	L	G	G	T	G	S	G	M	G	T	L	L	I	S	K	I	R	E	E	Y	P	160											
At2	DRMMLTFSVFPSPKVS	D	T	V	V	E	P	Y	N	A	T	L	S	V	H	Q	L	V	E	N	A	D	E	C	M	V	L	D	N	E	A	L	Y	D	I	C	F	R	T	L	K	L	T	P	S	F	G	D	L	N	H	L	I	S	A	T	M	S	G	V	T	C	C	L	240	
Zm1	DRMMLTFSVFPSPKVS	D	T	V	V	E	P	Y	N	A	T	L	S	V	H	Q	L	V	E	N	A	D	E	C	M	V	L	D	N	E	A	L	Y	D	I	C	F	R	T	L	K	L	T	P	S	F	G	D	L	N	H	L	I	S	A	T	M	S	G	V	T	C	C	L	240	
La1	DRMMLTFSVFPSPKVS	D	T	V	V	E	P	Y	N	A	T	L	S	V	H	Q	L	V	E	N	A	D	E	C	M	V	L	D	N	E	A	L	Y	D	I	C	F	R	T	L	K	L	T	P	S	F	G	D	L	N	H	L	I	S	A	T	M	S	G	V	T	C	C	L	240	
Ps1	DRMMLTFSVFPSPKVS	D	T	V	V	E	P	Y	N	A	T	L	S	V	H	Q	L	V	E	N	A	D	E	C	M	V	L	D	N	E	A	L	Y	D	I	C	F	R	I	L	K	L	S	N	P	S	F	G	D	L	N	H	L	I	S	A	T	M	S	G	V	T	C	C	L	240
At4	DRMMLTFSVFPSPKVS	D	T	V	V	E	P	Y	N	A	T	L	S	V	H	Q	L	V	E	N	A	D	E	C	M	V	L	D	N	E	A	L	Y	D	I	C	F	R	T	L	K	L	A	N	P	T	F	G	D	L	N	H	L	I	S	A	T	M	S	G	V	T	C	C	L	240
Os2	DRMMLTFSVFPSPKVS	D	T	V	V	E	P	Y	N	A	T	L	S	V	H	Q	L	V	E	N	A	D	E	C	M	V	R	D	N	E	A	L	Y	D	M	C	F	R	T	L	K	L	A	T	P	T	F	G	D	L	N	H	L	I	S	A	T	M	S	G	V	T	C	C	L	239
Zm2	DRMMLTFSVFPSPKVS	D	T	V	V	E	P	Y	N	A	T	L	S	V	H	Q	L	V	E	N	A	D	E	C	M	V	L	D	N	E	A	L	Y	D	I	C	F	R	T	L	K	L	T	P	S	F	G	D	L	N	H	L	I	S	A	T	M	S	G	V	T	C	C	L	240	
Os1	DRMMLTFSVFPSPKVS	D	T	V	V	E	P	Y	N	A	T	L	S	V	H	Q	L	V	E	N	A	D	E	C	M	V	R	D	N	E	A	L	Y	D	I	C	F	R	T	L	K	L	T	P	S	F	G	D	L	N	H	L	I	S	A	T	M	S	G	V	T	C	C	L	240	
Dc1	DRMMLTFSVFPSPKVS	D	T	V	V	E	P	Y	N	A	T	L	S	V	H	Q	L	V	E	N	A	D	E	C	M	V	L	D	N	E	A	L	Y	D	I	C	F	R	T	L	K	L	S	T	P	S	F	G	D	L	N	H	L	I	S	A	T	M	S	G	V	T	C	C	L	240
Gm1	DRMMLTFSVFPSPKVS	D	T	V	V	E	P	Y	N	A	T	L	S	V	H	Q	L	V	E	N	A	D	E	C	M	V	L	D	N	E	A	L	Y	D	I	C	F	R	T	L	K	L	T	N	P	S	V	G	D	L	N	H	L	I	S	T	T	M	S	G	V	T	C	C	L	240
At2	RFPGQLNSDLRKLAVNL	I	P	F	P	R	L	H	F	F	M	V	G	F	A	P	L	T	S	R	G	S	Q	Q	Y	R	S	L	T	V	P	E	L	T	Q	Q	M	W	D	A	K	N	M	C	A	A	D	P	R	H	G	R	Y	L	T	A	S	A	M	F	R	G	K	320		
Zm1	RFPGQLNSDLRKLAVNL	I	P	F	P	R	L	H	F	F	M	V	G	F	A	P	L	T	S	R	G	S	Q	Q	Y	R	A	L	T	V	P	E	L	T	Q	Q	M	W	D	A	K	N	M	C	A	A	D	P	R	H	G	R	Y	L												

<i>Ss</i> 1*	MRECI SIHVGGAGVQIGNACWELYCLEHGIQPDGQMP	SDKTIGGGDDSFNTFFSETGAGK	60
<i>Rn</i> 1	MRECI SIHVGGAGVQIGNACWELYCLEHGIQPDGQMP	SDKTIGGGDDSFNTFFSETGAGK	60
<i>Mm</i> 1	MRECI SIHVGGAGVQIGNACWELYCLEHGIQPDGQMP	SDKTIGGGDDSFNTFFSETGAGK	60
<i>Hs</i> 1	MRECI SIHVGGAGVQIGNACWELYCLEHGIQPDGQMP	SDKTIGGGDDSFNTFFSETGAGK	60
<i>Cg</i> 1	MRECI SIHVGGAGVQIGNACWELYCLEHGIQPDGQMP	SDKTIGGGDDSFNTFFSETGAGK	60
<i>Hs</i> 2	MRECI SIHVGGAGVQIGNACWELYCLEHGIQPDGQMP	SDKTIGGGDDSFNTFFSETGAGK	60
<i>Hs</i> 4	MRECI SVHVGGAGVQIGNACWELYCLEHGIQPDGQMP	SDKTIGGGDDSFNTFFSETGAGK	60
<i>Ss</i> 1	HVPRAVFDLEPTVIDEVRTGTYRQLFHPEQLITGKEDA	AANNYARGHYTIGKEIIDLVLD	120
<i>Rn</i> 1	HVPRAVFDLEPTVIDEVRTGTYRQLFHPEQLITGKEDA	AANNYARGHYTIGKEIIDLVLD	120
<i>Mm</i> 1	HVPRAVFDLEPTVIDEVRTGTYRQLFHPEQLITGKEDA	AANNYARGHYTIGKEIIDLVLD	120
<i>Hs</i> 1	HVPRAVFDLEPTVIDEVRTGTYRQLFHPEQLITGKEDA	AANNYARGHYTIGKEIIDLVLD	120
<i>Cg</i> 1	HVPRAVFDLEPTVIDEVRTGTYRQLFHPEQLITGKEDA	AANNYARGHYTIGKEIIDLVLD	120
<i>Hs</i> 2	HVPRAVFDLEPTVIDEVRTGTYRQLFHPEQLITGKEDA	AANNYARGHYTIGKEIIDLVLD	120
<i>Hs</i> 4	HVPRAVFDLEPTVIDEIRNGPYRQLFHPEQLITGKEDA	AANNYARGHYTIGKEIIDPVL	120
<i>Ss</i> 1	RIRKLADQCTGLQGFVFSFGGGTSGGFTSLLMERLSVD	YGKSKLEFSIYPAPQVSTA	180
<i>Rn</i> 1	RIRKLADQCTGLQGFVFSFGGGTSGGFTSLLMERLSVD	YGKSKLEFSIYPAPQVSTA	180
<i>Mm</i> 1	RIRKLADQCTGLQGFVFSFGGGTSGGFTSLLMERLSVD	YGKSKLEFSIYPAPQVSTA	180
<i>Hs</i> 1	RIRKLADQCTGLQGFVFSFGGGTSGGFTSLLMERLSVD	YGKSKLEFSIYPAPQVSTA	180
<i>Cg</i> 1	RIRKLADQCTGLQGFVFSFGGGTSGGFTSLLMERLSVD	YGKSKLEFSIYPAPQVSTA	180
<i>Hs</i> 2	RIRKLADQCTGLQGFVFSFGGGTSGGFA	SLLMERLSVDYGKSKLEFAIYPAPQVSTA	180
<i>Hs</i> 4	RIRKLSQDCTGLQGFVFSFGGGTSGGFTSLLMERLSVD	YGKSKLEFSIYPAPQVSTA	180
<i>Ss</i> 1	VVEPYNSILTTHTTLEHSDCAFMDNEAIYDICRRNLDIER	PTYTNLNRLLIGQIVSSITA	240
<i>Rn</i> 1	VVEPYNSILTTHTTLEHSDCAFMDNEAIYDICRRNLDIER	PTYTNLNRLLIGQIVSSITA	240
<i>Mm</i> 1	VVEPYNSILTTHTTLEHSDCAFMDNEAIYDICRRNLDIER	PTYTNLNRLLISQIVSSITA	240
<i>Hs</i> 1	VVEPYNSILTTHTTLEHSDCAFMDNEAIYDICRRNLDIER	PTYTNLNRLLISQIVSSITA	240
<i>Cg</i> 1	VVEPYNSILTTHTTLEHSDCAFMDNEAIYDICRRNLDIER	PTYTNLNRLLISQIVSSITA	240
<i>Hs</i> 2	VVEPYNSILTTHTTLEHSDCAFMDNEAIYDICRRNLDIER	PTYTNLNRLLIGQIVSSITA	240
<i>Hs</i> 4	VVEPYNSILTTHTTLEHSDCAFMDNEAIYDICRRNLDIER	PTYTNLNRLLISQIVSSITA	240
<i>Ss</i> 1	SLRFDGALNVDLTEFQTNLVPYPRGHFPLATYAPVI	SAEKAYHEQLSVAEITNACFEPAN	300
<i>Rn</i> 1	SLRFDGALNVDLTEFQTNLVPYPRGHFPLATYAPVI	SAEKAYHEQLSVAEITNACFEPAN	300
<i>Mm</i> 1	SLRFDGALNVDLTEFQTNLVPYPRGHFPLATYAPVI	SAEKAYHEQLSVAEITNACFEPAN	300
<i>Hs</i> 1	SLRFDGALNVDLTEFQTNLVPYPRGHFPLATYAPVI	SAEKAYHEQLSVAEITNACFEPAN	300
<i>Cg</i> 1	SLRFDGALNVDLTEFQTNLVPYPRGHFPLATYAPVI	SAEKAYHEQLSVAEITNACFEPAN	300
<i>Hs</i> 2	SLRFDGALNVDLTEFQTNLVPYPRGHFPLATYAPVI	SAEKAYHEQLSVAEITNACFEPAN	300
<i>Hs</i> 4	SLRFDGALNVDLTEFQTNLVPYPRGHFPLATYAPVI	SAEKAYHEQLSVAEITNACFEPAN	300
<i>Ss</i> 1	QMVKCDPRHGKYMACCLLYRGDVVPKDVNAAIATIKTKRT	IQFVDWCPTGFKVGINYEPP	360
<i>Rn</i> 1	QMVKCDPRHGKYMACCLLYRGDVVPKDVNAAIATIKTKRT	IQFVDWCPTGFKVGINYEPP	360
<i>Mm</i> 1	QMVKCDPRHGKYMACCLLYRGDVVPKDVNAAIATIKTKRT	IQFVDWCPTGFKVGINYEPP	360
<i>Hs</i> 1	QMVKCDPRHGKYMACCLLYRGDVVPKDVNAAIATIKTKRS	IQFVDWCPTGFKVGINYEPP	360
<i>Cg</i> 1	QMVKCDPRHGKYMACCLLYRGDVVPKDVNAAIATIKTKRS	IQFVDWCPTGFKVGINYEPP	360
<i>Hs</i> 2	QMVKCDPRHGKYMACCLLYRGDVVPKDVNAAIATIKTKRT	IQFVDWCPTGFKVGINYEPP	360
<i>Hs</i> 4	QMVKCDPRHGKYMACCLLYRGDVVPKDVNAAIATIKTKRS	IQFVDWCPTGFKVGINYEPP	360
<i>Ss</i> 1	TVVPGGDLAKVQRAVCMLSNTTAIAEAWARLDHKFDL	MYAKRAFVHWYVGEEMEEGFSE	420
<i>Rn</i> 1	TVVPGGDLAKVQRAVCMLSNTTAIAEAWARLDHKFDL	MYAKRAFVHWYVGEEMEEGFSE	420
<i>Mm</i> 1	TVVPGGDLAKVQRAVCMLSNTTAIAEAWARLDHKFDL	MYAKRAFVHWYVGEEMEEGFSE	420
<i>Hs</i> 1	TVVPGGDLAKVQRAVCMLSNTTAIAEAWARLDHKFDL	MYAKRAFVHWYVGEEMEEGFSE	420
<i>Cg</i> 1	TVVPGGDLAKVQRAVCMLSNTTAIAEAWARLDHKFDL	MYAKRAFVHWYVGEEMEEGFSE	420
<i>Hs</i> 2	TVVPGGDLAKVQRAVCMLSNTTAIAEAWARLDHKFDL	MYAKRAFVHWYVGEEMEEGFSE	420
<i>Hs</i> 4	TVVPGGDLAKVQRAVCMLSNTTAIAEAWARLDHKFDL	MYAKRAFVHWYVGEEMEEGFSE	420
<i>Ss</i> 1	AREDMAALEKDYEEVGVDVSEGESEEEGEEY	451	<div style="border: 1px solid black; padding: 5px; width: fit-content;"> <p>Amino acid colour:</p> <p>Conserved</p> <p>Semi-conserved</p> <p>Non-conserved</p> </div>
<i>Rn</i> 1	AREDMAALEKDYEEVGVDVSEGESEEEGEEY	451	
<i>Mm</i> 1	AREDMAALEKDYEEVGVDVSEGESEEEGEEY	451	
<i>Hs</i> 1	AREDMAALEKDYEEVGVDVSEGESEEEGEEY	451	
<i>Cg</i> 1	AREDMAALEKDYEEVGVDVSEGESEEEGEEY	451	
<i>Hs</i> 2	AREDLAALKDYEEVGVDVSEAEAE-GEY	450	
<i>Hs</i> 4	AREDMAALEKDYEEVGVDVSE--DEDEGEE-	448	

Figure 6.8. Comparison of the amino acid sequences of the α -tubulins of dinitroaniline-insensitive mammals. Shown are the sequences for *Sus scrofa* (*Ss*), *Rattus norvegicus* (*Rn*), *Mus musculus* (*Mm*), *Homo sapiens* (*Hs*), and *Cricetulus griseus* (*Cg*) (number following name corresponds to α -tubulin isotype); the accession numbers are as in Table 2.3. Colouring indicates amino acid differences in mammal types relative to the most common residue at each position. **S. scrofa* 1 was the chosen α -tubulin representative sequence.

<i>Hs2</i>	MREIVH L QAGQCGNQIGAKFW E VI S DEHGIDPTGTYHGSD L QLERIN V YNEATGGKYV	60
<i>Mm3</i>	MREIVH L QAGQCGNQIGAKFW E VI S DEHGIDPTGTYHGSD L QLERIN V YNEATGGKYV	60
<i>Hs5</i>	MREIVH L QAGQCGNQIGAKFW E VI S DEHGIDPTGTYHGSD L QLERIN V YNEATGG N YV	60
<i>Rn1</i>	MREIVH I QAGQCGNQIG P KFW E VI S DEHGIDPTG S YHGSD L QLERIN V YNEA A GNKYV	60
<i>Ss1</i> *	MREIVH I QAGQCGNQIGAKFW E VI S DEHGIDPTG S YHGSD L QLERIN V YNEA A GNKYV	60
<i>Hs1</i>	MREIVH I QAGQCGNQIGAKFW E VI S DEHGIDPTGTYHGSD L Q L DRI S VYNEATGGKYV	60
<i>Hs4</i>	MREIVH I QAGQCGNQIGAKFW E VI S DEHGIDP S GN Y VGSD L QLER I S V YNEA S SHKYV	60
<i>Hs2</i>	PRAVLVDLEPGTMD S VRSGPF Q IFRPDNF V FGQ S GAGNNWAKGHY T EGAE L VDSV L DV V	120
<i>Mm3</i>	PRAVLVDLEPGTMD S VRSGPF Q IFRPDNF V FGQ S GAGNNWAKGHY T EGAE L VDSV L DV V	120
<i>Hs5</i>	PRAVLVDLEPGTMD S VRSGPF Q IFRPDNF V FGQ S GAGNNWAKGHY T EGAE L VDSV L DV V	120
<i>Rn1</i>	PRA L VLVDLEPGTMD S VRSGPF Q IFRPDNF V FGQ S GAGNNWAKGHY T EGAE L VDSV L DV V	120
<i>Ss1</i>	PRA L VLVDLEPGTMD S VRSGPF Q IFRPDNF V FGQ S GAGNNWAKGHY T EGAE L VDSV L DV V	120
<i>Hs1</i>	PRA L VLVDLEPGTMD S VRSGPF Q IFRPDN F I F Q S GAGNNWAKGHY T EGAE L VDSV L DV V	120
<i>Hs4</i>	PRA L VLVDLEPGTMD S VR S G A F G H L FRPDNF V FGQ S GAGNNWAKGHY T EGAE L VDSV L DV V	120
<i>Hs2</i>	RKEAES C D L Q G F L THSLGGGT G SGMG T LL I SK I RE E Y P DRIM N T F S V VP S PK V SD T V V	180
<i>Mm3</i>	RKEAES C D L Q G F L THSLGGGT G SGMG T LL I SK I RE E Y P DRIM N T F S V VP S PK V SD T V V	180
<i>Hs5</i>	RKEAES C D L Q G F L THSLGGGT G SGMG T LL I SK I RE F P D RI M N T F S V V P S PK V SD T V V	180
<i>Rn1</i>	RKE S E S C D LQ G F L THSLGGGT G SGMG T LL I SK I RE E Y P DRIM N T F S V M P S P K V SD T V V	180
<i>Ss1</i>	RKE S E S C D LQ G F L THSLGGGT G SGMG T LL I SK I RE E Y P DRIM N T F S V VP S PK V SD T V V	180
<i>Hs1</i>	RKEAES C D L Q G F L THSLGGGT G SGMG T LL I SK I RE E Y P DRIM N T F S V VP S PK V SD T V V	180
<i>Hs4</i>	RKE C E N C D LQ G F L THSLGGGT G SGMG T LL I SK V RE E Y P DRIM N T F S V VP S PK V SD T V V	180
<i>Hs2</i>	EPYNATLS V H Q L V ENTDE T Y C IDNEAL Y D I CF R TL K L T TP T Y G DL N H L V S AT M S G V T T C L	240
<i>Mm3</i>	EPYNATLS V H Q L V ENTDE T Y C IDNEAL Y D I CF R TL K L T TP T Y G DL N H L V S AT M S G V T T C L	240
<i>Hs5</i>	EPYNATLS V H Q L V ENTDE T Y C IDNEAL Y D I CF R TL K L T TP T Y G DL N H L V S AT M S G V T T C L	240
<i>Rn1</i>	EPYNATLS V H Q L V ENTDE T Y C IDNEAL Y D I CF R TL K L T TP T Y G DL N H L V S AT M S G V T T C L	240
<i>Ss1</i>	EPYNATLS V H Q L V ENTDE T Y C IDNEAL Y D I CF R TL K L T TP T Y G DL N H L V S AT M S G V T T C L	240
<i>Hs1</i>	EPYNATLS V H Q L V ENTDE T Y C IDNEAL Y D I CF R TL R L T TP T Y G DL N H L V S GT M E C V T T C L	240
<i>Hs4</i>	EPYNATLS I H Q L V ENTDE T Y C IDNEAL Y D I CF R TL K L A T P TY G DL N H L V S AT M S G V T T S L	240
<i>Hs2</i>	RFP Q L N AD L R K LAV N M V FP R L H FF M PG F AP L TS R GS Q Y R AL T VP E L T Q Q M F DA K N M	300
<i>Mm3</i>	RFP Q L N AD L R K LAV N M V FP R L H FF M PG F AP L TS R GS Q Y R AL T VP E L T Q Q M F DA K N M	300
<i>Hs5</i>	RFP Q L N AD L R K LAV N M V FP R L H FF M PG F AP L TS R GS Q Y R AL T VP E L T Q Q M F DA K N M	300
<i>Rn1</i>	RFP Q L N AD L R K LAV N M V FP R L H FF M PG F AP L TS R GS Q Y R AL T VP E L T Q Q M F D S K N M	300
<i>Ss1</i>	RFP Q L N AD L R K LAV N M V FP R L H FF M PG F AP L TS R GS Q Y R AL T VP E L T Q Q M F DA K N M	300
<i>Hs1</i>	RFP Q L N AD L R K LAV N M V FP R L H FF M PG F AP L TS R GS Q Y R AL T VP D L T Q Q V F DA K N M	300
<i>Hs4</i>	RFP Q L N AD L R K LAV N M V FP R L H FF M PG F AP L TR R GS Q Y R AL T VP E L T Q Q M F DA K N M	300
<i>Hs2</i>	AACDPRHGR Y L T VAA V FRGRMS K EV D E Q ML N V Q N K NS S Y F VE I P N N V K T AV C D I PP R G	360
<i>Mm3</i>	AACDPRHGR Y L T VAA V FRGRMS K EV D E Q ML N V Q N K NS S Y F VE I P N N V K T AV C D I PP R G	360
<i>Hs5</i>	AACDPRHGR Y L T VAA V FRGRMS K EV D E Q ML S V Q S K NS S Y F VE I P N N V K T AV C D I PP R G	360
<i>Rn1</i>	AACDPRHGR Y L T VAA I FRGRMS K EV D E Q ML N V Q N K NS S Y F VE I P N N V K T AV C D I PP R G	360
<i>Ss1</i>	AACDPRHGR Y L T VAA V FRGRMS K EV D E Q ML N V Q N K NS S Y F VE I P N N V K T AV C D I PP R G	360
<i>Hs1</i>	AACDPRHGR Y L T VAA V FRGRMS K EV D E Q ML N V Q N K NS S Y F VE I P N N V K T AV C D I PP R G	360
<i>Hs4</i>	AACDPRHGR Y L T V A T V FRGRMS K EV D E Q ML A I Q S K NS S Y F VE I P N N V K V AV C D I PP R G	360
<i>Hs2</i>	L K MS A T F I G N S T A I Q E L F K R I S E Q F T A M F R R K A F L H W Y T G E G M D E M E F T E A E S N M N D L V S	420
<i>Mm3</i>	L K MS A T F I G N S T A I Q E L F K R I S E Q F T A M F R R K A F L H W Y T G E G M D E M E F T E A E S N M N D L V S	420
<i>Hs5</i>	L K M A T F I G N S T A I Q E L F K R I S E Q F T A M F R R K A F L H W Y T G E G M D E M E F T E A E S N M N D L V S	420
<i>Rn1</i>	L K MS A T F I G N S T A I Q E L F K R I S E Q F T A M F R R K A F L H W Y T G E G M D E M E F T E A E S N M N E L V S	420
<i>Ss1</i>	L K MS A T F I G N S T A I Q E L F K R I S E Q F T A M F R R K A F L H W Y T G E G M D E M E F T E A E S N M N D L V S	420
<i>Hs1</i>	L K M A V T F I G N S T A I Q E L F K R I S E Q F T A M F R R K A F L H W Y T G E G M D E M E F T E A E S N M N D L V S	420
<i>Hs4</i>	L K MS S T F I G N S T A I Q E L F K R I S E Q F T A M F R R K A F L H W Y T G E G M D E M E F T E A E S N M N D L V S	420
<i>Hs2</i>	E Y Q Q Y Q D A T A E E E G F E F E E E A E E V A----- 445	
<i>Mm3</i>	E Y Q Q Y Q D A T A E E E G F E F E E E A E E V A----- 445	
<i>Hs5</i>	E Y Q Q Y Q D A T A E - G E F E E E A E E V A----- 444	
<i>Rn1</i>	E Y Q Q Y Q D A T A D E Q G F E F E E E G E D E A----- 445	
<i>Ss1</i>	E Y Q Q Y Q D A T A D E Q G F E F E E E G E D E A----- 445	
<i>Hs1</i>	E Y Q Q Y Q D A T A E E E D F G E E E A E E A----- 444	
<i>Hs4</i>	E Y Q Q Y Q D A T A E E G E M Y E D D E E S E A Q G P K 450	

Amino acid colour:
Conserved
Semi-conserved
Non-conserved

Figure 6.9. Comparison of the amino acid sequences of the β -tubulins of dinitroaniline-insensitive mammals. Shown are the sequences for *S. scrofa* (*Ss*), *R. norvegicus* (*Rn*), *M. musculus* (*Mm*), and *H. sapiens* (*Hs*) (number following name corresponds to β -tubulin isotype); the accession numbers are as in Table 2.3. Colouring indicates amino acid differences in mammal types relative to the most common residue at each position. **S. scrofa* 1 was the chosen representative β -tubulin sequence.

group. From the sequence alignments the level of tubulin conservation among both groups was seen to be very high (see Figs. 6.6 - 6.9), with most differences occurring within the C-termini (amino acid positions 428 - 452) of both tubulin monomers. From the alignments *Eleusine indica* (goosegrass) α -tubulin (isotype 1) and *Arabidopsis thaliana* (thalecress) β -tubulin (isotype 2) were selected to be representative of tubulins from dinitroaniline-sensitive plants and *Sus scrofa* (pig) α - and β -tubulin were chosen to represent tubulins from dinitroaniline-insensitive mammals.

The selected sequences were then aligned with *P. falciparum* tubulins as shown in Fig. 6.10 and 6.11. *P. falciparum* strain K1/Thailand was used for this analysis, as it has been used for experimentation throughout this project and shares 100% identity with both α - and β - tubulin of the strain 3D7 (data not shown). It is also noted that *P. falciparum* strains NF54 and FCR-3/Gambia contain three non-conserved, 1 semi-conserved and 5 conserved amino acid changes on β -tubulin compared to strains used in this study, which bear no significant effect on subsequent alignments (data not shown). From the alignments, amino acids were then highlighted which were similar or identical in *E. indica* / *A. thaliana* and *P. falciparum* but different in *S. scrofa*. The differences were then categorised as being conserved, semi-conserved or non-conserved, reflecting similarities or differences in amino acid size, shape, polarity, and charge. A total of 30 conserved, 4 semi-conserved and 9 non-conserved amino acid differences were found in the α -tubulin sequences. Less variation was observed in the β -tubulin amino acid sequences, with 13 conserved, 3 semi-conserved and 3 non-conserved differences noted.

6.2.4.2. Homology modeling of *P. falciparum* tubulins

The amino acid differences (43 on α -tubulin and 19 on β -tubulin) noted in section 6.2.4.1 were distributed throughout the primary sequence of *P. falciparum* tubulins. To visualise their tertiary structure location, we modeled the α I/ β -tubulin heterodimer of *P. falciparum* based on most of the three-dimensional structure of mammalian $\alpha\beta$ -tubulin (see section 2.10.3). The *P. falciparum* tubulin model (see Fig. 6.12) displayed an overall structural likeness to that of the bovine tubulin structure. In addition, the modeled N-loop region of modeled *P. falciparum* α -tubulin also displayed a similar overall structure to the analogous bovine β -tubulin N loop structure (data not shown).

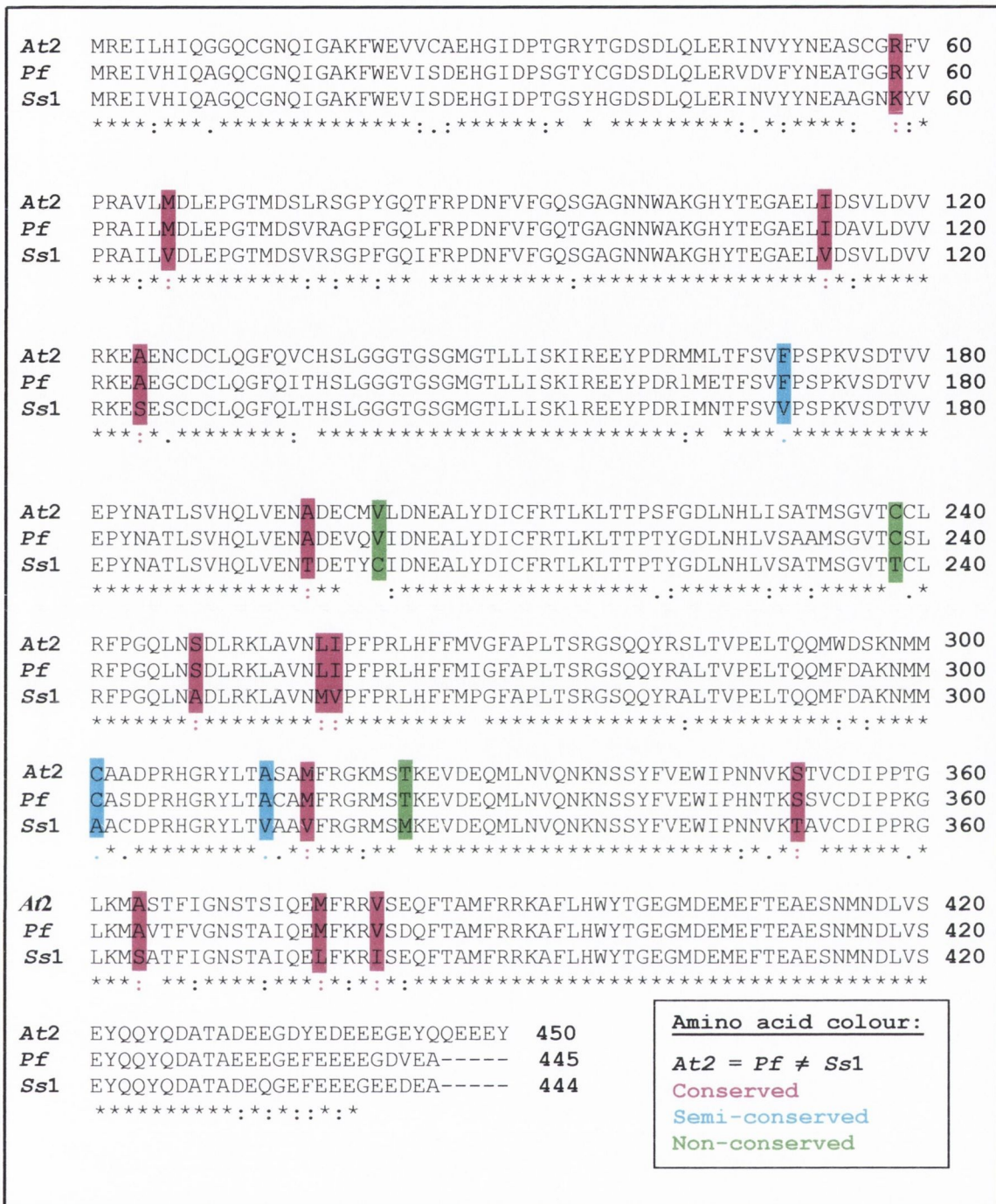


Figure 6.11. Alignment of representative plant [*A. thaliana* (*At 2*)] and animal [*S. scrofa* (*Ss 1*)] β -tubulin amino acid sequences with those of *P. falciparum* (*Pf*). The colouring scheme denotes amino acid residues which are common to *P. falciparum* and plant but different from mammalian β -tubulins. Asterisks, colons, and periods indicate amino acid regions of exact identity, similarity and relatedness, respectively. The accession numbers are as in Table 2.3. Sequence alignments were performed using ClustalW 1.8 (Higgins *et al*, 1996).

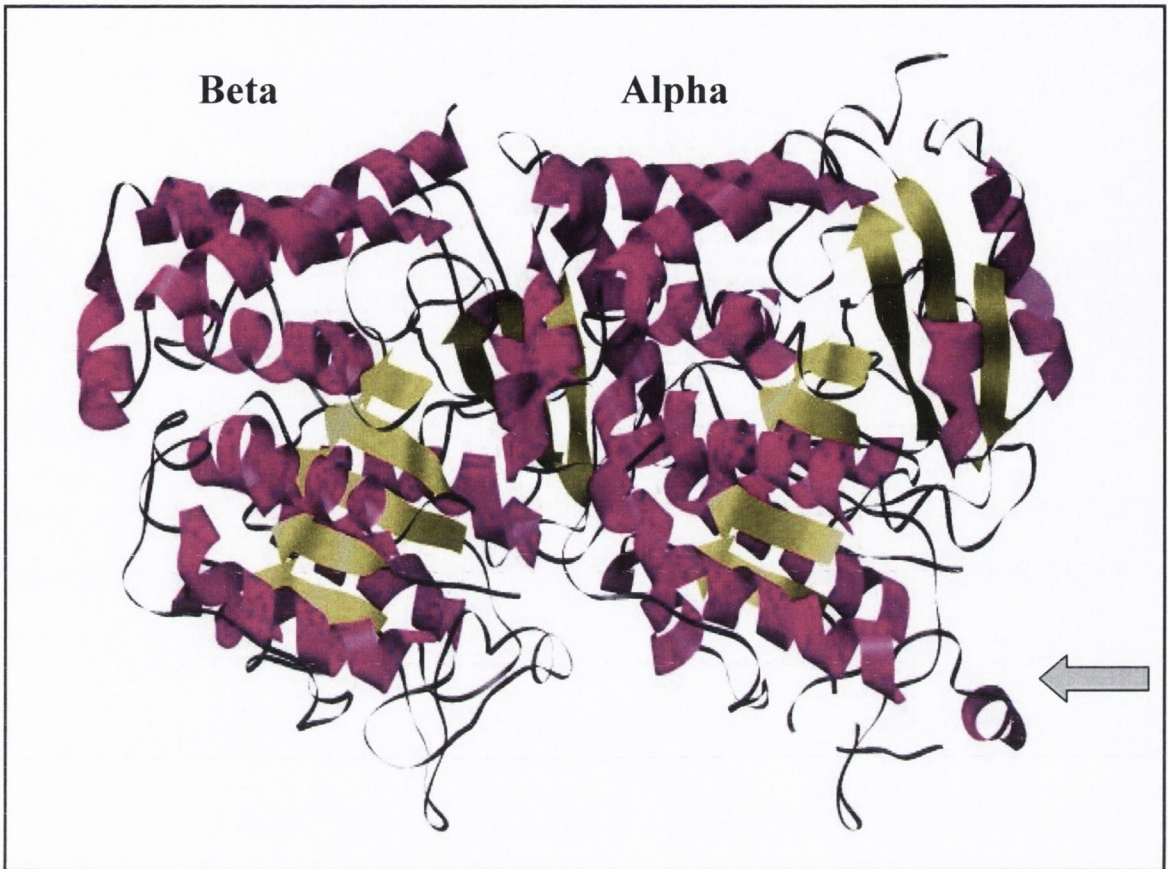


Figure 6.12. Ribbon diagram of the proposed structure of the α I/ β -tubulin heterodimer of *P. falciparum* obtained by homology modelling. The amino acid sequences of *P. falciparum* α I- and β -tubulin were fit to the structure of the bovine tubulin heterodimer using the Insight II, Biopolymer and Discover software from Accelrys (San Diego, CA, USA), running on a Silicon Graphics O₂ workstation. The N-loop region of α I-tubulin was modelled on the analogous N-loop of bovine β -tubulin. α -helices are shown as purple helical ribbons and β -strands as yellow arrows. Loop regions are in black. Alpha indicates the α I-tubulin subunit and beta indicates the β -tubulin subunit. The arrow indicates the position of the modelled N-loop region on α I-tubulin.

The spatial distribution of the amino acid differences determined in section 6.2.4.1 were then mapped onto the structural model of the *P. falciparum* α I/ β -tubulin heterodimer (see Fig. 6.13). The conserved amino acid differences were found to be distributed throughout the tubulin heterodimer with the majority of the non-conserved amino acid differences clustering around the core of both tubulin monomers. In addition, some of the semi-conserved amino acid differences were found located close to the modeled tubulin surface (Fig. 6.13).

6.2.4.3. Identification of a possible trifluralin-binding cavity

Using the highlighted residues (Fig. 6.13) and equivalent amino acids on the mammalian tubulin crystal structure as a guide, a possible trifluralin-binding domain was located on the *P. falciparum* modeled α I-tubulin just below the protein surface (Fig. 6.14). Residues in the modeled *P. falciparum* α I-tubulin important for forming the putative trifluralin-binding cavity included Val141, Pro173, Ser187, Thr191, Leu194, Ala201, Met203, Phe267, Phe388, Met 391, Leu425 and Leu428. Of these, Val141 and Phe388 (phenylalanine and tryptophan, respectively, in mammals) were of principal importance in creating the binding domain for docking of trifluralin.

The putative target-binding region of trifluralin was demarcated for a docking study by including all residues in α I-tubulin that were within 18 Å of C α of the residue valine (141) on the modeled α I-tubulin. The final trifluralin-binding configuration within the modeled α I-tubulin cavity was selected using a combination of manual and automatic docking techniques. In parallel studies, we also investigated the interaction and docking of trifluralin with the equivalent region of *S. scrofa* α -tubulin. However, no such trifluralin-binding cavity existed, primarily due to the presence of the bulky amino acids Phe141 and Trp388. Docking studies were unsuccessful as numerous energetically-unfavourable negative contacts formed between trifluralin and surrounding amino acids and as a result, no binding was observed (data not shown). Similarly, no such dinitroaniline-binding cavity was identified on modeled *P. falciparum* β -tubulin (data not shown).

Analysis of the possible trifluralin-binding site indicated that most of the residues surrounding the docked trifluralin molecule are hydrophobic. The side chains of Leu425, Met391, Pro173 and Phe388 and the CH₃ group of Thr191 could make hydrophobic interactions with the C₃H₇ groups that branch of the top of the trifluralin molecule (see Fig. 6.1). Similarly Leu428, Val141 and Phe267 may form

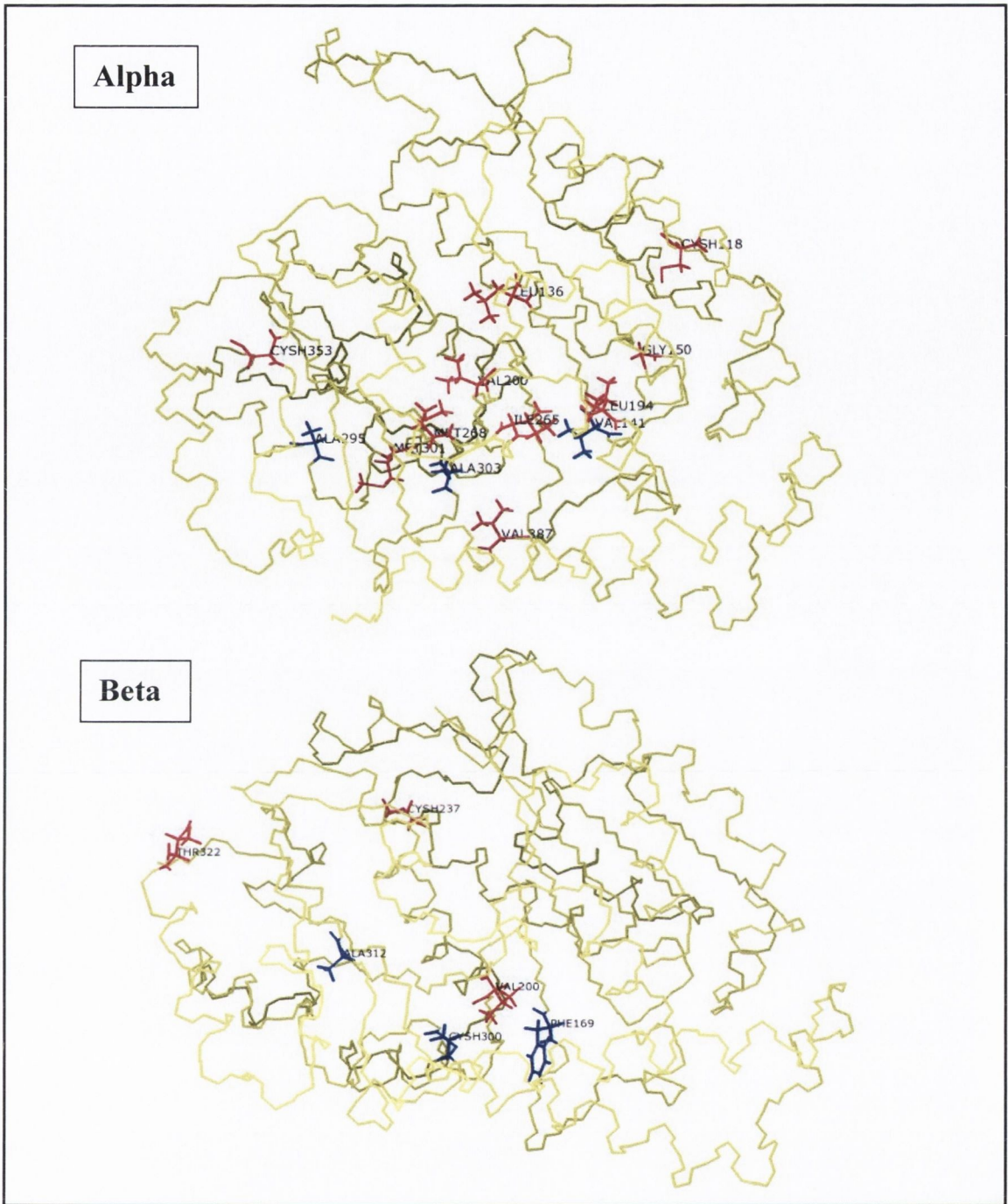


Figure 6.13. Spatial distribution and location of amino acid positions where *P. falciparum* and dinitroaniline-sensitive plant tubulins differ from mammalian tubulins. The backbones of modelled *P. falciparum* α - and β -tubulin are shown (lighter and darker shades of green indicate backbone at the front and back positions, respectively) along with side chains of non-conserved (coloured red) and semi-conserved (coloured blue) amino acids as indicated in alignments in section 6.10 and 6.11 (conserved differences are not shown). Numbers refer to the amino acid positions in *P. falciparum* α - and β -tubulin sequences (note: for technical reasons β -tubulin residue numbers shown are out by one compared to the alignment in section 6.11, e.g. Phe169 above actually corresponds to Phe170).



Figure 6.14. Potential binding site for the dinitroaniline trifluralin in the modelled *P. falciparum* α I-tubulin. Amino acid differences between trifluralin-sensitive (*P. falciparum* and plants) and trifluralin-resistant (mammals) species mapped onto the modelled *P. falciparum* tubulin dimer as shown in Fig. 6.13 were used to identify a possible dinitroaniline-binding site by physical scanning techniques. Trifluralin (red) was docked by manual and autodocking techniques into a cavity formed principally by the residues Val141 (yellow) and Phe388 (yellow). α -helices and β -strands are shown as grey helical ribbons and arrows, respectively. The arrow indicates the position of the modelled N-loop.

hydrophobic/aromatic interactions with the benzene ring of trifluralin. Both NO₂ groups of trifluralin would appear to be in relatively unreactive positions and thus unlikely to form H-bonds with surrounding residues. Finally the CF₃ moiety is in a mixed environment of alternating hydrophobic and hydrophilic residues (Cys170, Asp168, Leu194 and Ser190). Thus, it would appear that the main interactions between trifluralin and the surrounding residues in the possible trifluralin-binding cavity in modelled *P. falciparum* α I-tubulin are hydrophobic in nature.

6.3. DISCUSSION

The primary goal of this chapter was to explore the cellular and molecular mechanisms of action of antimitotic herbicides on *P. falciparum*, with particular focus on tubulin. To initiate this study, a number of compounds and derivatives were selected from the dinitroaniline class of herbicide and tested for their ability to inhibit *P. falciparum* in culture. Compounds were found to display modest antimalarial activity (IC₅₀ values between 2.9 and 8.1 μ M), compared for example with microtubule inhibitors from the dolastatin/auristatin family (IC₅₀ < 240 nM). The antimalarial activity of trifluralin was found to be superior to its precursor chloralin. Our results are in agreement with the data of Dow *et al* (2002) who showed that trifluralin was more potent than chloralin against *P. berghei* in culture. These results suggest that the superior potency of chloralin over trifluralin (~ 100-fold difference) against *Trypanosoma cruzi* epimastigotes (Traub-Cseko *et al*, 2001) does not extend to *Plasmodium* spp. In addition, the absence of both nitro groups on the benzyl ring of chloralin resulted in loss of antimalarial activity. This finding is consistent with previous structure-antiprotozoal activity studies on dinitroaniline compounds, which have shown that at least one of the nitro-groups is necessary for anti-trypanosomatid activity (Chan *et al*, 1993). Thus the electronegative domain of dinitroaniline compounds would appear to play an important role in protein-ligand interactions in a range of protozoan parasites including *P. falciparum*.

Studies to date on the effects of antimitotic herbicides on *Plasmodium* spp. have focused primarily on agents from the dinitroaniline stable. To extend this investigation, microtubule inhibitors from the phosphoric amide and *N*-phenylcarbamate herbicide classes were tested for their ability to inhibit *P. falciparum* growth in culture. Interestingly APM, the most commonly-used member

of the phosphoro amide herbicides in the control of broadleaf weeds (Anthony *et al*, 1999b), displayed antimalarial activity in the low micromolar range (IC₅₀ 3.5 µM). This is the first report of anti-malarial activity of a compound from this class of herbicide and it is possible that other compounds may be uncovered from this source with more potent activity. In addition, phosphorothioamidate herbicides lack anti-mammalian cell activity (Murthy *et al*, 1994) and display superior aqueous solubility to that of dinitroanilines (maximum aqueous solubility of APM is 2.3×10^{-4} M compared to 8.2×10^{-7} M for trifluralin) (Morejohn *et al*, 1991). The poor aqueous solubility of dinitroanilines has been suggested to create problems in the maintenance of constant drug concentrations for biological studies. For example in a pharmacokinetic study involving the rat model of malaria, *Rattus norvegicus*, it was thought that the lack of *in vivo* antimalarial activity was possibly due to the low water-solubility of trifluralin resulting in its poor adsorption and insufficient plasma concentrations (Dow *et al*, 2002). Therefore, the more favourable physical properties of APM together with its highly selective mode of action would appear to offer more hope than dinitroanilines as potential antimalarials and possibly warrants further evaluation as a lead compound in a similar animal model of malaria.

Unfortunately, chloroprotham, which belongs to the *N*-phenyl carbamate class of herbicides, displayed no antimalarial activity at all of the concentrations tested. This result is unsurprising as some of the related carbamates (benzimidazole-2-yl carbamates), which are used as fungicides and antihelminthics, also display poor antimalarial activity (Bell, 1998). Furthermore, studies with tobacco cells also suggest that the binding site for chloroprotham on plant tubulin is distinct from that of trifluralin and amiprothos-methyl (Young *et al*, 2000). Thus, the most likely explanation for the lack of antimalarial activity of chloroprotham is poor tubulin binding or the absence of a benzamide-binding site on the parasite tubulin heterodimer.

Features of antimalarial activity of antimetabolic herbicides were found to deviate from those of the dolastatin, “*Vinca*” alkaloid and taxoid classes of microtubule inhibitors. The plateau effect which was discussed in chapter 3 was not significant in either 48 or 72 h dose response curves of any of the antimetabolic herbicides tested. A possible reason for this could be superior uptake kinetics for antimetabolic herbicides into parasites. Compounds such as trifluralin and APM have simple aromatic chemistries in contrast to the complex chemical structures of the

dolastatins and taxoids (see Figs. 3.2 and 6.1). Such structural differences may allow herbicides to diffuse more rapidly across erythrocytic and parasitic membranes, allowing rapid accumulation in and inhibition of the parasite. Previous reports have indicated the relatively quick uptake of trifluralin by its ability to inhibit *in vivo* flagellar regeneration on *Chlamydomonas* zoospores almost directly upon addition at concentrations $> 5 \mu\text{M}$ (Hess, 1979). The possibility also exists that ring and early trophozoite stages of parasite development (0 - 18 h post invasion), which are resistant to the dolastatins and taxoids at concentrations up to $10 \mu\text{M}$, are more susceptible to the antimitotic herbicides and therefore result in the sigmoidal dose response curves as seen in Fig. 6.2. Thus while it appears that the dolastatins/auristatins, taxoids and "Vinca" alkaloids interact with high and low affinity targets in the sub-nanomolar to nanomolar and micromolar ranges respectively, antimitotic herbicides appear to interact with a target(s) only in the low micromolar range.

The effects of antimitotic herbicides on *P. falciparum* microtubular architecture were in contrast to those of dolastatin 10/vinblastine and Taxol (see Fig. 6.3). The dinitroanilines trifluralin, chloralin and oryzalin all caused loss of normal microtubular structures and their replacement by speckles or dots of discrete tubulin labelling throughout the parasite. The failure of parasites to maintain their characteristic mitotic architecture in the presence of such agents, which is crucial to cell functioning, is a likely reason for the antimalarial action of the dinitroanilines. A related effect of trifluralin and pendimethalin (0.1 - 1 mM) on the narrow band of subpellicular microtubules (f-MAST) of *P. falciparum* merozoites has also been reported (Fowler *et al.*, 1998). The f-MAST, which normally appears as a single band of tubulin-associated fluorescence, was replaced by a single apical dot of fluorescence upon herbicide treatment. However, our observations are likely to be more relevant to growth inhibition because of the lower concentrations of antimitotic herbicides used here (5 - 50 fold less).

The dot-like fragments of tubulin labelling throughout the parasite after herbicide treatment were in contrast to the diffuse/fragmented labelling seen with dolastatin 10 and vinblastine (see Fig. 3.5 b - d) and the thick rods of tubulin formed after Taxol treatment (see Fig. 3.5 e). The reason for this is uncertain but may reflect net depolymerisation of parasite microtubules in a fashion different from that caused by other classes of microtubule inhibitor. In plants, herbicides have been shown to

cause rapid dissociation of tubulin dimers from the positive end of microtubules (Anthony *et al*, 1999), so the dot-like structures of parasite tubulin as seen in Fig. 6.3 (b - d) could represent severed or stunted microtubule structures due to herbicide action. The particles may also represent tubulin-herbicide complexes, which may have aggregated following herbicide-induced depolymerisation of parasite microtubules. These results also indicate that antimitotic herbicides probably bind to parasite tubulin at a location distinct from the “*Vinca*” domain or Taxol binding site.

Our immunofluorescence studies also illustrated the similar effect of APM on parasite microtubules to that of the dinitroanilines (Fig. 6.3 e) and would appear to agree with the analysis of Ellis *et al* (1994), who suggest that these two chemically-distinct classes of herbicide share a common intracellular target, and possibly the same binding site(s). This observation may also be extended to other protozoan parasites, as both oryzalin and APM have recently been shown to inhibit the assembly of purified leishmanial tubulin *in vitro* with IC₅₀ values of approximately 25 and 50 μ M, respectively (Werbovetz, 2002).

As stated earlier, the binding site(s) on either plant or protozoan tubulin for dinitroaniline compounds have not yet been identified but recent reports have proposed a number of locations based on molecular modeling studies (Blume *et al*, 2003; Morrissette *et al*, 2004; Nyporko *et al*, 2002). Knowing features of this site and tubulin-herbicide interactions could substantially help in the design of more potent antimitotic, antiprotozoal agents. Therefore, further studies based on molecular and homology-modelling techniques were undertaken to investigate the interaction of dinitroaniline herbicides with *P. falciparum* tubulins.

The first approach was to identify features of tubulin structure (amino acids) which were common to dinitroaniline-sensitive plants and *P. falciparum* but different in mammals. From alignment studies, the majority of amino acid differences including non-conservative substitutions were found to reside on α I-tubulin (see Figs. 6.10 and 6.11). The differences were then mapped onto a homology model of the *P. falciparum* tubulin heterodimer, which was facilitated by the determination of most of the three-dimensional structure of bovine α/β -tubulin by electron crystallography at 3.7 Å resolution (Nogales *et al*, 1998). Although most amino acid differences resided in the core of both tubulin monomers, a possible dinitroaniline-binding site was identified on modeled *P. falciparum* α I-tubulin (see Fig. 6.14) with residues Val141 and Phe388 playing a central role in its identification. In contrast, docking of

trifluralin into the equivalent site on bovine α -tubulin was hindered by the combination of Phe141 and Trp388 due to the presence of their bulky aromatic rings. In addition, an equivalent site was not observed on modeled *P. falciparum* β -tubulin.

The location of the possible dinitroaniline cavity on modeled *P. falciparum* α -tubulin was below the protein surface, which raises solvent accessibility issues. However, reports suggest that binding sites for other classes of microtubule inhibitor exist in the interior of the tubulin heterodimer (Robinson *et al*, 2004; Traub-Cseko *et al*, 2001). Structural movements within the tubulin heterodimer could possibly accommodate trifluralin into the proposed site. For example, movement of the H8 helix and the T7 loop structures within the β -subunit of bovine tubulin resulted in the release of space for colchicine binding (Ravelli *et al*, 2004). Conformational changes within the monomer of β -tubulin have also been implicated with benzimidazole binding to *H. contortus* tubulin (Robinson *et al*, 2004). Thus, conformational changes in *P. falciparum* tubulins could possibly allow dinitroanilines access to the proposed site to bind to specific residues and exert their antimalarial effects.

A similar, putative dinitroaniline-binding site may also exist on plant and *Leishmania* tubulins. A study by Yamamoto *et al* (1998) suggested that two locations exist where goosegrass and *Leishmania* α -tubulins differ significantly from those of mammalian. One of these, as in the case of *P. falciparum*, is around Val141, which they propose to have an effect on tubulin hydrophobicity and secondary structure. However, further investigations were not reported. Recently a number of alternative dinitroaniline-binding sites have been put forward based on resistant mutations and simulated docking studies on modelled tubulins. One report suggests that the dinitroaniline/phosphorothioamidate-binding site on plant (*E. indica*) tubulin is predominantly located in a hydrophobic pocket below the surface of the α -monomer near the tubulin dimer interface (Blume *et al*, 2003). Out of the eight amino acid residues proposed to form this cavity, six are conserved, 1 is semi-conserved and 1 is non-conserved with the equivalent amino acids in *P. falciparum* α I-tubulin (data not shown). Another group suggest that the dinitroaniline-binding site on *Toxoplasma gondii* is also located on α -tubulin at a site beneath the N-loop, which is involved in protofilament interactions (Morrissette *et al*, 2004). In this case, *P. falciparum* shares identity with 12 out of the 13 residues involved in forming the putative binding site. Thus a number of putative dinitroaniline sites on plant and protozoan parasite tubulins now exist, but all still require molecular validation and characterisation.

To date there have been no reports probing the interaction of dinitroaniline herbicides with *P. falciparum* tubulin, probably due to difficulties in purifying the protein direct from the parasite as discussed in chapter 4. In an attempt to overcome this obstacle, we examined the molecular interaction of *P. falciparum* recombinant tubulin fusion proteins (as described in chapter 4) with a radiolabelled form of trifluralin. Results showed that [¹⁴C]trifluralin bound to MBP- α I- and MBP- β -tubulin fusions to a similar extent, had a reduced affinity for mammalian tubulin (6 - 6.5 fold less) and little or no affinity for MBP alone. The level of binding to recombinant *P. falciparum* tubulin fusions was 1437 dpm for 195 μ g MBP α I and 1580 dpm for 199 μ g MBP β with 16.8 mCi of [¹⁴C]trifluralin per millimole. This result is comparable to that of trifluralin binding to the flagellar tubulin of *Chlamydomonas* (942 dpm for 196 μ g of protein with 1.03 mCi of [¹⁴C]trifluralin per millimole: Hess *et al*, 1977) and that of partially-purified tubulin of *Leishmania mexicana amazonensis* (258 \pm 27 dpm with 30 μ g of protein and 566 \pm 93 dpm with 40 μ g of protein with 3 mCi of [¹⁴C]trifluralin per millimole: Chan *et al*, 1990). Chan *et al* (1990) also found the specificity of trifluralin binding to *Leishmania* over rat tubulin to be \sim 3.6 - 11.1 fold. In our experiments the specificity of trifluralin binding for recombinant over bovine brain tubulin was lower, but this may reflect the greater quantities of protein used in our study which may have resulted in a higher amount of non-specific binding.

The observed binding of trifluralin to both tubulin fusion monomers was unexpected and could be due to a number of reasons including the presence of a dinitroaniline site on both monomers. Although both monomers share approximately only 40% amino acid sequence identity, their overall structural fold should be quite similar as suggested by the crystal structure of bovine tubulin, making it possible for similar binding sites to exist. However, our homology modeling studies provide little evidence for a dinitroaniline binding site on β -tubulin. The only evidence for dinitroanilines interacting with β -tubulin comes from a number of colchicine-resistant *Chlamydomonas reinhardtii* mutants, which were shown to possess a single amino acid substitution in the β -tubulin monomer, Lys350 to glutamate or methionone, which conferred cross-resistance to dinitroanilines and amiprofos-methyl (Lee *et al*, 1990). However, as these mutants are cross resistant to very diverse classes of microtubule inhibitors (colchicine and antimitotic herbicides) and supersensitive to Taxol, the resistance displayed is probably due to increased

microtubule stability in the cells compared with the wild type rather than modification in a dinitroaniline or colchicine-binding site (Schibler *et al*, 1991).

The possibility also exists that a cavity or cleft may have formed between the recombinant tubulins and the MBP fusion, which may have allowed trifluralin to bind to both monomers, although this is unlikely in that [¹⁴C]trifluralin showed no affinity for MBP alone. It could also be possible that the fold in the recombinant tubulins may be different from that of native *P. falciparum* tubulins, which may have resulted in the observed binding of trifluralin to both monomers. However, Hollomon *et al* (1998) showed that fungal β -tubulin expressed as a fusion protein bound benzimidazole and phenylcarbamate fungicides as expected, suggesting the fungicide-binding sites can fold correctly in fusion proteins. It is also of interest to note that other microtubule inhibitors have been reported to bind to both tubulin monomers to varying extents. For example, photoaffinity labelling experiments with vinblastine (Wolff *et al*, 1991) and two photoactive derivatives of this compound (Safa *et al*, 1987; Nasioulas *et al*, 1990) were found to label α -tubulin more than β -tubulin, with 57 - 75% of the incorporated radiolabel being in the α -subunit. Similarly, a photoaffinity analog of maytansine was found to be incorporated in a ~ 4 : 5 ratio into α - and β -tubulin respectively (Sawada *et al*, 1993). In addition, [¹⁴C]mebendazole, a benzimidazole compound, was found to bind with highest affinity to recombinant *H. contortus* α -tubulin ($K_d = 1.35 \mu\text{M}$) followed by recombinant β -tubulin isotypes 2 and 1 ($K_d = 2.31 \mu\text{M}$ and $3.95 \mu\text{M}$, respectively) (Oxberry *et al*, 2001a). These results suggest that microtubule inhibitors from different classes may have different binding sites and affinities for both or either tubulin monomer. Thus, even though studies associate α -tubulin with the dinitroaniline binding site, β -tubulin may also play a role in the binding of antimitotic herbicides to parasite tubulin. Perhaps the measurement of dinitroaniline binding to *P. falciparum* recombinant tubulins by fluorescence quenching or a related technique would relay more accurate data on the affinity of trifluralin for the different parasite tubulin monomers.

In summary, this chapter has provided experimental evidence both directly in the parasite and *in vitro* that *P. falciparum* tubulins are the target for antimitotic herbicides. In addition, based on the selective antimalarial activity and superior physical properties to the dinitroaniline compounds, APM is a potential lead compound for antimalarial drug design.

Chapter 7

General Discussion

7.1. EFFECTS OF MICROTUBULE INHIBITORS ON *P. FALCIPARUM*

Prior to the commencement of this work, studies had suggested that tubulin from the malarial parasite, *P. falciparum*, may present a potential drug target (Bell 1998; Taraschi *et al*, 1998). This is due to the crucial cellular role of microtubules and the established record of tubulin as a chemotherapeutic target for applications that include anti-tumour agents, fungicides, herbicides, and anthelmintics (Lacey, 1988). However, before this project began, biochemical work concerning *P. falciparum* tubulins had been extremely limited due to the inability to isolate these proteins from the parasite cell. In response to this, we initially characterised the cellular effects of novel and known classes of antimicrotubule agents against *P. falciparum* to aid in target validation and to verify the cellular mechanism of action of candidate antimalarial compounds. The following section outlines the classes of microtubule inhibitor that were chosen for this analysis:

“*Vinca*” site agents: The dolastatin/auristatin class

Concentrations of dolastatin 10 in the picomolar to low nanomolar range impeded the process of parasite schizogony and nuclear division and resulted in loss of mitotic microtubular structures and their replacement by diffuse or fragmented tubulin labelling. Such effects are consistent with an anti-tubulin mechanism of action and were similar to those of the “*Vinca*” alkaloid vinblastine. In addition, several peculiar effects on *P. falciparum* cell biology were observed.

One such effect was the morphologically-abnormal cell types that presumably materialised due to the inhibition of microtubule-mediated processes. Similarly, “*Vinca*” domain agents have illustrated profound developmental effects on a range of other protozoan parasites. For example, treatment of procyclic forms of *T. brucei* with rhizoxin resulted in irregular morphological changes and prevented mitotic spindle formation (Robinson *et al*, 1995), while hemiasterlin blocked nuclear division and cytokinesis in cultures of *L. donovani* (Havens *et al*, 2000).

The unusual dose-response curves displayed by dolastatin 10/auristatins against asynchronous, asexual parasites, which has previously been observed with the structurally-unrelated inhibitor Taxotere (Schrével *et al*, 1994), were deemed to reflect the varying susceptibilities of the different stages of asexual erythrocytic parasites. While ring-stage parasites were generally resistant to the effects of dolastatin 10 and auristatin PE, trophozoite- and schizont-stage parasites showed

greater susceptibilities. These findings may help explain the widely differing IC₅₀ values that have been reported for certain microtubule inhibitors against *P. falciparum* cultures, using various exposure times and degrees of synchrony (Bell, 1998). In addition, if such agents were to be used for clinical therapy, they may be fast- or slow-acting in malaria patients, depending on the age range of parasites present.

Prior to this study, there had been no reports outlining detailed structure-activity relationships (SAR) for “*Vinca*” domain agents or any other microtubule inhibitors on *P. falciparum*. Our detailed SAR analysis for the dolastatin/auristatin series of compounds against *P. falciparum* revealed a number of interesting observations; however, no agent had markedly stronger antimalarial than antimammalian cell activity. Thus, it seems likely that *P. falciparum* tubulin, like kinetoplastid tubulin (Werbovetz, 2002), has a similar sensitivity to “*Vinca*” domain agents as mammalian tubulin. However, limited molecular information currently exists pertaining to the “*Vinca*” binding site on mammalian or protozoan tubulins, so differences may exist that could be exploited for the discovery of parasite-biased ligands. Perhaps the use of our homology model of the *P. falciparum* $\alpha\beta$ -tubulin heterodimer coupled with further screening of available chemical databases may uncover compounds from the “*Vinca*” class of microtubule inhibitors that bind specifically to *P. falciparum* tubulin.

Herbicides: The dinitroaniline and phosphorothioamidate classes

Antimitotic agents from both classes of herbicide inhibited growth and differentiation of *P. falciparum* in the low micromolar range, caused a block on nuclear division and caused loss of normal microtubular structures with their replacement by speckles or dots of discrete tubulin labelling throughout the parasite. The failure of parasites to maintain their characteristic mitotic architecture in the presence of such agents, in contrast to mammalian cells (Hugdahl *et al*, 1993), is consistent with an anti-tubulin mechanism of action. Thus, such selective disruption of *P. falciparum* microtubules provided the grounds for further explorations into the nature of the interaction between antimitotic herbicides and parasite tubulin.

However, biochemical studies concerning *P. falciparum* tubulin up until now have been unfeasible due to an inability to purify the proteins directly from the parasite (Bell, 1998). This technical difficulty has probably arisen due to the scarcity

of tubulin in the parasite cell. Our studies have confirmed this belief, as tubulin in asexual stages of parasite development were found to comprise no more than 0.25% of cellular proteins at most, in contrast to a figure of at least 10% for tubulin-rich parasites such as *L. mexicana* (Fong *et al*, 1981) and *T. brucei* (MacRae *et al*, 1990). To address this problem and to further investigate the molecular basis of the interaction of antimitotic herbicides with parasite tubulin, we utilised an *E.coli*-based expression system to produce recombinant *P. falciparum* tubulins as soluble MBP-fusion proteins. Both recombinant α I- and β -tubulin were found to have a higher affinity for a radiolabelled version of the dinitroaniline trifluralin than had bovine brain tubulin. No binding to MBP alone was detected. This result is consistent with the premise that the inhibition of cultured *P. falciparum* was caused by binding of these ligands to parasite tubulin.

The apparent interaction between dinitroanilines/phosphorothioamidates and tubulin of *P. falciparum* is by no means unique, as ligands from both herbicide classes have been shown specifically to bind to and inhibit tubulin polymerisation *in vitro* from a range of protozoan parasites and plant species (Werbovets *et al*, 1999, 2002; Chan *et al*, 1990; Morejohn *et al*, 1991). Moreover, tubulins isolated from tobacco plants and the kinetoplastid parasite *L. donovani* were bound by the dinitroaniline oryzalin with moderate affinities, displaying dissociation constants (K_d) of 117 nm and 19 μ m, respectively (Murthy *et al*, 1994; Werbovets *et al*, 2003). The work described here could be expanded in future to measure K_d for dinitroanilines, phosphorothioamidates and other related agents on *P. falciparum* tubulin, for example by fluorescence quenching or surface plasmon resonance. In this way it may be possible to identify agents with lower K_d and greater potency against cultured parasites. Thus, the identification of the herbicide-binding site on tubulin would appear to constitute a very promising approach to new antimalarial drug design.

7.2. TUBULINS OF *P. FALCIPARUM*

The key to gaining a biological appreciation of *P. falciparum* tubulin and its potential usefulness as a target for drug therapy is through its characterisation, something only feasible if the tubulin is purified in an assembly-competent form. As outlined earlier, this has yet to be achieved with *P. falciparum* tubulins and consequently most studies of parasite microtubules have been confined to intact-cell techniques. In response to this, our approach was to produce recombinant forms of

these proteins. Although it was previously believed that recombinant tubulin produced in *E. coli* does not fold properly and is non-functional (Yaffe *et al*, 1988), this appears not be the case, as indicated by our studies and recent reports which have outlined the characterisation of assembly-competent recombinant tubulins expressed in *E. coli* from various protozoan parasites (see Table 4.1).

Although our initial attempts at characterising authentic, refolded, recombinant *P. falciparum* tubulins were unsuccessful, more encouraging results were achieved with the tubulins expressed in *E. coli* with the fusion partner MBP. Recombinant MBP- α I tubulin fusion displayed assembly competency as it was incorporated in the microtubules of bovine brain tubulin. Previous studies have shown similar findings in that intracellular and *in vitro* co-polymerisation of protozoan and higher plant/animal tubulins have given rise to such hybrid polymers (Linder *et al*, 1998; Lubega *et al*, 1993; Phadtare *et al*, 1994; Prescott *et al*, 1989; Vantard *et al*, 1990). However, the results achieved with MBP- β -tubulin were less clear-cut. The reason why α I-tubulin fusion should be incorporated into microtubules more efficiently than the β -tubulin fusion remains unclear. Nevertheless, although further work remains to be done, including the successful removal of the MBP-tag, we have clearly paved the way towards gaining a better understanding of *P. falciparum* tubulin and associated microtubular structures *in vitro*. In addition to the characterisation of recombinant *P. falciparum* tubulins, it will also be important to determine if native parasite tubulins are post-translationally modified. This may be accomplished using specialised techniques such as mass spectrometry or tandem-mass spectrometry or by use of antibodies that specifically recognise the presence of such modifications.

7.3. PLASMODIUM FALCIPARUM TUBULIN AS A CHEMOTHERAPEUTIC TARGET: FUTURE DIRECTIONS

With ~ 41% of the world's population at risk of malaria (Olliaro *et al*, 2001) and the continual spread of drug resistance among the malarial parasites to most established anti-malarial agents, there is a urgent need to develop new drugs. In response to this, we have investigated the likelihood that the microtubular cytoskeleton and its protein tubulin of *P. falciparum* might constitute a fruitful chemotherapeutic target. Differences in amino acid sequences and in a number of biochemical properties of tubulin (e.g. drug binding, peptide mapping patterns,

electrophoretic mobilities) from lower eukaryotes such as the parasitic protozoa and helminths compared with those of higher eukaryotes like mammals makes it possible selectively to target parasite tubulin (Dawson *et al*, 1984; Traub-Cseko *et al*, 2001; this study).

Although our studies (as well as those of other groups) with microtubule inhibitors from anti-cancer programmes such as dolastatin 10, vinblastine and Taxol have proved useful in probing microtubule function in the parasite, such non-selective agents have no prospects as antimalarial drugs. However, the selective antimalarial activity of dinitroaniline herbicides, which we have now extended to include the phosphorothioamidate herbicides, and their interaction with *P. falciparum* tubulin both in culture and *in vitro* provides motivation for their further exploration as antimalarial agents. Much needs to be addressed, however, before antimitotic herbicides can be considered for clinical use. Firstly, the potencies of dinitroanilines and the phosphorothioamidate APM for parasite growth inhibition lie far behind those of established antimalarials such as chloroquine and mefloquine (Geary *et al*, 1989). For further pre-clinical development, antimitotic herbicides effective at least in the sub-micromolar range will be required. To this end, encouraging results have recently been reported by Werbovetz and co-workers who have developed analogs of the dinitroaniline oryzalin that were more potent in culture against *L. donovani* and *T. brucei brucei* than the parent compound (Werbovetz *et al*, 2003; Bhattacharya *et al*, 2004). One agent (compound 35) possessed an IC₅₀ value of 120 nM against cultured *T. brucei*, inhibited the assembly of *Leishmania* tubulin with an IC₅₀ of 6.9 µM, and showed little effect on purified mammalian tubulin. Therefore, it does seem reasonable that antimitotic herbicides with heightened efficacy against cultured *P. falciparum* are a realistic target. Perhaps the synthetic modification of APM, based on the success of the new oryzalin analogues, may be a worthwhile pursuit in the search for more potent antimitotic herbicides.

Knowing details of the antimitotic herbicide-binding site on *P. falciparum* tubulin would surely prove to be the most rational way to aid in the design of more effective ligands. While a number of putative sites, based predominantly on homology modelling of the crystal structure of the bovine αβ-tubulin heterodimer (Nogales *et al*, 1998) have now been suggested (Blume *et al*, 2003; Morrissette *et al*, 2004; this study), these remain to be experimentally verified. An X-ray crystal

structure of recombinant *P. falciparum* tubulins would provide greater insight into structural differences between *P. falciparum* and mammalian tubulins. The large affinity-tag, MBP, may possibly hinder crystal growth due to conformational heterogeneity, but recently crystal structures of fusion proteins with such tags have been reported (Smyth *et al*, 2003). The use of analogues of antimetabolic herbicides in affinity labelling experiments could also help in locating this site on *Plasmodium* tubulin, just as affinity labelling experiments provided information pertaining to the colchicine, taxol and “*Vinca*” alkaloid binding sites on mammalian tubulin (Nogales *et al*, 1998; Ravelli *et al*, 2004). At the very least, the determination of dissociation constants between antimetabolic herbicides and recombinant *P. falciparum* tubulins will be helpful in quantifying selectivity.

Secondly, the fact that these compounds may be implicated in host toxicity, possibly due to the presence of aromatic nitro groups, is of concern. The U.S. Environmental Protection Agency (EPA) has classified the dinitroaniline trifluralin as a Category C (possible human) carcinogen (U.S. Environmental Protection Agency, 1987). A recent study has also shown that trifluralin induced some side effects in animals at the highest dose tested (six doses of 600 mg/kg), although histopathological examination of sacrificed rats displayed no abnormalities (Dow *et al*, 2002). However, there are studies that fail to demonstrate that trifluralin is carcinogenic. For example, in a 2-year study in which trifluralin was fed to B6C3F₁ mice, no increase of benign or malignant neoplasms was observed (Francis *et al*, 1991). Similarly, trifluralin was also found to protect against benzo(a)pyrene induction of lung and forestomach tumors in A/J mice (Triano *et al*, 1985). Overall, such disputed indications of potential carcinogenicity suggest that such herbicides would have to be modified extensively in order to progress towards clinical development.

Thirdly, the low aqueous solubility of dinitroanilines has been suggested to be a major contributor to their poor pharmacokinetics (Morejohn *et al*, 1991). In the aforementioned rodent model of malaria, it was found that the lack of *in vivo* antimalarial activity of trifluralin was possibly due to the low water-solubility of trifluralin resulting in its poor adsorption and insufficient plasma concentrations (Dow *et al*, 2002). In an attempt to overcome the low solubility and poor transport profiles of the dinitroanilines, trifluralin has been linked to a number of different sugar moieties to give glycoconjugated dinitroanilines (Mead *et al*, 2003). The

resulting analogues were found to retain moderate activity (IC₅₀ 3 - 8 μ M) against cultured *Cryptosporidium parvum*. In conclusion, such agents as well as APM, which displays superior solubility to the dinitroanilines, could give greater efficacy in a similar rodent model of malaria and may merit further investigation.

While our studies have indicated an interaction between microtubule inhibitors and *P. falciparum* tubulins both intracellularly and *in vitro*, much work pertaining to the characterisation of *P. falciparum* tubulin and its validation as a drug target remains. Our initial attempts to refold native recombinant *P. falciparum* tubulin to form functional microtubules proved unsuccessful. Perhaps the use of rabbit reticulocyte lysates (RRL), enriched in tubulin folding machinery could prove be a more successful method for the *in vitro* refolding of bacterially-expressed, insoluble *P. falciparum* tubulins as has proved to be the case with recombinant mammalian tubulins (Shah *et al*, 2001). However, given that this technique is labour-intensive and yields of functional tubulin are moderate (tens of micrograms), soluble tubulin expressed in *E. coli* remains a more attractive option. This is confirmed by our encouraging results with *P. falciparum* α I-tubulin expressed as a soluble recombinant fusion protein, which appears to be assembly-competent. In addition, a recent study of MacDonald *et al* (2004) has indicated the formation of microtubules from recombinant α - and β - tubulins of a number of protozoan parasites expressed in the soluble form in *E. coli*.

The fact that MacDonald and co-workers used a similar *E. coli*-based expression system to ours for the production of functional tubulin and achieved the successful removal of the MBP-tag encourages us to believe that *P. falciparum* microtubule formation from soluble recombinant tubulins may be realised. Key to this will be the removal of the large MBP-tag. The ability of *P. falciparum* MBP- α I-tubulin to copolymerise with bovine tubulin will, however, facilitate subsequent experimentation with antimitotic herbicides and other microtubule inhibitors. In addition, it will be important to establish the extent and distribution of recombinant α I-tubulin incorporation into the hybrid microtubules by use of immunofluorescence and electron microscopy.

Although microtubules are composed chiefly of the α - and β -polypeptides of tubulin, a variety of microtubule-associated proteins (MAPs) are imputed to diversify the function of microtubules and thus, may represent potential drug candidates. A number of MAP's have been identified in mammalian cells and

examples of these include the microtubule motor proteins kinesin and dynein that are involved in intracellular transport (Scholey *et al*, 1994), the MAP 1, 2 and 4 family (Bullinski, 1994) involved in microtubule stabilisation, stathmin (Ravelli *et al*, 2004), which is involved in microtubule destabilisation, and tektins (Stephens, 1998), which form extended filaments in the walls of flagellar microtubules. Little information on MAPs in the malarial parasites exists apart from the identification of the microtubule motor proteins dynein and kinesin in *P. falciparum* merozoites (Fowler *et al*, 2001). Therefore, *P. falciparum* recombinant tubulins could be used to for *in vitro* pull-down assays with parasite extracts to aid in the identification of such MAPS. Alternatively, the interaction of *P. falciparum* recombinant tubulins with “candidate” binding partners could be analysed, for example using surface plasma resonance technology (BIAcore®). This has proved successful in identifying a bimolecular interaction between the recombinant GST- β -tubulin fusion protein of *Tetrahymena pyriformis* and elongation factor 1 α (EF-1 α) which plays an essential role in translation of mRNA in ribosomes of eukaryotic cells (Nakazawa *et al*, 1999).

Although the genetic manipulation of *Plasmodium* species is possible (de Konig-Ward *et al*, 2000), establishment of stable transfections has been notoriously difficult. Recently, however, strains of *P. falciparum* and *P. berghei* that constitutively express GFP have been established (Franke-Fayard *et al*, 2004 and Rug *et al*, 2004). Available data strongly support the view that expression of GFP-tubulin and its incorporation into microtubules does not detectably interfere with microtubule function in a range of eukaryotes (Rusan *et al*, 2001). Therefore, *Plasmodium* species expressing such GFP-tubulin constructs may prove to be a valuable tool for the analysis of microtubule dynamics, organisation and behaviour throughout the parasite cell cycle, and may also play an important role in the analysis of the effects of candidate microtubule inhibitors in intact cells.

In addition to tubulins’ promise as a potential drug target, Lubega and co-workers have recently suggested it may also represent a possible vaccine candidate against African trypanosomiasis (Lubega *et al*, 2002a). Intriguingly, mice immunised with a tubulin-rich preparation from *T. brucei* conferred broad protection against African trypanosomiasis (Lubega *et al*, 2002a). The same group have also shown that anti-tubulin antibodies specifically inhibit trypanosome growth in culture (Lubega *et al*, 2002b). Their reasoning for the inhibition of parasite growth was unclear, but the antibodies did appear to be internalised by the trypanosomes, which may have led to

tubulin binding and subsequently microtubule depolymerisation. This raises the issue of the usefulness of *P. falciparum* tubulin as a similar vaccine candidate. This is unlikely, however, given the fact that most stages of the asexual cycle of *P. falciparum* are confined within the erythrocyte and the relative scarcity of tubulin in the parasite cell compared to trypanosomes. On the other hand, the *P. falciparum* merozoite, the only extracellular stage of development in the blood, which encloses a narrow band of subpellicular microtubules (f-MAST) important for erythrocyte invasion (Bejon *et al*, 1997; Fowler *et al*, 1998), may comprise a potential target. As we have both purified *P. falciparum* recombinant tubulins and have antibodies specific to both proteins, an investigation into the potential of *P. falciparum* tubulin as an immunotherapeutic target may constitute a worthwhile enterprise.

The work described in this thesis clearly shows the potential of *P. falciparum* tubulins as a chemotherapeutic target. Knowledge of the molecular interactions between microtubule inhibitors and *P. falciparum* tubulin is fundamental to the development of novel antimalarial agents with low host toxicity, suitable pharmacokinetic properties and potent activity. By employing an extensive drug development strategy to allow for the evaluation of lead compounds against cultured parasites and mammalian cells, their use in animal malaria models and in biochemical tubulin-binding assays together with computer modeling of *Plasmodium* tubulins may help to facilitate the development of selective antimalarial agents of chemotherapeutic value.

References

- Adoutte, A., Claisse, M., and Cance, J.** 1984. Tubulin evolution: an electrophoretic and immunological analysis. *Origins life* **13**: 177-182.
- Aikawa, M.** 1967. Ultrastructure of the pellicular complex of *Plasmodium fallax*. *J Cell Biol* **35**: 103-113.
- Aikawa, M.** 1971. Parasitological review. *Plasmodium*: the fine structure of malarial parasites. *Exp Parasitol* **30**: 284-320.
- Akella, R., Arasu, P., and Vaidya, A. B.** 1988. Molecular clones of alpha-tubulin genes of *Plasmodium yoelii* reveal an unusual feature of the carboxy terminus. *Mol Biochem Parasitol* **30**: 165-174.
- Algaier, J., and Himes, R. H.** 1988. The effects of dimethyl sulfoxide on the kinetics of tubulin assembly. *Biochim Biophys Acta* **954**: 235-243.
- Al-Olayan, E. M., Williams, G. T., and Hurd, H.** 2002. Apoptosis in the malaria protozoan, *Plasmodium berghei*: a possible mechanism for limiting intensity of infection in the mosquito. *Int J Parasitol* **32**: 1133-1143.
- Altmann, K. H.** 2001. Microtubule-stabilising agents: a growing class of important anticancer drugs. *Curr Opin Chemical Biology* **5**: 424-431.
- Altschul, S. F., Gish, W., Miller, W., Myers, E. W., and Lipman, D. J.** 1990. Basic local alignment search tool. *J Mol Biol* **25**: 403-410.
- Amos, L. A.** 2000. Focusing-in on microtubules. *Curr Opin Struct Biol* **10**: 236-241.
- Amos, L. A.** 2004. Microtubule structure and its stabilisation. *Org Biomol Chem* **2**: 2153-2160.
- Andreu, J. M., Oliva, M. A., and Monasterio, O.** 2002. Reversible unfolding of FtsZ cell division proteins from archaea and bacteria. Comparison with eukaryotic tubulin folding and assembly. *J Biol Chem* **277**: 43262-43270.
- Andresen, M., Schmitz-Salue, R., and Jakobs, S.** 2004. Short tetracysteine tags to β -tubulin demonstrate the significance of small labels for live cell imaging. *Mol Biol Cell* **15**: 5616-5622.
- Ansorge, W.** 1985. Fast and sensitive detection of protein and DNA bands by treatment with potassium permanganate. *J Biochem Biophys Meth* **11**: 13-20.
- Anthony, R. G., and Hussey, P. J.** 1999a. Dinitroaniline herbicide resistance and the microtubule cytoskeleton. *Trends Plant Sci* **4**: 112-116.
- Anthony, R. G., and Hussey, P. J.** 1999b. Double mutation in *Eleusine indica* α -tubulin increases the resistance of transgenic maize calli to dinitroaniline and phosphorothioamidate herbicides. *Plant J* **18**: 669-674.

Baca, A. M., and Hol, W. G. J. 2000. Overcoming codon bias: a method for high-level overexpression of *Plasmodium* and other AT-rich parasite genes in *Escherichia coli*. *Int J Parasitol* **30**: 113-118.

Bai, R., Covell, D. G., Taylor, G. F., Kepler, J. A., Copeland, T. D., Nguyen, N. Y., Pettit, G. R., and Hamel, E. 2004. Direct photoaffinity labelling by dolastatin 10 of the amino-terminal peptide of β -tubulin containing cysteine 12. *J Biol Chem* **279**: 30731-30740.

Bajer, A. S., and Molé-Bajer, J. 1986. Drugs with colchicine-like effects that specifically disassemble plant but not animal microtubules. *Ann NY Acad Sci* **466**: 767-784.

Banerjee, R., and Goldberg, D. E. 2001. The *Plasmodium* food vacuole. In: Antimalarial Chemotherapy. Mechanisms of action, resistance, and new directions in drug discovery. Rosenthal, P. J. (Ed), Humana Press, Totowa, New Jersey. pp 43-63.

Bannister, L. H., Hopkins, J. M., Dluzewski, A. R., Margos, G., Williams, I. T., Blackman, M. J., Kocken, C. H., Thomas, A. W., and Mitchell, G. H. 2003. *Plasmodium falciparum* apical membrane antigen 1 (PfAMA-1) is translocated within micronemes along subpellicular microtubules during merozoite development. *J Cell Science* **116**: 3825-3834.

Bannister, L. H., Hopkins, J. M., Fowler, R. E., Krishna, S., and Mitchell, G. H. 2000. A brief illustrated guide to the ultrastructure of *Plasmodium falciparum* asexual blood stages. *Parasitol Today* **16**: 427-433.

Bannister, L., and Mitchell, G. 2003. The ins, outs and roundabouts of malaria. *Trends Parasitol* **19**: 209-213.

Barahona, I., Soares, H., Cyrne, L., Penque, D., Denoulet, P., and Rodrigues-Pousada, C. 1988. Sequence of one α - and two β -tubulin genes of *Tetrahymena pyriformis*. *J Mol Biol* **202**: 365-382.

Basco, L. K., Marquet, F., Makler, M. T., and Le Bras, J. 1995. *Plasmodium falciparum* and *Plasmodium vivax*: lactate dehydrogenase activity and its application for *in vitro* drug susceptibility assay. *Exp Parasitol* **80**: 260-271.

Bejon, P. A., Bannister, L. H., Fowler, R. E., Fookes, R. E., Webb, S. E., Wright, A., and Mitchell, G. H. 1997. A role for microtubules in *Plasmodium falciparum* merozoite invasion. *Parasitol* **114**: 1-6.

Belkum, A. V., Janse, C., and Mons, B. 1991. Nucleotide sequence variation in the β -tubulin genes from *Plasmodium berghei* and *Plasmodium falciparum*. *Mol Biochem Parasitol* **47**: 251-254.

Bell, A. 1998. Microtubule inhibitors as potential antimalarial agents. *Parasitol Today*. **14**: 234-240.

Bell, A. 2000. Recent developments in the chemotherapy of malaria. *Curr Op Anti Infect Invest Drugs* **2**: 63-70.

Bell, A. 2000-2004. Personal communication

Bell, A., Wernli, B., and Franklin, R. M. 1993. Effect of microtubule inhibitors on protein synthesis in *Plasmodium falciparum*. *Parasitol Res* **79**: 146-152.

Bell, A., Wernli, B., and Franklin, R. M. 1995. Expression and secretion of malarial parasite β -tubulin in *Bacillus brevis*. *Biochimie* **77**: 256-261.

Berman, M. H., Westbrook, J., Feng, G., Gilliland, T. N., Bhat, H., Weissig, I. N., Sindyalov, P. E., and Bourne, P. E. 2000. The protein data bank. *Nucleic Acids Res* **28**: 235-242.

Best, D., Warr, P. J., and Gull, K. 1981. Influence of the composition of commercial sodium dodecyl sulfate preparations on the separation of α - and β -tubulin during polyacrylamide gel electrophoresis. *Anal Biochem* **114**: 281-284.

Bhattacharya, G., Herman, J., Delfin, D., Salem, M. M., Barszcz, T., Mollet, M., Riccio, G., Brun, R., and Werbovetz, K. A. 2004. Synthesis and antitubulin activity of N¹- and N⁴-substituted 3,5-dinitrosulfanilamides against African trypanosomes and *Leishmania*. *J Med Chem* **47**: 1823-1832.

Bloom, G. S. 1992. Motor proteins for cytoplasmic microtubules. *Curr Opin Cell Biol* **4**: 66-73.

Blume, Y. B., Nyporko, A. Y., Yemets, A. I., and Baird, W. V. 2003. Structural modeling of the interaction of plant α -tubulin with dinitroaniline and phosphoramidate herbicides. *Cell Biol Int* **27**: 171-174.

Borisy, G. G., and Taylor, E. W. 1967. The mechanism of action of colchicine. Binding of colchicine-³H to cellular protein. *J Cell Biol* **34**: 525-533.

Bradford, M. M. 1976. A rapid and sensitive method for the quantitation of microgram quantities of protein utilising the principle of protein-dye binding. *Anal Biochem* **72**: 248-254.

Breman, J. G. 2001. The ears of the hippopotamus: manifestations, determinants, and estimates of the malaria burden. *Am J Trop Med Hyg* **64**: 1-11.

Breman, J. G., Alilio, M. S., and Mills, A. 2004. Conquering the intolerable burden of malaria: what's new, what's needed: a summary. *Am J Trop Med Hyg* **71**: 1-15.

Bryan, J., and Wilson, L. 1971. Are cytoplasmic microtubules heteropolymers? *Proc Natl Acad Sci USA* **8**: 1762-1766.

Bulinski, J. C. 1994. MAP4. *In: Microtubules*. Hyams, J. S., and Lloyd, C. W. (Eds.), Wiley-Liss, Inc., New York, NY. pp 167-182.

- Burns, R. G., and Surridge, C. D.** 1994. Tubulin: conservation and structure. *In: Microtubules.* Hyams, J. S., and Lloyd, C. W. (Eds.), Wiley-Liss, Inc., New York, NY. pp 3-31.
- Butler, D., Maurice, J., and O' Brien, C.** 1997. Time to put malaria control on the global agenda. *Nature* **386**: 535-541.
- Callahan, H. L., Kelley, C., Pereira, T., and Grogl, M.** 1996. Microtubule inhibitors: structure-activity analyses suggest rational models to identify potentially active compounds. *Antimicrob Agents Chemother* **40**: 947-952.
- Calvo, E., Rubiano, C., Vargas, A., and Wasserman, M.** 2002. Expression of housekeeping genes during the asexual cell cycle of *Plasmodium falciparum*. *Parasitol Res* **88**: 267-271.
- Canning, E. U., and Sinden, R. E.** 1973. The organisation of the ookinete and observations on nuclear division in oocysts of *Plasmodium berghei*. *Parasitol* **67**: 29-40.
- Chan, M. M-Y., and Fong, D.** 1990. Inhibition of Leishmanias but not host macrophages by the antitubulin herbicide trifluralin. *Science* **249**: 924-926.
- Chan, M. M-Y, Triemer, R. E., and Fong D.** 1991. Effect of the anti-microtubule drug oryzalin on growth and differentiation of the parasitic protozoan *Leishmania mexicana*. *Differentiation* **46**: 15-21.
- Chan, M. M-Y., Tzeng, J., Emge, T. J., Ho, C-T., and Fong D.** 1993. Structure-function analysis of antimicrotubule dinitroanilines against promastigotes of the parasitic protozoan *Leishmania mexicana*. *Antimicrob Agents Chemother* **37**: 1909-1913.
- Clark, I. A., and Schofield, L.** 2000. Pathogenesis of malaria. *Parasitol Today* **16**: 451-454.
- Clayton, L., Quinlan, R. A., Roobol, A., Pogson, C. I., and Gull, K.** 1980. A comparison of tubulins from mammalian brain and *Physarum polycephalum* using SDS-polyacrylamide gel electrophoresis and peptide mapping. *FEBS Lett* **115**: 301-305.
- Cleveland, D. W., Lopata, M. A., Sherline, P., and Kirschner, M. W.** 1981. Unpolymerised tubulin modulates the level of tubulin mRNAs. *Cell* **25**: 537-546.
- Cleveland, D. W., and Sullivan, K. F.** 1985. Molecular biology and genetics of tubulin. *Annu Rev Biochem* **54**: 331-365.
- Clough, B., and Wilson, R. J. M.** 2001. Antibiotics and the plasmodial plastid organelle. *In: Antimalarial Chemotherapy. Mechanisms of action, resistance, and new directions in drug discovery.* Rosenthal, P. J. (Ed), Humana Press, Totowa, New Jersey. pp 265-286.

- Cowan, N. J.** 1998. Mammalian cytosolic chaperonin. *Methods Enzymol* **290**: 230-241.
- Cowman, A. F., and Crabb, B. S.** 2002. The *Plasmodium falciparum* genome - a blueprint for erythrocyte invasion. *Science* **298**: 126-128.
- Cruz-Monserrate, Z., Mullaney, J. T., Harran, P. G., Pettit, G. R., and Hamel, E.** 2003. Dolastatin 15 binds in the vinca domain of tubulin as demonstrated by hummel-dreyer chromatography. *Eur J Biochem* **270**: 3822-3828.
- Culvenor, J. G., Day, K. P., and Anders, R. F.** 1991. *Plasmodium falciparum* ring-infected erythrocyte surface antigen is released from merozoite dense granules after erythrocyte invasion. *Infect Immun* **59**: 1183-1187.
- Cytoskeleton Inc., (anonymous).** 2004. Instruction manual for tubulin polymerisation assay kit. pp. 1-7.
- Cyr, R. J., Sotak, M., Bustos, M. M., Gultinan, M. J., and Fosket, D. E.** 1987. Changes in the relative electrophoretic mobility of higher plant tubulin subunits in SDS-polyacrylamide gels. *Biochim Biophys Acta* **914**: 28-34.
- Das, A., Elmendorf, H. G., Li, W., and Haldar, K.** 1994. Biosynthesis, export and processing of a 45 kDa protein detected in membrane clefts of erythrocytes infected with *Plasmodium falciparum*. *Biochem J* **302**: 487-496.
- Dawson, P. J., Gutteridge, W. E., and Gull, K.** 1984. A comparison of the interaction of anthelmintic benzimidazole, with tubulin isolated from mammalian tissue and the parasite nematode *Ascaridia galli*. *Biochem Pharmacol* **33**: 1069-1074.
- de Koning-Ward, F., Janse, C. J., and Waters, A. P.** 2000. The development of genetic tools for dissecting the biology of malaria parasites. *Annu Rev Microbiol* **54**: 157-185.
- Delgado, P., Romero, M. D. R., and Torres, A.** 1991. Alpha/beta inversion of the *Euplotes* and *Oxytricha* tubulins. *Cytobios* **66**: 87-91.
- Delves, C. J., Ridley, R. G., Goman, M., Holloway, S. P., Hyde, J. E., and Scaife, J. G.** 1989. Cloning of a β -tubulin gene from *Plasmodium falciparum*. *Mol Microbiol* **3**: 1511-1519.
- Delves, C. J., Alano, P., Ridley, R. G., Goman, M., Holloway, S. P., Hyde, J. E., and Scaife, J. G.** 1990. Expression of α and β tubulin genes during the asexual and sexual blood stages of *Plasmodium falciparum*. *Mol Biochem Parasitol* **43**: 271-278.
- Dieckmann-Schuppert, A., and Franklin, R. M.** 1989. Compounds binding to cytoskeletal proteins are active against *Plasmodium falciparum* *in vitro*. *Cell Biol Int Rep* **13**: 411-418.

- Dow, G. S., Armson, A., Boddy, M. R., Itenge, T., McCarthy, D., Parkin, J. E., Thompson, R. C. A., and Reynoldson, J. A.** 2002. *Plasmodium*: assessment of the antimalarial potential of trifluralin and related compounds using a rat model of malaria, *Rattus norvegicus*. *Exp Parasitol* **100**: 155-160.
- Downing, K. H.** 2000. Structural basis for the interaction of tubulin with proteins and drugs that affect microtubule dynamics. *Annu Rev Cell Dev Biol* **16**: 89-111.
- Downing, K. H., and Nogales, E.** 1999. Crystallographic structure of tubulin: implications for dynamics and drug binding. *Cell Struct Func* **24**: 269-275.
- Dumontet, C.** 2000. Mechanisms of action and resistance to tubulin-binding agents. *Exp Opin Invest Drugs* **9**: 779-788.
- Ellis, J. R., Taylor, R., and Hussey, P. J.** 1994. Molecular modeling indicates that two chemically distinct classes of anti-mitotic herbicide bind to the same receptor site(s). *Plant Physiol* **105**: 15-18.
- Fennell, B. J., Carolan, S., Pettit, G.R., and Bell, A.** 2003. Effects of the antimitotic natural product dolastatin 10, and related peptides, on the human malarial parasite *Plasmodium falciparum*. *J Antimicrob Chemother* **51**: 833-841.
- Fidock, D. A., Rosenthal, P. J., Croft, S. L., Brun, R., and Nwaka, S.** 2004. Antimalarial drug discovery: efficacy models for compound screening. *Nature Rev* **3**: 509-520.
- Fong, D., and Chang, K.** 1981. Tubulin biosynthesis in the developmental cycle of a parasitic protozoan, *Leishmania mexicana*: changes during differentiation of motile and nonmotile stages. *Proc Natl Acad Sci USA* **78**: 7624-7628.
- Fowler, R. E., Fookes, R. E., Lavin, F., Bannister, L. H. and Mitchell, G. H.** 1998. Microtubules in *Plasmodium falciparum* merozoites and their importance for invasion of erythrocytes. *Parasitol* **117**: 425-433.
- Fowler, R. E., Smith, A. M. C., Whitehorn, J., Williams, I. T., Bannister, L. H. and Mitchell, G. H.** 2001. Microtubule associated motor proteins of *Plasmodium falciparum* merozoites. *Mol Biochem Parasitol* **117**: 187-200.
- Francis, P. C., Emmerson, J. L., Adams, E. R., and Owens, N. V.** 1991. Oncogenicity study of trifluralin in B6C3F1 mice. *Food Chem Toxicol* **29**: 549-555.
- Franke-Fayard, B., Trueman, H., Ramesar, J., Mendoza, J., van der Keur, M., van der Linden, R., Sinden, R. E., Waters, A. P., and Janse, C. J.** 2004. A *Plasmodium berghei* reference line that constitutively expresses GFP at a high level throughout the complete life cycle. *Mol Biochem Parasitol* **137**: 23-33.
- Fulton, C., and Simpson, P. A.** 1976. Selective synthesis and utilisation of flagellar tubulin. The multitubulin hypothesis. *In*: Cell motility. Goldman, R., Pollard, T., and Rosenbaum, J. (Eds.), Cold Spring Harbor Laboratory, Cold Spring Harbour, New York. pp 987-1005.

Ganesh, T., Guza, R. C., Bane, S., Ravindra, R., Shanker, N., Lakdawala, A. S., Snyder, J. P., and Kingston, D. G. I. 2004. The bioactive Taxol conformation on β -tubulin: experimental evidence from highly active constrained analogs. *Proc Natl Acad Sci USA* **101**: 10006-10011.

Gao, Y., Vainberg, I. E., Chow, R. L., and Cowan, N. J. 1993. Two cofactors and cytoplasmic chaperonin are required for the folding of α - and β -tubulin. *Mol Cell Biol* **13**: 2478-2485.

Gardner, M. J., Hall, N., Fung, E., White, O., Berriman, M., Hyman, R. W., Carlton, J. M., Pain, A., Nelson, K. E., Bowman, S., Paulsen, I. T., James, K., Eisen, J. A., Rutherford, K., Salzberg, S. L., Craig, A., Kyes, S., Chan, M. S., Nene, V., Shallom, S. J., Suh, B., Peterson, J., Angiuoli, S., Pertea, M., Allen, J., Selengut, J., Haft, D., Mather, M. W., Vaidya, A. B., Martin, D. M., Fairlamb, A. H., Fraunholz, M. J., Roos, D. S., Ralph, S. A., McFadden, G. I., Cummings, L. M., Subramanian, G. M., Mungall, C., Venter, J. C., Carucci, D. J., Hoffman, S. L., Newbold, C., Davis, R. W., Fraser, C. M., and Barrell, B. 2002. Genome sequence of the human malaria parasite *Plasmodium falciparum*. *Nature* **419**: 498-511.

Gavigan, C. S., Kiely, S. P., Hirtzlin, J., and Bell, A. 2003. Cyclosporin-binding proteins of *Plasmodium falciparum*. *Int J Parasitol* **33**: 987-996.

Geary, T. G., Divo, A. A., and Jensen, J. B. 1989. Stage specific actions of antimalarial drugs on *Plasmodium falciparum* in culture. *Am J Trop Med Hyg* **40**: 240-244.

Greenwood, B. 2004. Between hope and a hard place. *Nature* **430**: 926-927.

Guha, S., and Bhattacharyya, B. 1997. Refolding of urea-denatured tubulin: recovery of natively like structure and colchicine binding activity from partly unfolded states. *Biochemistry* **36**: 13208-13213.

Guinet, F., Dvorak, J. A., Fujioka, H., Keister, D. B., Muratova, O., Kaslow, D. C., Aikawa, M., Vaidya, A. B., and Wellems, T. E. 1996. A developmental defect in *Plasmodium falciparum* male gametogenesis. *J Cell Biol* **135**: 269-278.

Gull, K. 1999. The cytoskeleton of trypanosomatid parasites. *Annu Rev Microbiol* **53**: 629-655.

Gull, K. 2001. Protist tubulins: new arrivals, evolutionary relationships and insights to cytoskeletal function. *Curr Opin Microbiol* **4**: 427-432.

Hadfield, J. A., Ducki, S., Hirst, N., and McGowan, A. T. 2003. Tubulin and microtubules as targets for anticancer drugs. *Prog Cell Cycle Res* **5**: 309-325.

Haldar, K., and Akompong, T. 2001. Transport and trafficking in *Plasmodium*-infected red cells. *In: Antimalarial Chemotherapy. Mechanisms of action, resistance, and new directions in drug discovery.* Rosenthal, P. J. (Ed), Humana Press, Totowa, New Jersey. pp 27-41.

- Havens, C. G., Bryant, N., Asher, L., Lamoreaux, L., Perfetto, S., Brendle, J. J., and Werbovetz, K. A.** 2000. Cellular effects of leishmanial tubulin inhibitors on *L. donovani*. *Mol Biochem Parasitol* **110**: 223-236.
- Haynes, R. K., and Krishna, S.** 2004. Artemisinins: activities and actions. *Microb Infect* **6**: 1339-1346.
- Heald, R., and Nogales, E.** 2002. Microtubule dynamics. *J Cell Science* **115**: 3-4.
- Hess, F. D. and Bayer, D. E.** 1977. Binding of the herbicide trifluralin to *Chlamydomonas* flagellar tubulin. *J Cell Sci* **24**: 351-360.
- Hess, F. D.** 1979. The influence of the herbicide trifluralin on flagellar regeneration in *Chlamydomonas*. *Exp Cell Res* **119**: 99-109.
- Higgins, D. G., Thompson, J. D., and Gibson, T. J.** 1996. Using CLUSTAL for multiple sequence alignments. *Methods Enzymol* **266**: 383-402.
- Hollomon, D. W., Butters, J. A., Barker, H., and Hall, L.** 1998. Fungal β -tubulin, expressed as a fusion protein, binds benzimidazole and phenylcarbamate fungicides. *Antimicrob Agents Chemother* **42**: 2171-2173.
- Holloway, S. P., Sims, P. F. G., Delves, C. J., Scaife, J. G., and Hyde, J. E.** 1989. Isolation of α -tubulin genes from the human malaria parasite, *Plasmodium falciparum*: sequence analysis of α -tubulin. *Mol Microbiol* **3**: 1501-1510.
- Holloway, S. P., Gerousis, M., Delves, C. J., Sims, P. F. G., Scaife, J. G., and Hyde, J. E.** 1990. The tubulin genes of the human malaria parasite *Plasmodium falciparum*, their chromosomal location and sequence analysis of the α -tubulin II gene. *Mol Biochem Parasitol* **43**: 257-270.
- Hugdahl, J. D., and Morejohn, L. C.** 1993. Rapid and reversible high-affinity binding of the dinitroaniline herbicide oryzalin to tubulin from *Zea mays* L. *Plant Physiol* **102**: 725-740.
- Hussey, P. J., and Gull, K.** 1985. Multiple isotypes of α - and β -tubulin in the plant *Phaseolus vulgaris*. *FEBS* **181**: 113-118.
- Ifediba, T., and Vanderberg, J. P.** 1981. Complete *in vitro* maturation of *Plasmodium falciparum* gametocytes. *Nature* **294**: 364-366
- Ikeda, Y., and Steiner, M.** 1976. Isolation of platelet microtubule protein by an immunosorptive method. *J Biol Chem* **251**: 6135-6141.
- Inclán, Y. F., and Nogales, E.** 2001. Structural models for the self-assembly and microtubule interactions of γ -, δ - and ϵ -tubulin. *J Cell Science* **114**: 413-422.
- Jarvik, J., and Rosenbaum, J. L.** 1980. Oversized flagellar membrane protein in paralyzed mutants of *Chlamydomonas reinhardtii*. *J Cell Biol* **85**: 258-272.

- Jomaa, H., Wiesner, J., Sanderbrand, S., Altincicek, B., Weidemeyer, C., Hintz, M., Turbachova, I., Eberl, M., Zeidler, J., Lichtenthaler, H. K., Soldati, D., and Beck, E.** 1999. Inhibitors of the nonmevalonate pathway of isoprenoid biosynthesis as antimalarial drugs. *Science* **285**: 1573-1576.
- Kaidoh, T., Nath, J., Fujioka, H., Okoye, V., and Aikawa, M.** 1995. Effect and localisation of trifluralin in *Plasmodium falciparum* gametocytes: an electron microscopic study. *J Euk Microbiol* **42**: 61-64.
- Kapust, R. B., and Waugh, D. S.** 1999. *Escherichia coli* maltose-binding protein is uncommonly effective at promoting the solubility of polypeptides to which it is fused. *Protein Sci* **8**: 1668-1674.
- Kaytes, P. S., Theriault, N. Y., Poorman, R. A., Murakami, K., and Tomich, C-S. C.** 1986. High-level expression of human rennin in *Escherichia coli*. *J Biotechnol* **4**: 205-218.
- Kavallins, M., Verrillis, N. M., and Hill, B. T.** 2001. Anti-cancer therapy with novel tubulin interacting drugs. *Drug Resistance Update* **6**: 392-401.
- Kumar, N.** 1981. Taxol-induced polymerisation of purified tubulin. *J Biol Chem* **256**: 10435-10441.
- Kumar, N., Aikawa, M., and Grotendorst, C.** 1985. *Plasmodium gallinaceum*: critical role for microtubules in the transformation of zygotes into ookinetes. *Exp Parasitol* **59**: 239-247.
- Kurland, C., and Gallant, J.** 1996. Errors of heterologous protein expression. *Curr Opin Biotechnol* **7**: 489-493.
- Kwa, M. S. G., Veenstra, J. G., and Roos, M. H.** 1994. Benzimidazole resistance in *Haemonchus contortus* is correlated with a conserved mutation at amino acid 200 in β -tubulin isotype 1. *Mol Biochem Parasitol* **63**: 299-303.
- Lacey, E.** 1988. The role of the cytoskeletal protein, tubulin, in the mode of action and mechanism of drug resistance to benzimidazoles. *Int J Parasitol* **18**: 885-936.
- Laemmli, U. K.** 1970. Cleavage of structural proteins during assembly of the head of bacteriophage T4. *Nature* **227**: 680-685.
- Lajoie-Mazenc, I., Tollon, Y., Detraves, C., Julian, M., Moisand, A., Gueth-Hallonet, C., Debec, A., Salles-Passador, I., Puget, A., Mazarguil, H., Raynaud-Messina, B., and Wright, M.** 1994. Recruitment of antigenic γ -tubulin during mitosis in animal cells: presence of γ -tubulin in the mitotic spindle. *J Cell Sci* **107**: 2825-2837.
- Lambros, C., and Vanderberg, J. P.** 1979. Synchronisation of *Plasmodium falciparum* erythrocytic stages in culture. *J Parasitol* **65**: 418-420.
- Landfear, S. M., McMahon-Pratt, D., and Wirth, D. F.** 1983. Tandem

arrangement of tubulin genes in the protozoan parasite *Leishmania enriettii*. *Mol Cell Biol* **3**: 1070-1076.

Lee, V. D., and Huang, B. 1990. Missense mutations at lysine 350 in β -tubulin confer altered sensitivity to microtubule inhibitors in *Chlamydomonas*. *Plant Cell* **2**: 1051-1057.

Le Roch, K. G., Zhou, Y., Blair, P. L., Grainger, M., Moch, J. K., Haynes, J. D., De La Vega, P., Holder, A. A., Batalov, S., Carucci, D. J., and Winzeler, E. A. 2003. Discovery of gene function by expression profiling of the malaria parasite life cycle. *Science* **301**: 1503 - 1508.

Li, H., DeRosier, D. J., Nicholson, W. V., Nogales, E., and Downing, K. H. 2002. Microtubule structure at 8 Å resolution. *Structure* **10**: 1317-1328.

Linder, S., Schliwa, M., and Kube-Granderath, E. 1997. Sequence analysis and immunofluorescence study of α - and β -tubulins in *Reticulomyxa filosa*: implications of the high degree of 2-tubulin divergence. *Cell Motil Cytoskel* **36**: 164-178.

Linder, S., Schliwa, M., and Kube-Granderath, E. 1998. Expression of *Reticulomyxa filosa* α - and β -tubulins in *Escherichia coli* yields soluble and partially correctly folded material. *Gene* **212**: 87-94.

Llorca, O., Martin-Benito, J., Gomez-Puertas, P., Ritco-Vonso-vici, M., Willison, K. R., Carrascosa, J. L., and Valpuesta, J. M. 2001. Analysis of the interaction between the eukaryotic chaperonin CCT and its substrates actin and tubulin. *J Struct Biol* **135**: 205-218.

López-Antuñano, F. J., and Schmunis, G. A. 1992. Plasmodia in humans. *In: Parasitic Protozoa*. Kreier, J. P., and Baker, J. R. (Eds), Academic Press, San Diego. **5**: 135-266.

Löwe, J., and Amos, L. A. 1998. Crystal structure of the bacterial cell-division protein FtsZ. *Nature* **391**: 203-206.

Löwe, J., Li, H., Downing, K. H., and Nogales, E. 2001. Refined structure of $\alpha\beta$ -tubulin at 3.5 Å resolution. *J Mol Biol* **313**: 1045-1057.

Lubega, G. W., Geary, T. G., Klein, R. D., and Prichard, R. K. 1993. Expression of cloned β -tubulin genes of *Haemonchus contortus* in *Escherichia coli*: interaction of recombinant β -tubulin with native tubulin and mebendazole. *Mol Biochem Parasitol* **62**: 281-292.

Lubega, G. W., Byarugaba, D. K., and Prichard, R. K. 2002a. Immunisation with a tubulin-rich preparation from *Trypanosoma brucei* confers broad protection against African trypanosomiasis. *Exp Parasitol* **102**: 9-22.

Lubega, G. W., Ochola, D. O. K., and Prichard, R. K. 2002b. *Trypanosoma*

brucei: anti-tubulin antibodies specifically inhibit trypanosome growth in culture. *Exp Parasitol* **102**: 134-142.

Ludueña, R. F., Banerjee, A., and Khan, I. A. 1992. Tubulin structure and biochemistry. *Curr Opin Cell Biol* **4**: 53-57.

Ludueña, R. F. 1998. Multiple forms of tubulin: different gene products and covalent modifications. *Int Rev Cytology* **178**: 207-275.

MacDonald, L. M., Armson, A., Thompson, R. C. A., and Reynoldson, J. A. 2003. Characterisation of factors favouring the expression of soluble protozoan tubulin proteins in *Escherichia coli*. *Prot Expr Purif* **29**: 117-122.

MacDonald, L. M., Armson, A., Thompson, R. C. A., and Reynoldson, J. A. 2004. Characterisation of benzimidazole binding with recombinant tubulin from *Giardia duodenalis*, *Encephalitozoon intestinalis*, and *Cryptosporidium parvum*. *Mol Biochem Parasitol* **138**: 89-96.

Macrae, T. H., and Gull, K. 1990. Purification and assembly *in vitro* of tubulin from *Trypanosoma brucei brucei*. *Biochem J* **265**: 87-93.

Makler, M. T., Ries, J. M., Williams, J. A., Bancroft, J. E., Piper, R. C., Gibbins, B. L., and Hinrichs, D. J. 1993. Parasite lactate dehydrogenase as an assay for *Plasmodium falciparum* drug sensitivity. *Am J Trop Med Hyg* **48**: 739-741.

Mandelkow, E., and Mandelkow, E-M. 1995. Microtubules and microtubule-associated proteins. *Curr Opin Cell Biol* **7**: 72-81.

Maniatis, T., Fritsch, E. F., and Sambrook, J. 1982. Molecular cloning: a laboratory manual. Cold Spring Harbour, New York.

McIntosh, J. R. 1994. The roles of microtubules in chromosome movement. *In: Microtubules*. Hyams, J. S., and Lloyd, C. W. (Eds.), Wiley-Liss, Inc., New York, NY. pp 413-434.

McKean, P. G., Vaughan, S., and Gull, K. 2001. The extended tubulin superfamily. *J Cell Science* **114**: 2723-2733.

Mooberry, S. L., Tien, G., Hernandez, A. H., Plubrukarn, A., and Davidson, B. S. 1999. Laulimalide and isolaulimalide, new paclitaxel-like microtubule-stabilising agents. *Cancer Res* **59**: 653-660.

Maessen, S., Wesseling, J. G., Smits, M. A., Konings, R. N. H., and Schoenmakers, J. G. G. 1993. The γ -tubulin gene of the malaria parasite *Plasmodium falciparum*. *Mol Biochem Parasitol* **60**: 27-36.

Marston, F. A. O. 1987. The purification of eukaryotic polypeptides expressed in *Escherichia coli*. *In: DNA Cloning, Vol. III, A Practical Approach* (D. M. Glover, ed.), pp. 59-88. IRL Press, Oxford, Washington.

- Mead, J. R., Fauq, A. H., Khan, M. A., and McNair, N.** 2003. Efficacy of glycoconjugated dinitroanilines against *Cryptosporidium parvum*. *J Eukaryot Microbiol* **50**: 550-552.
- Meshnick, S. R., and Dobson, M. J.** 2001. The history of antimalarial drugs. *In: Antimalarial Chemotherapy. Mechanisms of action, resistance, and new directions in drug discovery.* Rosenthal, P. J. (Ed), Humana Press, Totowa, New Jersey. pp 15-26.
- Miller, L. H., Baruch, D. I., Marsh, K., and Doumbo, O. K.** 2002. The pathogenic basis of malaria. *Nature* **415**: 673-679.
- Mizuno, K., Perkin, J., Sek, F., and Gunning, B.** 1985. Some biochemical properties of higher plant tubulins. *Cell Biol Int Rep* **9**: 5-12.
- Mohri, H.** 1968. Amino-acid composition of "tubulin" constituting microtubules of sperm flagella. *Nature* **217**: 1053-1054.
- Moorthy, V. S., Good, M. F., and Hill, A. V. S.** 2004. Malaria vaccine developments. *Lancet* **363**: 150-156.
- Morejohn, L. C., and Fosket, D. E.** 1982. Higher plant tubulin identified by self-assembly into microtubules *in vitro*. *Nature* **297**: 426-428.
- Morejohn, L. C., and Fosket, D. E.** 1984. Inhibition of plant microtubule polymerisation *in vitro* by the phosphoric amide herbicide amiprofos-methyl. *Science* **224**: 874-876.
- Morejohn, L. C., and Fosket, D. E.** 1991. The biochemistry of compounds with anti-microtubule activity in plant cells. *Pharmac Ther* **51**: 217-230.
- Morrisette, N. S., and Sibley, L. D.** 2002. Cytoskeleton of apicomplexan parasites. *Microbiol Mol Biol Rev* **66**: 21-38.
- Morrisette, N. S., Mitra, A., Sept, D., and Sibley, L. D.** 2004. Dinitroanilines bind α -tubulin to disrupt microtubules. *Mol Biol Cell* **15**: 1960-1968.
- Murthy, J. V., Kim, H-H., Hanesworth, V. R., Hugdahl, J. D., and Morejohn, L. C.** 1994. Competitive inhibition of high-affinity oryzalin binding to plant tubulin by the phosphoric amide herbicide amiprofos-methyl. *Plant Physiol* **105**: 309-320.
- Nakazawa, M., Moreira, D., Laurent, J., Le Guyader, H., Fukami, Y., and Ito, K.** 1999. Biochemical analysis of the interaction between elongation factor 1 α and α/β -tubulins from a ciliate, *Tetrahymena pyriformis*. *FEBS Lett* **453**: 29-34.
- Nasioulas, G., Grammbitter, K., Himes, R. H., and Ponstingl, H.** 1990. Interaction of a new photosensitive derivative of vinblastine, NAPAVIN, with tubulin and microtubules *in vitro*. *Eur J Biochem* **192**: 69-74.
- Nare, B., Lubega, G., Prichard, R. K., and Georges, E.** 1996. *p*-Azidosalicyl-5-

amino-6-phenoxybenzimidazole photolabels the N-terminal 63-103 amino acids of *Haemonchus contortus* β -tubulin. *J Biol Chem* **271**: 8575-8581.

Nath, J., and Schneider, I. 1992. Anti-malarial effects of the anti-tubulin herbicide trifluralin: studies in *Plasmodium falciparum*. *Clin Res* **40**: 331A

Nath, J., Okoye, V., and Schneider, I. 1994. Anti-malarial effects of the anti-tubulin herbicide trifluralin: studies with *Plasmodium falciparum*. *Storming Media Report No*: A934682.

News. 2002. Creatures of our own making. *Science* **298**: 80-81.

Nogales, E., Wolf, S. G., and Downing, K. H. 1998. Structure of the alpha beta tubulin dimer by electron crystallography. *Nature* **391**: 199-203.

Nogales, E. 2000. Structural insights into microtubule function. *Annu Rev Biochem* **69**: 277-302.

Nyporko, A. Y., Yemets, A. I., Klimkina, L. A., and Blume, Y. B. 2002. Sensitivity of *Eleusine indica* callus to trifluralin and amiprofos methyl in correlation with the binding of these compounds to tubulin. *Russian J Plant Physiol* **49**: 413-418.

Oakley, B. R. 2000. An abundance of tubulins. *Trends Cell Biol* **10**: 537-542.

Oakley, C. E., and Oakley, B. R. 1989. Identification of γ -tubulin, a new member of the tubulin superfamily encoded by *mipA* gene of *Aspergillus nidulans*. *Nature* **338**: 662-664.

Ochola, D. O. K., Prichard, R. K., and Lubega, G. W. 2002. Classical ligands bind tubulin of trypanosomes and inhibit their growth *in vitro*. *J Parasitol* **88**: 600-604.

Olliaro, P. L., and Bloland, P. B. 2001. Clinical and public health implications of antimalarial drug resistance. *In*: Antimalarial Chemotherapy. Mechanisms of action, resistance, and new directions in drug discovery. Rosenthal, P. J. (Ed), Humana Press, Totowa, New Jersey. pp 65-83.

Olsen, M. K., Rockenbach, S. K., Curry, K. A., and Tomich, C-S, C. 1989. Enhancement of heterologous polypeptide expression by alterations in the ribosome-binding-site sequence. *J Biotechnol* **9**: 179-190.

Oxberry, M. E., Geary, T. G., and Prichard, R. K. 2001a. Assessment of benzimidazole binding to individual recombinant tubulin isotypes from *Haemonchus contortus*. *Parasitol* **122**: 683-687.

Oxberry, M. E., Geary, T. G., Winterrowd, C. A., and Prichard, R. K. 2001b. Individual expression of recombinant α - and β -tubulin from *Haemonchus contortus*: polymerisation and drug effects. *Prot Expr Purif* **21**: 30-39.

- Pettit, G. R., Srirangam, J. K., Barkoczy, J., Williams, M. D., Boyd, M. R., Hamel, E., Pettit, R. K., Hogan, F., Bai, R., Chapuis, J. C., McAllister, S. C. and Schmidt, J. M.** 1998. Antineoplastic agents 365. Dolastatin 10 SAR probes. *Anti-cancer Drug Design* **13**: 243-277.
- Pettit, G. R., Srirangam, J. K., Barkoczy, J., Williams, M. D., Durkin, K. P. M., Boyd, M. R., Bai, R., Hamel, E., Schmidt, J. M. and Chapuis, J. C.** 1995. Antineoplastic agents 337. Synthesis of dolastatin 10 structural modifications. *Anti-cancer Drug Design* **10**: 529-544.
- Phadtare, S., Fisher, M. T., and Yarbrough, L. R.** 1994. Refolding and release of tubulins by a functional immobilised *groEL* column. *Biochimica et Biophysica Acta* **1208**: 189-192.
- Pinder, J., Fowler, R., Bannister, L., Dluzewski, A., and Mitchell, G. H.** 2000. Motile systems in malaria merozoites: how is the red blood cell invaded? *Parasitol Today* **16**: 240-245.
- Plessmann, U., Reiter-Owona, I., and Lechtreck, K-F.** 2004. Posttranslational modifications of α -tubulin of *Toxoplasma gondii*. *Parasitol Res* **94**: 386-389.
- Poncet, J.** 1999. The dolastatins, a family of promising antineoplastic agents. *Curr Pharma Design* **5**: 139-162.
- Pouvelle, B., Farley, P. J., Long, C. A., and Taraschi, T. F.** 1994. Taxol arrests the development of blood-stage *Plasmodium falciparum* *in vitro* and *Plasmodium chabaudi adami* in malaria-infected mice. *J Clin Invest* **94**: 413-417.
- Prescott, A. R., Foster, K. E., Warn, R. M., and Gull, K.** 1989. Incorporation of tubulin from an evolutionarily diverse source, *Physarum polycephalum*, into the microtubules of a mammalian cell. *J Cell Sci* **92**: 595-605.
- Pucciarelli, S., Miceli, C., and Melki, R.** 2002. Heterologous expression and folding analysis of a β -tubulin isotype from the antarctic ciliate *Euplotes focardii*. *Eur J Biochem* **269**: 6271-6277.
- Raff, E. C.** 1994. The role of multiple tubulin isoforms in cellular microtubule function. *In: Microtubules*. Hyams, J. S., and Lloyd, C. W. (Eds.), Wiley-Liss, Inc., New York, NY. pp 85-109.
- Rai, S. S., and Wolff, J.** 1996. Localisation of the vinblastine-binding site on β -tubulin. *J Biol Chem* **271**: 14707-14711.
- Ravelli, R. B. G., Gigant, B., Curmi, P. A., Jourdain, I., Lachkar, S., Sobel, A., and Knossow, M.** 2004. Insight into tubulin regulation from a complex with colchicine and a stathmin-like domain. *Nature* **428**: 198-202.
- Rawlings, D. J., Fujioka, H., Fried, M., Keister, D. B., Aikawa, M., and Kaslow, D. C.** 1992. α -tubulin II is a male-specific protein in *Plasmodium falciparum*. *Mol Biochem Parasitol* **56**: 239-250.

- Read, M., Sherwin, T., Holloway, S. P., Gull, K., and Hyde, J. E.** 1993. Microtubular organisation visualised by immunofluorescence microscopy during erythrocytic schizogony in *Plasmodium falciparum* and investigation of post-translational modifications of parasite tubulin. *Parasitol* **106**: 223-232.
- Ridley, R. G.** 2002. Medical need, scientific opportunity and the drive for antimalarial drugs. *Nature* **415**: 686-693.
- Ridley, R., and Toure, Y.** 2004. Winning the drugs war. *Nature* **430**: 942-943.
- Robinson, D. R., Sherwin, T., Ploubidou, A., Byard, E. H., and Gull, K.** 1995. Microtubule polarity and dynamics in the control of organelle positioning, segregation, and cytokinesis in the trypanosome cell cycle. *J Cell Biol* **128**: 1163-1172.
- Robinson, M. W., McFerran, N., Trudgett, A., Hoey, L., and Fairweather, I.** 2004. A possible model of benzimidazole binding to β -tubulin disclosed by invoking an inter-domain movement. *J Mol Graph Model* **23**: 275-284.
- Rosenberg, R., Wirtz, R. A., Schneider, I., and Burge, R.** 1990. An estimation of the number of malaria sporozoites ejected by a feeding mosquito. *Trans R Soc Trop Med Hyg* **84**: 209-212.
- Rosenthal, P. J.** 2001. Protease inhibitors. *In: Antimalarial Chemotherapy. Mechanisms of action, resistance, and new directions in drug discovery.* Rosenthal, P. J. (Ed), Humana Press, Totowa, New Jersey. pp 325-346.
- Rubio, J. P., and Cowman, A. F.** 1996. The ATP-binding cassette (ABC) gene family of *Plasmodium falciparum*. *Parasitol Today* **12**: 135-140.
- Rug, M., Wickham, M. E., Foley, M., Cowman, A. F., and Tilley, L.** 2004. Correct promoter control is needed for trafficking of the ring-infected erythrocyte surface antigen to the host cytosol in transfected malaria parasites. *Infect Immun* **72**: 6095-6105.
- Rusan, N. M., Fagerstrom, C. J., Yvon, A-M. C., and Wadsworth, P.** 2001. Cell cycle-dependent changes in microtubule dynamics in living cells expressing green fluorescent protein- α tubulin. *Mol Biol Cell* **12**: 971-980.
- Russell, D. G., Miller, D., and Gull, K.** 1984. Tubulin heterogeneity in the trypanosome *Crithidia fasciculata*. *Mol Cell Biol* **4**: 779-790.
- Sachdev, D., and Chirgwin, J. M.** 1998. Solubility of proteins isolated from inclusion bodies is enhanced by fusion to maltose-binding protein or thioredoxin. *Protein Expr Purif* **12**: 122-132.
- Sachs, J., and Malaney, P.** 2002. The economic and social burden of malaria. *Nature* **415**: 680-685.

Safa, A. R., Hamel, E., and Felsted, R. L. 1987. Photoaffinity labeling of tubulin subunits with a photoactive analogue of vinblastine. *Biochemistry* **26**: 97-102.

Salmon, B. L., Oksman, A., and Goldberg, D. E. 2001. Malaria parasite exit from the host erythrocyte: a two-step process requiring extraerythrocytic proteolysis. *Proc Natl Acad Sci USA* **98**: 271-276.

Sawada, T., Kato, Y., Kobayashi, H., Hashimoto, Y., Watanabe, T., Sugiyama, Y., and Iwasaki, S. 1993a. A fluorescent probe and a photoaffinity labeling reagent to study the binding site of maytansine and rhizoxin on tubulin. *Bioconjug Chem* **4**: 284-289.

Sawada, T., Kobayashi, H., Hashimoto, Y., and Iwasaki, S. 1993b. Identification of the fragment photoaffinity-labeled with azidodansyl-rhizoxin as Met-363-Lys-379 on beta-tubulin. *Biochem Pharmacol* **45**: 1387-1394.

Schein, C. H., and Noteborn, M. H. M. 1988. Formation of soluble recombinant proteins in *Escherichia coli* is favoured by lower growth temperatures. *Bio/Technology* **6**: 291-294.

Schibler, M. J., and Huang, B. 1991. The col^R4 and col^R15 β -tubulin mutations in *Chlamydomonas reinhardtii* confer altered sensitivities to microtubule inhibitors and herbicides by enhancing microtubule stability. *J Cell Biol* **113**: 605-614.

Schneider, A., Plessmann, U., and Weber, K. 1997. Subpellicular and flagellar microtubules of *Trypanosoma brucei* are extensively glutamylated. *J Cell Sci* **110**: 431-437.

Scholey, J. M. and Vale, R. D. 1994. Kinesin-based organelle transport. *In: Microtubules.* Hyams, J. S., and Lloyd, C. W. (Eds.), Wiley-Liss, Inc., New York, NY. pp 343-365.

Sen, K., and Godson, G. N. 1990. Isolation of α - and β - tubulin genes of *Plasmodium falciparum* using a single oligonucleotide probe. *Mol Biochem Parasitol* **39**: 173-182.

Senge, M. O., and Hatscher, S. 2000. The malaria pigment haemozoin – a focal point of action for antimalarial drugs. *ChemBiochem* **1**: 247-249.

Schneider, A., Sherwin, T., Sasse, R., Russell, D. G., Gull, K., and Seebeck, T. 1987. Subpellicular and flagellar microtubules of *Trypanosoma brucei brucei* contain the same α -tubulin isoforms. *J Cell Biol* **104**: 431-438.

Schrével, J., Sinou, V., Grellier, P., Frappier, F., Guénard, D., and Potier, P. 1994. Interactions between docetaxel (Taxotere) and *Plasmodium falciparum*-infected erythrocytes. *Proc Natl Acad Sci USA* **91**: 8472-8476.

Shah, C., Xu, C. Z-Q., Vickers, J., and Williams, R. 2001. Properties of microtubules assembled from mammalian tubulin synthesised in *Escherichia coli*. *Biochemistry* **40**: 4844-4852.

- Shea, D. K., and Walsh, C. J.** 1987. mRNAs for α - and β -tubulin and flagellar calmodulin are among those coordinately regulated when *Naegleria gruberi* amoebae differentiate into flagellates. *J Cell Biol* **105**: 1303-1309.
- Shelanski, M. L., Gaskin, F., and Cantor, C. R.** 1973. Microtubule assembly in the absence of added nucleotides. *Proc Nat Acad Sci USA* **70**: 765-768.
- Sinden, R. E., Canning, E. U., Bray, R. S., and Smalley, M. E.** 1978. Gametocyte and gamete development in *Plasmodium falciparum*. *Proc Roy Soc Lond Biol Sci* **201**: 375-399.
- Sinden, R. E., Canning, E. U., and Spain, B. J.** 1976. Gametogenesis and fertilisation in *Plasmodium yoelii nigeriensis*: a transmission electron microscope study. *Proc Roy Soc Lond Biol Sci* **193**: 55-76.
- Sinden, R. E., Hartley, R. H., and King, N. J.** 1985. Gametogenesis in *Plasmodium*; the inhibitory effects of anticytoskeletal agents. *Int J Parasitol* **15**: 211-217.
- Sinden, R. E., and Smalley, M. E.** 1979. Gametocytogenesis of *Plasmodium falciparum* *in vitro*: the cell-cycle. *Parasitol* **79**: 277-296.
- Sinou, V., Boulard, Y., Grellier, P., and Schrével, J.** 1998. Host cell and malarial targets for docetaxel (Taxotere™) during the erythrocytic development of *Plasmodium falciparum*. *J Euk Microbiol* **45**: 171-183.
- Sinou, V., Grellier, P., and Schrével, J.** 1996. *In vitro* and *in vivo* inhibition of erythrocytic development of malarial parasites by docetaxel. *Antimicrob Agents Chemother* **40**: 358-361.
- Smith, E. F., and Sale, W. S.** 1994. Mechanisms of flagellar movement: functional interactions between dynein arms and the radial spoke – central apparatus complex. *In: Microtubules.* Hyams, J. S., and Lloyd, C. W. (Eds.), Wiley-Liss, Inc., New York, NY. pp 381-392.
- Smyth, D. R., Mrozkiewicz, M. K., McGrath, W. J., Listwan, P., and Kobe, B.** 2003. Crystal structures of fusion proteins with large-affinity tags. *Protein Science* **12**: 1313-1322.
- Stephens, R. E.** 1972. Thermal fractionation of outer fiber doublet microtubules into A- and B-subfiber components: A- and B-tubulin. *J Mol Biol* **47**: 353-363.
- Stephens, R. E.** 1998. Electrophoretic resolution of tubulin and tektin subunits by differential interaction with long-chain alkyl sulfates. *Anal Biochem* **265**: 356-360.
- Stokkermans, T. J. W., Schwartzman, J. D., Keenan, K., Morrissette, N. S., Tilney, L. G., and Roos, D. S.** 1996. Inhibition of *Toxoplasma gondii* replication by dinitroaniline herbicides. *Exp Parasitol* **84**: 355-370.

- Su, X-Z., Wu, Y., Sifri, C. D., and Wellems, T. E.** 1996. Reduced extension temperatures required for PCR amplification of extremely A + T-rich DNA. *Nucleic Acids Res* **24**: 1574-1575.
- Suh, K. N., Kain, K. C., and Keystone, J. S.** 2004. Malaria. *J Canadian Medical Assoc* **170**: 1693-1702.
- Suhrbier, A., Sinden, R. E., Couchman, A., Fleck, S. L., Kumar, S., and McMillan, D.** 1993. Immunological detection of cytoskeletal proteins in the exoerythrocytic stages of malaria by fluorescence and confocal laser scanning microscopy. *J Euk Microbiol* **40**: 18-23.
- Suprenant, K. A., Hays, E., LeCluyse, E., and Dentler, W. L.** 1985. Multiple forms of tubulin in the cilia and cytoplasm of *Tetrahymena thermophila*. *Proc Natl Acad Sci USA* **82**: 6908-6912.
- Taraschi, T. F., Trelka, D., Schneider, T., and Matthews, I.** 1998. *Plasmodium falciparum*: characterisation of organelle migration during merozoite morphogenesis in asexual malaria infections. *Exp Parasitol* **88**: 184-193.
- Tian, G., Lewis, S. A., Feierbach, B., Stearns, T., Rommelaere, H., Ampe, C., and Cowan, N. J.** 1997. Tubulin subunits exist in an activated conformational state generated and maintained by protein cofactors. *J Cell Biol* **138**: 821-832.
- Tilney, L. G., and Tilney, M. S.** 1996. The cytoskeleton of protozoan parasites. *Curr Opin Cell Biol* **8**: 43-48.
- Torres, K., and Horwitz, S. B.** 1998. Mechanisms of Taxol-induced cell death are concentration dependent. *Cancer Res* **58**: 3620-3626.
- Trager, W., Rozario, C., Shio, H., Williams, J., and Perkins, M. E.** 1992. Transfer of a dense granule protein of *Plasmodium falciparum* to the membrane of ring stages and isolation of dense granules. *Infect Immun* **60**: 4656-4661.
- Trager, W., and Jensen, J. D.** 1976. Human malarial parasites in continuous culture. *Science* **193**: 673-675.
- Traub-Cseko, Y. M., Ramalho-Ortigão, J. M., Dantas, A. P., de Castro, S. L., Barbosa, H. S., and Downing, K. H.** 2001. Dinitroaniline herbicides against protozoan parasites: the case of *Trypanosoma cruzi*. *Trends Parasitol* **17**: 136-141.
- Triano, E. A., Simpson, J. B., Kratky, M., Lang, W. R., and Triolo, A. J.** 1985. Protective effects of trifluralin on benzo(a)pyrene-induced tumors in A/J mice. *Cancer Res* **45**: 601-607.
- U.S. Environmental Protection Agency.** 1987. Guidance for the reregistration of pesticide products containing trifluralin as the active ingredient, p 8. Office of Pesticides and Toxic Substances, U.S. Environmental Protection Agency, Washington, D. C.

- Usanga E. A., O'Brien, E., and Luzzato, L.** 1986. Mitotic inhibitors arrest the growth of *Plasmodium falciparum*. *FEBS* **209**: 23-27.
- Vantard, M., Levilliers, N., Hill, A-M., Adoutte, A., and Lambert, A-M.** 1990. Incorporation of *Paramecium* axonemal tubulin into higher plant cells reveals functional sites of microtubule assembly. *Proc Natl Acad Sci USA* **87**: 8825-8829.
- Vickerman, K., and Cox, F. E. G.** 1967. Merozoite formation in the erythrocytic stages of the malaria parasite *Plasmodium vinckei*. *Trans Roy Soc Trop Med Hyg* **61**: 303-312.
- Wellems, T., and Plowe, C.** 2001. Chloroquine-resistant malaria. *J Infect Dis* **184**: 770-776.
- Werbovetz, K. A.** 2002. Tubulin as an antiprotozoal drug target. *Mini Rev Med Chem* **2**: 519-529.
- Werbovetz, K. A., Brendle, J., and Sackett, D.** 1999. Purification, characterisation, and drug susceptibility of tubulin from *Leishmania*. *Mol Biochem Parasitol* **98**: 53-65.
- Werbovetz, K. A., Sackett, D. L., Delfin, D., Bhattacharya, G., Salem, M., Obrzut, T., Rattendi, D., and Bacchi, C.** 2003. Selective antimicrotubule activity of *N*1-phenyl-3,5-dinitro-*N*4,*N*4-di-*n*-propylsulfanilamide (GB-II-5) against kinetoplastid parasites. *Mol Pharmacol* **64**: 1325-1333.
- Wesseling, J. G., Dirks, R., Smits, M. A., and Schoenmakers, J. G. G.** 1989. Nucleotide sequence and expression of a β -tubulin gene from *Plasmodium falciparum*, a malarial parasite of man. *Gene* **83**: 301-309.
- Westermann, S., and Weber, K.** 2003. Post-translational modifications regulate microtubule function. *Nature Rev* **4**: 938-947.
- Wilson, L., Anderson, K., and Chin, D.** 1976. Nonstoichiometric poisoning of microtubule polymerisation: a model for the mechanism of action of the *vinca* alkaloids, podophyllotoxin, and colchicine. *In: Cell motility*. Cold Spring Harbor, New York; Cold Spring Harbour Laboratory. (Goldman R, Pollard T, Rosenbaum JL eds.), pp. 1051-1064.
- Wilson, L., and Jordan, M. A.** 1994. Pharmacological probes of microtubule function. *In: Microtubules*. Hyams, J. S., and Lloyd, C. W. (Eds.), Wiley-Liss, Inc., New York, NY. pp 59-83.
- Wolff, J., Knipling, L., Cahnmann, H. J., and Palumbo, G.** 1991. Direct photoaffinity labeling of tubulin with colchicine. *Proc Natl Acad Sci USA*. **88**: 2820-2824.
- Wu, J., and Yarbrough, L. R.** 1987. Expression of the alpha and beta tubulin genes of the African trypanosome in *Escherichia coli*. *Gene* **61**: 51-62.

Wheatley, S. P., Kandels-Lewis, S. E., Adams, R. R., Ainsztein, A. M., and Earnshaw, W. C. 2001. INCENP binds directly to tubulin and requires dynamic microtubules to target to the cleavage furrow. *Exp Cell Res* **262**: 122-127.

Yaffe, M. B., Levison, B. S., Szasz, J., and Sternlicht, H. 1988. Expression of a human α -tubulin: properties of the isolated subunit. *Biochemistry* **27**: 1869-1880.

Yamamoto, E., Zeng, L., and Baird, W. V. 1998. α -tubulin missense mutations correlate with antimicrotubule drug resistance in *Eleusine indica*. *Plant Cell* **10**: 297-308.

Yoshida, M., Narusaka, Y., Minami, E., and Ishii, H. 1999. Expression of *Neurospora crassa* β -tubulin, target protein of benzimidazole fungicides, in *Escherichia coli*. *Pestic Sci* **55**: 362-364.

Young D. H., and Lewandowski, V. T. 2000. Covalent binding of the benzamide RH-4032 to tubulin in suspension-cultured tobacco cells and its application in a cell-based competitive-binding assay. *Plant Physiol* **124**: 115-124.

Zuckerman, A. 1967. Harvesting of *Plasmodium falciparum* with saponin. *Bull WHO* **37**: 431-436.